Stretto di Messina

Concessionaria per la progettazione, realizzazione e gestione del collegamento stabile tra la Sicilia e il Continente Organismo di Diritto Pubblico
(Legge n°1158 del 17 dicembre 1971, modificata dal D.Lgs. n°114 del 24 aprile 2003)

EurolinK

PONTE SULLO STRETTO DI MESSINA

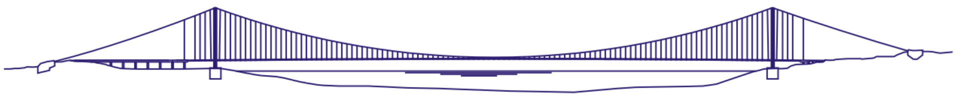

PROGETTO DEFINITIVO

EUROLINK S.C.p.A.

IMPREGILO S.p.A. (MANDATARIA)
SOCIETÀ ITALIANA PER CONDOTTE D'ACQUA S.p.A. (MANDANTE)
COOPERATIVA MURATORI E CEMENTISTI - C.M.C. DI RAVENNA SOC. COOP. A.R.L. (MANDANTE)
SACYR S.A.U. (MANDANTE)
ISHIKAWAJIMA - HARIMA HEAVY INDUSTRIES CO. LTD (MANDANTE)
A.C.I. S.C.P.A. - CONSORZIO STABILE (MANDANTE)

IL PROGETTISTA	IL CONTRAENTE GENERALE	STRETTO DI MESSINA	STRETTO DI MESSINA
COWI Ing. E.M. Veje Dott. Ing. E. Pagani Ordine Ingegneri Milano n°15408 EurolinK	Project Manager (Ing. P.P. Marcheselli)	Direttore Generale e RUP Validazione (Ing. G. Fiammenghi)	Amministratore Delegato (Dott. P. Ciucci)

PB0029_F0

Unità Funzionale	OPERA DI ATTRAVERSAMENTO
Tipo di sistema	STUDI DI BASE
Raggruppamento di opere/attività	ANALISI GLOBALI
Opera - tratto d'opera - parte d'opera	Basic Studies
Titolo del documento	Runability, Safety and Comfort Analysis, Annex

CODICE: C G 1 0 0 0 | P | R X | D | P | S B | A 2 | 0 0 | 0 0 | 0 0 | 0 0 | 0 2 | F0

REV	DATA	DESCRIZIONE	REDATTO	VERIFICATO	APPROVATO
F0	20-06-2011	EMISSIONE FINALE	PKAN/GB/SG	JCA/FB	JCA/EYA

NOME DEL FILE: PB0029_F0

INDICE

1 Executive summary

The Messina Bridge is a highly innovative bridge design for the world's longest span (3300m) to link Sicily with mainland Italy. The bridge is to be a suspension bridge formed from 4 main cables, a steel triple box girder, and 399m tall steel towers. Not only are the bounds of current bridge experience being pushed to the limit with a structure that is significantly larger than the current world's longest span of 1991m (the Akashi Kaikyo bridge), the aerodynamic stability of the deck structure is reliant on the beneficial characteristics provided by the innovative triple deck box structure. Thus the railway runability, safety and comfort have to be proven for the structural design.

This report covers the scope of and approach to the train runability, safety and comfort study carried out for the Messina Strait Bridge.

The basic scope of the runability study is to verify that the actual trains likely to be operating on the bridge subject to the loads specified in the Design Basis, document GCG.F.04.01 will meet the requirements with regards to runability as well as safety and comfort. These requirements are specified specifically for each limit state (SLS1 and SLS2) and each load combination belonging to these.

The analyses that have been carried out can be subdivided into two classes:

- Global analyses carried out with COWI's in-house developed FE-software IBDAS with a train model comprising 7 degrees of freedom (DOF) per bogie. IBDAS allows for direct dynamic train-bridge interaction analysis, i.e. the dynamic trains are interacting directly with the global FE-model utilizing a frequency domain modal approach. This group of analyses is performed on a global bridge FE model, with a simplified model of the trains in the sense that no modelling of rails and fittings are included. The full number of analysis cases is considered, so as to obtain a broad picture of the train and bridge behaviour and response parameters.
- Local analyses with a refined large number of DOF train model, as well as rail and fittings modelled. The local analysis has been carried out with ADTreS, which is a software package entirely developed and validated by the Mechanical Engineering Department of Politecnico di Milano. It is fully dedicated to the mathematical modelling of train-track-bridge interaction. It is based on a multi-body model of the rail vehicle and on a finite element approach for the bridge, which can also include the track structure itself.This group of analyses is aimed at the

assessment of the local dynamic behaviour of the trains, determining dynamic loadings caused by real trains on rails, fittings and onto the underlying primary stringers and rail box girder, to be compared with the conventional static loads adopted for the design of the same elements.

One of the main concerns regarding train runability on the Messina Strait Bridge is the sensitivity to wind loads acting on the bridge and in particular on the trains. Especially empty freight coaches are an issue in this regard. Further the accelerations induced on the trains when passing the expansion joints is an area of interest. Apart from these obvious issues the automatic train-bridge interaction assessment in the analysis models ensures that potential dynamic amplification effects are covered as well.

With two railway tracks on the bridge, six different dynamic trains calibrated from real train types, three structural key positions on the bridge at which the trains will meet and two limit states comprising a total of 6 load combinations the total number of possible analysis combinations amounts roughly 600. This large amount of analysis calls for a very automated and systematic calculation approach.

1.1 Design Basis, Rail Dynamics

The Tender Design Basis document GCG F.04.01 (Design basis and expected performance levels) outlines derailment and train overturning checks to be carried out. The design basis has been further elaborated in document "*CG1000-P-RG-D-P-GE-00-00-00-00-00-02-A Basis of Design*"

1.1.1 Runability

The following railway runability performance levels is to be fulfilled according to Design Basis, document *CG1000-P-RG-D-P-GE-00-00-00-00-00-02-A Basis of Design*:

1.1.2 Safety

The derailment verification is based on the variations of the lateral force, Y, and the vertical force, P, at the wheel-rail contact points for the dynamic train-bridge system.

Tests carried out by the ORE C-138 group have shown that derailment can occur in the extreme case where the Y/P ratio over a distance of more than 2 m is greater than 1.2. For this reason the following value is usually retained as the criterion for safety against derailment:

$$\frac{Y}{P} < 1.2$$

However, in order to keep a satisfactory safety margin the ratio shall under normal operation not exceed:

$$\frac{Y}{P} < 0.8$$

The risk of overturning is evaluated by the maximum wheel unloading coefficient, ΔP/P. The European Standard EN 14067-6, subsections 5.4.3.4 and 5.4.4.1, discuss the limit ratio ΔP/P < 0.9 for trains subjected to cross winds supported by the Technical Specifications for Interoperability (TSIs) High Speed Rolling Stock, Annex G. In order to accommodate for all dynamic actions including rail irregularities and cross wind it has been agreed by discussion in between SdM, Parsons and Eurolink to use the ratio:

$$\frac{\Delta P}{P} < 0.9$$

1.2 Dynamic Properties of the RFI Trains

All relevant parameters for coaches and locomotives are based on the dynamic properties informed in Document No. DT.ISP.F.E.R3.001 [1] and further as corrected by SdM.

1.3 Loads and Load Combinations

The analyses carried out include combinations of several parameters:

- Environmental loads, i.e. temperature, wind and seismic
- Number of trains
- Position of trains
- Train speed.

The individual loads to be included in the analysis are defined in the Design Basis [2]. Loads are as follows:

- Dead Load Deformation (PP + PN)
- Roadway and Railway Loading (QR)
- Wind Action (VV)
- Seismic Action (VS)
- Temperature Action (VT)

1.4 Train Combinations

The analysed train combinations are composed by in total 27 different cases analysed by complete and individual computer runs.

In cases where two trains pass each other on the bridge, three different relative positions of the trains are considered in order to evaluate the most unfavourable positions of the trains:

The three relative positions of two trains correspond to:

1 The trains meet at the middle of the main span.

2 The trains meet approximately at the tower.

3 The trains meet approximately at the expansion joint.

However, for some of the analyses only the meeting point at the middle of the bridge has been carried out due to extensive calculation time. This applies for the analyses including seismic loading or dynamic wind load. The outcome of the analyses with all three meeting points investigated has revealed that the influence of this is absolutely minor.

1.5 IBDAS Global model description

The trains are modelled by means of a 7 DOF/bogie model containing two separate masses: Bogie mass and coach mass. The bogie mass contains four DOF: Vertical and horizontal lateral translation as well as rolling and pitching. The coach mass contains the same two translational DOF in addition to rolling. The contact interface between wheels and the rails is modelled as a fully stiff connection in the IBDAS model. Hence no representative wheel/rail contact forces can be computed. Due to this modelling approach negative wheel forces, i.e. tensile forces, can occur if the uplift wheel forces exceed the compressive force from the train dead load. As such results are reliably only when the wheel/rail contact force is compressive.

Between the wheel/rail rail contact points and the bogie mass the primary suspension is modelled by means of a vertical as well as lateral spring/damper system. An identical composition exists for the secondary suspension between the bogie and the coach mass. All springs and dampers in the model are characterized by constant coefficients, i.e. there's a fully linear relation between displacement/velocity and force.

The different criteria to be investigated in connection with runability, safety and comfort assessment are provided as a direct output in the result files generated by IBDAS. Hence the user need not to perform tedious data processing of large history files in order to compute the relevant quantities. Similarly, IBDAS can automatically report envelope extreme quantities of a full time series.

1.6 AdTreS Local Analysis for Wheel / Track Runability

In this section, the dynamic local interaction between train transit and structure response across diaphragms and cross girders is particularly investigated. To achieve this objective, a detailed local model of the railway girder is developed, modeled, and validated. The entire railway girder box is separated from the four T beams located underneath the rail track and they are all modelled individually.

The rail vehicle model is based on a multi-body approach which accounts for both vertical and lateral dynamics of the train-structure interaction. Each vehicle consists of seven rigid bodies (i.e., car body, two bogies, and four wheelsets) connected together through primary and secondary suspensions. Linear and nonlinear elastic and damping elements are used for the suspensions schematization. The car body and the bogies are taken as having 5 degrees of freedom each: vertical and lateral translational rigid body motions, and yaw, pitch, and roll rigid body rotations. Each wheelset is modeled as a 2 degrees of freedom system which includes lateral translational motion and yaw rotation. The vertical translational motion of the wheelset is a variable which depends on the relative lateral displacement between rail and wheelset in a nonlinear fashion.

The full multi-body model of the vehicle consists of a total of 23 DOF, where the longitudinal motion is given by selecting the vehicle speed. The lateral, vertical displacement and the roll rotation of the whole railway is computed as the superposition of rail irregularity and deformability. The rail lateral motion is taken into account through the so called term “Gravitational Stiffness“ [15].

1.6.1 Embedded rail track and fittings model

The schematization of the structural local model is improved by introducing a model of the embedded rail track. Both rails are laid on a continuous layer of rubber elements along their entire length. The embedded rail mathematical model is developed as follows:

- rails are modeled as beam-type finite elements;
- rubber beds are modeled as a continuous layer of a uniformly distributed set of visco-elastic elements which links the multi-beam finite element model and the rails together.

Values of the parameters have been chosen such that the vertical and lateral displacements of the rails are less than 2 mm when a vertical load equal to 20 ton/axis and a lateral force of 20 kN are respectively applied.

1.7 Local Analysis scope

Local interaction between train and railway girder is investigated for a short-span structure. A 300 m long finite element local model is developed according to the geometrical and physical characteristics of the full-length scale global finite element model.

The dynamic amplification factor defined as the ratio between the maximum dynamic value and the maximum static value of a quantity Q, such as deflection or stress has been analysed.

Dynamic train transit simulations are compared to the static transit of equivalent axle loads nearby cross girders and diaphragms. Impact Factors are computed from quantities Q representing nodal forces and displacements, particularly :

- force transmitted to the visco-elastic beds on the left and right hand side of the track fittings;
- maximum vertical wheel-rail contact force at different vehicle speeds;

- nodal vertical displacement difference between rail and T beam on the left and right hand side of the track.

Analysis of local effects is also performed by computing track and vehicle acceleration peaks:

- nodal vertical acceleration peaks of right and left rails and T beams;
- nodal vertical acceleration peaks of the railway girder;

1.8 Analysis main results - Railway runability, safety and comfort

The only violation of requirements when no environmental loads (wind or seismic) are applied is the unweighted RMS vertical acceleration for the train type RFI 4. This train type is a double decker train and hence contains a rather stiff suspension in order to prevent excessive dynamic movements. As such this minor violation is not a matter of concern. In addition to this, recoil, which is considered as a comfort criterion and hence applies only for passenger trains, is exceeded considerably for all analysis cases. However, the low values of the Sperling Ride comfort index implies that passenger comfort is kept at a very satisfactory level, and the recoil criterion has in recent years been replaced with a comfort filter approach on accelerations ref. EN 12299.

For the load combination introducing dynamic lateral horizontal wind loading on the structure as well as the moving vehicles the critical transverse wind speed has to be relaxed in order to comply with the overturning criterion $\Delta P/P$ and as such the value for train type RFI 6 (empty freight train) close to 0.9 has been determinate for the wind speed applying for all train types (38 m/s 10 min mean, 50.5 m/s gust wind). This causes certain other train types to have a considerable safety margin, but a unified wind speed for all train types has been adopted for the sake of operation simplicity. If it's chosen to distinguish between freight and passenger trains during the operation of the bridge, the passenger trains can comply with the safety requirements (overturning and derailment) when exposed to a SLS2 wind load. In this case RFI 3 is the most wind sensitive train.

The seismic loading has proved to be most adverse when the earth quake peaks at the time when the trains are crossing the pylon region. This is expectable as the highly increased stiffness in this region will tend to induce significantly larger accelerations on the railway girder. The seismic loading applied in SLS1 generally causes no problems in terms of overturning and derailment. However, the two freight trains (RFI 5 + RFI6) show a violation of the overturning ratio already at this level of ground acceleration. In SLS2 several trains exceed the limits for overturning and/or derailment whereas others are below the limits. The modelling approach of the dynamic trains running directly on the bridge deck prevents reliable results to be calculated when passing the expansion joint. The risk studies (ORA Natural Hazards - CG1000-P-SR-D-P-GE-R5-00-00-00-00-04-C) address whether the trains actually overturn or just lift from the track and falls back.

From the comparison analyses follows that the ADTreS calculated dynamic forces never exceed the amplified RFI static worst case loads. For this reason no further analysis is required.

By the modelling approach special cases as follows are all included in the numerical models:

- Detailed modelling of the expansion joint structure
- Detailed local model of a girder section with all cross beams etc. included

1.9 Analysis main results - Roadway runability

In the broad picture, roadway runability has not been considered nearly as challenging as railway runability. Hence it has been agreed between COWI and EDIN to address the analysis by calculating roadway deck accelerations when the bridge is subject to dynamic wind loads corresponding to SLS1 wind load. I.e. no dynamic vehicles has been modelled as is the case with railway runability. Apart from the fact that roadway runability is not really a key focus area, no dynamic properties are currently available for cars and trucks.

The results show a significant margin between actual calculated accelerations and the limits stated in Design Basis document GCG F.04.01.

2 Introduction

This report covers the scope of and approach to the train runability, safety and comfort study carried out for the Messina Strait Bridge.

The basic scope of the runability study is to verify that the actual trains likely to be operating on the bridge subject to the loads specified in the Design Basis, document GCG.F.04.01 will meet the requirements with regards to runability as well as safety and comfort. These requirements are specified specifically for each limit state (SLS1 and SLS2) and each load combination belonging to these. For the runability and safety assessments the nominal train speed of 120 km/h is multiplied with a factor of 1.2, i.e. 144 km/h, whereas the comfort analysis is run with 120 km/h in accordance with EC/TSI. Requirements stated in the Design Basis are summarized in Section 3, with the subsequent Section 4 summarizing all the individual loads (e.g. wind, seismic, temperature) to be applied simultaneously with the running trains. The relevant load combinations are also described. This leads to a matrix outlining the analyses which have to be completed in order to cover the scope, see Section 6. These three sections hence give an overview of the runability scenarios and of the expected performance levels for both the trains and the bridge.

The data assumptions adopted for the trains (e.g. stiffness, damping, inertial properties as well as geometrical data and drag coefficients) are presented in Section 5.

The subsequent Sections are devoted to the analyses that have been carried out and to the results obtained. The analyses and models can be subdivided in two classes:

- Global analyses carried out with COWI's in-house developed FE-software IBDAS with a train model comprising 7 degrees of freedom (DOF) per bogie. IBDAS allows for direct dynamic train-bridge interaction analysis, i.e. the dynamic trains are interacting directly with the global FE-model utilizing a frequency domain approach. This group of analyses is performed on a global bridge FE model, with a simplified model of the trains in the sense that no modelling of rails and fittings are included. The full number of analysis cases is considered, so as to obtain a broad picture of the train and bridge behaviour and response parameters. Section 7 gives an introduction to the software used and the calculation approach utilized. Section 8 contains an overview of the results obtained in accordance with the analysis programme.
- Local analyses with a refined large number of DOF train model, as well as rail and fittings modelled. The local analysis has been carried out with ADTreS, a software package entirely

developed and validated by the Mechanical Engineering Department of Politecnico di Milano. It is fully dedicated to the mathematical modelling of train-track-bridge interaction. It is based on a multi-body model of the rail vehicle and on a finite element approach for the bridge, which can also include the track. This group of analyses is aimed at the assessment of the local dynamic behaviour of the trains, determining dynamic loadings caused by real trains on rails, fittings and onto the underlying primary stringers and rail box girder, to be compared with the conventional static loads adopted for the design of the same elements. Numerical methods and software is described in Section 9.1. The analyses are carried out on a segment of bridge deck of 300 m in length, whose FE modelling is refined so as to be able to represent effectively the local dynamics of the rail box girder, with the explicit inclusion of primary stringers and diaphragms, together with rails and fittings.

One of the main concerns regarding train runability on the Messina Strait Bridge is the sensitivity to wind loads acting on the bridge and in particular on the trains. Especially empty freight coaches are an issue in this regard. Further the accelerations induced on the trains when passing the expansion joints is an area of interest. Apart from these obvious issues the automatic train-bridge interaction assessment in the analysis models ensure that potential dynamic amplification effects are covered as well.

With two railway tracks on the bridge, six different dynamic trains calibrated from real train types, three structural key positions on the bridge at which the trains will meet and two limit states comprising a total of 6 load combinations the total number of possible analysis combinations amounts roughly 600. This large amount of analysis calls for a very automated and systematic calculation approach.

3 Runability, Safety and Comfort requirements

The performance levels with regards to railway runability have been determined in order to ensure acceptable comfort and safety levels for passengers as well as to minimize the wear on the rail structures. In the following the scope and the actual performance levels are presented. Furthermore the background for the quantification of the two safety criteria is presented.

3.1 Scope

The Design Basis document GCG.F.04.01 outlines the requirements for the operation of trains on the bridge with regards to runability, safety and comfort. The overall distinction between these three groups of requirements reads:

- The runability requirements ensure that various parameters with regards to the motion of the train and the track remain within reasonable limits so as to avoid excessive wear and tear.
- The safety criteria define two hazardous and potentially fatal scenarios which will compromise safety for the train passengers and staff; derailment and overturning.
- The comfort criteria are defined in order to ensure a satisfactory level of the comfort experienced by the train passengers during the crossing of the bridge. This comprises both short duration peak impacts and time averaged impacts.

3.2 Limit states

According to Design Basis GCG.F.04.01 rail runability has to be guaranteed in both SLS1 and SLS2 as opposed to roadway runability which doesn't have to be guaranteed in SLS2. The environmental actions corresponding to SLS1 and SLS2 have been determined on the basis of a 50 and 200 years return period, respectively. However, as discussed in Section 4, the wind speeds defined even in SLS1 exceeds the critical values with regards to overturning of certain train types. Hence the critical wind speed adopted for all train types as the lowest common denominator corresponds to a shorter return period.

3.3 Criteria

The below table states the requirements with regards to runability, safety and comfort as a function of the limit state and load combination in question,

				Runability, Safety and Comfort criteria						
				SLS1			SLS2			
			Combination	2	4	5	2	4	5	
Runability	Train speed		[km/h]	144	144	144	144	144	144	RFI train 1-6
	Equivalent longitudinal slope	One train in one track	[%]	< 1.80	< 1.80	n/a	n/a	n/a	n/a	
		Two trains in two tracks	[%]	< 2.00	< 2.00	n/a	< 2.20	< 2.20	n/a	
	Transverse slope		[%]	< 8.00	< 8.00	n/a	< 10.00	< 10.00	n/a	
	Total rate of change of cant of the track	Short base, bases from 1.3 to 4.5m	[%]	< 0.250	< 0.250	n/a	< 0.400	< 0.400	n/a	
		Short base, bases from 4.5 to 20.0m	[%]	< 0.200	< 0.200	n/a	< 0.275	< 0.275	n/a	
	Non-compensated acceleration		[m/s^2]	< 0.6	< 0.6	n/a	< 0.84	< 0.84	n/a	
	Roll speed		[rad/s]	< 0.033	< 0.033	n/a	< 0.036	< 0.036	n/a	
	Vertical acceleration of the trackbed		[m/s^2]	< 0.70	< 0.70	n/a	< 1.00	< 1.00	n/a	
	Longitudinal acceleration		[m/s^2]	< 2.50	< 2.50	n/a	< 2.50	< 2.50	n/a	
Safety	Train speed		[km/h]	144	144	144	144	144	144	
	Derailment check		Y/P	< 0.8	< 0.8	< 0.8	< 0.8	< 0.8	< 0.8	
	Overturning check		dP/P	< 0.9	< 0.9	< 0.9	< 0.9	< 0.9	< 0.9	
Comfort	Train speed		[km/h]	120	120	n/a	120	120	n/a	
	Comfort index Wz	Passenger trains only		< 2.2	< 2.2	n/a	n/a	n/a	n/a	
	Peak vehicle acceleration	Passenger trains only	[m/s^2]	≤ 2.0	≤ 2.0	n/a	n/a	n/a	n/a	
	RMS transverse acceleration	Passenger trains only	[m/s^2]	< 0.5	< 0.5	n/a	n/a	n/a	n/a	
	RMS vertical acceleration [duration = 2.0 s]	Passenger trains only	[m/s^2]	< 0.75	< 0.75	n/a	n/a	n/a	n/a	
	Recoil	Passenger trains only	[m/s^3]	< 0.25	< 0.25	n/a	< 0.58	< 0.58	n/a	

Table 3-1: Runability, Safety and Comfort criteria.

As seen the vehicle velocity for all runability and safety checks has to be 20% larger than the nominal design speed.

Note that the limits for the acceleration levels in the comfort criteria are calculated with and without a frequency weighting filter calibrated to reflect the comfort as experienced by a human. The Sperling Ride (Wz) frequency filter has been used. As no further information has been provided, the same upper limits are used for both cases according to the above table. The

3.4 Safety

In the following a short introduction to the background of the two safety criteria is given.

3.4.1 Derailment

The derailment verification is based on the variations of the lateral force, Y, and the vertical force, P, at the wheel-rail contact points for the dynamic train-bridge system.

Tests carried out by the ORE C-138 group and further stated by EN14363 have shown that derailment can occur in the extreme case where the Y/P ratio over a distance of more than 2 m is greater than 1.2. For this reason Y/P < 1.2 is usually retained as the criterion for safety against derailment. However, in order to keep a satisfactory safety margin the ratio shall under normal operation not exceed:

$$\frac{Y}{P} < 0.8$$

This criterion applies for both SLS1 and SLS2.

3.4.2 Overturning

The risk of overturning is evaluated by the maximum wheel unloading coefficient, ΔP/P, i.e. the ratio between the static compressive force from the train dead load and the tensile forces generated by lateral forces acting on the train masses as well as the train masses rotation about the longitudinal bridge axis.

Depending on which source is referred to, the overturning criterion is determined differently.

- UIC 518
- Esveld: Modern railway track
- ORE 138
- EN 14067-6, subsections 5.4.3.4 (p. 29) and 5.4.4.1 (p. 29)
- Technical Specifications for Interoperability (TSIs) High Speed Rolling Stock, Annex G

The overturning criterion has been set in the interval ΔP/P < 0.6 - 0.9. The tests carried out by first ERRI, then ORE and finally UIC has mostly been regarding overturning safety when running in tight curves.

Based upon a safety approach the criterion could be argued to be ΔP/P < 0.6. However the runability analysis indicates this may be too conservative as the criterion applies for curves with radius less than 17200 m and not for a straight rail line on a bridge. Analyses carried out by COWI indicate wind induced curves on the bridge with radius at minimum 50000 m. Furthermore this ratio is only valid in the case of static tests on the vehicle, and does not consider the effect dynamic actions, such as track irregularity, wind forces etc and speed limits apply for the bridge, and as such the need for very strict overturning criteria vanishes.

Fiche UIC 518 [R03] and Fiche UIC 518-1 [R04] discuss the dynamic case to yield for a ratio ΔP/P < 0.8, however, still not including the effects of rail irregularities.

The European Standard EN 14067-6, subsections 5.4.3.4 and 5.4.4.1, discuss the limit ratio ΔP/P < 0.9 for trains subjected to cross winds supported by the Technical Specifications for Interoperability (TSIs) High Speed Rolling Stock, Annex G. In order to accommodate for all dynamic actions including rail irregularities and cross wind it has been agreed by discussion in between SdM, Parsons and Eurolink to use the ratio:

$$\frac{\Delta P}{P} < 0.9$$

4 Load Specifications

The design and performance checks of the Bridge shall in general consider at least the actions indicated in Table 4.1-1.

Table 4-1 Design actions.

Par. 1	**Permanent Actions (P)**		
	Structural Self Weight		PP
	Self Weight of non-structural elements		PN
Par. 2	**Variable man-generated actions (Q)**		
	Actions for local sizing of the structural system (strength and deformation at the micro- and meso- level[1])		QL
	Actions for the global sizing of the structural system and for serviceability checks (strength and deformation at the macro-level[2])	Dense variable load	QA
		Rarefied variable load	QR
Par. 3	**Variable natural and environmental actions (V)**		
	Wind action		VV
	Seismic action		VS
	Thermal action		VT
	Water in drainage pipes (rain)		VR
Par. 4	**Accidental actions (A)**		A

The runability, safety and comfort checks will be a subset of the above shown design and performance checks. The subset is discussed in the below. Design and Performance Checks

The analyses carried out include combinations of several loads:

- Environmental loads, i.e. temperature, wind and seismic actions
- Roadway loading in one girder
- Number of trains
- Position of trains
- Train speed.

[1] QL load is applied for road and rail box girders, cross girders, hanger system and hanger groups

[2] QA and QR load is applied for the restraint and support system, main cables and saddles and tie down hangers

The individual loads to be included in the analysis are defined in the Design Basis [2].

The aim for runability, safety and comfort is to provide a full overview of the analyses which has to be carried out in order to cover the content stated in the design and performance check table.

4.1.1 Dead Load Deformation (PP + PN)

Since it is assumed that local deformations in the girder from dead load are eliminated during track laying in construction, it is assumed that the train runs on a track with no dead load deformations

Deformations from 200 years of creep and shrinkage in the concrete piers are not applied.

4.1.2 Roadway and Railway Loading (QR)

The effect of static and dynamic interaction from roadway vehicles on railway locomotives and coaches are verified by static deformations only, since the frequencies of roadway and railway vehicles are much higher that the natural frequencies of the bridge. The latter implies that no dynamic amplification causing the static loads to be above the limits will occur.

This has been proven by use of the local model ADTreS in section 12.6 by comparing the maximum vertical dynamic load for a RFI 5 loaded freight train wagon running at 144 km/h with the so called LM71 train described in RFI instruction “ISTRUZIONI PER LA PROGETTAZIONE E L’ESECUZIONE DEI PONTI FERROVIARI - RFIDTC-ICI-POSPINF001A”.

From the comparison analyses follows that the ADTreS calculated dynamic forces never exceed the amplified RFI static worst case loads. For this reason no further analysis is required.

4.1.3 Wind Action (VV)

The wind forces are applied as static deformations on the bridge structure using the mean wind profile defined in the Design Basis.

Wind forces acting on the train are calculated as:

$$w = \tfrac{1}{2}\rho v^2 C \quad \text{[N/m2]}$$

where

ρ is the air density equal to 1.28 kg/m^3

v is the wind speed acting on the train

C is the drag coefficient

The drag coefficients for wind at an effective attack angle of 90 degrees (lateral) taking the train speed into account have been verified with reference to the following notes,

- "Crosswind action on rail vehicles: Wind tunnel experimental analyses" , Marco Bocciolone, Federico Cheli, Roberto Corradi, Sara Muggiasca, Gisella Tomasini, Journal of Wind Engineering and Industrial Aerodynamics, 96 (2008) 584–610.
- "Wind tunnel tests on train scaled models to investigate the effect of infrastructure scenario", Federico Cheli, Roberto Corradi, Daniele Rocchi, Gisella Tomasini and Emilio Maestrini, BBAA VI International Colloquium on Bluff Bodies Aerodynamics & Applications, Milano, Italy, July, 20-24, 2008.

Table 4.1-2: Drag coefficients, CD, of Real Trains

Train	Type	Vehicle	Available measurements		Similar vehicles		CD lateral	Reference lateral area [m^2]
RFI1	ETR500	loco	ETR500	loco	-	-	0.9568	71.174
	ETR500	coach	ETR500	coach	-	-	0.9839	91.700
RFI2	ETR470	loco	-	-	ETR480	loco	1.1363	88.032
	ETR470	coach	-	-	ETR480	coach	0.9959	93.912
RFI3	E402B	loco	-	-	UICZ1	loco	0.7793	81.700
	"semipilota MD"	coach	UICZ1	loco	-		0.7793	92.204
RFI4	TAF	loco	-	-	UICZ1	loco	0.7793	111.000
	TAF	coach	-	-	UICZ1	coach	0.8610	112.000
RFI5	E402B	loco	-	-	UICZ1	loco	0.7793	81.700
	SHIMMINS	coach	-	-	ETR500	coach	0.9839	39.000
RFI6	E402B	loco	-	-	UICZ1	loco	0.7793	81.700
	HBILLS	coach	-	-	ETR500	coach	0.9839	77.000

The wind speed on the train is smaller than that induced to the bridge deck due to wind screens.

This effect was originally investigated by Politecnico di Milano and reported in Wind Tunnel Test Report "APPROFONDIMENTO DEL COMPORTA-MENTO AERODINAMICO E AEROELASTICO DELL'IMPALCATO III FASE", section 4.2. as part of the Tender Design requirements.

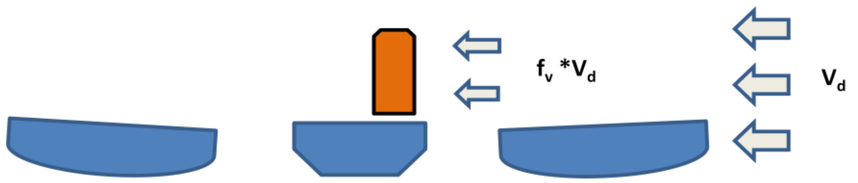

Figure 4-1 Wind reduction due to outer road way girders.

Below the influence from wind perpendicular to the train from varying angles of the bridge, i.e. -4, -2, 0, +2, +4 degrees is illustrated(refer to Wind Tunnel Test by Politecnico di Milano).

The coefficient on the wind has been evaluated by integrating over the train height, using the -2 degrees (3.5%) slope of the bridge, corresponding to the actual transverse slope of the bridge for variable loads.

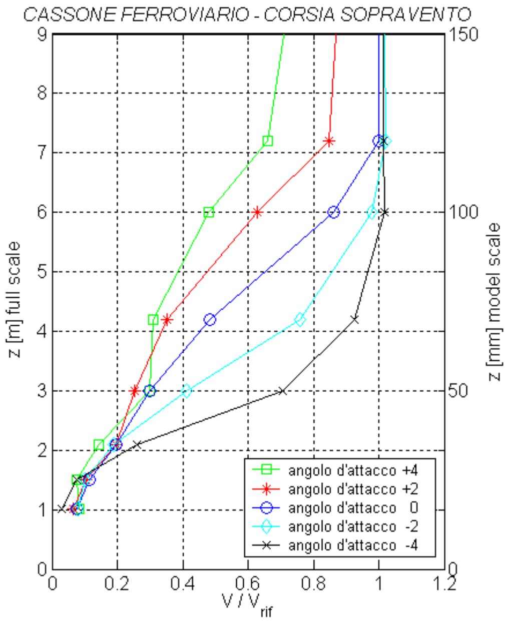

Figure 4-2: Wind reduction factor as function of transverse slope.

The result gives a factor of 0.65 measured in almost 4m elevation. As the height of trains is in the range 3.47m to 4.2m this reduction factor is conservative as it is applied along the entire height, even when taking into consideration that the wind load is related squared to the wind speed.

The analysis cases with wind have been carried out with full dynamic wind load on the structure as well as the train, i.e. the deformation of the structure is evaluated in every time step. The basis for the wind load is a time series describing the wind speed in all three directions to all time steps (10Hz sampling frequency) at 369 points on the bridge, see figure 4-3. A Monte Carlo simulation of the wind field has been utilized. Linear interpolation of the wind speed has been used between the discrete points, and the wind speed applied to the train has been taken as the same as for the railway girder at the actual stationing in a given time step.

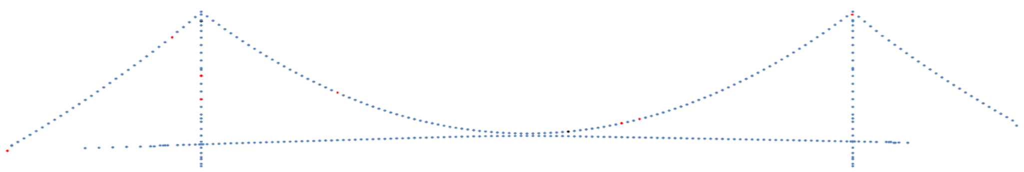

Figure 4-3: Locations on the bridge choosen for the wind time series simulation.

The wind speed experienced by the train is evaluated as the effective wind speed, i.e. wind field speed plus transverse speed of the train itself. The same applies for the bridge structure. Furthermore, the drag, lift and moment coefficients of the bridge are updated in every time step according to the actual deformation of the bridge. The calculation approach for this is the same as for the wind gust analyses carried out.

The time series for the wind speed in SLS1 has a mean wind speed of 44 m/s and a maximum gust wind speed of 58.5 m/s. Figure 4-4 shows the wind speed as a function of time in SLS1 at the centre of the main span. Note that the analyses carried out with a reduced wind speed due to violation of the overturning criteria are based on a uniform scalar scaling of the SLS1 wind time series.

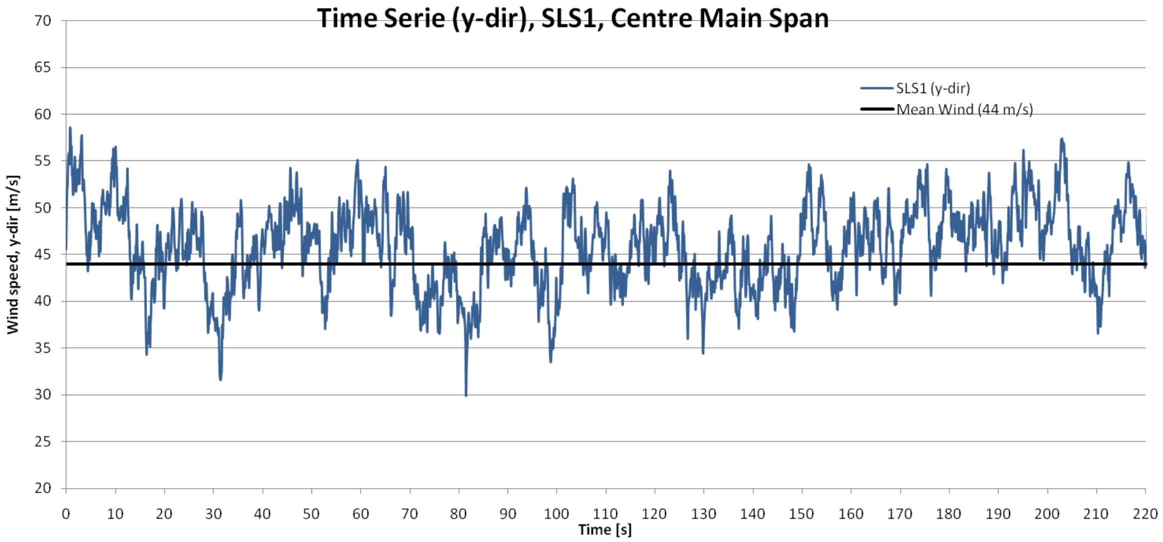

Figure 4-4: Wind speed history for SLS1.

The time series for the wind speed in SLS2 has a mean wind speed of 47 m/s and a maximum gust wind speed of 62.1 m/s. Figure 4-5 shows the wind speed as a function of time in SLS2 at the centre of the main span.

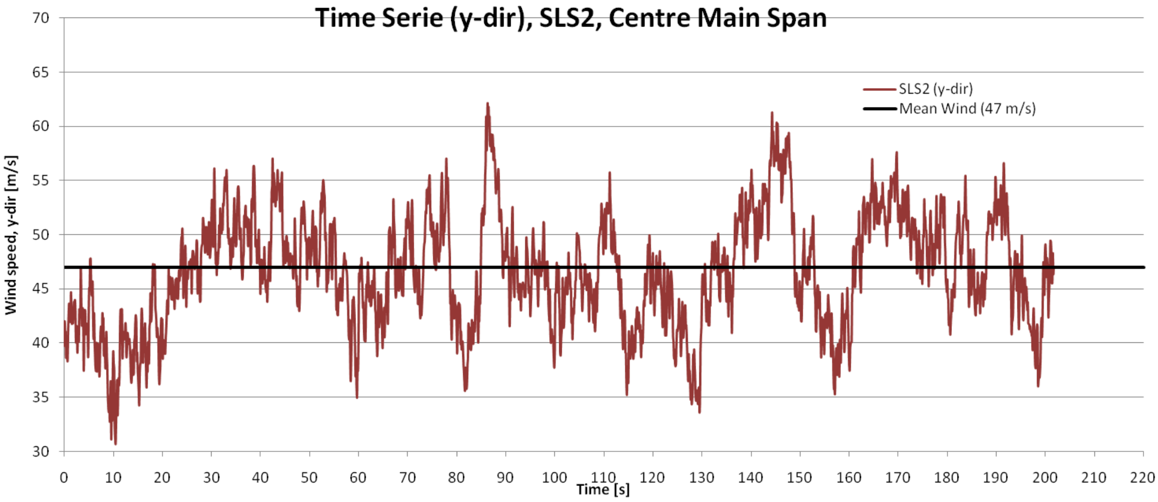

Figure 4-5: Wind speed history for SLS2.

Both time series for wind have been generated utilizing the Monte Carlo simulation method.

Convergence studies have revealed that the parameters searched for in the runability, safety and comfort study become practically independent of the number of eigen modes included in the analysis when exceeding 800 modes. Hence, 800 modes have been used in the analyses including wind load.

It should be emphasized that no connection exists between the individual bogies apart from a fixed spacing. Hence the model is not capable of modelling the twisting effect from an overturning bogie on neighbouring wagons. And as such an overturning wagon cannot benefit from possibly restraint forces transferred through the connection to the neighbouring wagons. The approach, however, is obviously conservative.

4.1.4 Seismic Action (VS)

Seismic actions have been applied by inducing a total of 8 time series of accelerations specified for each direction on the supported nodes in the global FE-model. Each of these 8 time series represent a distinct simulated earth quake. The available time series correspond to ULS earth quakes defined with a peak ground acceleration of 5.7 m/s^2. To convert the time series for application in SLS1 and SLS2, which are only relevant in the runability study, a simple scaling has been carried out, i.e

$$[A_{SLS1}] = \frac{1.2}{5.7}\,[A_{ULS}]$$

$$[A_{SLS2}] = \frac{2.6}{5.7}\,[A_{ULS}]$$

The accelerations for the individual directions have been scaled in accordance with the common practise on the project, ref. IBDAS report CG1000-P-RG-D-P-SV--00-00-00-00-01-B. This means that any of the three directions can be chosen as dominating according to the below shown scaling.

Table 4-2: Adjustment factors.

Direction	Adjustment factor
1 (dominating)	1.00
2	0.80
3	0.75

However, as the obvious most critical direction of accelerations for trains in terms of overturning and derailment is transverse, only this directing has been analysed as the dominating direction.

The seismic loading has proved to be most adverse when the earth quake peaks at the time when the trains are crossing the pylon region. This is expectable as the highly increased stiffness in this area will tend to induce significantly larger accelerations on the railway girder.

The actual deformations, velocities and accelerations transferred to the train tracks is solved through a modal analysis approach including 1000 eigen modes as opposed to the load combinations not containing seismic loading which are based on only 500 eigen modes without wind load and 800 eigen modes with wind load. A sensitivity study carried out with IBDAS shows this is sufficient for the global model.

The below figure shows the acceleration in the three directions as well as total for a SLS2 earth quake (E3-02). The figure also shows at what time the first and the last axle in each of the six real trains passes the Sicily pylon.

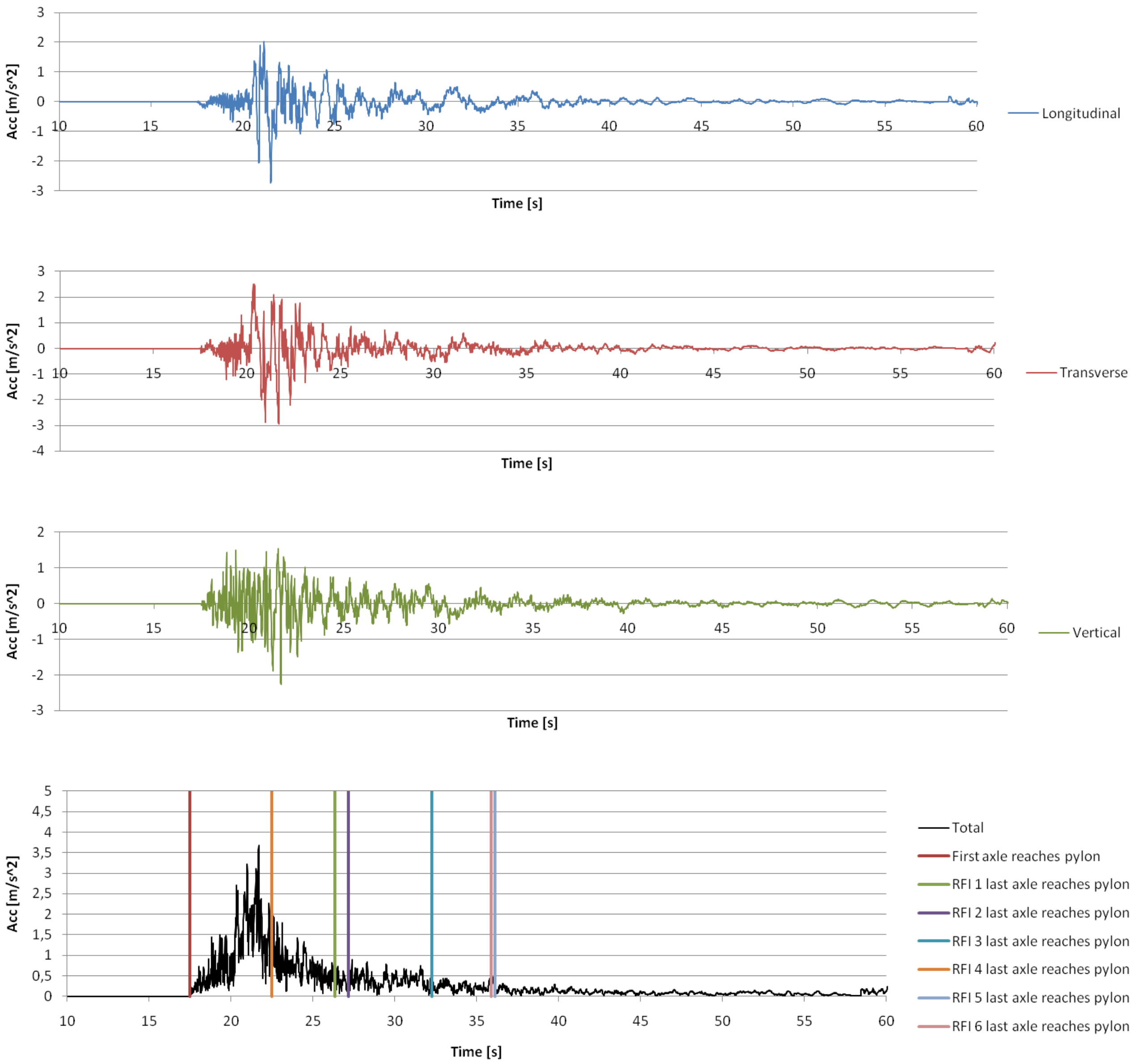

Figure 4-6: Time record of SLS2 earth quake.

4.1.5 Temperature Action (VT)

Temperature variation is applied as static deformations as described in doc. PG 2R B0-001 N03 p1 (GLOBAL MODEL) [3]. Static deformations from either uniform or non-uniform distributed temperature change are applied.

4.2 Load combinations

The below shown table outlines the loads for the individual load combinations. Note, that the wind loads in load combination 4 are defined as 10 minute average wind speeds.

Figure 4-6: Load combinations relevant for the runability study.

SLS1 / SLS2 load combinations - key parameters for use with runability study												
SLS1 / SLS2	Dead load				Variable man-generated loads		Variable natural and environmental loads					
Combination	PP Structural self weight		PN Self weight of non-structural elements		QR Road and rail traffic loads		VV Wind load		VS Seismic load		VT Thermal load	
2	As calculated geometrically	1.0	Includes all secondary equipment	1.0	Road: Most heavily loaded lane: 3.75 kN/m One of the other two lanes: 1.25 kN/m Braking = 1/10 vertical Rail: One dynamic RFI train in each track	1.0					Reference daily air temperatures: Summer: 22.5 °C - 41.0 °C Winter: -0.5 °C - 12.0 °C	0 / 1.0
4	As calculated geometrically	1.0	Includes all secondary equipment	1.0	Road: Most heavily loaded lane: 3.75 kN/m One of the other two lanes: 1.25 kN/m Braking = 1/10 vertical Rail: One dynamic RFI train in each track	1.0	Level of velocity: **SLS1:** 44 m/s **SLS2:** 47 m/s	1.0			Reference daily air temperatures: Summer: 22.5 °C - 41.0 °C Winter: -0.5 °C - 12.0 °C	0 / 1.0
5	As calculated geometrically	1.0	Includes all secondary equipment	1.0	Road: Most heavily loaded lane: 3.75 kN/m One of the other two lanes: 1.25 kN/m Braking = 1/10 vertical Rail: One dynamic RFI train in each track	1.0			Seismic frequency response spectrum **SLS1:** Peak ground acc.: 1.2 m/s^2 **SLS2:** Peak ground acc.: 2.6 m/s^2	1.0	Reference daily air temperatures: Summer: 22.5 °C - 41.0 °C Winter: -0.5 °C - 12.0 °C	0 / 1.0

5 Real Train modelling

In order to simulate the train vehicles running on the global FE-model including dynamic effects, several properties with regards to mass, stiffness, damping, mass inertial moments etc. have to be determined. Further, when wind load is acting on the vehicles themselves, aerodynamic coefficients becomes crucial as well in addition to parameters describing centre of mass locations. Train parameters have been adopted from document DT.ISP.F.E.R3.001 where ever possible. The remaining parameters have been confirmed and agreed with SdM.

5.1 IBDAS model of dynamic train

The trains are modelled by means of a 7 DOF/bogie model containing two separate masses: Bogie mass and coach mass. The bogie mass contains four DOF: Vertical and horizontal lateral translation as well as rolling and pitching. The coach mass contains the same two translational DOF in addition to rolling. The contact interface between wheels and the rails is modelled as a fully stiff connection in the IBDAS model. Hence no representative wheel/rail contact forces can be computed. Due to this modelling approach negative wheel forces, i.e. tensile forces, can occur if the lateral moments exceed the compressive force from the train dead load. As such results are reliably only when the wheel/rail contact force is compressive.

Between the wheel/rail rail contact points and the bogie mass the primary suspension is modelled by means of a vertical as well as lateral spring/damper system. An identical composition exists for the secondary suspension between the bogie and the coach mass. All springs and dampers in the model are characterized by constant coefficients, i.e. there's a fully linear relation between displacement/velocity and force.

The figure below provides a diagram overview of the dynamic model for one bogie.

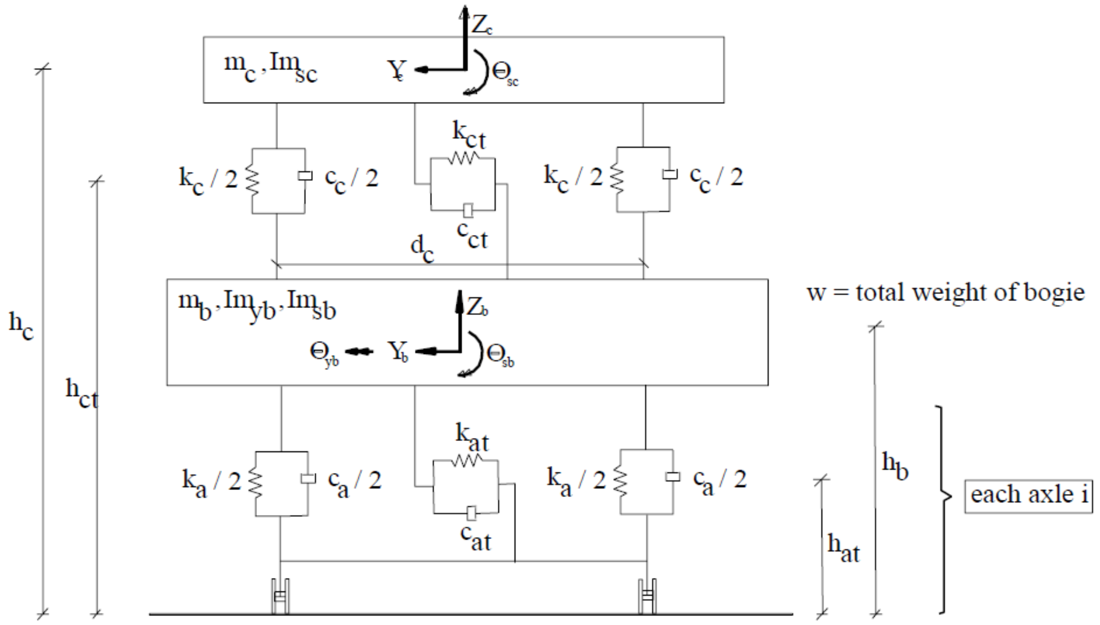

Figure 5-1: Schematization of the dynamic representation of a train bogie in IBDAS.

5.2 ADTreS model of dynamic train

The rail vehicle model is based on a multi-body approach which accounts for both vertical and lateral dynamics of the train-structure interaction. Each vehicle consists of seven rigid bodies (i.e., car body, two bogies, and four wheelsets) connected together through primary and secondary suspensions. Linear and nonlinear elastic and damping elements are used for the suspensions schematization. The car body and the bogies are taken as having 5 degrees of freedom each: vertical and lateral translational rigid body motions, and yaw, pitch, and roll rigid body rotations. Each wheelset is modelled as a 2 degrees of freedom system which includes lateral translational motion and yaw rotation. The vertical translational motion of the wheelset is a variable which depends on the relative lateral displacement between rail and wheelset in a nonlinear fashion. Bending and torsional deformable modes can also be modelled, but they are not included here.

The full multi-body model of the vehicle consists of a total of 23 degrees of freedom, where the longitudinal motion is given by selecting the vehicle speed. The lateral, vertical displacement and the roll rotation of the whole railway is computed as the superposition of rail irregularity and deformability. The rail lateral motion is taken into account through the so called term “Gravitational Stiffness“ [15].

Rail flexibility and wheel-rail contact profiles are introduced in the model according to the standard specifications described in UNI60 and ORE S1002 for the rail and wheel profiles, respectively, assuming mono-contact conditions. As such, the computation of wheel-rail contact forces is exploited to perform the vehicle-structure interaction [13].

Figure 9-1shows the schematic of the vehicle multi-body model which consists of car body, bogies and wheelsets. Stiffness and damping parameters of primary and secondary suspensions are set according to the standard specifications of real trains RFI [1, 12, 13, 14].

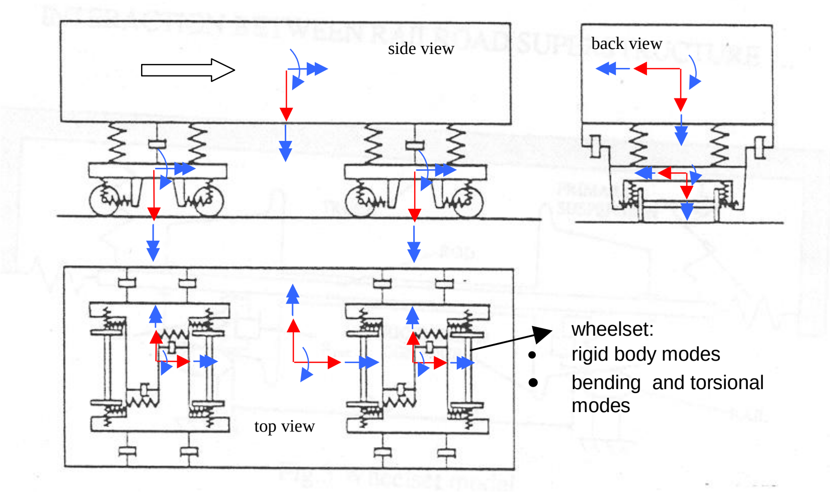

Figure 5-2: Schematic of the multi-body model of the vehicle: degrees of freedom of car body and bogies are indicated

5.3 Train properties

The below table states the full set of parameters describing the six train types included as informed by the Design Basis (2) including later corrections received from SdM.

			Passenger trains								Freight trains			
			RFI 1		RFI 2		RFI 3		RFI 4		RFI 5		RFI 6	
			Locomotive	Coach	Locomotive	Coach	Locomotive	Coach	Locomotive	Coach	Locomotive	Coach	Locomotive	Coach
	Coach mass (half of full coach mass)	kg	27420	17116	21736	18800	25920	13250	28550	24648	25920	45000	25920	8907
	Damping coefficient of suspended coach system	MNs/m	0.1196	0.0624	0.0686	0.0687	0.1016	0.0730	0.056	0.056	0.1016	0.2000	0.1016	0.2000
	Spring stiffness of suspended coach system	MN/m	1.776	0.788	0.924	0.926	2.640	1.288	1.44	1.620	2.640	20	2.640	20
	Bogie mass	kg	3150	2875	2455	2587	12800	2950	6430	2817	12800	2100	12800	2100
	Mass inertia moment of bogie about s axis	kgm^2	2420	1740	1552	1589	3320	1940	2360	1720	3320	1200	3320	1200
	Mass inertia moment of bogie about y axis	kgm^2	5168	2789	1655	1694	10371	1660	6740	2686	10371	925	10371	925
	Damping coefficient of each suspended bogie axle	MNs/m	0.0294	0.0206	0.0196	0.0250	0.0442	0.0032	0.0190	0.0060	0.0442	0.0484	0.0442	0.0484
	Spring stiffness of each suspended bogie axle	MN/m	4.670	1.6150	2.270	2.270	4.570	1.665	3.70	1.900	4.570	4.840	4.570	4.840
	Total weight of bogie (bogie, wheels, half coach)	MN	0.341	0.228	0.278	0.250	0.445	0.192	0.401	0.311	0.445	0.497	0.445	0.136
	Length between axles in bogie	m	3	3	2.7	2.7	2.85	2.4	2.75	2.55	2.85	1.80	2.85	1.80
	Number og bogie axles		2	2	2	2	2	2	2	2	2	2	2	2
	Length of train	m	353		386		591		200		744		735	
	Number of coaches and locomotives		14		15		23		8		59		34	
	Bogie distances between coaches/locomotives	m	4.28	3.50	3.00	3.00	4.25	3.50	3.65	2.30	4.25	2.50	4.25	2.50
	Bogie distance in coach/locomotive	m	11.45	19	19	19	10.45	18	19	19	10.45	7.00	10.45	15.40
	Height of center of gravity of coach	m	*1.5*	*1.5*	*1.464*	*1.5*	*1.924*	*1.7*	*2.145*	*1.89*	*1.924*	*1.5*	*1.924*	*1.56*
	Height of center of gravity of bogie	m	*0.65*	*0.544*	*0.393*	*0.39*	*0.847*	*0.6*	*0.55*	*0.46*	*0.847*	*0.46*	*0.847*	*0.46*
	Height of center of gravity of wheels	m	*0.52*	*0.445*	*0.445*	*0.585*	*0.625*	*0.43*	*0.55*	*0.46*	*0.625*	*0.44*	*0.625*	*0.44*
	Mass of wheels	kg	*1765*	*1425*	*1824*	*1824*	*2882*	*1510*	*2560*	*1809*	*2882*	*1278*	*2882*	*1278*
	Height of center of gravity (weighted average)	m	1.320	1.264	1.236	1.236	1.446	1.332	1.686	1.594	1.446	2.33	1.446	1.73
	Height of center of wind load	m	1.85	1.85	1.74	1.74	2.03	2.03	2.10	2.10	2.03	1.90	2.03	1.90
	Drag coefficient		0.96	0.98	1.14	1	0.78	0.78	0.78	0.86	0.78	0.98	0.78	0.98
	Height of coach (for wind load evaluation)	m	3.7	3.7	3.47	3.47	4.05	4.05	4.2	4.2	4.05	3.8	4.05	3.8
Additional 7DOF parameters	Mass intertia moment about S-axis of coach	kgm^2	32600	27350	34550	30147	27410	23500	34800	27500	27410	52605	27410	19177
	Transversal spring stiffness of suspended coach system	MN/m	0.42	0.2352	0.24	0.226	0.428	0.328	0.24	0.27	0.428	20	0.428	20
	Transversal damping coef. of suspended coach system	MNs/m	0.0392	0.0392	0.0344	0.0343	0.065	0.028	0.0526	0.0526	0.065	0.2	0.065	0.2
	Transversal spring stiffness of suspended axle	MN/m	41.8	17	23.7	23	53.6	5.88	3.1	8.3	53.6	3.42	53.6	3.42
	Transversal damping coef. of suspended axle	MNs/m	0	0	0	0	0	0	0	0	0	0	0	0
	Height of axle transversal suspension above top of rail	m	0.52	0.445	0.445	0.585	0.625	0.43	0.55	0.46	0.625	0.44	0.625	0.44
	Height of coach transversal suspension above top of rail	m	0.95	0.76	0.612	0.63	1.4315	0.661	0.9425	0.845	1.4315	0.5	1.4315	0.56
	Height of centre of gravity of bogie above top of rail	m	0.65	0.544	0.393	0.393	0.847	0.6	0.55	0.46	0.847	0.46	0.847	0.46
	Height of centre of gravity of coach above top of rail	m	1.5	1.5	1.464	1.5	1.924	1.7	2.145	1.89	1.924	1.5	1.924	1.56
	Transverse horizontal distance between the two vertical springs of the coach	m	2.05	2	2	2	2.1	2	1.94	2	2.1	2	2.1	2

Figure 5-3: Train properties.

6 Analysis matrix

With six different real trains operating alone or two at a time on the bridge, 27 combinations of train types can be established. For each of these, three different meeting points have been investigated: Middle of bridge, near a pylon and at an expansion joint. However, for the load cases with seismic loading only the six load cases with each train type running alone on the bridge has been considered as the influence from other trains on safety with regards to seismic loading is negligibly.

Furthermore, each load combination can include thermal loading. As IBDAS cannot automatically determine whether temperature load is adverse or relieving in connection with dynamic train models, combinations have to be run with and without temperature. However, once again the seismic load combinations aren't run with temperature load as the only focus in these is safety.

As covered in the above sections, the limit for transverse wind speed in terms of violation of the overturning criterioen has been found to be in the order of magnitude of the mean wind speed corresponding to SLS1. As such, it doesn't make sense to increase the wind speed beyond this level in SLS2. Hence load combination 4 in SLS2 has been cancelled.

As load combination 2 only contains thermal loading this one has only been analysed in SLS1.

All criteria with regards to runability and safety are investigated at train speeds 20% above the nominal speed limit, i.e. 120 kph x 1.20 = 144 kph. The comfort criteria are investigated at 120 kph.

The below shown matrix presents a graphical overview of the total analysis programme analysed in accordance with the above.

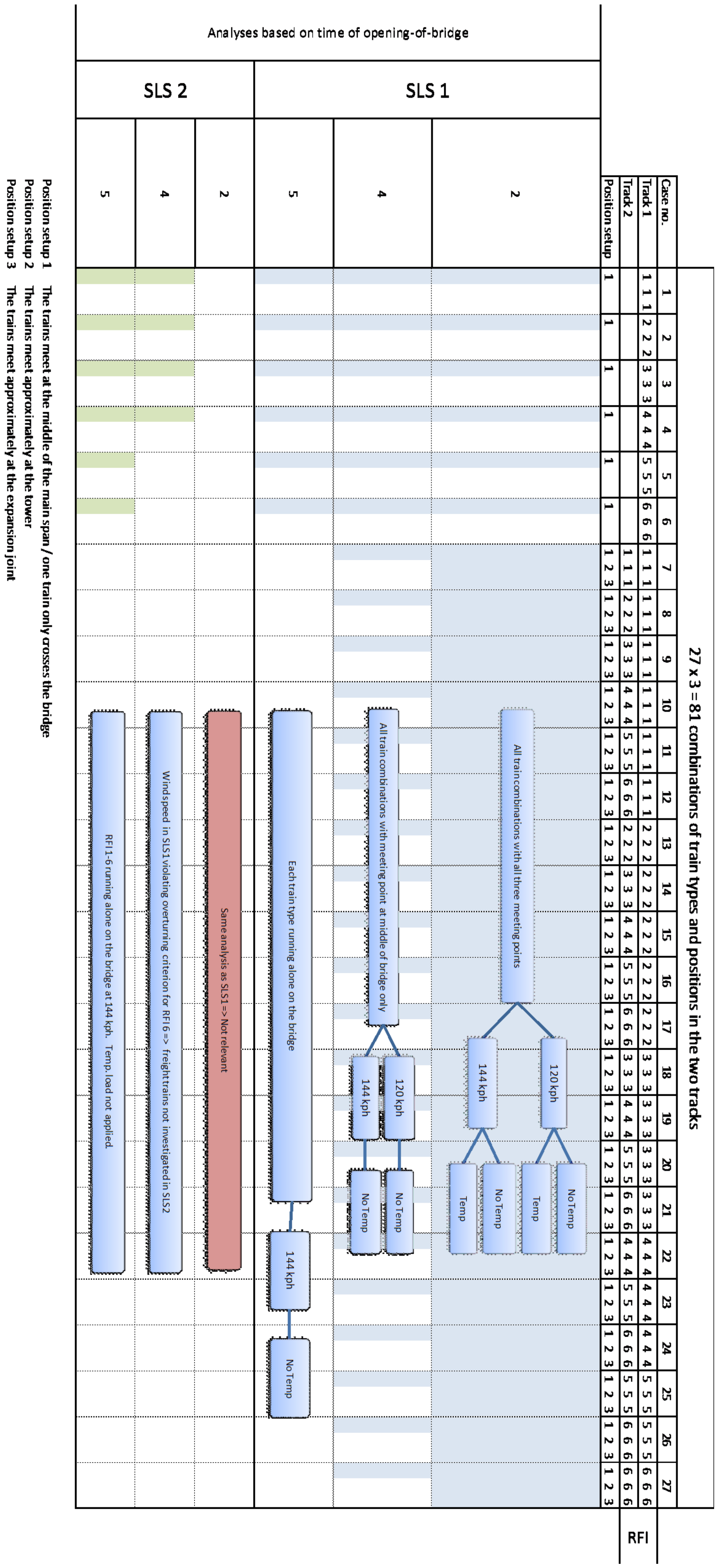

Figure 6-1: Analysis matrix.

7 Introduction to the IBDAS model

For a full description of the global FE-model developed in IBDAS, see. Doc No. CG1000-P-RG-D-P-SV-00-00-00-00-00-01 "*Global IBDAS Model, Description*"

7.1 IBDAS dynamic train modelling

A comfort module is available within the standard IBDAS analysis package offering dynamic train modelling to be made on top of an existing FE-model. In the following the main calculation approach is outlined whereas a description of parameters defining the dynamic vehicles is given in Section 5.

The overall principle for the dynamic calculations is a modal analysis approach, i.e. the response is computed as a linear combination of a number of eigen modes chosen by the modeller. Each eigen mode describes the displacement of every degree of freedom in the model associated with the eigen mode in question. The amplitude of each eigen mode at a given time step is introduced through the so called modal coordinates which are a scalar quantity dependent on time, only. Exploiting the orthogonality properties of the eigen modes the equations of motion decouple when expressed in an m-dimensional space spanned by the mode shapes instead of a three dimensional space spanned by physical axes. Hence a system of n DOF can be solved as if n systems of only one DOF. The outcome is then the modal coordinates which should be multiplied with the corresponding eigen modes. This can then be transformed back to geometrical coordinates, i.e. physical DOF.

When the global FE-model has been expressed by means of the modal approach, it no longer contains n physical DOF but m modal DOF, where $m \leq n$. The dynamic vehicles are then introduced by utilizing the condition that each axle is coupled stiff to the railway track, i.e. the surface of the bridge model. The movements of the deck are described for any position at any time step by means of the modal coordinates and mode shapes. Via this condition the vehicles couple to the bridge and introduces a number of additional DOF corresponding to the total number of DOF for the trains, in this case 7 DOF x number of bogies. In this manner the mutual interaction between bridge and trains is established.

In IBDAS the system of equations of motion to be solved are expressed as first order differential equations where all second derivatives, i.e. accelerations, of the DOF have been defined as functions of all other variables. The system of first order differential equations is then solved by means of a Runge-Kutta method which automatically subdivides each time step as necessary to obtain an accurate solution.

The dynamic interaction of the bridge and train will depend upon stiffness's, mass and damping properties of the two parts. The global IBDAS FE-model includes full dynamic interaction between bridge and trains.

7.2 Output

The different criteria to be investigated in connection with runability, safety and comfort assessment are provided as a direct output in the result files generated by IBDAS. Hence the user need not to perform tedious data processing of large history files in order to compute the relevant quantities. Similarly, IBDAS can automatically report envelope extreme quantities of a full time series.

7.3 IBDAS Bridge Model

The IBDAS model has been refined to such detail that all static and dynamic effects are represented with sufficient accuracy for the analyses.

GLOBAL AND LOCAL DEFLECTIONS

The deformation of the rail subject to a running wheel set may arise due to the following reasons:

- global deflection of the bridge girder due to train loads
- local deflection of the bridge girder and deck slab
- deflection of the bridge girder due to temperature effects
- deflection of the piers due to long term creep and shrinkage effects
- deflection of the bridge girder due to transverse and longitudinal wind
- deflections and accelerations due to seismic actions
- local deformations at expansion joints

- Wheel/rail interaction in relation to mode shapes

7.3.1 14 DOF Approach

For the IBDAS model using the 14 DOF train model direct checks can be made for runability, comfort, and safety requirements.

These requirements include:

- Transverse slope
- Rate of change of cant
- Non-compensated acceleration
- Recoil
- Roll speed
- Vertical acceleration of the suspended coach
- Vertical acceleration of the trackbed
- Derailment and overturning check.

Each vehicle (coach or locomotive) is modelled by two 7 DOF bogies, i.e. 14 DOF per vehicle as shown in figure 2.

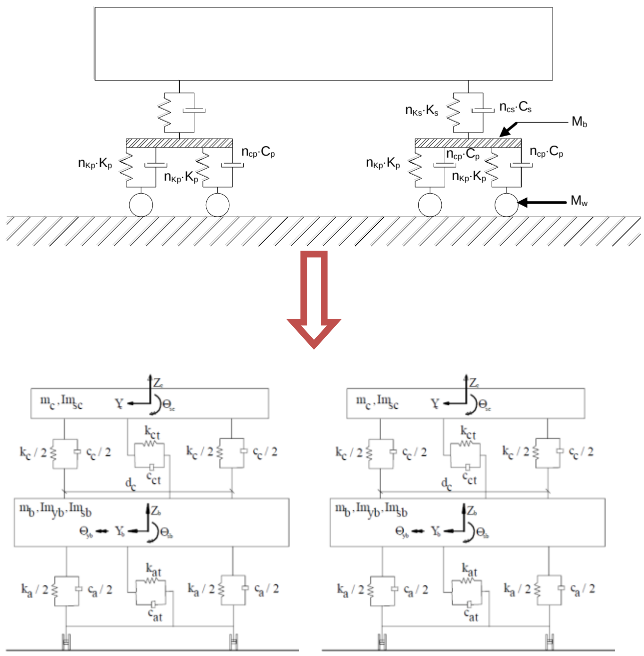

Figure 7-1 Dynamic coach or locomotive model for schematic bogie support. Simplified model (7DOF, Zc, Zb,Θy and Θs) spatial bogie model (bogie with 2 out of 4 wheels shown) corresponding to each bogie support is shown below.

7.3.1.1 Equivalent mass, stiffness, and damping

The 14 DOF vehicles are described in 3 dimensions by a bogie and coach mass m_b and m_c, a primary and secondary suspension defined by the vertical springs k_a and k_c and the dashpots c_a and c_c at each bogie in addition to the horizontal lateral springs and dashpots k_{at}, k_{ct}, c_{at}, c_{ct}. The coach mass is equal to half the mass of the real vehicle coach mass. The spring and dashpot parameters are obtained from the primary and secondary springs and dashpots specified in DT.ISP.F.E.R3.001 where p and s refer to the primary and secondary suspension system of the vehicle.

For each bogie the model calculates the vertical and horizontal lateral deflection of the bogie and coach and the roll and pitch of the bogie as well as the roll of the coach.

For the 14 DOF model the envelope for the true dynamic variations of the vertical and lateral wheel forces P and Y is calculated, while the lateral wind force component contributing to Y is calculated as a static wind force.

8 Global IBDAS Analysis Results

In the following the main conclusions from the analysis programme performed in IBDAS is outlined. A distinction will be made corresponding to limit states. Only results for each of the six RFI train types running alone at the bridge will be shown as interaction between oncoming trains has proved marginal. The remaining results including two trains running at the bridge simultaneously can be found in section 13 (Appendix 1).

Furthermore the roadway runability levels is briefly addressed.

8.1 Load combination 2, No environmental loads

In load combination two neither wind nor seismic loading apply. Hence the results belonging to this load combination provides an overview of the level of performance stemming from the dynamic interaction between structure and vehicle alone.

Below the results for the case with no thermal loading is presented.

RFI type	Train speed [km/h]	Transverse slope [m/m]	Change of cant [m/m]	Non-compensated lateral acc. [m/s^2]	Roll speed [rad/s]	Derailment ratio incl. wind [-]	Derailment ratio excl. wind [-]	Overturning ratio incl. wind [-]	Sperling Ride index, Wz (unweighted) [-]	Sperling Ride index, Wz (weighted) [-]	Peak vertical acc. (unweighted) [m/s^2]	Peak vertical acc. (weighted) [m/s^2]	RMS vertical acc. (2.0 s.) (unweighted) [m/s^2]	RMS vertical acc. (2.0 s.) (weighted) [m/s^2]	Recoil (based on 2.0 s. RMS coach acc.) [m/s^3]	Vertical peak acc., trackbed (unweighted) [m/s^2]	Vertical peak acc., trackbed (weighted) [m/s^2]
		0.08	0.0025	0.6	0.033	0.8	0.8	0.9	2.2	2.2	2.00	2.00	0.75	0.75	0.25	0.70	0.70
1	144	0.0095	0.0000	0.134	0.006	0.105	0.105	0.192								0.040	0.025
1	120								0.61	0.51	1.37	0.84	0.60	0.33	0.84		
2	144	0.0098	0.0001	0.138	0.009	0.068	0.068	0.119								0.038	0.018
2	120								0.61	0.52	1.40	0.87	0.60	0.34	0.87		
3	144	0.0099	0.0001	0.139	0.017	0.100	0.100	0.241								0.050	0.033
3	120								0.63	0.55	1.84	1.22	0.77	0.51	1.22		
4	144	0.0094	0.0000	0.132	0.003	0.022	0.022	0.195								0.060	0.043
4	120								0.70	0.60	1.81	1.07	0.91	0.54	0.97		
5	144	0.0201	0.0001	0.281	0.019	0.124	0.124	0.284								0.110	0.043
6	144	0.0099	0.0001	0.138	0.016	0.097	0.097	0.450								0.041	0.027

Table 8-1: Load combination 2 results.

As seen the unweighted RMS vertical acceleration is violated for RFI 3 and especially RFI 4. The latter is a double decker train type and hence contains a rather stiff suspension in order to prevent excessive dynamic movements. As such this minor violation is not a matter of concern as the weighted RMS values are still below the limits. In addition to this, recoil, which is considered as a comfort criterion and hence applies only for passenger trains, is exceeded considerably. However, the low values of the Sperling Ride comfort index implies that passenger comfort is kept at a very satisfactory level.

8.2 Load combination 4, Wind load

Load combination 4 introduces lateral horizontal wind load on the structure as well as the moving vehicles. The wind load on the bridge as well as the train is applied as a fully dynamic wind load based on time series describing the wind speed in all three directions to all time steps at 369 locations on the bridge. Linear interpolation is used between these discrete points and the train is subjected to the same wind speed as the railway girder (before reduction due to wind screens). The transverse velocity of the train and bridge is taken into account to find the effective wind speed, and the drag, lift and moment coefficients for the bridge are continuously updated according to the actual deformation of the structure.

In order to put the dynamic analyses in load combination 4 into perspective a very simplified static approach has been carried out, see below. The outcome of this study serves to give an idea of to which extend the results from the full dynamic analysis is dominated by effects due to inertia and damping.

8.2.1 Static calculation approach

By a simple static equilibrium approach for a train with mass m subjected to a wind load of magnitude P_{wind} attacking $h/2$ from the top of the rail and the point of overturning defined as the magnitude of the wind load P_{wind} causing the compression force from the dead load to be equal to the tension force from the overturning moment introduced by the wind load, the critical wind speed can be found when assuming the wind pressure is constant over the height and the length of the train:

$$v_{crit} = \sqrt{\frac{0.9mw}{\rho C_D \alpha^2 l h_1 \left(\frac{h_1}{2} + h_2\right)}}$$

Note that the factor 0.9 in the numerator is introduced in order to calculate the critical wind speed in accordance with the overturning criterion of dP/P < 0.9.

The table below states the values used for the different variables in the formula for critical wind speed for each of the six real trains specified. These properties are identical to the ones used in the dynamic analysis carried out in IBDAS. Note that values from coaches/wagons only have been used, i.e. the locomotives are not investigated in the static approach.

Air density, rho [kg/m3]	1.28
Wind reduction factor, alpha [-]	0.65

	mass [N]	h2 [m]	w [m]	l [m]	C_d [-]	h1 [m]
RFI 1	456820	0.9	1.51	25.2	0.98	3.7
RFI 2	500700	0.9	1.51	25.7	1.00	3.47
RFI 3	384400	0.9	1.51	25.7	0.78	4.05
RFI 4	621660	0.9	1.51	25	0.86	4.2
RFI 5	993120	0.9	1.51	12.6	0.98	3.8
RFI 6	271260	0.9	1.51	21.6	0.98	3.8

With the formula for the critical wind speed quantified the graphs below can be established. As seen the critical wind speed is shown as a function of the height of the coach h_1. This makes it easy to see how close a given train type is to the limit in SLS1 and SLS2 containing a gust wind speed of 58.5 and 62.1 m/s, respectively. However, the dashed lines mark the actual heights with the colour scheme corresponding to the graphs for the critical wind speed. Hence, the intersection points mark the critical static wind speed for the train type in question. These intersection points should be located above the SLS1 and SLS2 gust wind speeds in order not to violate the overturning criterion in a static fashion.

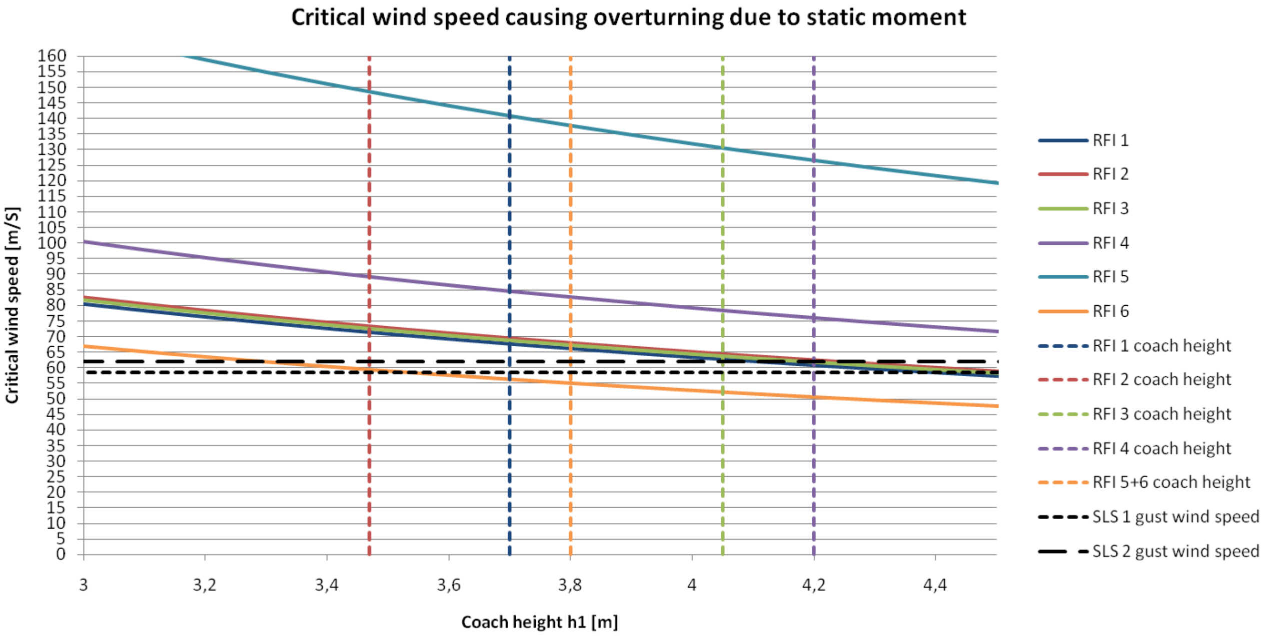

Figure 8-1: Critical static wind speeds.

The main conclusions from the static approach are as follows:

- RFI 3 is among the passenger trains especially sensitive to transverse wind load and will violate the overturning criterion at static wind speeds about 60-65 m/s
- RFI 6 (empty freight train) will violate the overturning criterion around 55 m/s static wind speed.

All stated critical wind speeds are before reduction of the wind screens and hence not the ones the trains will actually be subjected to. In this case they will be only 65% of the unreduced wind speeds due to the wind screens.

Note that this static approach has not been determinate for the outcome of the overturning simulations. It only serves a comparison to the full dynamic analyses in order to outline to which extend the dynamics dominate the results.

8.2.2 Dynamic calculation approach

Analyses utilizing COWI's analysis system IBDAS with the full dynamic wind load approach, indicate that **overturning requirements can be met for all six RFI trains if the 10 min average**

design wind speed for train runability in specific is lowered to 38 m/s corresponding to 50.5 m/s gust wind speed when scaling the Monte Carlo simulated SLS1 wind time series with a factor (38 m/s) / (44 m/s) = 0.864. The stated critical limit corresponds to an effective overturning criterion of *dP/P* ≤ 0.9. The governing train type is the empty freight train, RFI 6.

If it is chosen to distinguish between freight and passenger trains the passenger trains can operate in wind speeds corresponding to a SLS 2 wind time series (47 m/s 10 min mean wind speed, 62.1 m/s gust wind speed). As for SLS 1, the wind time series belonging to SLS 2 has been generated using the Monte Carlo simulation method. The governing train type among the passenger trains is RFI 3.

By risk analysis it has been foreseen that the return period of 38 m/s 10 min mean wind speed will be 6 years while 47 m/s 10 min mean wind corresponds to a return period of 200 years.

Below the peak values of the runability, safety and comfort criteria are stated for each of the six real train types in load combination 4 (no thermal load). Furthermore a series of history plots are subsequently presented to illustrate the spatial variation of selected parameters. These plots does not necessarily represent the worst bogie or axle in the train with regards to the parameter in question, but serves to provide an understanding of the principal variation across the bridge.

The below table shows the calculated runability and safety properties for RFI 1 to 6 when applying an unscaled SLS1 wind time series. As seen the empty freight train (RFI 6) exceeds 1 in overturning ratio. Hence the overall critical threshold wind speed for all train types has to be lowered. Apart from this, the roll speed criterion is violated considerably when the trains are exposed to this heavy dynamic wind load.

Limit state	Load combination	Train combination case	Track no.	RFI type	Meeting point	Train speed [km/h]	Wind load type	Mean wind speed [m/s]	Maximum gust wind speed in time series [m/s]	Thermal load	Seismic peak ground acc. [m/s^2]	Transverse slope [m/m]	Change of cant [m/m]	Non-compensated lateral acc. [m/s^2]	Roll speed [rad/s]	Derailment ratio [-]	Overturning ratio [-]	Vertical peak acc., trackbed (unweighted) [m/s^2]	Vertical peak acc., trackbed (weighted) [m/s^2]
Limit												0.08	0.0025	0.6	0.033	0.8	0.9	0.70	0.70
SLS1	4	1	1	1	One train only	144	Dynamic time series	44	58.5	No	0.0	0.0161	0.0001	0.226	0.044	0.536	0.529	1.383	0.924
SLS1	4	2	1	2	One train only	144	Dynamic time series	44	58.5	No	0.0	0.0165	0.0001	0.231	0.085	0.655	0.538	8.777	2.357
SLS1	4	3	1	3	One train only	144	Dynamic time series	44	58.5	No	0.0	0.0181	0.0001	0.254	0.107	0.511	0.684	1.383	0.932
SLS1	4	4	1	4	One train only	144	Dynamic time series	44	58.5	No	0.0	0.0162	0.0001	0.227	0.034	0.208	0.471	1.359	0.881
SLS1	4	5	1	5	One train only	144	Dynamic time series	44	58.5	No	0.0	0.0282	0.0001	0.396	0.090	0.422	0.424	1.424	0.994
SLS1	4	6	1	6	One train only	144	Dynamic time series	44	58.5	No	0.0	0.0185	0.0001	0.260	0.093	0.517	1.029	1.383	0.941

Figure 8-2: 44 m/s dynamic 10 min mean wind speed results.

When scaling the SLS1 wind time series with a factor of 0.864 in order to come down to 38 m/s 10 min mean wind speed (50.5 m/s gust wind speed) all train types fulfil the safety criteria. As seen RFI 6 is just on the limit with the overturning criterion. The roll speed violations are not considered critical as it doesn't relate to safety, and the wind load is indeed still extreme. As seen in section 8.1 the roll speed is not an issue without wind load, and furthermore the roll speed is only violated at very few discrete points along the bridge as shown on figure 8-11. **Hence this level of wind speed is adopted as a unified threshold critical wind speed for all six real train types**.

Limit state	Load combination	Train combination case	Track no.	RFI type	Meeting point	Train speed [km/h]	Wind load type	Mean wind speed [m/s]	Maximum gust wind speed in time series [m/s]	Thermal load	Seismic peak ground acc. [m/s^2]	Transverse slope [m/m]	Change of cant [m/m]	Non-compensated lateral acc. [m/s^2]	Roll speed [rad/s]	Derailment ratio [-]	Overturning ratio [-]	Vertical peak acc., trackbed (unweighted) [m/s^2]	Vertical peak acc., trackbed (weighted) [m/s^2]
Limit												0.08	0.0025	0.6	0.033	0.8	0.9	0.70	0.70
SLS1	4	1	1	1	One train only	144	Dynamic time series	38	50.5	No	0.0	0.0144	0.0001	0.202	0.034	0.388	0.418	1.036	0.713
SLS1	4	2	1	2	One train only	144	Dynamic time series	38	50.5	No	0.0	0.0151	0.0001	0.211	0.064	0.540	0.414	7.851	5.083
SLS1	4	3	1	3	One train only	144	Dynamic time series	38	50.5	No	0.0	0.0164	0.0001	0.229	0.082	0.405	0.675	1.027	0.718
SLS1	4	4	1	4	One train only	144	Dynamic time series	38	50.5	No	0.0	0.0141	0.0001	0.199	0.026	0.164	0.401	1.025	0.718
SLS1	4	5	1	5	One train only	144	Dynamic time series	38	50.5	No	0.0	0.0265	0.0001	0.371	0.069	0.338	0.412	1.088	0.710
SLS1	4	6	1	6	One train only	144	Dynamic time series	38	50.5	No	0.0	0.0166	0.0001	0.233	0.073	0.430	0.879	1.039	0.714

Figure 8-3: 38 m/s dynamic 10 min mean wind speed results.

The calculated comfort properties applicable for the four passenger trains corresponding to 38 m/s 10 min mean wind speed is listed below. As seen the only violation of the requirements are the 2 sec RMS vertical acceleration of the coach and the recoil. As the RMS values are not violated when applying the Sperling Ride comfort frequency filter this is not considered an issue. The recoil criterion has shown practically impossibly to comply with, and as previously mentioned the frequency filter approach ref. EN12299 is currently replacing the recoil criterion.

Limit state	Load combination	Train combination case	Track no.	RFI type	Meeting point	Train speed [km/h]	Wind load type	Mean wind speed [m/s]	Maximum gust wind speed in time series [m/s]	Thermal load	Seismic peak ground acc. [m/s^2]	Sperling Ride index, Wz (unweighted) [-]	Sperling Ride index, Wz (weighted) [-]	Peak vertical acc. (unweighted) [m/s^2]	Peak vertical acc. (weighted) [m/s^2]	RMS vertical acc. (2.0 s.) (unweighted) [m/s^2]	RMS vertical acc. (2.0 s.) (weighted) [m/s^2]	Recoil (based on 2.0 s. RMS coach acc.) [m/s^3]
Limit												2.2	2.2	2.00	2.00	0.75	0.75	0.25
SLS1	4	1	1	1	One train only	120	Dynamic time series	38	50.5	No	0.0	0.68	0.55	1.44	0.74	0.78	0.41	1.11
SLS1	4	2	1	2	One train only	120	Dynamic time series	38	50.5	No	0.0	0.68	0.55	1.45	0.74	0.74	0.38	1.01
SLS1	4	3	1	3	One train only	120	Dynamic time series	38	50.5	No	0.0	0.72	0.62	1.90	1.11	0.88	0.54	1.33
SLS1	4	4	1	4	One train only	120	Dynamic time series	38	50.5	No	0.0	0.75	0.62	1.89	1.04	1.07	0.59	1.24

Figure 8-4: 38 m/s dynamic 10 min mean wind speed results.

As mentioned the four passenger trains does not violate safety requirements when exposed to a SLS2 wind time series. The outcome of this scenario is shown in the below table.

Limit state	Load combination	Train combination case	Track no.	RFI type	Meeting point	Train speed [km/h]	Wind load type	Mean wind speed [m/s]	Maximum gust wind speed in time series [m/s]	Thermal load	Seismic peak ground acc. [m/s^2]	Transverse slope [m/m]	Change of cant [m/m]	Non-compensated lateral acc. [m/s^2]	Roll speed [rad/s]	Derailment ratio [-]	Overturning ratio [-]	Vertical peak acc., trackbed (unweighted) [m/s^2]	Vertical peak acc., trackbed (weighted) [m/s^2]
Limit												0.10	0.0040	0.8	0.036	0.8	0.9	1.00	1.00
SLS2	4	1	1	1	One train only	144	Dynamic time series	47	62.1	No	0.0	0.0195	0.0001	0.273	0.049	0.325	0.713	1.600	1.042
SLS2	4	2	1	2	One train only	144	Dynamic time series	47	62.1	No	0.0	0.0197	0.0001	0.277	0.034	0.302	0.586	1.600	1.042
SLS2	4	3	1	3	One train only	144	Dynamic time series	47	62.1	No	0.0	0.0198	0.0001	0.278	0.059	0.317	0.788	7.876	5.099
SLS2	4	4	1	4	One train only	144	Dynamic time series	47	62.1	No	0.0	0.0195	0.0001	0.273	0.042	0.255	0.604	1.610	1.040

Figure 8-5: 47 m/s dynamic 10 min mean wind speed results.

The following 8 graphs show the spatial variation of selected runability, safety and comfort properties for each train type. They do not, however, necessarily represent peak values. Hence the previously shown four tables is to be read in order to identify the overall outcome of the analysis. The purpose with the 8 graphs is to reveal the physical soundness of the calculations. For instance the impact of the approach bridges / terminal structure is very obvious on many of the plots. On plots where the property in question is violated for one or more train types the limit is shown. All plots are based on the unified critical dynamic 10 min mean wind speed, i.e. 38 m/s.

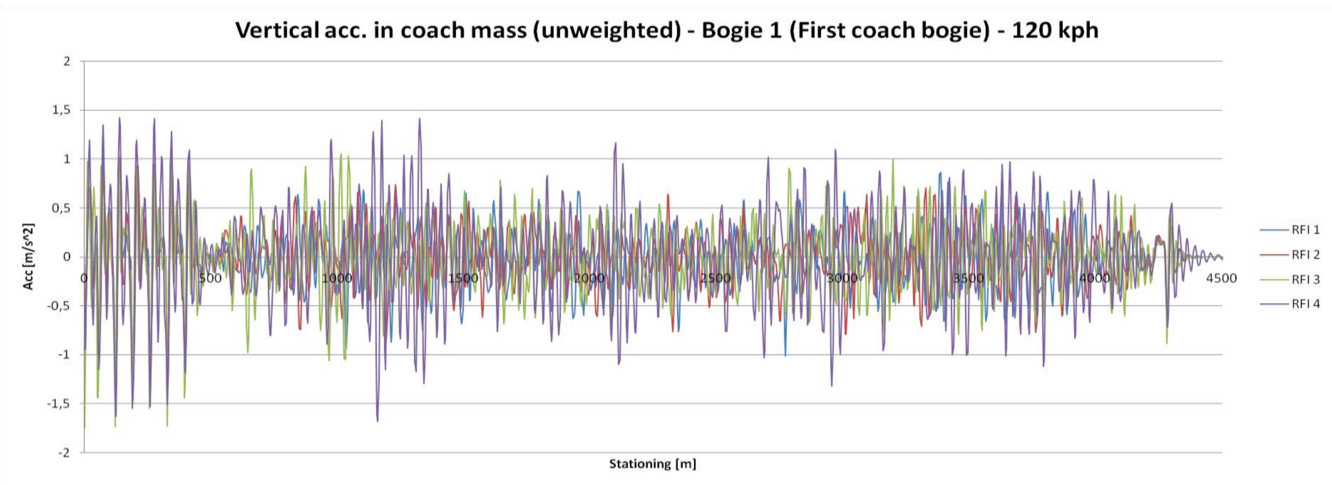

Figure 8-6: Vertical acc. in coach mass.

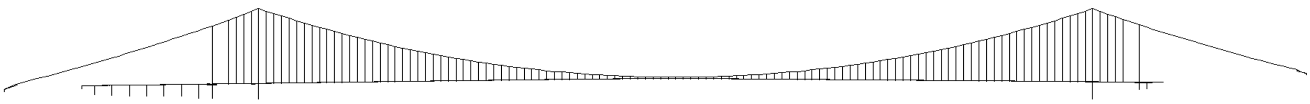

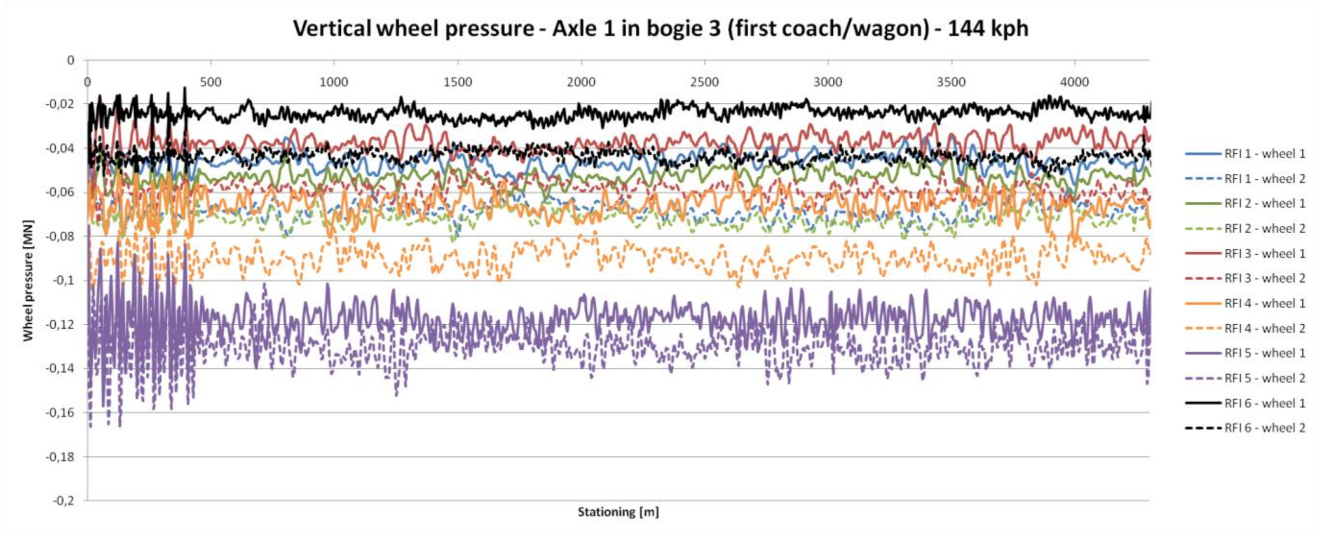

Figure 8-7: Wheel pressure.

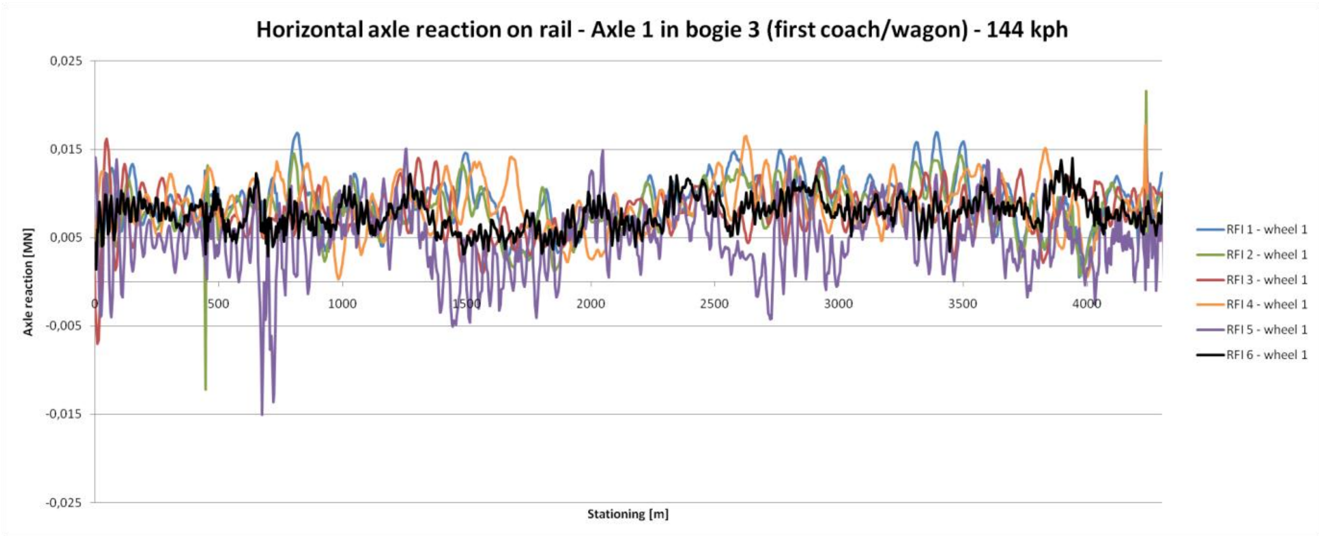

Figure 8-8: Horizontal axle reactions.

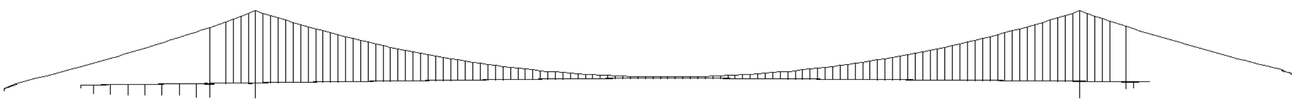

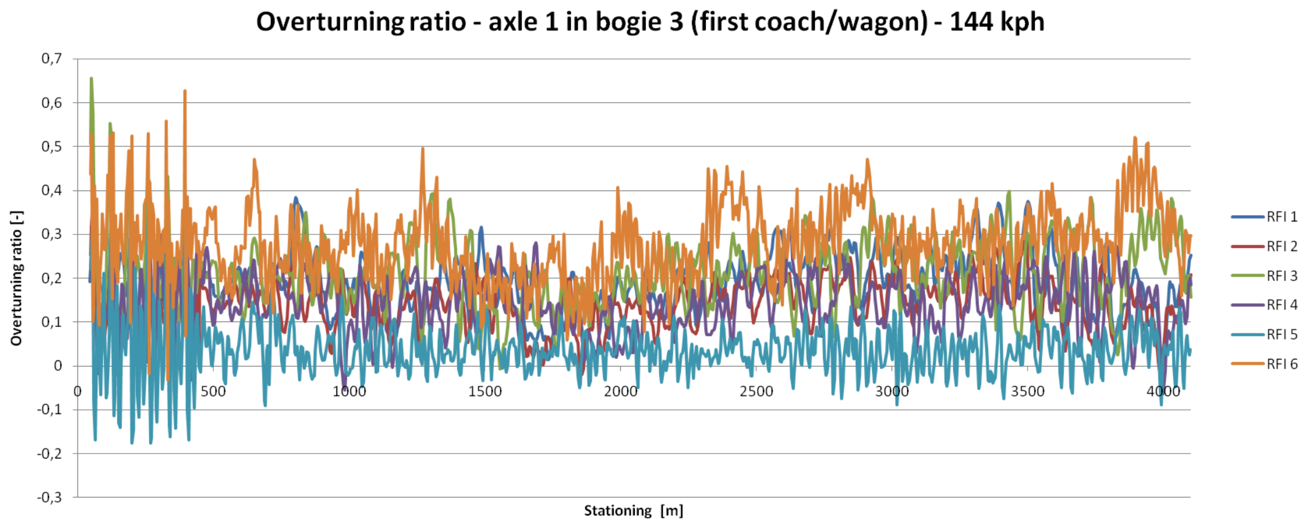

Figure 8-9: Overturning ratio.

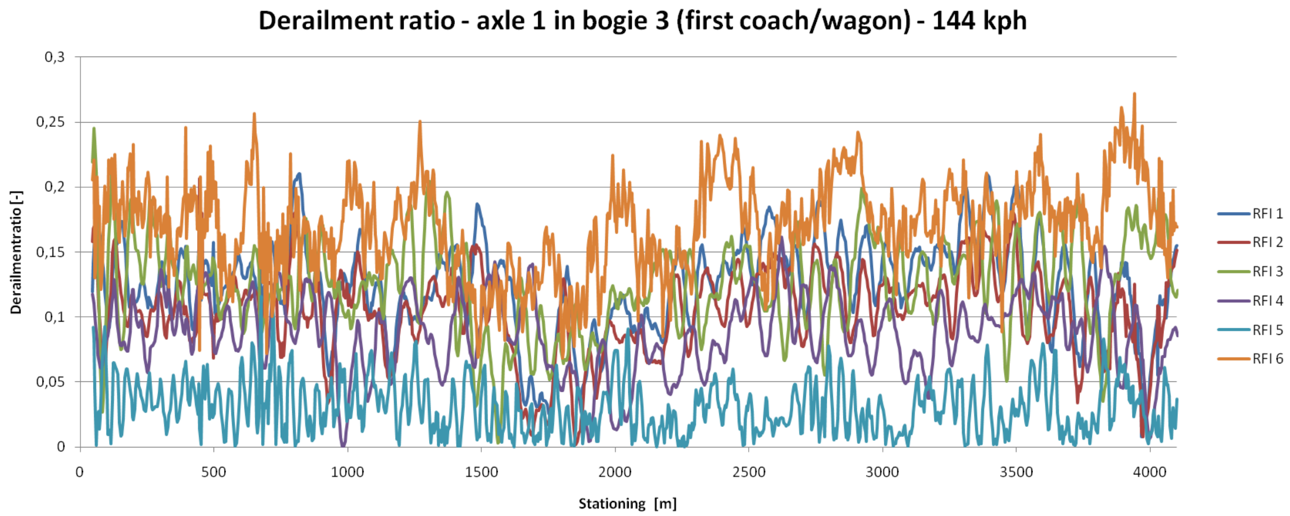

Figure 8-10: Derailment ratio.

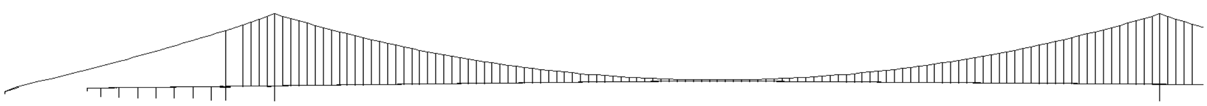

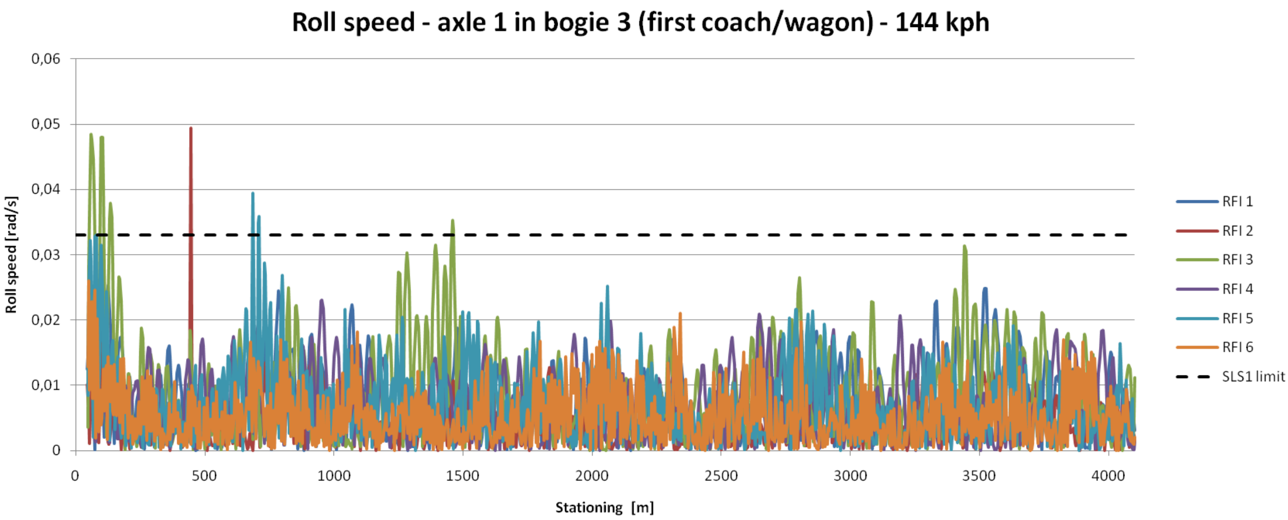

Figure 8-11: Roll speed

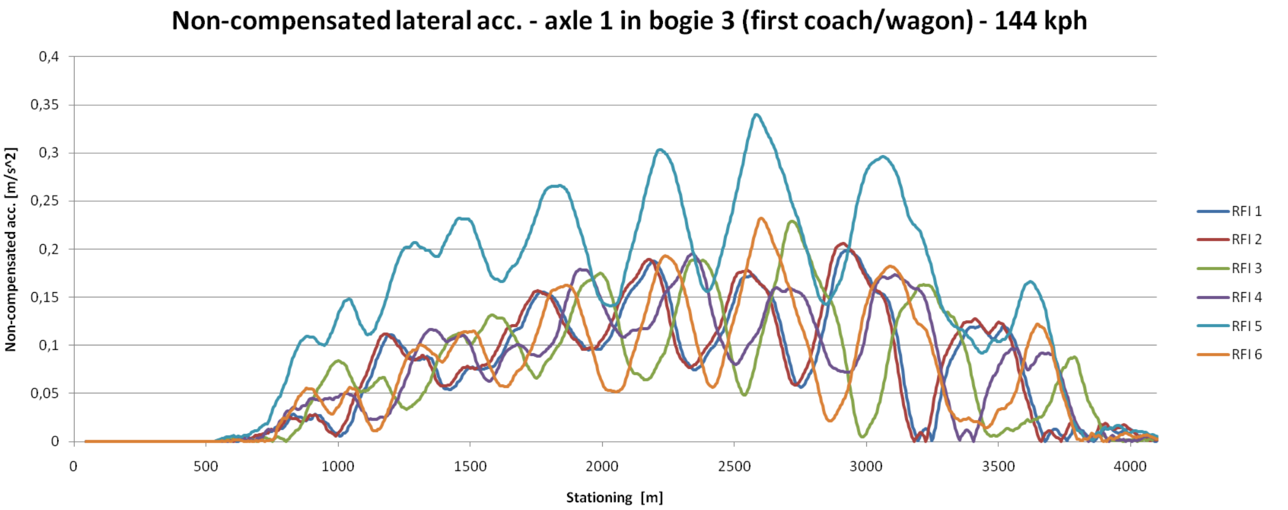

Figure 8-12: Non-compensated acceleration.

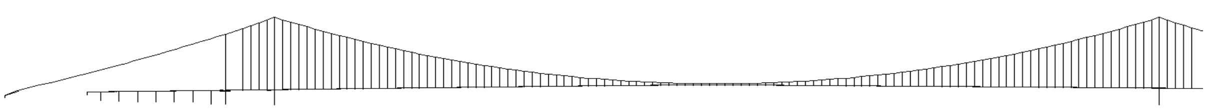

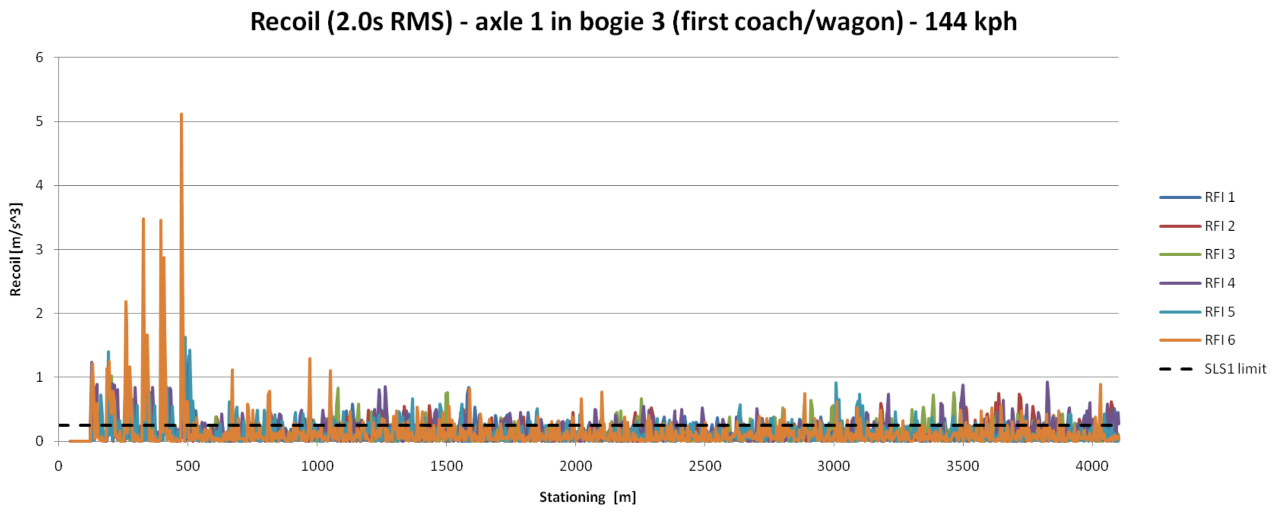

Figure 8-13: Recoil.

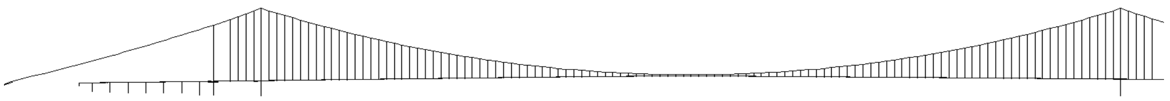

8.3 Load combination 5, Earth quake

In load combination 5 an earth quake is induced at the structure by applying a time series of accelerations on the supported nodes of the model. In SLS2 a total of 8 time series are investigated. The average of the overturning and derailment ratios from these analyses is then used to identify the most representative time series among the 8. This series is then solely used in the SLS1 verification. This procedure has been utilized due to computational time and is justified by the fact that the time series in SLS1 and SLS2 are identical apart from the scalar scaling. And since the runability study is based on linear dynamics no hidden effects will apply when running only one time series in SLS1 once this has been identified as representative for the full set of time series.

The resulting response at the railway tracks is determined through a modal solution approach as a linear combination of the eigen modes at any instance of time. As the loading on the vehicles is solely transferred by the structure itself as opposed to an partly external action like wind, this type of analysis calls for a large number of eigen modes to be included in order to be able to describe the response sufficiently. Convergence studies have revealed that 1000 eigen modes is sufficient.

The results are shown as peak values in tables as well as a function of stationing, however excluding the expansion joints. This deduction is introduced in order to keep a clear picture of the safety level in a spatial manner as it has been discovered that the analysis model causes some artificial peaks in derailment and overturning ratio at the expansion joints in connection with seismic loading. This is due to the fact that the dynamic train models in IBDAS are running directly at the railway girder rather than on a rail. When the expansion joint is subject to some relative horizontal and vertical displacements during an earth quake, the train in the model will experience this as a sudden kink in the track. In real life, obviously, the rail will produce a smooth deflection curve at the expansion joint. To provide an overview of the order of magnitude of the relative displacements a history plot has been included for the vertical and lateral horizontal direction for a representative seismic time series.

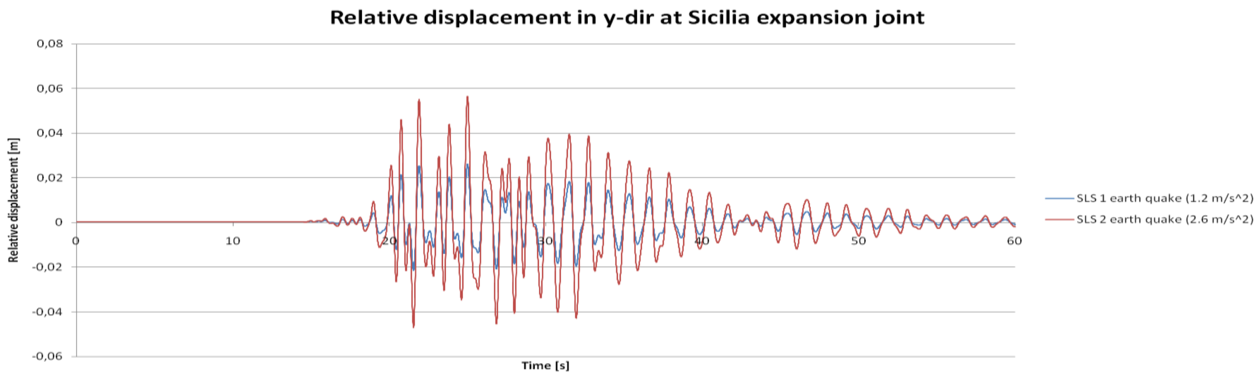

Figure 8-14: Relative displacements of expansion joint.

The two below shown plots illustrate the principal modelling problem at the expansion joint. The upper plot shows the overturning ratio across the entire bridge whereas the lower is excluding the expansion joint about stationing 450. As seen, in this case the overturning criterion is actually fulfilled as long as the train runs on the global FE-model not containing modelling flaws in terms of seismic impact.

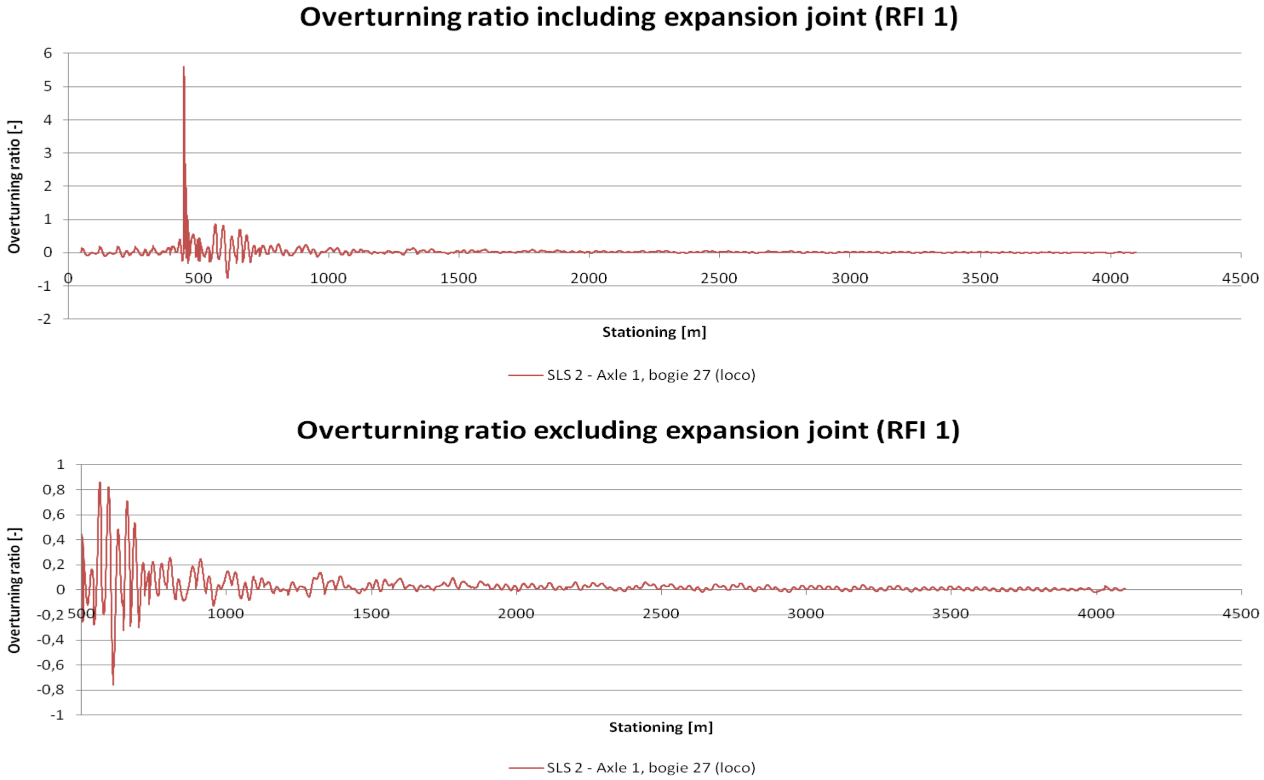

Figure 8-15: Overturning ratio with and without artificial peak due to modelling approach.

Should any further investigation be carried out, it would be possibly to model the rail itself rather than having the train running directly at the bridge deck.

In the following the peak values for overturning and derailment ratio is presented in tables followed by graphs showing the spatial variation for the worst axles in the most representative seismic time series (E1-02). This time series is the only one investigated in SLS1 as discussed earlier. Note that derailment results are unreliable when the overturning ratio exceeds 1.

Table 8-2: Overturning and derailment ratios for RFI1-6 in representative SLS1 earth quake.

Seismic event	Sub ID	RFI type	Axle 1 position at start of earth quake	**Overturning ratio**	Axle	Bogie	**Derailment ratio**	Axle	Bogie
				SLS1 (Peak ground acc. = 1.2 m/s^2)					
				Peak value			Peak value		
E1	2	1	Sicily pylon	0.52	1	1	0.29	2	3
		2		0.39	2	1	0.26	2	4
		3		0.74	2	8	0.5	1	9
		4		0.31	2	6	0.19	1	7
		5		2.08	1	4	1.11	2	52
		6		1.34	1	35	0.71	2	20

Legend
- (green) Value below design requirement
- (yellow) Value above design requirement but below physical critical value
- (red) Value above physical critical value

Table 8-3: Overturning and derailment ratios for RFI1-6 in the 8 SLS2 earth quakes.

Seismic event	Sub ID	RFI type	Axle 1 position at start of earth quake	**Overturning ratio**	Axle	Bogie	**Derailment ratio**	Axle	Bogie
				SLS2 (Peak ground acc. = 2.6 m/s^2)					
				Peak value			Peak value		
E1	1	1	Sicily pylon	0.8	2	2	0.46	2	3
		2		0.52	2	13	0.51	2	1
		3		1.26	2	5	4.42	2	4
		4		0.67	2	3	0.28	1	7
		5		4.48	1	4	164.6	2	21
		6		2.67	1	22	13.35	2	1
E1	2	1	Sicily pylon	1.11	1	1	0.58	2	3
		2		0.84	2	1	0.64	2	1
		3		1.59	2	8	836.2	1	3
		4		0.7	2	6	0.39	1	7
		5		4.54	1	4	3463.4	1	67
		6		2.9	1	29	943.2	1	45
E2	1	1	Sicily pylon	1.21	1	1	0.81	1	2
		2		0.72	1	1	0.8	2	4
		3		1.76	1	13	563.2	1	20
		4		0.99	1	3	0.53	2	2
		5		5.08	1	3	591	2	74
		6		2.86	2	21	2.94	1	60
E2	2	1	Sicily pylon	1.66	1	2	1.42	2	1
		2		0.96	1	3	1.49	2	1
		3		1.67	1	20	950.2	1	17
		4		0.73	1	6	0.34	1	1
		5		4.51	1	3	93.6	2	49
		6		2.34	1	30	135.3	1	47
E3	1	1	Sicily pylon	0.8	1	1	0.67	1	1
		2		0.61	1	3	0.47	1	3
		3		2.3	1	5	227.9	2	2
		4		0.75	2	14	0.45	2	10
		5		6.02	1	11	344.9	1	45
		6		3.6	1	15	446.5	2	29
E3	2	1	Sicily pylon	1.03	1	2	1.21	2	8
		2		0.77	1	9	0.96	2	10
		3		1.74	1	10	10863.9	1	8
		4		0.8	2	3	0.46	2	1
		5		4.72	1	3	58.2	2	98
		6		2.77	1	39	130.6	1	58
E4	1	1	Sicily pylon	1.48	2	1	0.67	2	5
		2		0.79	2	3	0.62	2	3
		3		1.48	2	1	10376.8	2	15
		4		0.61	2	3	0.44	2	4
		5		3.99	1	6	1673.4	1	55
		6		3.44	2	8	109.5	2	14
E4	2	1	Sicily pylon	0.76	1	27	0.45	2	4
		2		0.45	1	17	0.39	1	1
		3		1.02	1	8	85.3	1	3
		4		0.69	2	6	0.37	1	1
		5		5.66	2	3	275.4	2	49
		6		2.87	2	63	97.5	2	60

	Average	Average
RFI 1	1.11	0.78
RFI 2	0.71	0.74
RFI 3	1.60	2988.49
RFI 4	0.74	0.41
RFI 5	4.88	833.06
RFI 6	2.93	234.86

Legend
- (green) Value below design requirement
- (yellow) Value above design requirement but below physical critical value
- (pink) Value above physical critical value

As seen a violation of the overturning criterion occurs for both freight trains (RFI 5 and RFI 6) in SLS1. For RFI 5 the derailment criterion is also exceeded. In SLS 2, several train types experience problems. In average, only RFI 2 and RFI 4 stay below the limits in SLS2.

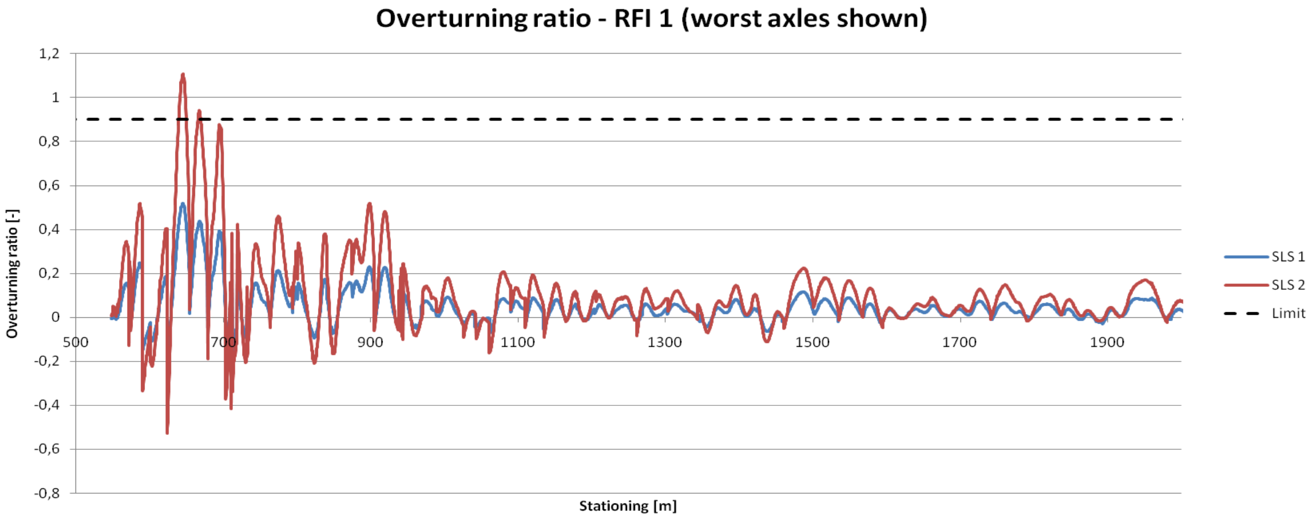

Figure 8-16: RFI 1 overturning ratio.

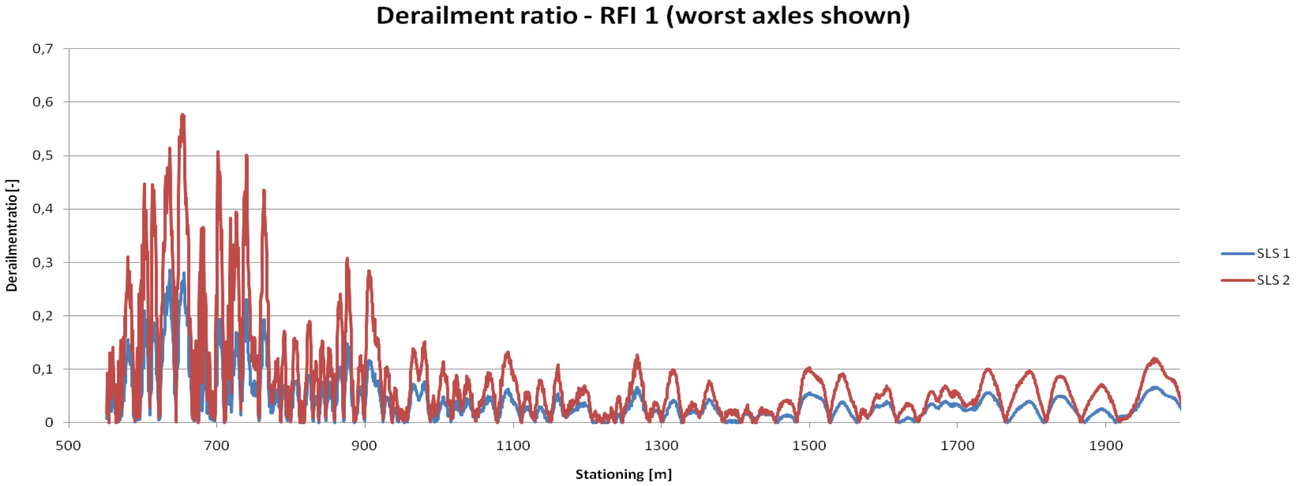

Figure 8-17: RFI 1 derailment ratio

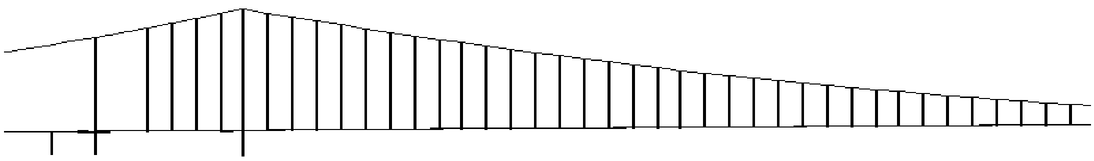

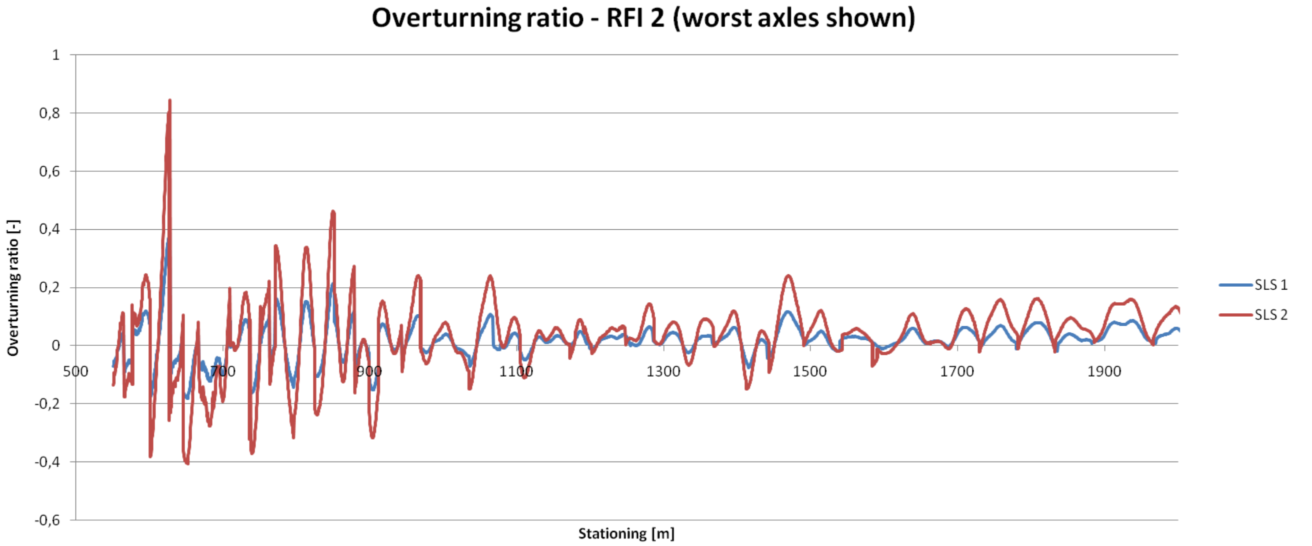

Figure 8-18: RFI 2 overturning ratio

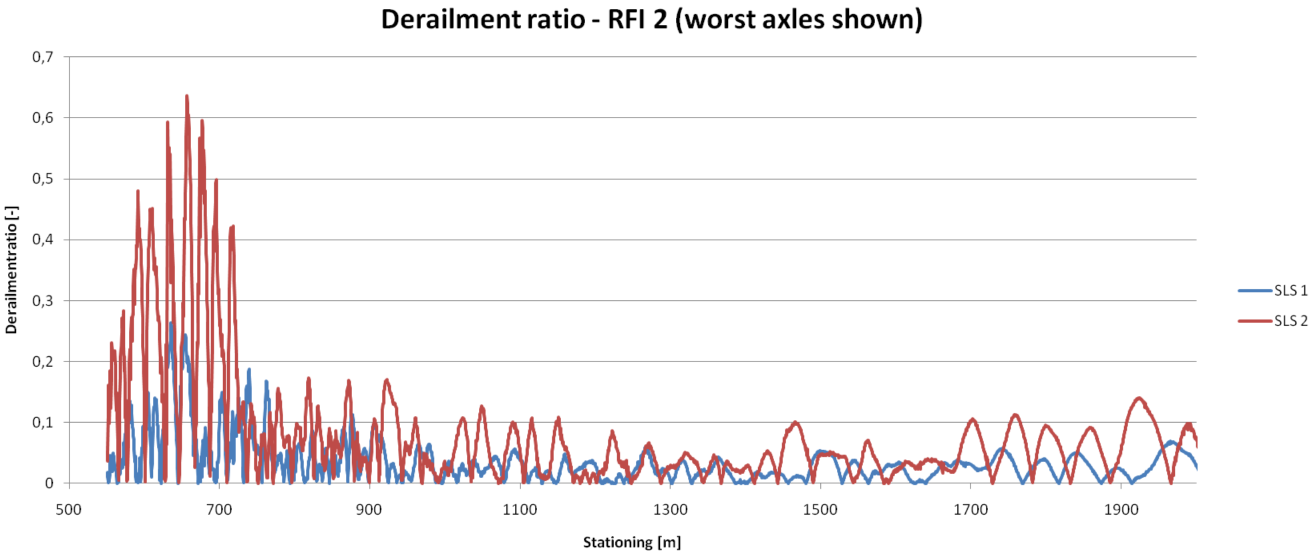

Figure 8-19: RFI 2 derailment ratio

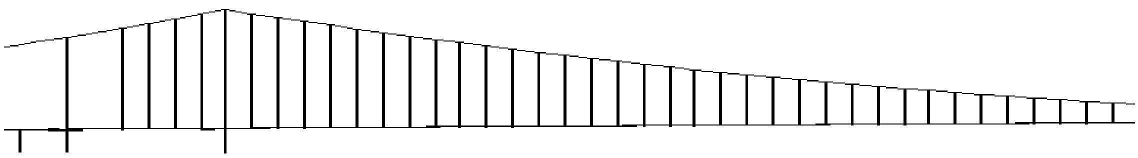

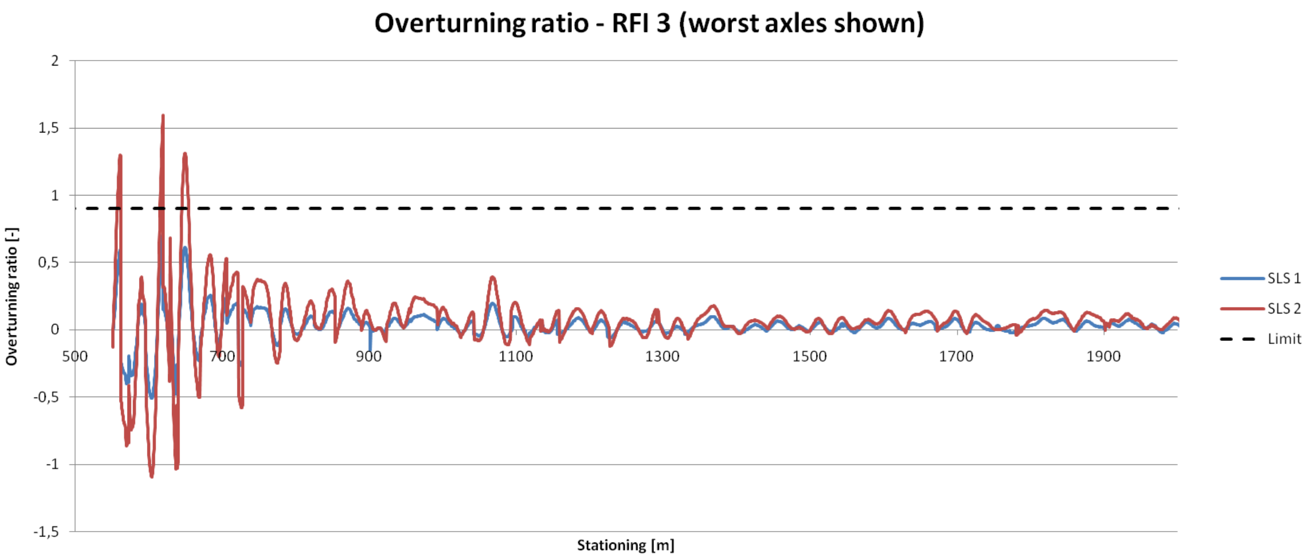

Figure 8-20: RFI 3 overturning ratio.

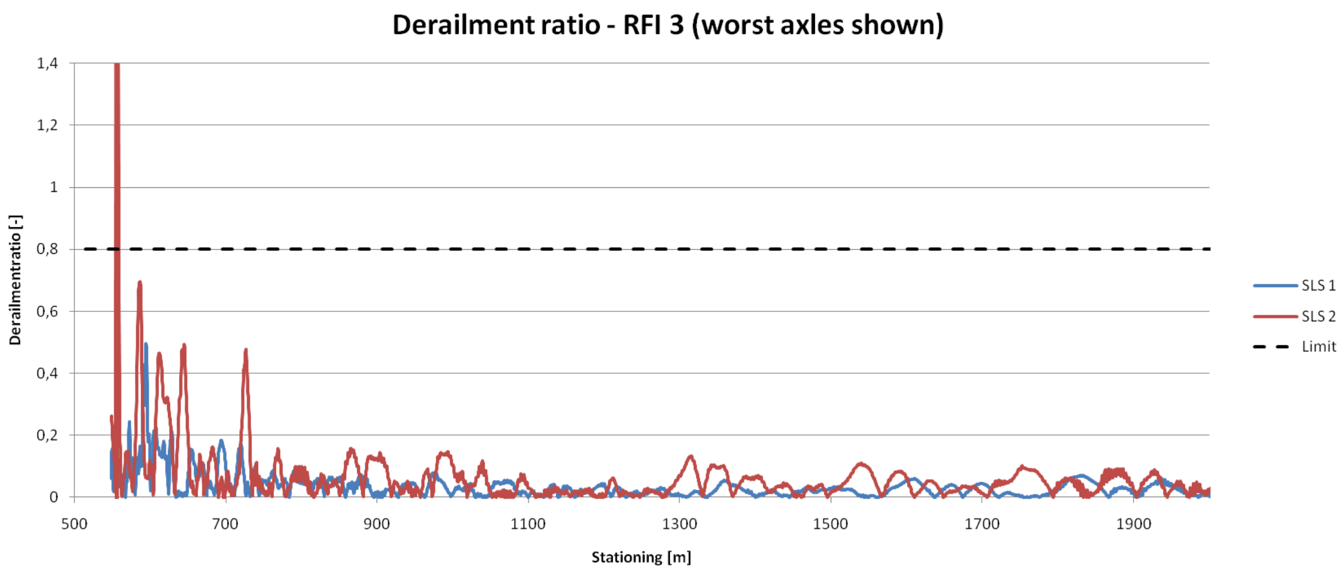

Figure 8-21: RFI 3 derailment ratio

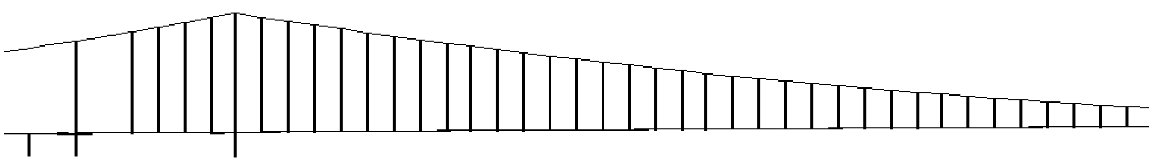

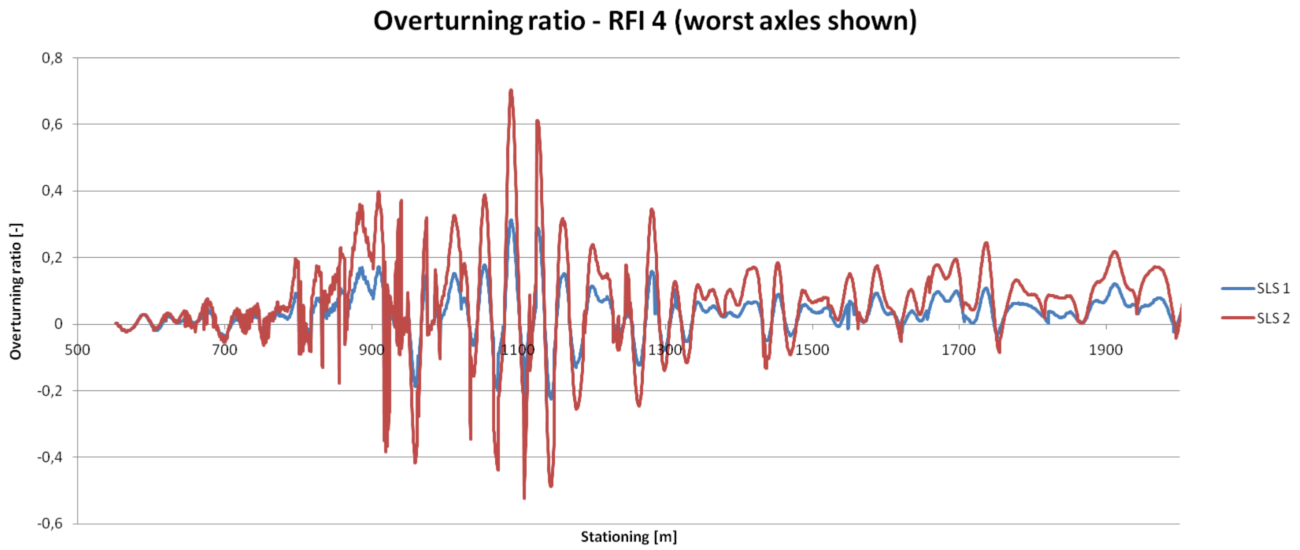

Figure 8-22: RFI 4 overturning ratio

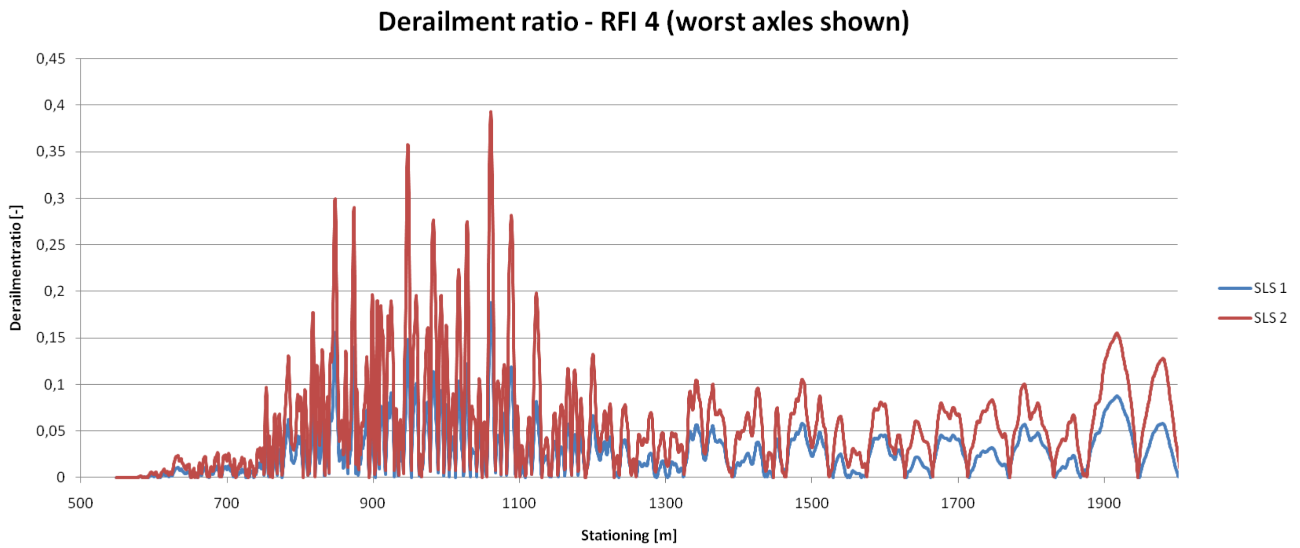

Figure 8-23: RFI 4 derailment ratio

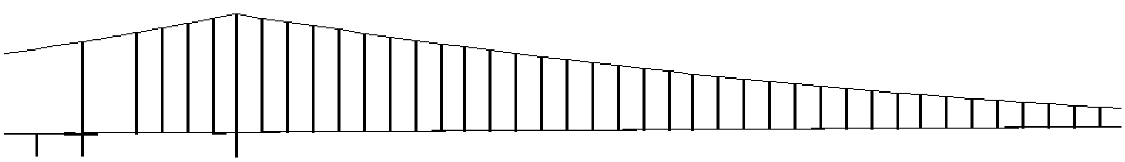

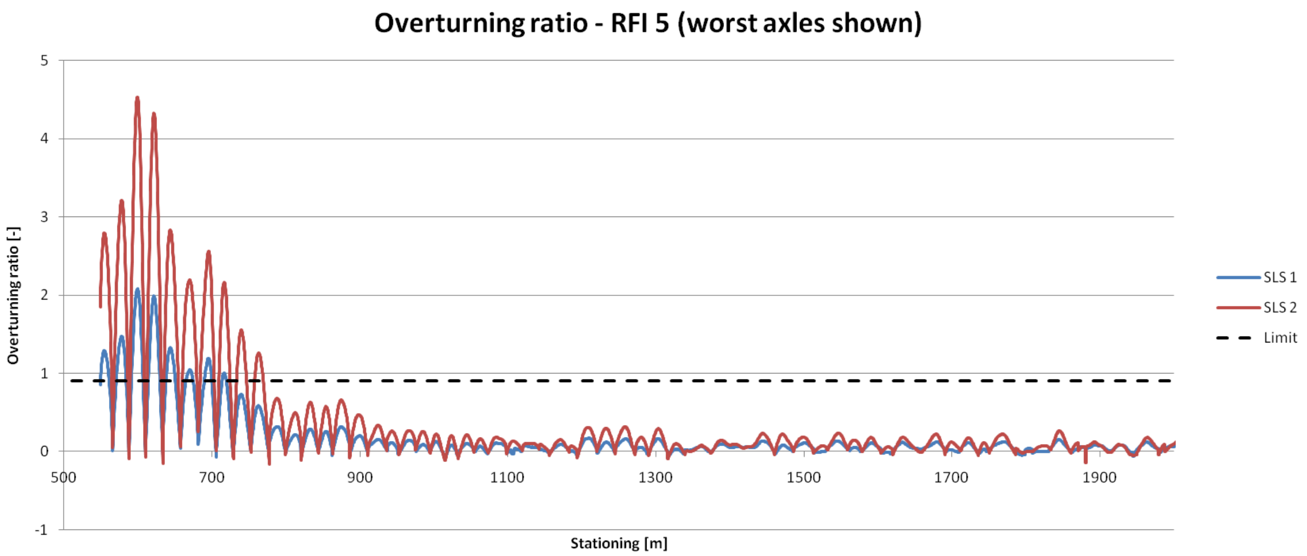

Figure 8-24: RFI 5 overturning ratio

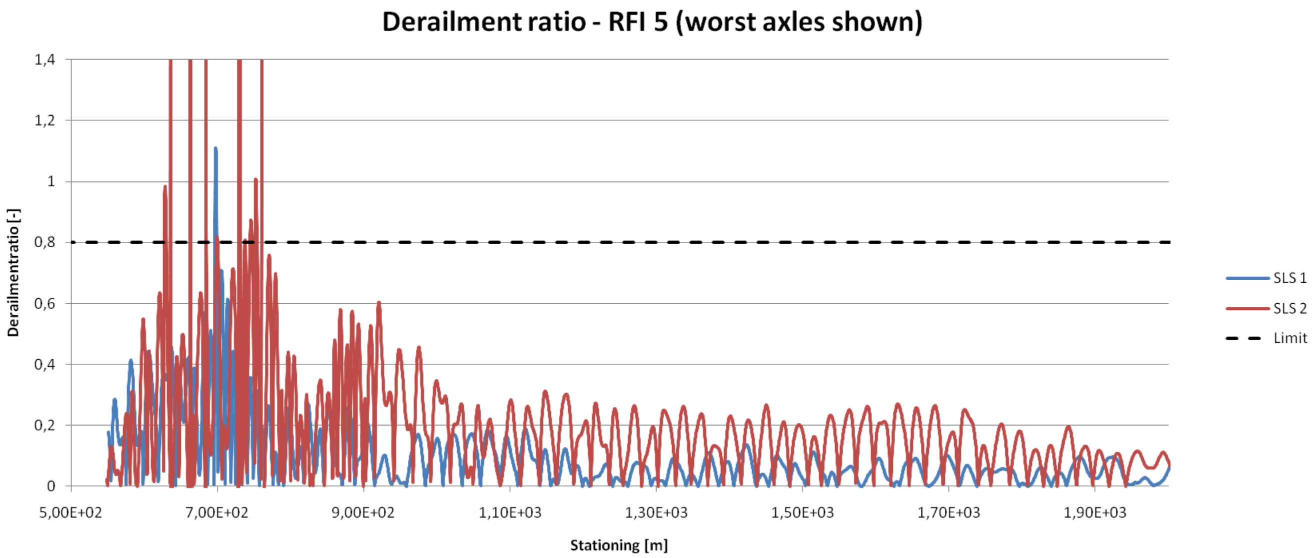

Figure 8-25: RFI 5 derailment ratio

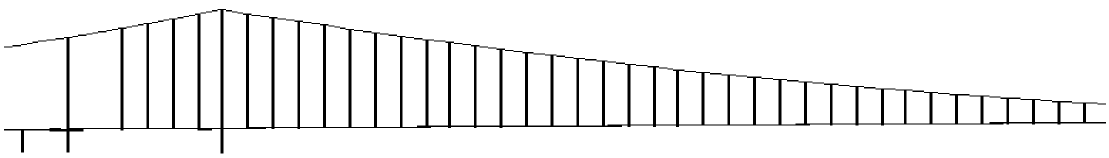

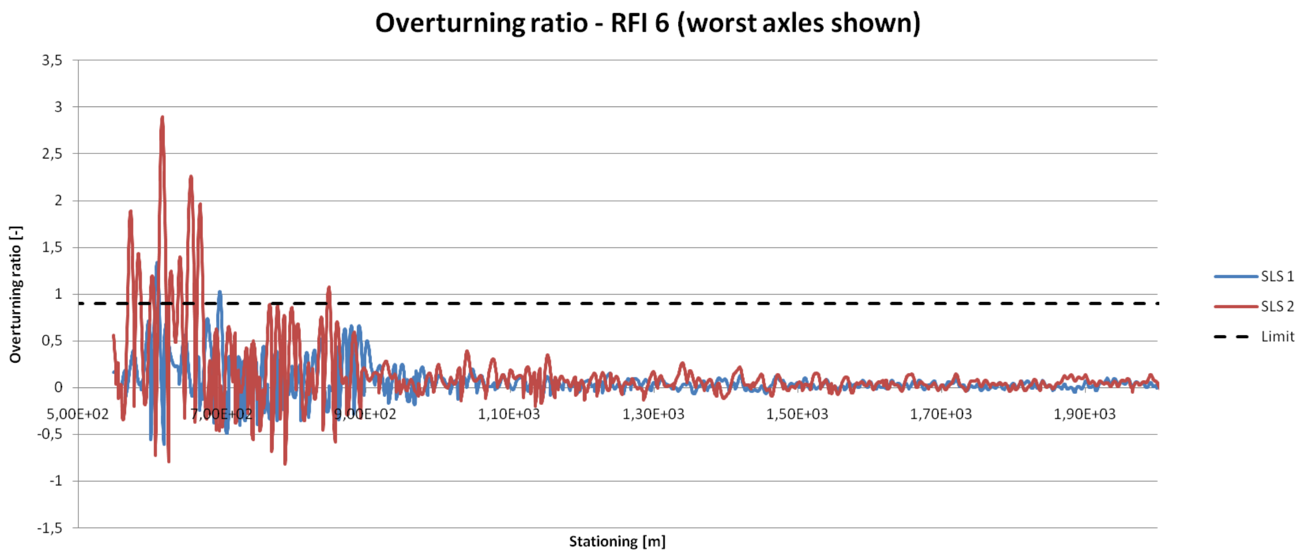

Figure 8-26: RFI 6 overturning ratio

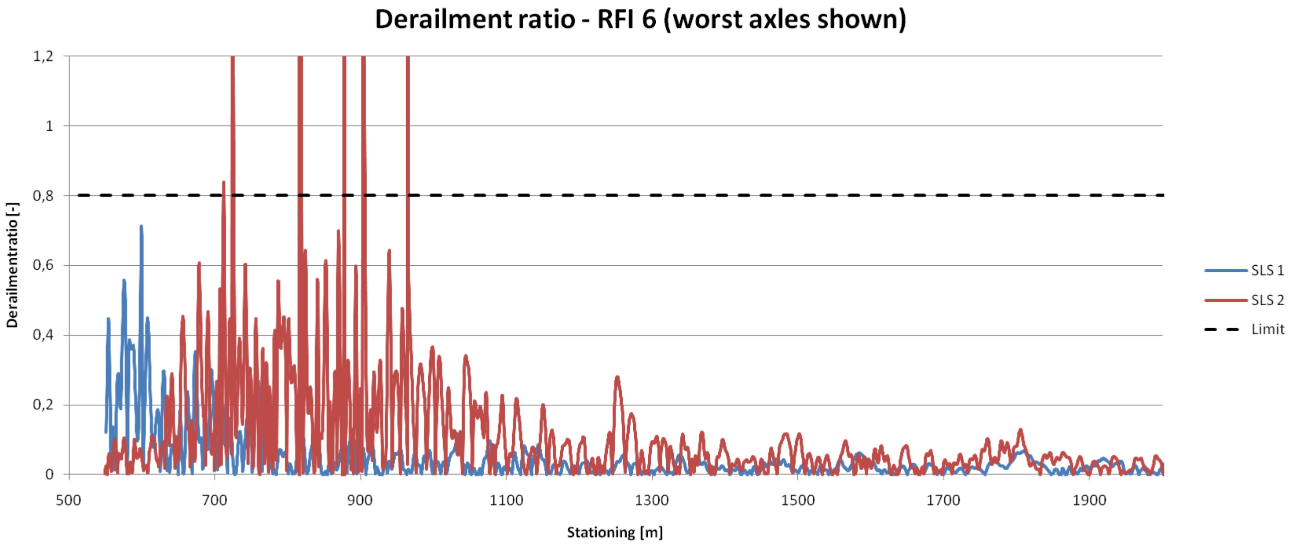

Figure 8-27: RFI 6 derailment ratio

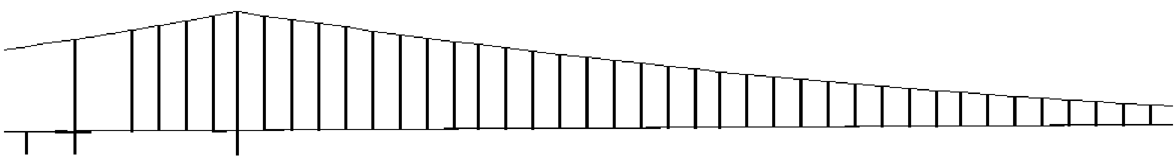

In order to illustrate the cause of the violations of the overturning and derailment criteria the time series for transverse accelerations of the ground are shown below for each of the 8 earth quakes applied in SLS2. In addition the plots show the resulting transverse acceleration at the railway girder at the Sicily pylon, which is the point the trains reach when the seismic activity is started. As seen, a significant amplification takes place. The amplification factor is similar for SLS1. The second time series, E1-02, is chosen as representative as a average earth quake used in SLS1.

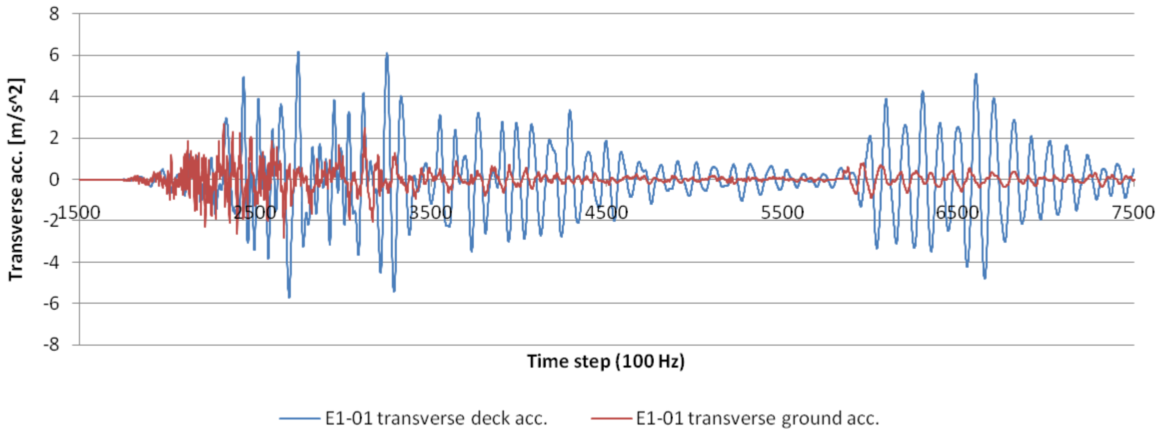

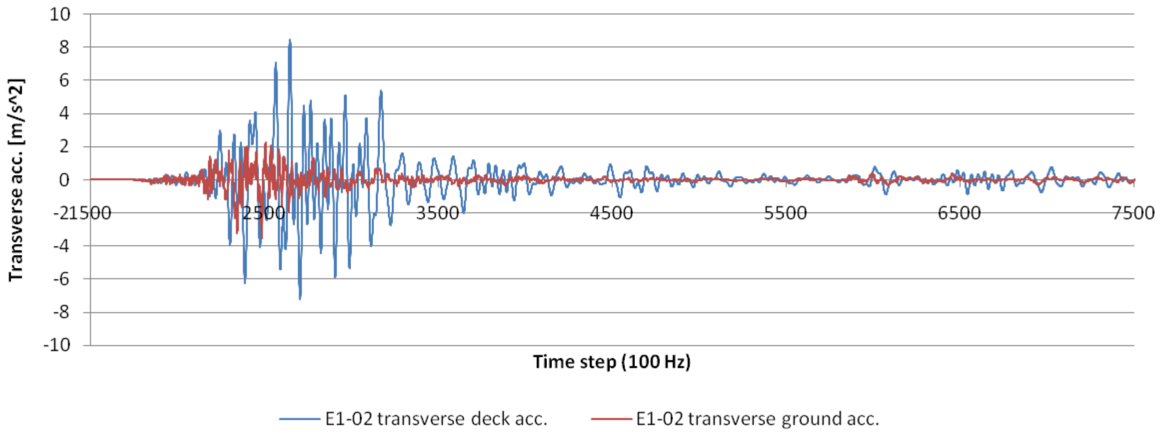

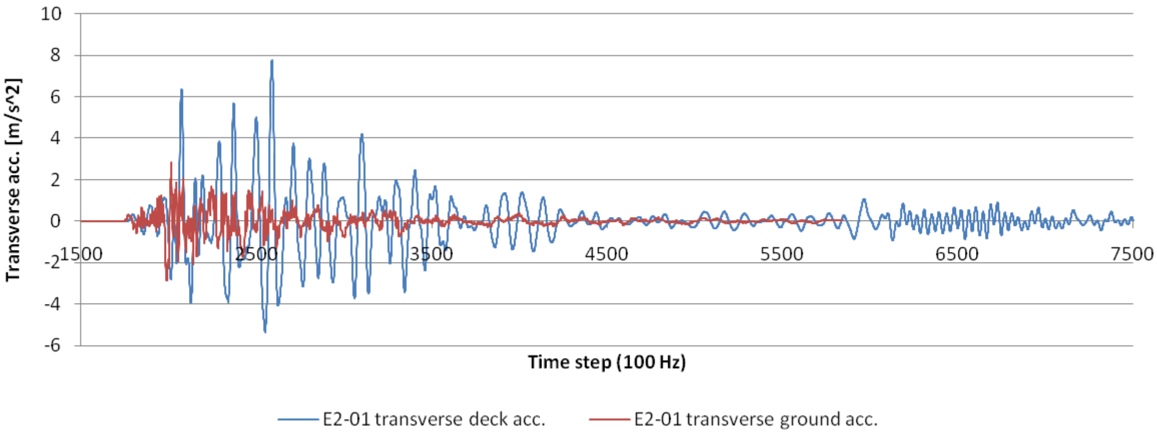
10
8
6
4
2
0
-2
-4
-6
1500
2500
3500
4500
5500
6500
7500
Transverse acc. [m/s^2]
Time step (100 Hz)
E2-01 transverse deck acc.
E2-01 transverse ground acc.

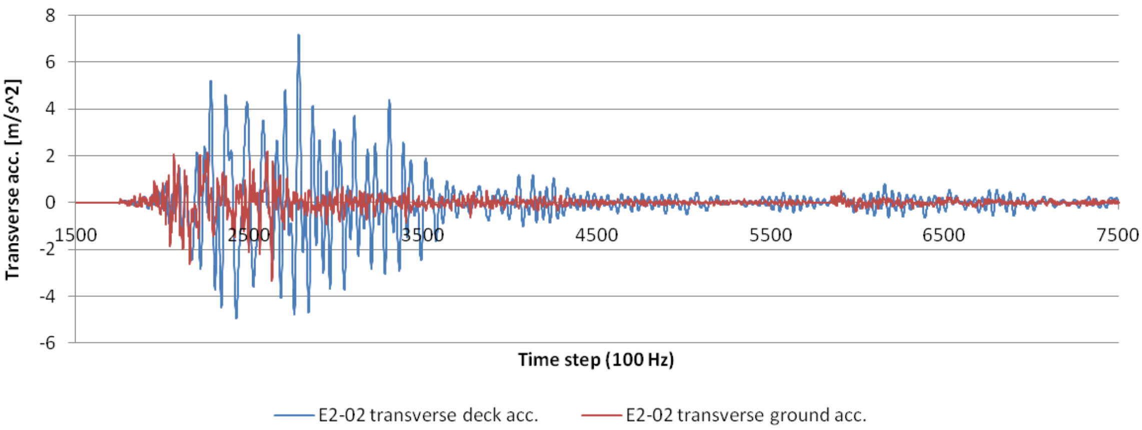
8
6
4
2
0
-2
-4
-6
1500
2500
3500
4500
5500
6500
7500
Transverse acc. [m/s^2]
Time step (100 Hz)
E2-02 transverse deck acc.
E2-02 transverse ground acc.

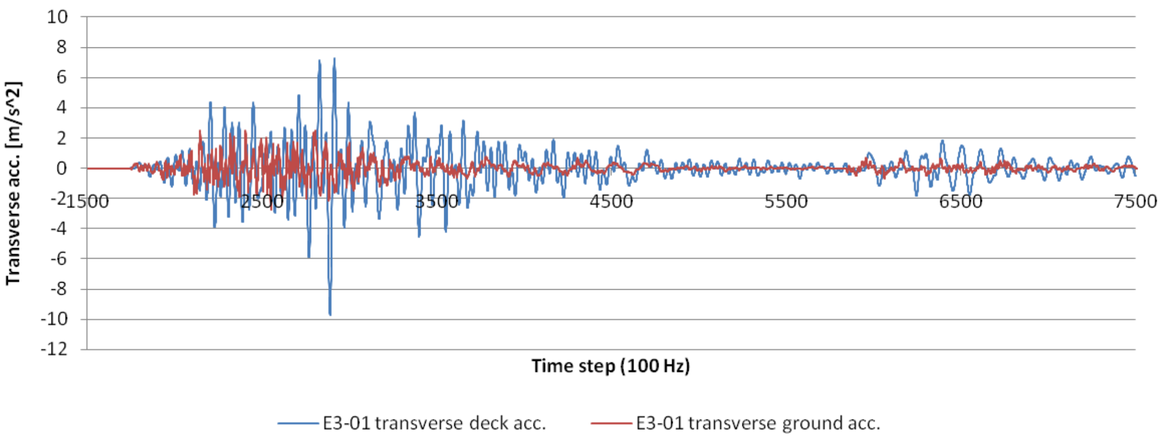
10
8
6
4
2
0
-2
-4
-6
-8
-10
-12
1500
2500
3500
4500
5500
6500
7500
Transverse acc. [m/s^2]
Time step (100 Hz)
E3-01 transverse deck acc.
E3-01 transverse ground acc.

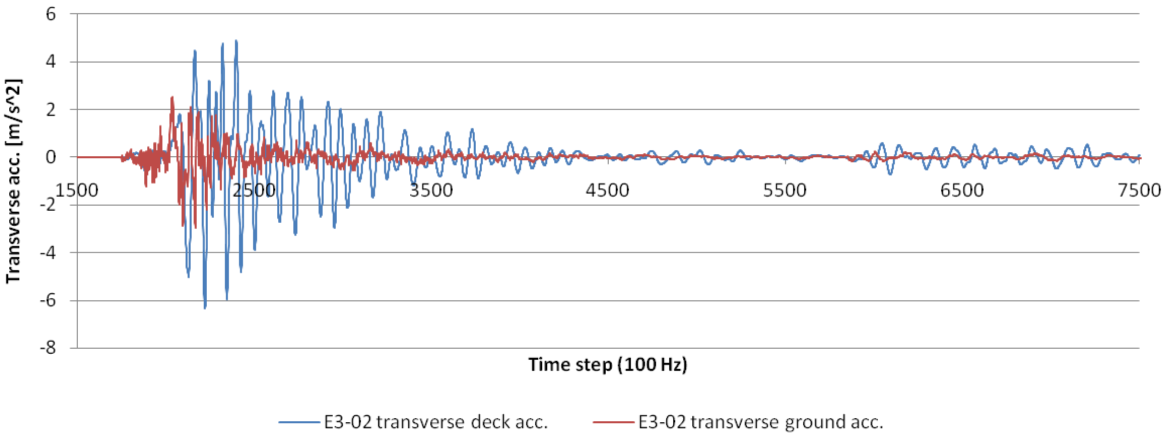
Transverse acc. [m/s^2]
Time step (100 Hz)
E3-02 transverse deck acc.
E3-02 transverse ground acc.

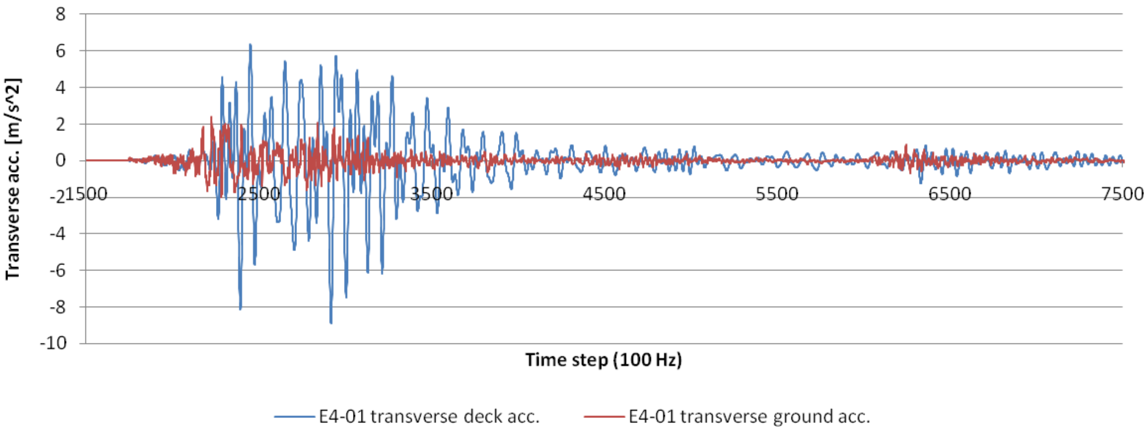
Transverse acc. [m/s^2]
Time step (100 Hz)
E4-01 transverse deck acc.
E4-01 transverse ground acc.

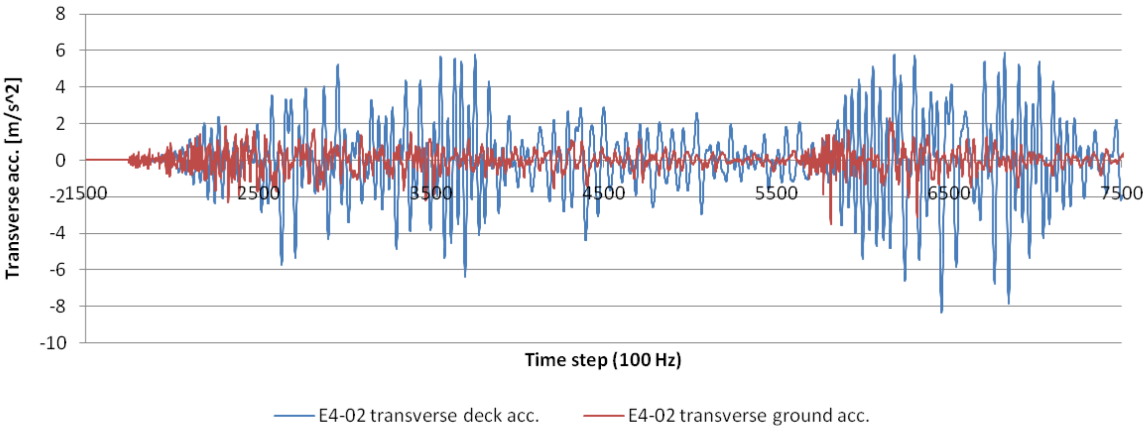
Transverse acc. [m/s^2]
Time step (100 Hz)
E4-02 transverse deck acc.
E4-02 transverse ground acc.

8.4 Roadway runability analyses

In the broad picture, roadway runability has not been considered nearly as challenging as railway runability. Hence it has been agreed between COWI and EDIN to address the analysis by calculating roadway deck accelerations when the bridge is subject to dynamic wind loads corresponding to SLS1 wind load. I.e. no dynamic vehicles has been modelled as is the case with railway runability. Apart from the fact that roadway runability is not really a key focus area, no dynamic properties are currently available for cars and trucks.

The below shown table states the accelerations at mid span for the longitudinal (S), transverse (Y) and vertical direction (Z). The values represent the largest accelerations induced when applying the wind load in 8 different wind directions spanning 180 degrees with an interval of 22.5 degrees.

Table 8-4: Roadway accelerations for dynamic wind load.

	AS [m/s^2]	AY [m/s^2]	AZ [m/s^2]
Actual acc.	0.110	0.345	0.535
Max. acc. allowed	0.500	0.500	1.500

8.5 Maximum vertical displacement

A special study has been carried out in order to examine the maximum vertical displacement of the bridge due to railway loading. The most adverse load case in this regard is when two loaded freight trains (RFI 5) are present at the bridge simultaneously. The below figure shows the vertical displacement throughout the bridge at the instant of time when the mid span is experiencing the largest displacement.

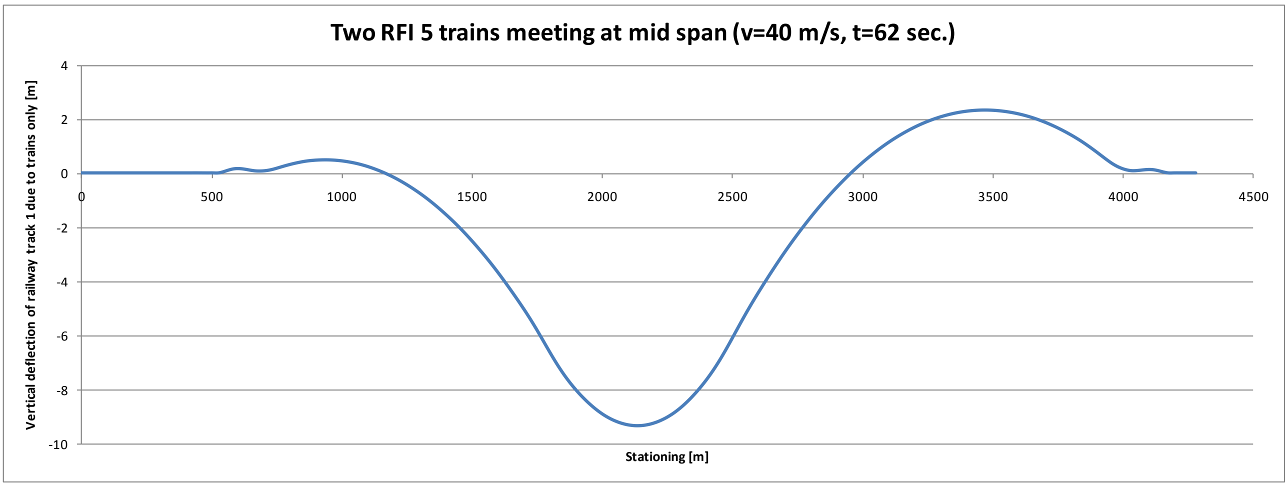

Figure 8-28: Maximum vertical displacement caused by trains.

9 Local Analysis for Wheel / Track Runability

In this section, the dynamic local interaction between train transit and structure response across diaphragms and cross girders is particularly investigated. To achieve this objective, a detailed local model of the railway girder is developed, modelled, and validated. The entire railway girder box is separated from the four T beams located underneath the rail track and they are all modelled individually. (to be expanded)

9.1 ADTres Bridge Model

ADTreS is a software entirely developed and validated by the Mechanical Engineering Department of Politecnico di Milano. It is fully dedicated to the mathematical modelling of train-track-bridge interaction. It is based on a multi-body model of the rail vehicle and on a finite element approach for the bridge, which can also include the track.

Two separate sets of governing differential equations are numerically integrated in time domain in a co-simulation process. They are separately expressed for the two subsystems composed by structure (bridge and track) and rail vehicles, and then solved in time domain. These equations are coupled by computing wheel-rail contact forces which depend on both vehicle and track generalized coordinates. The contact mechanics as it is applied to the wheel-rail system is solved using the mathematical models described by Kalker [11] and Shen-Elkins [12] theories. The first is implemented for the solution of the normal contact problem. Elastic and plastic rolling normal contact of bodies made of identical materials is included in the model. The second theory is implemented in order to model the tangential problem of the wheel-rail contact mechanics. Creep forces play an important role in determining the lateral dynamic performance of rail vehicles. Lateral stability (hunting), ride quality, wheel climb derailments, and wheel-rail wear are directly affected by the creep forces that occur in the contact patch between the wheel and the rail. These mathematical models aimed at predicting normal and lateral rail vehicle performance, have a very accurate representation of normal and lateral forces acting in the wheel-rail interface.

Runnability analyses are, finally, performed through a numerical procedure which accounts for train-bridge dynamic interaction, being the contact forces dependant on the motion of both subsystems [13,14].

9.1.1 Model of the rail vehicle

The rail vehicle model is based on a multi-body approach as described in section 5.2.

Figure 9-1shows the schematic of the vehicle multi-body model which consists of car body, bogies and wheelsets. Stiffness and damping parameters of primary and secondary suspensions are set according to the standard specifications of real trains RFI [1, 12, 13, 14].

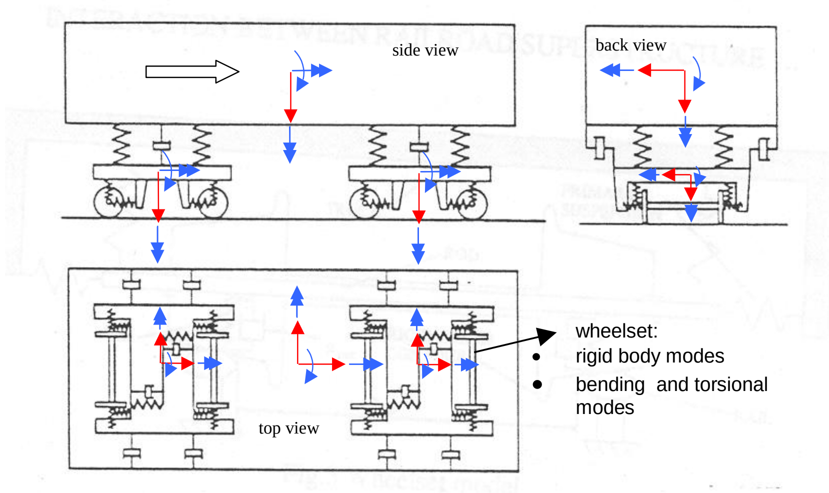

Figure 9-1: Schematic of the multi-body model of the vehicle: degrees of freedom of car body and bogies are indicated

9.2 Computational multibeam model description

9.2.1 FE model properties (structural elements)

From the global point of view, the dynamic behavior of the railway girder is approximated such that the whole contribution of girder, T beams, and local reinforcements is taken into account as one section property. Figure 12-2 shows a detail of the cross sectional area of the railway girder including all local reinforcements like T beams.

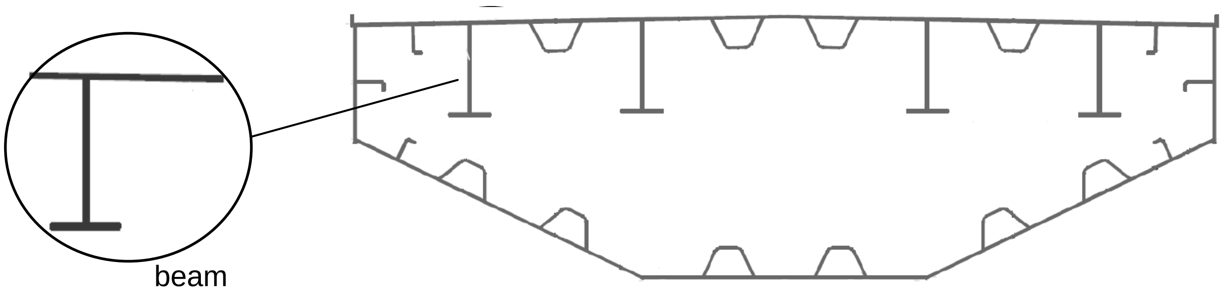

Figure 9-2 – Cross sectional area of the railway girder.

A front view of the global finite element model schematic of the railway girder is shown in Figure 9-3. The whole cross sectional area properties are concentrated in one single beam.

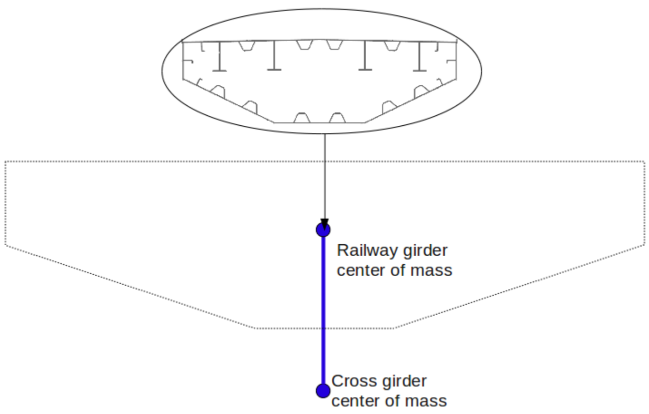

Figure 9-3 In the global model of the bridge, cross sectional area properties of the railway girder are concentrated in one single beam.

In the final local model the railway girder is connected to each T beam through rigid links kinematic constraints. Cross sectional area schematics of railway girder and T beams used for the local model are presented in Figure 9-4 and 9-5, respectively.

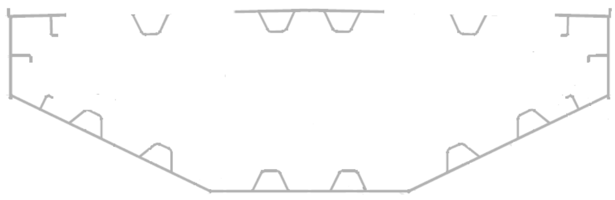

Figure 9-4 Railway girder cross sectional area used in the local multi-beam model.

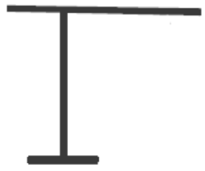

Figure 9-5 – T beam cross sectional area.

A sketch of the multi-beam model is shown in Figure 9-6. Each T beam is first separated and then rigidly connected to the railway girder. Rigid links, highlighted here in blue, are used to connect the railway girder to cross girder and T beams. The railway girder is, indeed, modelled as a five beams finite element model.

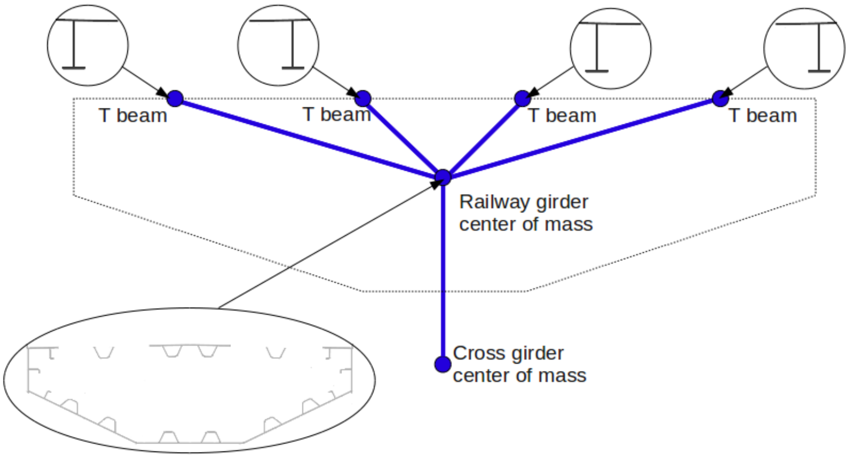

Figure 9-6 Front view of the railway girder multi-beam local model.

The front view of the local finite element multi-beam model of the railway girder is shown in Figure 9-7.

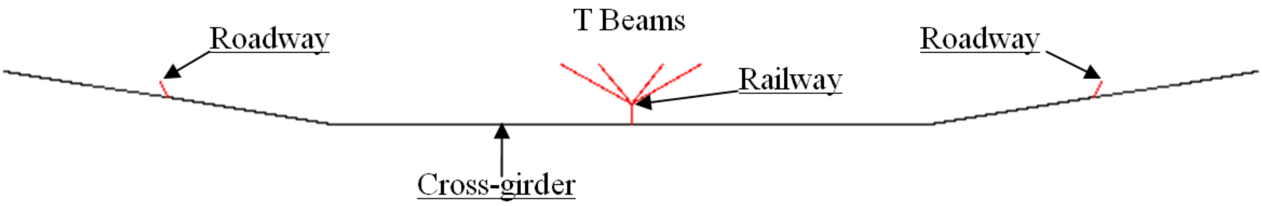

Figure 9-7 Front view of the multi-beam model. Kinematic rigid links, shown here in red, are used to connect the railway girder to cross girder and T beams.

The single-beam finite element schematization is adopted for the roadway girders modeling, for no local detail is needed for the purpose of this work. Kinematic rigid links are used to realize the constraint with the cross girders. The resulting five beams finite element model is then rigidly linked to the cross girder.

Top and isometric views of the 300 m long span local multi-beam model are shown in Figures 9-8 and 9-9.

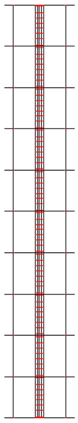

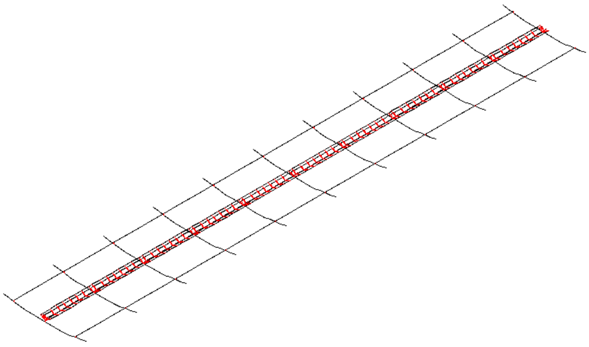

Figure 9-8 Top view of the multi-beam model.

Figure 9-9 Isometric view of the multi-beam model.

Figure 9-10 shows that each T beam is rigidly linked to the railway girder beam even at each diaphragm location.

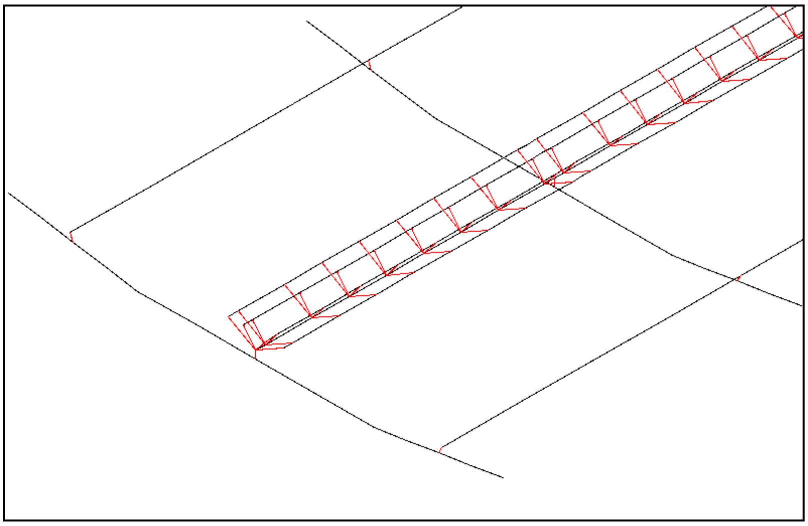

Figure 9-10 T beams are rigidly connected to the railway girder beam at each diaphragm location.

Figure 9-11 shows that each cross girder is rigidly connected to the railway girder beam through rigid links here represented in red.

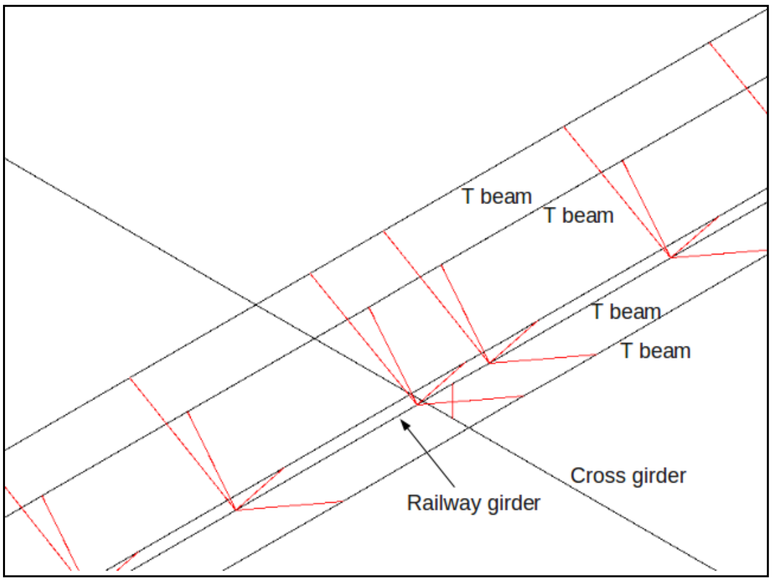

Figure 9-11 Each cross girder is rigidly connected to the railway girder beam.

Figure 9-13 shows the side view of a 30 m long structure where the cross girders are represented at the ends. The spacing among diaphragms is 3.75 m except for the diaphragms located on the cross girders which are placed 0.9375 m away from each cross girder center of mass.

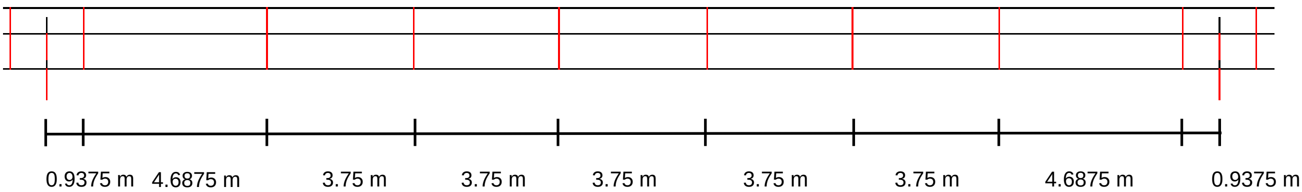

Figure 9-13 – Side view of the multi-beam model. T beams are rigidly linked to the railway beam at each diaphragms location.

A summary of the geometric characteristics of each finite element are presented in Table 9-1, for roadway, railway, cross girders, and T beams and are defined as:

- A = cross sectional area of the beam element [m2]

- Jp = polar moment of inertia [m4]
- Jt = torsional moment of inertia [m4]
- J2 = moment of inertia about the local 2 axis [m4]
- J3 = moment of inertia about the local 3 axis [m4]

	Section	A	J_p	J_t	J_2	J_3
Roadway girder	1	0.5250	9.4450	0.9550	0.4100	9.0350
Railway girder	2	0.2215	2.0391	0.5070	0.2319	1.8072
Cross girder 1	3	0.2380	0.4770	0.4770	0.0770	0.4000
Cross girder 2	4	0.2810	0.8530	0.8530	0.3010	0.5520
Cross girder 3	5	0.3120	1.2340	1.2340	0.5700	0.6640
Cross girder 4	6	0.3530	1.9090	1.9090	1.0950	0.8140
Cross girder 5	7	0.3670	2.1960	2.1960	1.3290	0.8670
Cross girder 6	8	0.3660	2.1920	2.1920	1.3260	0.8660
T beam	9	0.0366	0.0092	0.0000014	0.0065	0.0027

Table 9-1 Section properties of the beam elements.

9.2.2 Material properties

Material properties are set as

- E = 210000 MPa (Young Modulus)

- v = 0.3 (Poisson ratio)
- ρ = 7850 kg/m^3 (steel density)
- α = 0 or 4.23903E-05
- $\beta = 10^{-5}$ or 0.000207004

the α and β sensitivity to the model response have to be verified. The values α = 0 and β = 10^{-5} practically gives no damping associated with the structure, whereas the α = 4.23903E-05 and β = 0.000207004 coefficients are such that to have a 0.28% of damping ratio for the first multi-beam model first mode (4.3 Hz) and a 0.52 % damping ratio for the 14th mode (8.0 Hz), that is a flexural mode and depicted in the following. The correspondent Rayleigh damping graph is also shown).

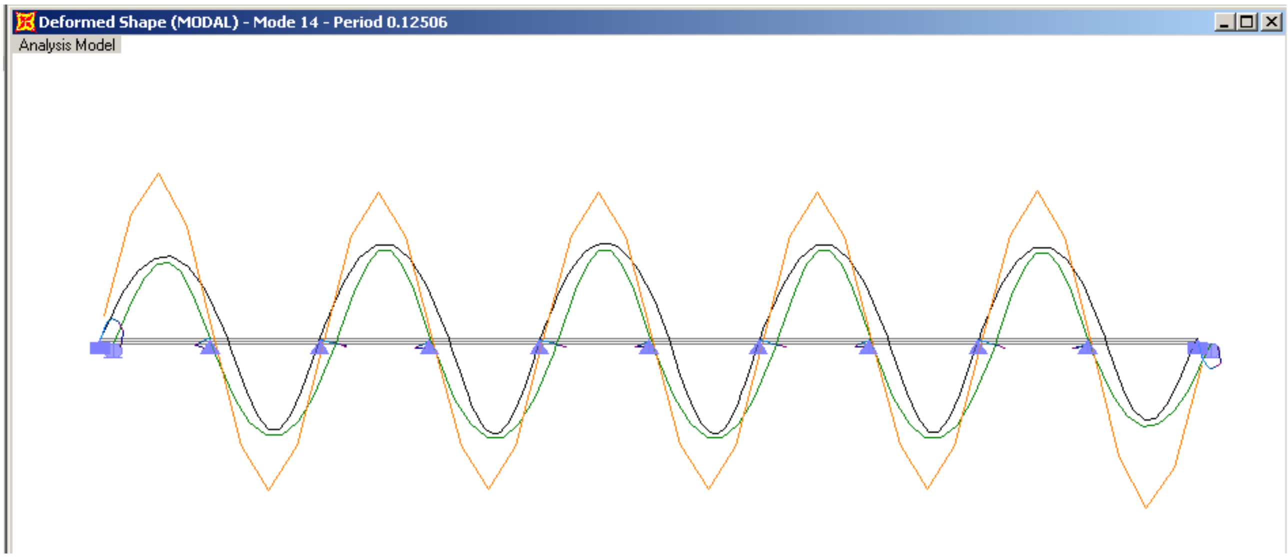

Figure 9-14 14th mode shape of the multi-beam local model (8 Hz).

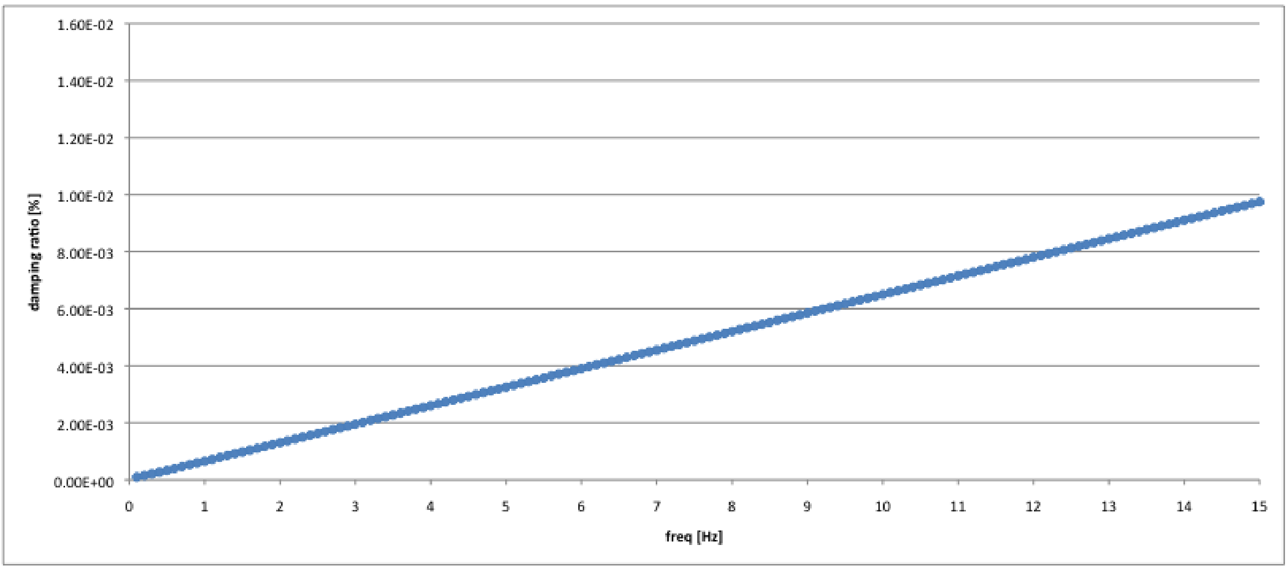

Figure 9-15 Rayleigh damping curve with α = 4.23903E-05 and β = 0.000207004

9.2.3 Girders discretization

Girders are modelled using beam-type finite elements. Each element has one node at each end and its cross sectional area is uniform. Only flexural deformability is taken into account.

Railway girder is discretized by placing one node at each diaphragm location resulting in 8 finite elements between cross girders.

Cross girders are discretized in 12 finite elements in order to account for the variable cross sectional area, as shown in Figure 9-16.

Roadway girders are discretized by placing one node every 7.5 m resulting in 4 finite elements between two cross girders.

T beams are discretized using a variable mesh for the purpose of local analysis. The first and the last spans, respectively, of 90 m and 120 m, are discretized using the same finite element mesh as the railway girder. The central 90 m span, located between 90 m and 180 m along the structure, is refined by placing two additional nodes between two diaphragms yielding 21 finite elements.

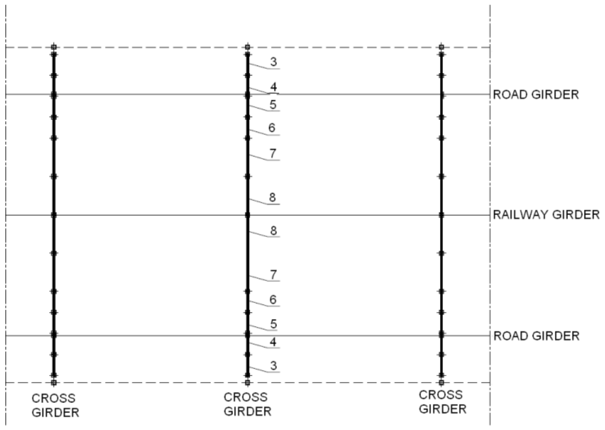

Figure 9-16 Top view of three cross girders. Schematic of variable cross sectional areas.

The initial 90 m and the final 120 m of the T beams have the same mesh as the railway girder. The central 90 m span between 90 m and 180 m is refined by placing two nodes between two diaphragms. Figures 9-17 and 9-18 show the mesh.

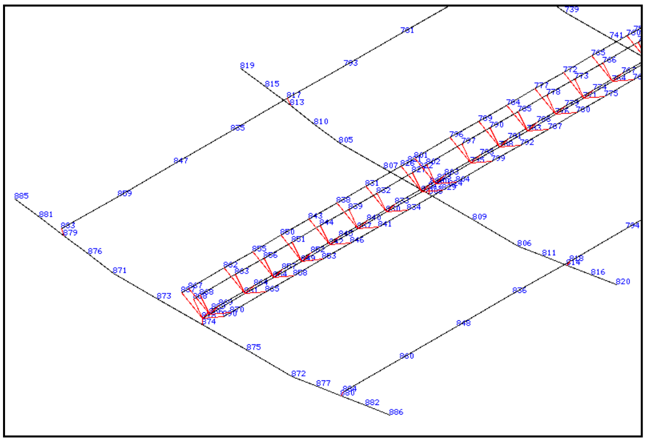

Figure 9-17 Schematic of nodal discretization for roadway, railway, cross girders, and T beams.

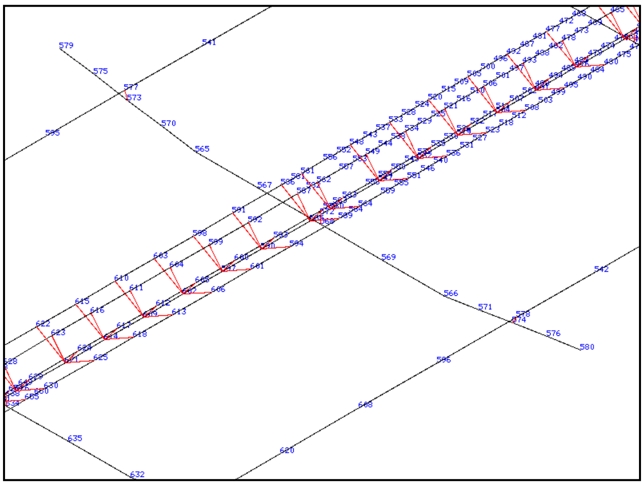

Figure 9-18 T beams are discretized with a finer mesh in the central part of the model.

Figure 9-19 presents the definition of the local system of reference used in the multi-beam model and section properties assignment.

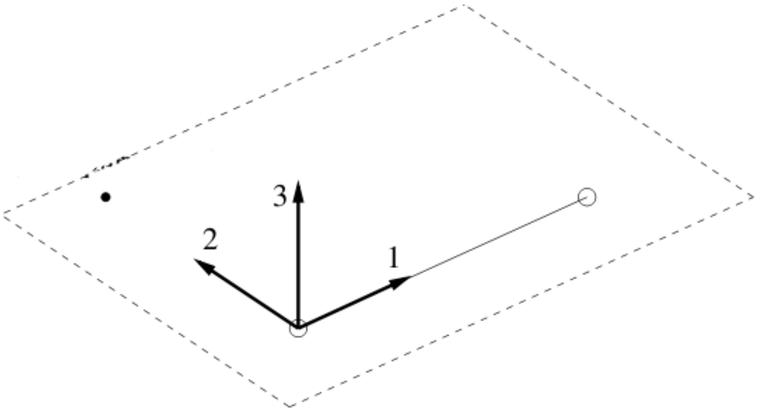

Figure 9-19 Definition of the local system of reference used in the multi-beam model and section properties assignment.

9.2.4 Validation of the structural model

Modal analysis is performed on the multi-beam structure using ADTreS and SAP2000. The objective of a second aid commercial software is based on validation purposes.

9.3 ADTreS Modal Analysis

FRF analysis of the multi-beam model is performed and the extracted modal parameters are listed in Table 9-2. Figure 9-20 shows the FRF plot where the first four peaks correspond to the first four eigenvalues. Figures 9-21 to 9-24 show the eigenvectors associated with their corresponding eigenvalues. Eigenvalues and eigenvectors represent, respectively, proper frequencies and modeshapes.

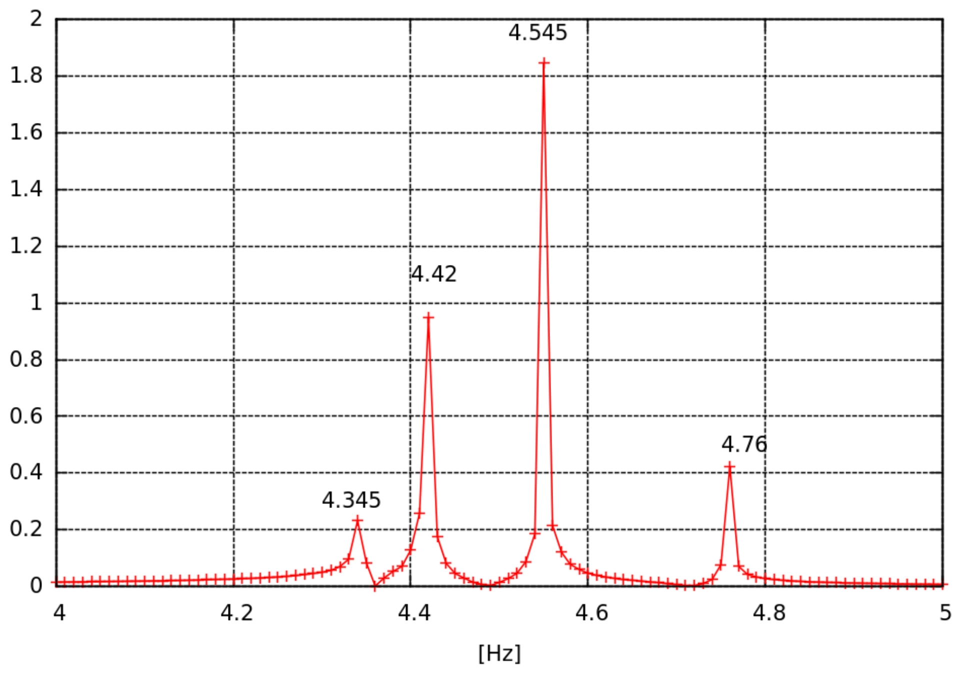

Figure 9-20 FRF plot of the multi-beam model.

Mode	Frequency [Hz]
1	4.345

Table 9-2 Modal frequencies.

2	4.42
3	4.545
4	4.76

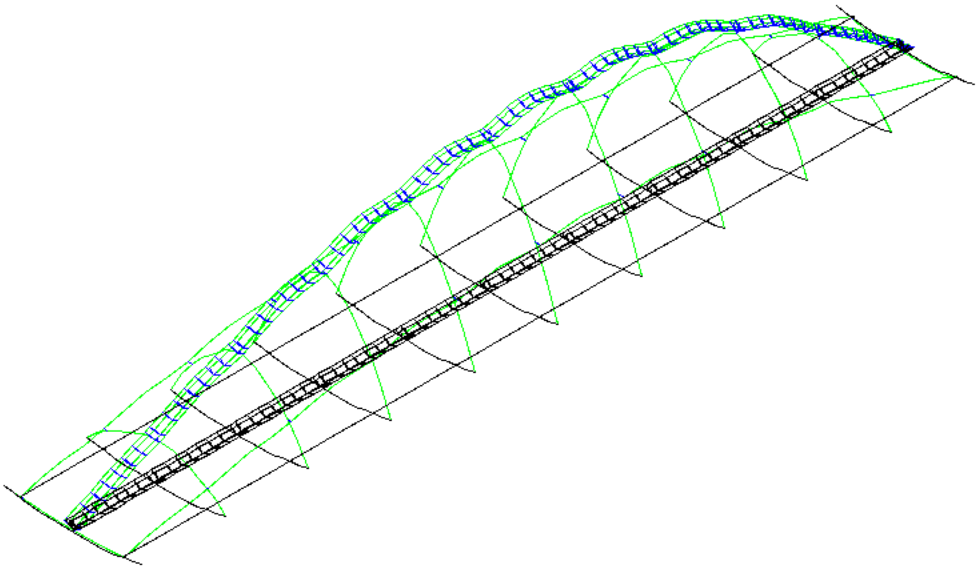

Figure 9-21 Modeshape 1 associated with a frequency equal to 4.345 Hz.

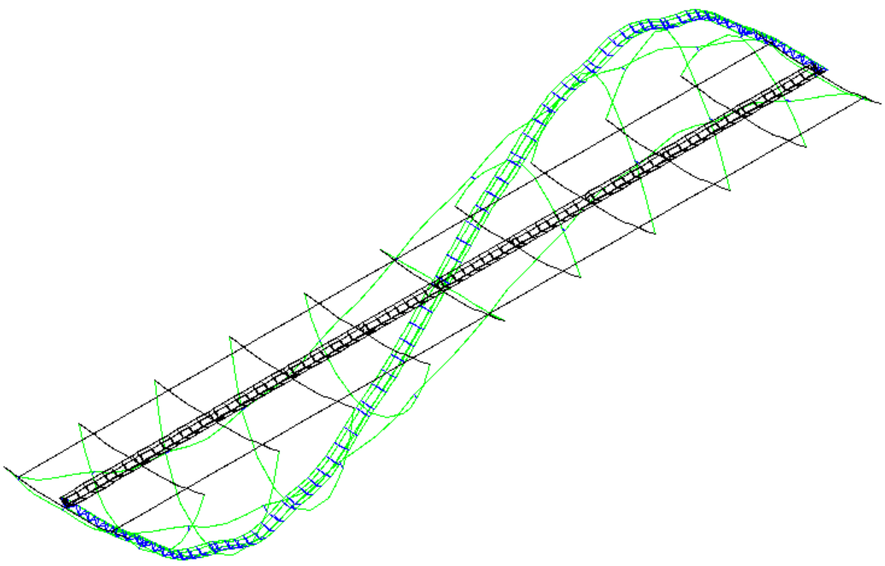

Figure 9-22 Modeshape 2 associated with a frequency equal to 4.42 Hz.

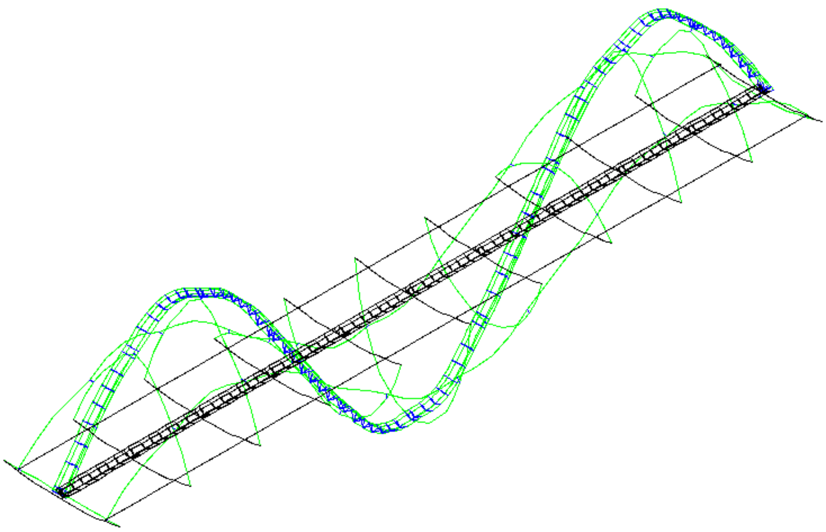

Figure 9-23 Modeshape 3 associated with a frequency equal to 4.545 Hz.

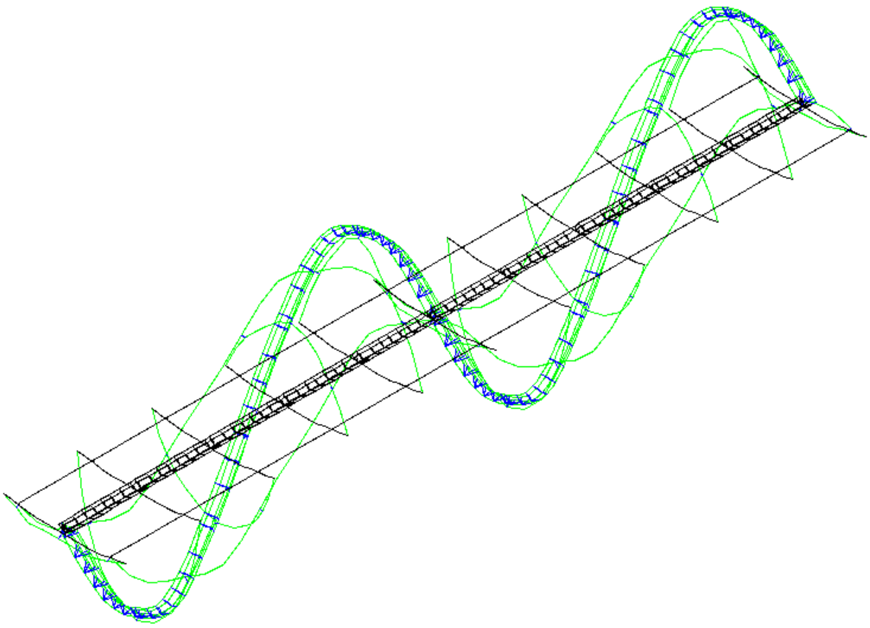

Figure 9-24 Modeshape 4 associated with a frequency equal to 4.76 Hz.

9.4 SAP2000 Modal analysis and comparison

The multi-beam model described in the previous sections is validated using the commercial software SAP2000 v.14 by selecting the same set of parameters and using the same finite element mesh. Modal frequencies and eigenvectors are then extracted and listed in Table 9-3.

Mode	Frequency [Hz] - SAP2000	Frequency [Hz] – ADTreS
1	4.364	4.345
2	4.433	4.42
3	4.560	4.545
4	4.760	4.76

Table 9-3 Modal frequencies SAP2000 vs. ADTreS.

Figures 9-25 – 9-28 show isometric, top, lateral, and front views of the model modeshapes as they are computed by SAP2000.

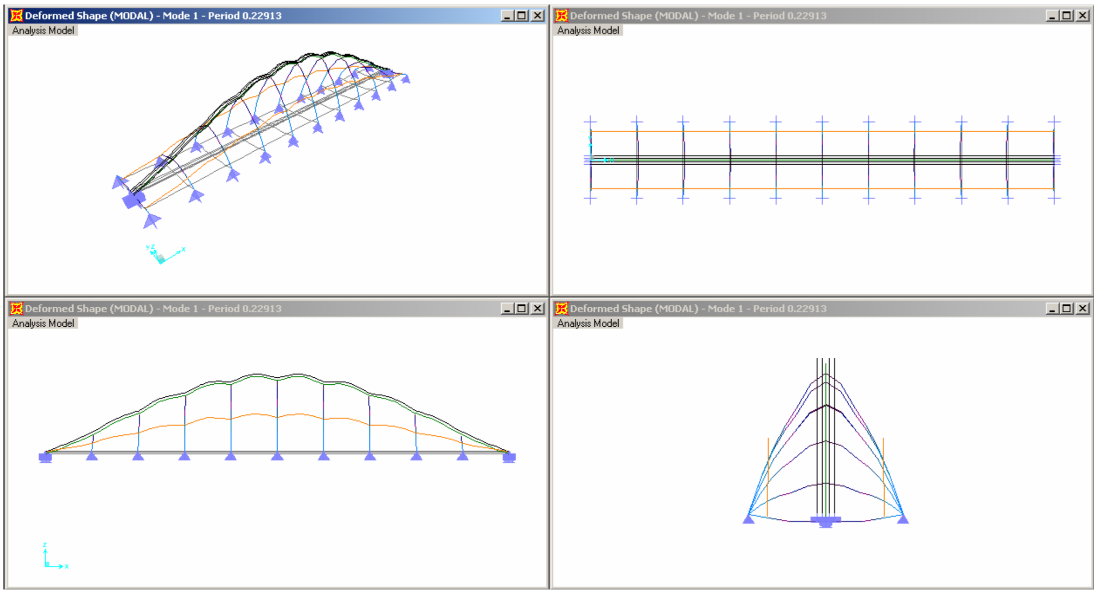

Figure 9-25 Modeshape 1 associated with a frequency equal to 4.364 Hz.

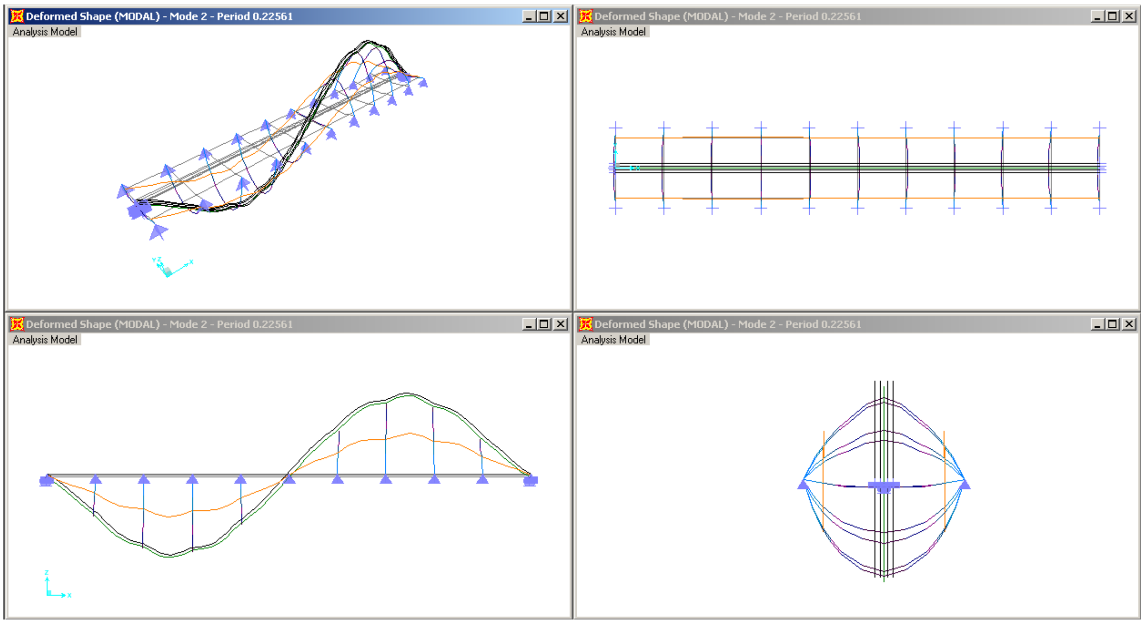

Figure 9-26 Modeshape 2 associated with a frequency equal to 4.433 Hz.

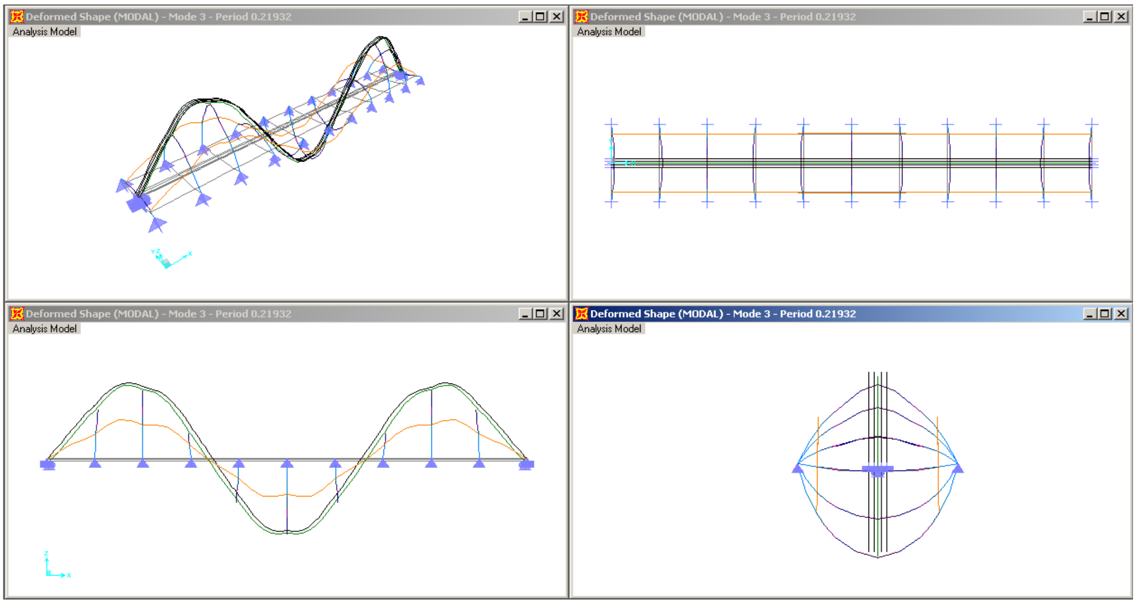

Figure 9-2 Modeshape 3 associated with a frequency equal to 4.56 Hz.

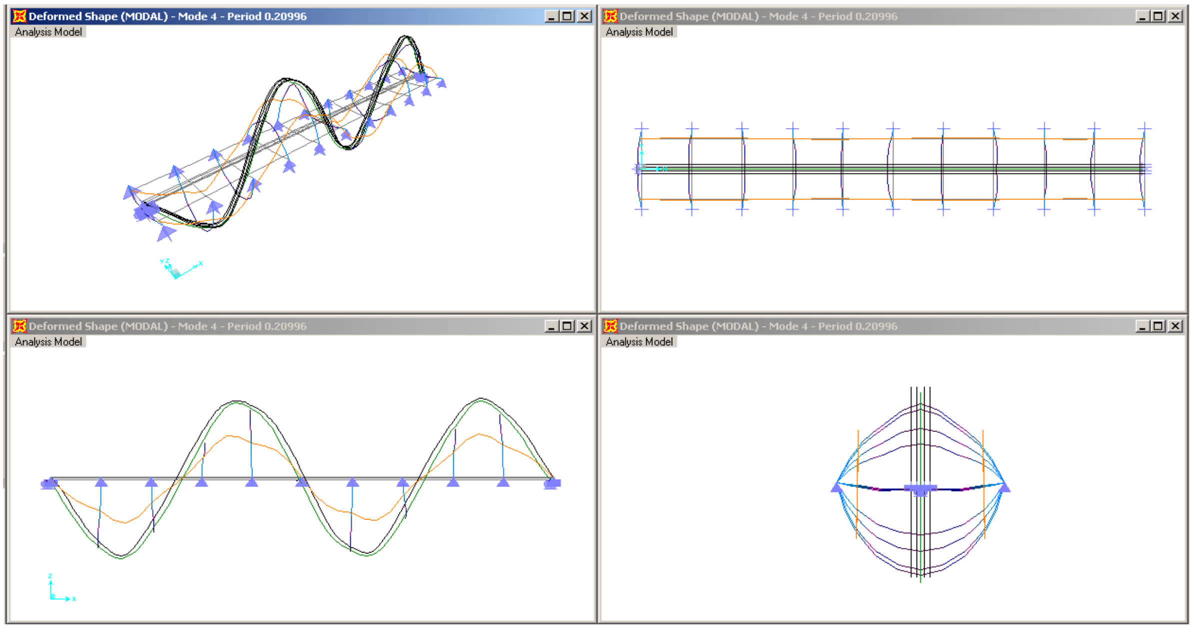

Figure 9-28 Modeshape 4 associated with a frequency equal to 4.76 Hz.

9.5 Embedded rail track and fittings model

The schematization of the structural local model is improved by introducing a model of the embedded rail track. Both rails are laid on a continuous layer of rubber elements along their entire length. The embedded rail mathematical model is developed as follows:

- rails are modeled as beam-type finite elements;
- rubber beds are modeled as a continuous layer of a uniformly distributed set of visco-elastic elements which links the multi-beam finite element model and the rails together.

9.5.1 Rail fittings (mesh properties and type)

A set of visco-elastic finite elements are evenly distributed along the track and located underneath the rails. Stiffness and damping properties are presented in Table 9-4.

Vertical stiffness Kv of the rail-structure link per unit area	1.48E+08 [N/m]/[m^2]
Lateral stiffness KL of the rail-structure link per unit area	0.846E+08 [N/m]/[m^2]
Torsional stiffness Kθx of the rail-structure link per unit length	0.83590E+10 [Nm/rad]/[m]
Vertical damping Cv of the rail-structure link per unit area	1.2E+04 [Ns/m]/[m^2]
Lateral damping CL of the rail-structure link per unit area	1.2E+04 [Ns/m]/[m^2]
Bed lateral (y) length	0.3 [m]

Table 9-4 Visco-elastic characteristics of the embedded rail track finite element model.

Values of the parameters presented in Table 9-4, are chosen such that the vertical and lateral displacements of the rails are less than 2 mm when a vertical load equal to 20 ton/axis and a lateral force of 20000 N are respectively applied.

Figure 9-29 shows a schematic of the two interacting subsystems: the multi-body model of the rail vehicle and the track fittings connected to the bridge structure. Spring and damper elements are also shown in the same figure [3,4].

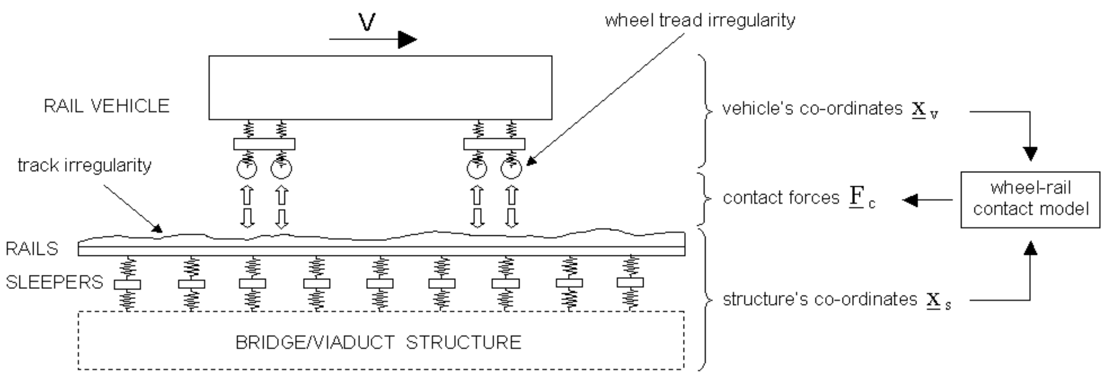

Figure 9-29 The multi-body model of the rail vehicle is coupledto the finite element model of track fittings and bridge structure.

Figure 9-30 shows the isometric view of the embedded rail track finite element model. Rails are modelled as beam-type finite elements and represented here in red. The continuous layer of rubber beds, which is located underneath the rails, is modelled as a set of visco-elastic finite elements and represented here as square black-contour prisms. A distributed set of spring and damper elements is also adopted in the model, but they are not shown in this figure. The whole embedded rail model consists of 2002 nodes.

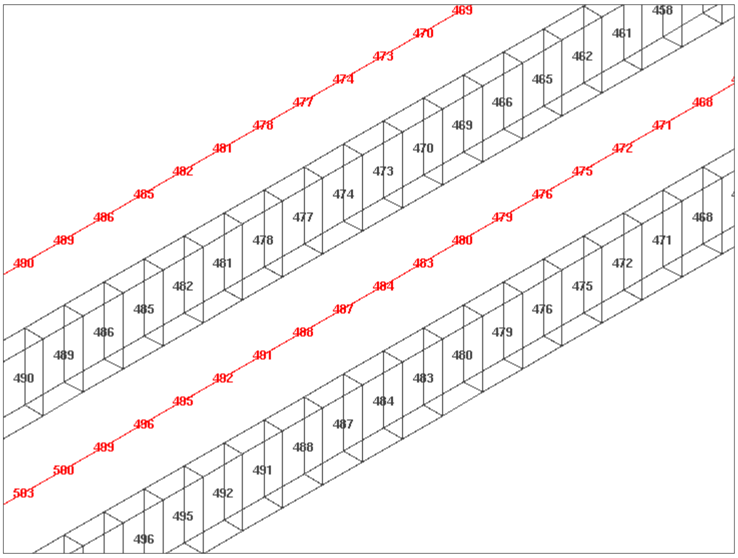

Figure 9-30 Finite element schematic of the embedded rail track model used in the simulations. Both rails and visco-elastic elements are sketched in this figure in red and black lines, respectively.

9.5.2 Rail irregularities (reference to codes)

Rail irregularities are taken into account according to the spectra functions specified by Code ORE B 176 Appendix 6.

9.6 Train Combinations

A detailed set of numerical simulations of train-structure interaction is performed. Table 9-5 shows the full list of numerical simulations performed for the local rail runability analyses.

			Speed [km/h]
RFI 1	ETR 500	Locomotive	144
	ETR 500	Coach	144
RFI 2	ETR470	Locomotive	144
	ETR470	Coach	144
RFI 3	E 402 B	Locomotive	144
			120
			110
			100
			90
			80
			70
			60
			50
	Semipilota MD	Coach	144
RFI 4	TAF	Locomotive	144
	TAF	Coach	144
RFI 5	Freight	Coach	144
RFI 6	Freight	Coach	144

Table 9-5 Set of numerical simulations for the local rail runnability analyses.

10 Local Analysis Results

10.1 Verification Method

Local interaction between train and railway girder is investigated for a short-span structure. A 300 m long finite element local model is developed according to the geometrical and physical characteristics of the full-length scale global finite element model. Figure 10-1 shows that the mid-span location is selected for local modelling and used for numerical simulations and local interaction analyses.

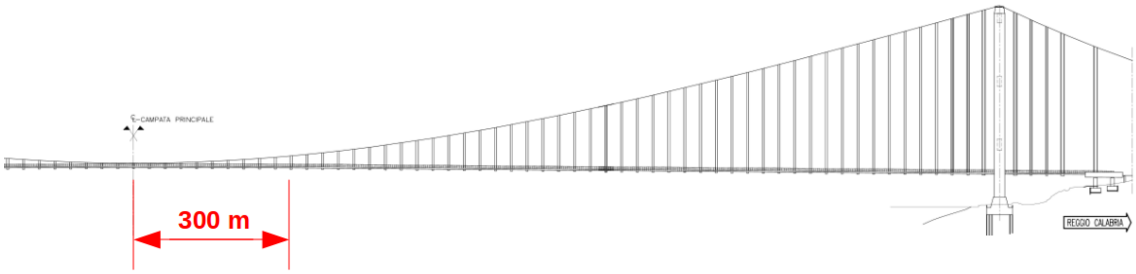

Figure 10-1 Local interaction analyses are performed for a 300 m long sub-model of the bridge at the mid-span location.

The full-length scale bridge used for global analyses is modelled according to a beam-type finite element schematization. A schematic of the 300 m deck model used for global interaction analyses is presented in Figures 10-2 and 10-3 in top and isometric views.

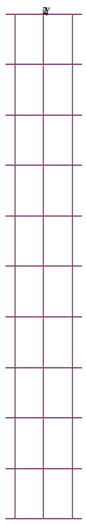

Figure 10-2 Top view of 300 m long deck model.

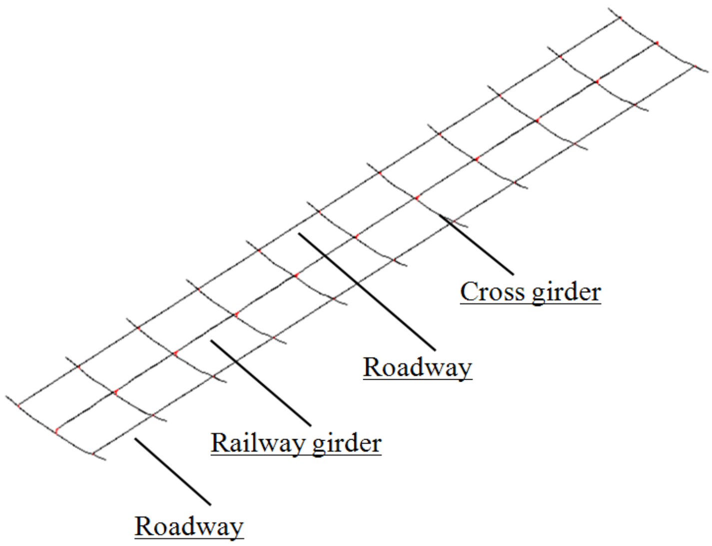

Figure 10-3 Isometric view of 300 m long deck model. Roadway, railway and cross girders are shown

The front view of the deck model is presented in Figure 10-4. It shows that roadway, railway, and cross girders are modeled as a single beam-type finite element model and kinematic constraints are set through a rigid links approach, here shown in red.

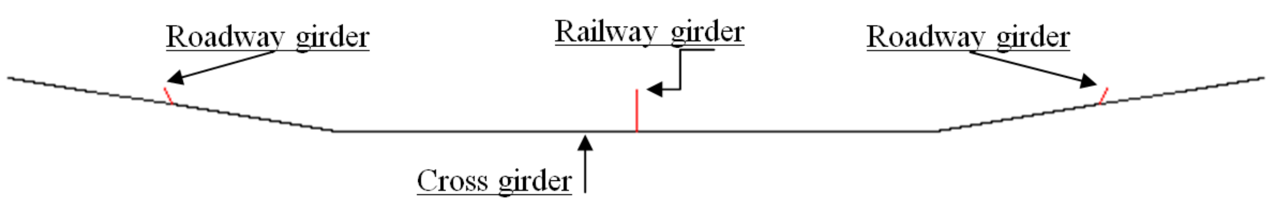

Figure 10-4 – Front view of the deck model. Roadways and railway girders are connected to cross girders through rigid links kinematic constraints, here shown in red.

10.2 Output locations

Four locations of the multi-beam model are accounted for local analyses: cross girders 5 and 6 and diaphragms 3 and 4 between cross girders 5 and 6, as shown in Figure 10-5 and 10-6:

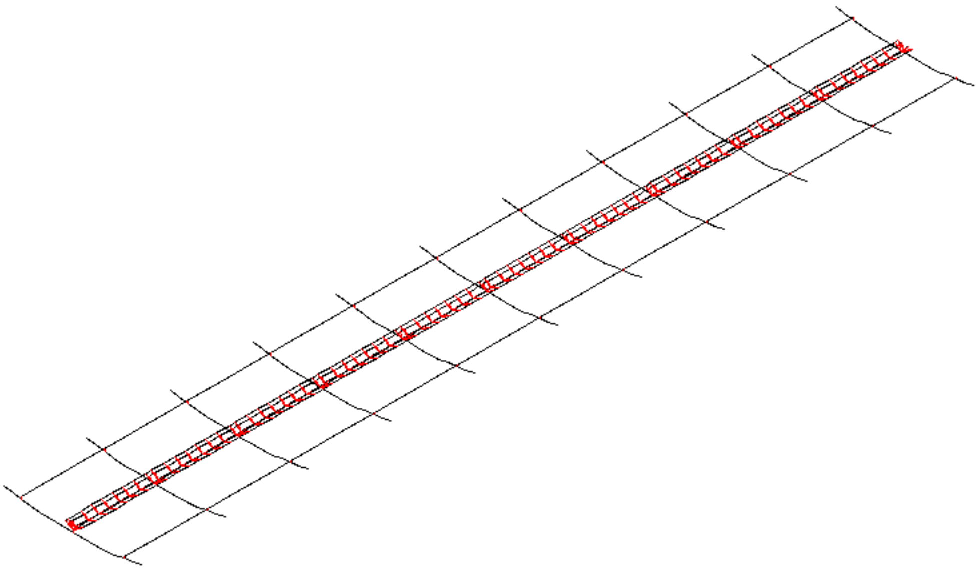

Figure 10-5 Output locations of the local multi-beam model.

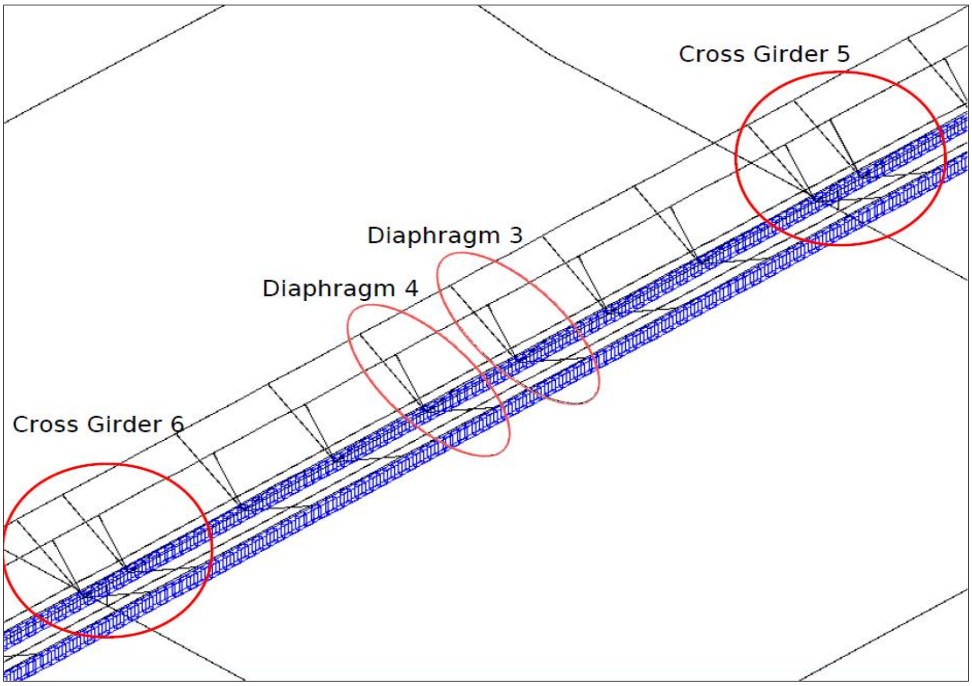

Figure 10-6 Local analyses are performed on the railway girder across cross girders 5 and 6 and diaphragms 3, 4.

Figure 10-7 shows the top view of the locations where analyses are performed.

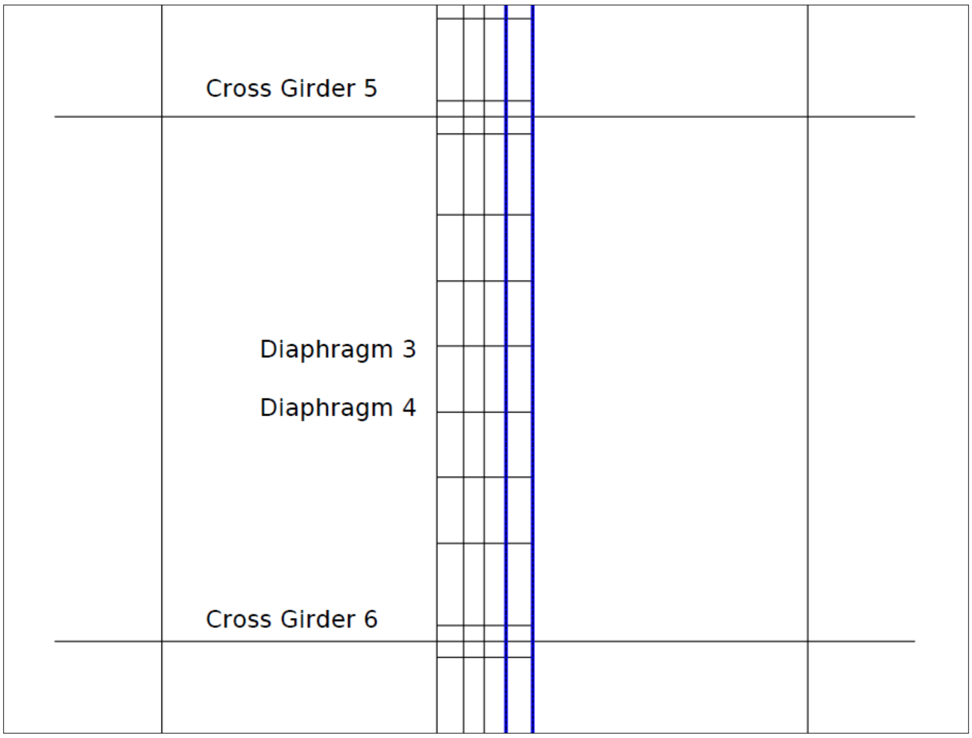

Figure 10-7 Top view of the locations where the analyses are performed.

Figure 10-9 shows the isometric view of the railway girder detail located at the cross girder 5.

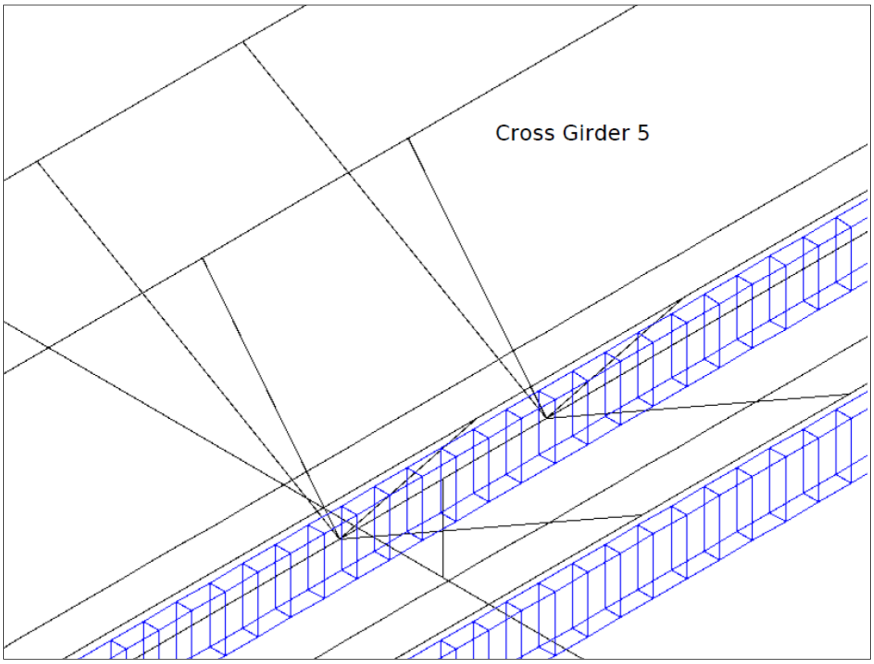

Figure 10-9 Isometric view of the railway girder across cross girder 5.

Figure 10-10 shows the nodal discretization of the railway girder at the cross girder 5.

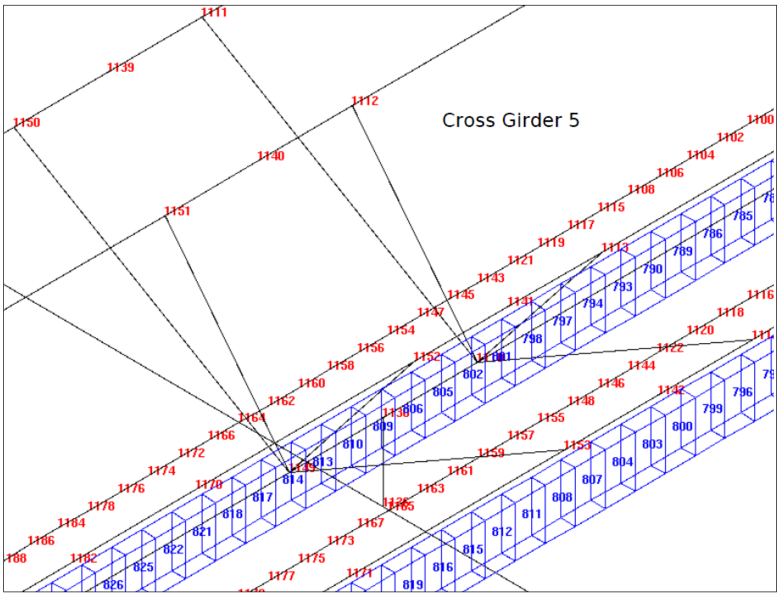

Figure 10-10 Isometric view of the railway girder across cross girder 5 and nodal discretization.

Figure 10-11 shows the top view of the railway girder located at the cross girder 5. Analyses are performed on the nodes circled in red.

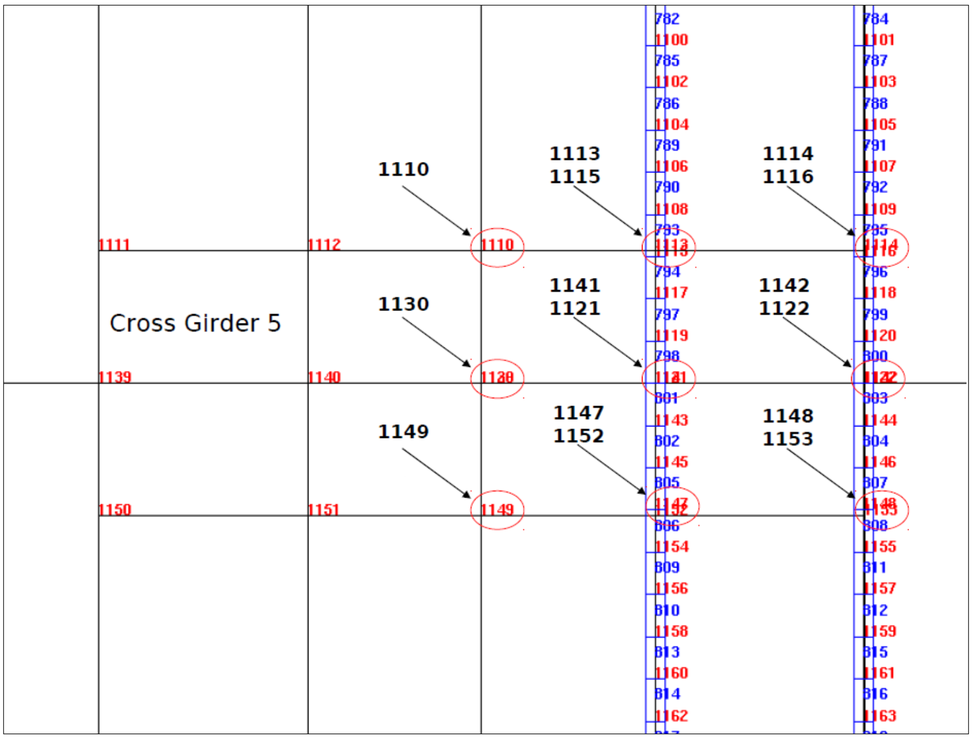

Figure 10-11 Top view of the railway girder across cross girder 5 and nodal discretization.

Figure 10-12 shows the isometric view of the railway girder detail located at the cross girder 5.

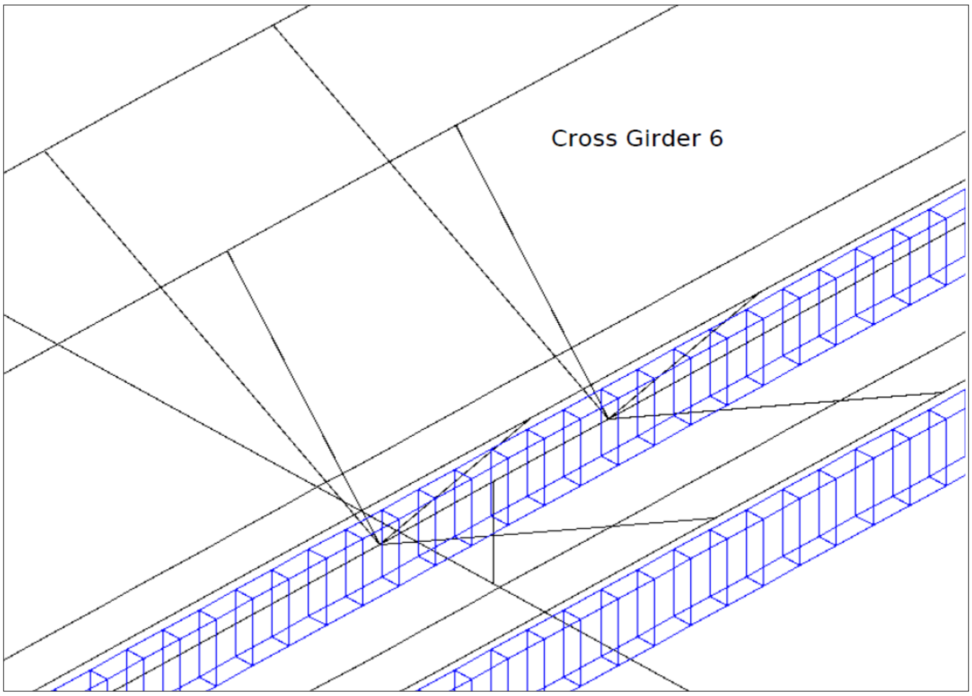

Figure 10-12 Isometric view of the railway girder across cross girder 6.

Figure 10-13 shows the nodal discretization of the railway girder at the cross girder 6.

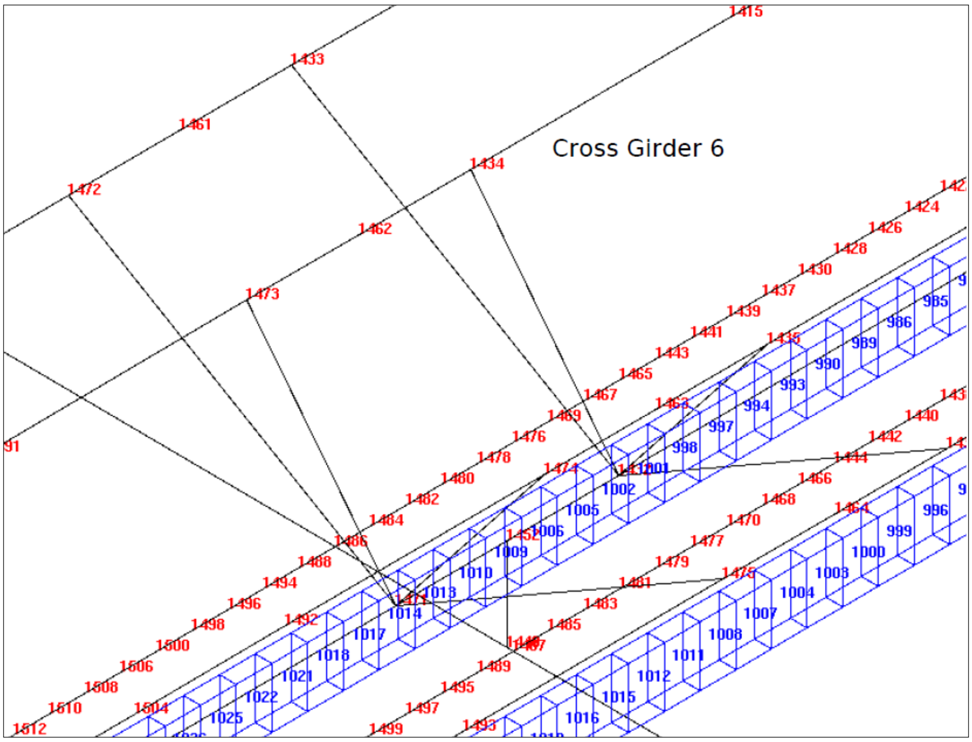

Figure 10-13 Isometric view of the railway girder across cross girder 6 and nodal discretization.

Figure 10-14 shows the top view of the railway girder located at the cross girder 6. Analyses are performed on the nodes circled in red.

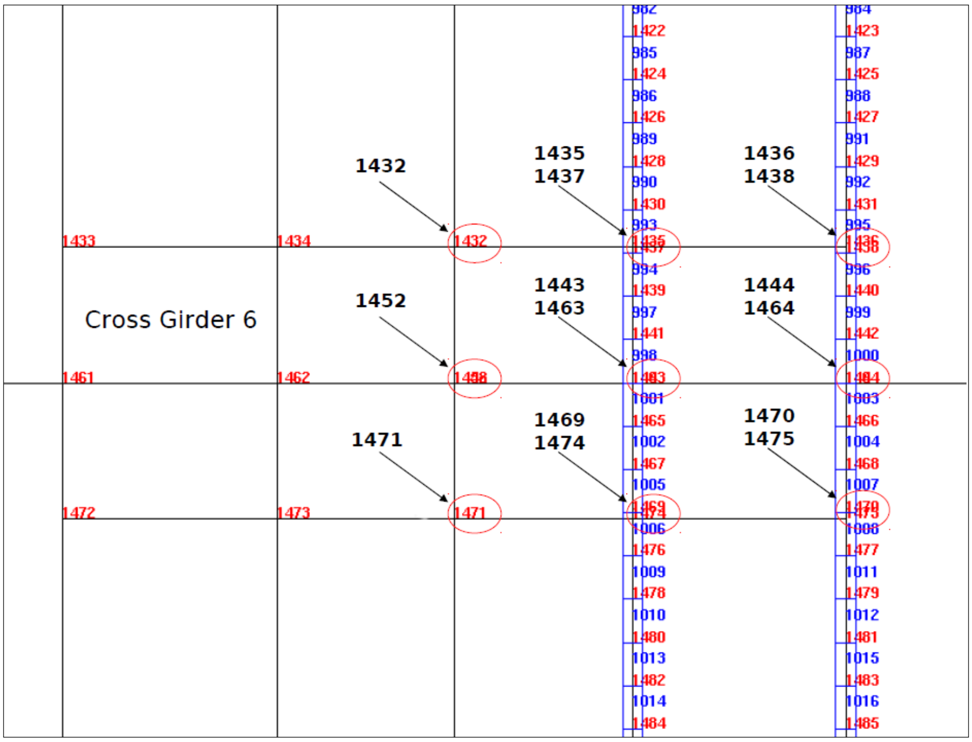

Figure 10-14 Top view of the railway girder across cross girder 6 and nodal discretization.

Figure 10-15 shows the isometric view of the railway girder detail between diaphragms 3 and 4 located between cross girders 5, 6.

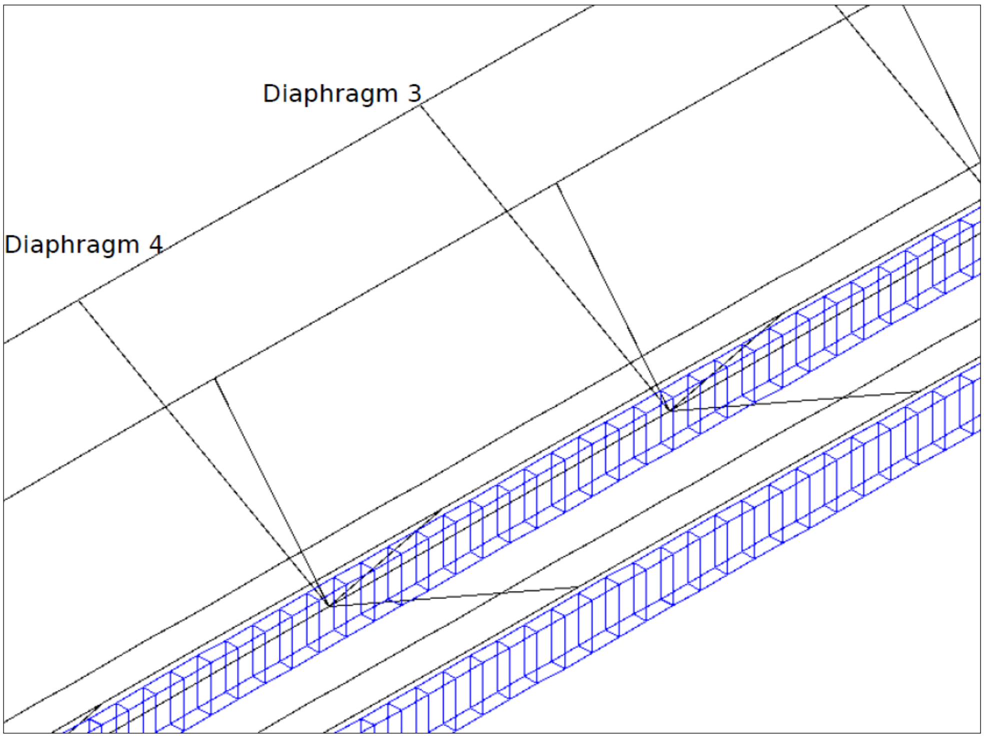

Figure 10-15 Isometric view of the railway girder across diaphragms 3 and 4.

Figure 10-16 shows the nodal discretization of the railway girder between diaphragms 3 and 4.

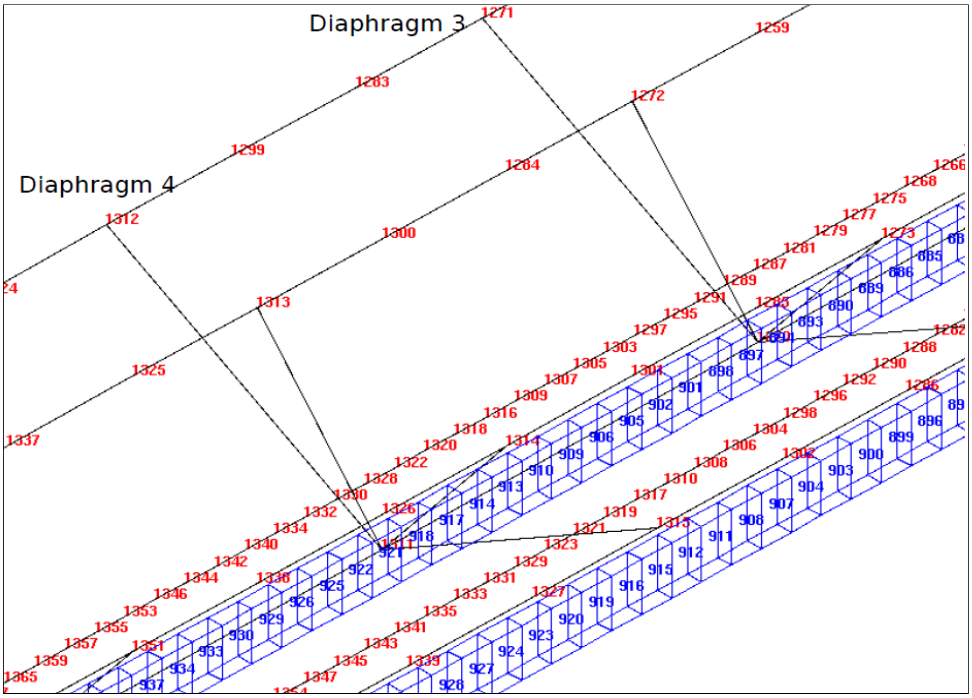

Figure 10-16 Isometric view of the railway girder across diaphragms 3 and 4 and nodal discretization.

Figure 10-17 and 10-18 show the top view of the railway girder detail located between diaphragms 3 and 4. Analyses are performed on the nodes circled in red.

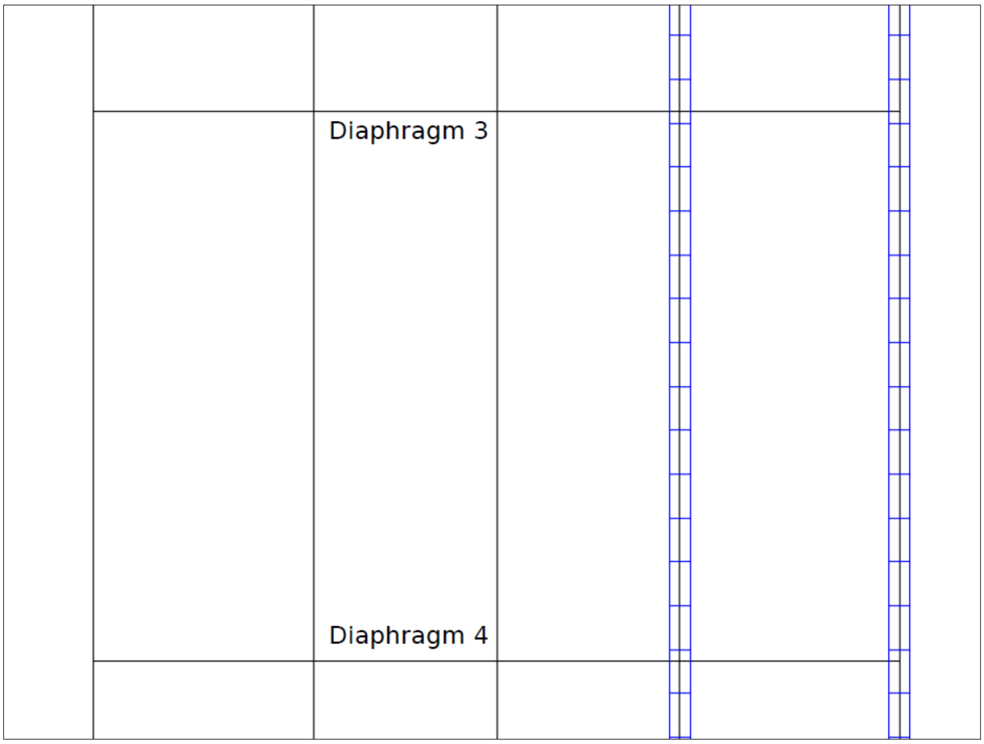

Figure 10-17 Top view of the railway girder across diaphragms 3 and 4.

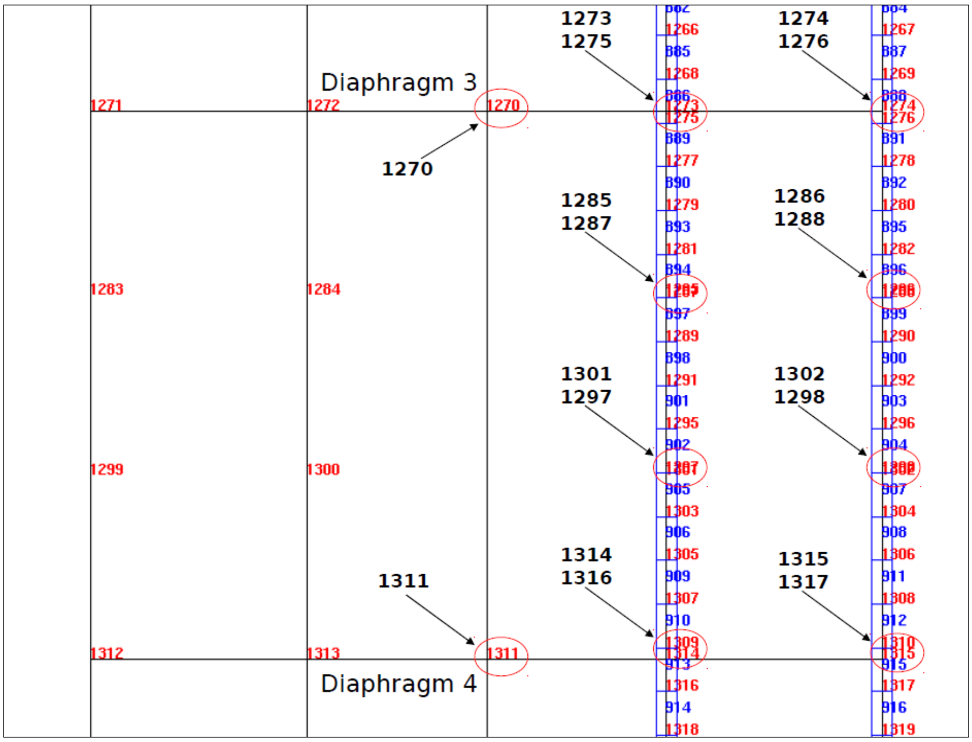

Figure 10-18 Isometric view of the railway girder across diaphragms 3 and 4 and nodal discretization.

10.3 Output quantities

The evaluation of dynamic effects of the train transit on the structural local model of the bridge is assessed in this section. The overall parameter which better synthesize these effects is a dynamic amplification factor defined as the ratio between the maximum dynamic value and the maximum static value of a quantity Q, such as deflection or stress. This ratio, from now on, will be referred to as Impact Factor: IF = Q MAX dyn / Q MAX st .

A full set of numerical simulations is performed according to the list presented in Table 9-5. Dynamic train transit simulations are compared to the static transit of equivalent axle loads nearby cross girders and diaphragms at the locations described in section 10.2. Impact Factors are computed from quantities Q representing nodal forces and displacements, particularly :

1 force transmitted to the visco-elastic beds on the left and right hand side of the track fittings;

2 maximum vertical wheel-rail contact force at different vehicle speeds;

3 nodal vertical displacement difference between rail and T beam on the left and right hand side of the track.

4 Analysis of local effects is also performed by computing track and vehicle acceleration peaks:

5 nodal vertical acceleration peaks of right and left rails and T beams;

6 nodal vertical acceleration peaks of the railway girder;

7 vertical acceleration peaks of the vehicle body;

8 non-compensated acceleration peaks of the vehicle body.

The Visco-elastic beds locations have been resumed from Appendix 2 and shown in figure 10-19 and the results have been summarized for the above simulations in table 10-1 and 10-2.

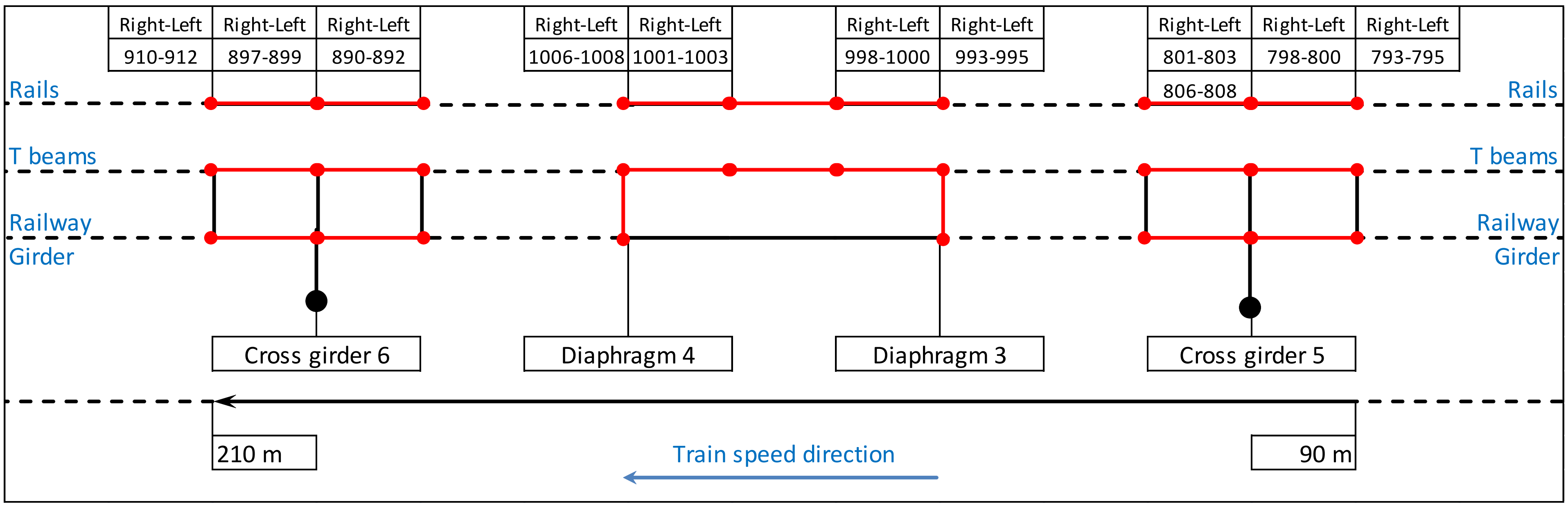

Figure 10-19 Visco-elastic beds locations

		Max Visco-Elastic Bed Force						Max Contact Force	Max Nodal Dynamic Vertical Displacement LEFT Rail-Tbeam				Max Nodal Dynamic Vertical Displacement RIGHT Rail-Tbeam			
RFI type	Speed [km/h]	Bed #	Left Bed [N]	I.F.	Bed #	Right Bed [N]	I.F.	Force [N]	Rail Node #	T beam Node #	Displacement [m]	I.F.	Rail Node #	T beam Node #	Displacement [m]	I.F.
1 - loco	144	795	13400	1,165	1006	15500	1,353	115000	1317	1315	-2,250E-03	1,216	1275	1273	-2,180E-03	1,172
1 - coach	144	795	7250	1,450	806	6889	1,378	58000	1116	1114	-1,079E-03	1,336	1275	1273	-1,152E-03	1,426
2 - loco	144	1000	11283	1,220	998	11260	1,217	88000	1470	1475	-1,790E-03	1,197	1297	1301	-1,794E-03	1,200
2 - coach	144	1000	9120	1,118	910	9670	1,184	80000	1148	1153	-1,540E-03	1,165	1275	1273	-1,554E-03	1,175
	144	995	17730	1,182	890	17600	1,173	150000	1438	1436	-2,830E-03	1,167	1316	1314	-2,700E-03	1,111
	120	795	17500	1,167	998	17500	1,171	142000	1298	1302	-2,900E-03	1,208	1275	1273	-2,800E-03	1,155
	110	795	17800	1,187	910	16700	1,113	140000	1298	1302	-2,750E-03	1,132	1275	1273	-2,700E-03	1,111
	100	795	17000	1,133	890	17000	1,133	135000	1298	1302	-2,740E-03	1,132	1287	1285	-2,670E-03	1,094
3 - loco	90	800	16900	1,134	890	17300	1,153	130000	1298	1302	-2,750E-03	1,136	1287	1285	-2,670E-03	1,103
	80	1008	16000	1,067	993	16500	1,100	131000	1116	1114	-2,650E-03	1,095	1437	1435	-2,655E-03	1,095
	70	795	16500	1,100	993	16500	1,100	127000	1116	1114	-2,650E-03	1,095	1437	1435	-2,600E-03	1,074
	60	795	16300	1,087	910	16100	1,073	128000	1122	1142	-2,620E-03	1,083	1316	1314	-2,580E-03	1,062
	50	808	17000	1,133	910	16100	1,073	123000	1122	1142	-2,700E-03	1,116	1316	1314	-2,600E-03	1,083
3 - coach	144	1000	8650	1,587	806	10300	1,597	82000	1148	1153	-1,550E-03	1,483	1147	1152	-1,658E-03	1,585
4 - loco	144	995	16000	1,185	1006	16000	1,185	125000	1444	1464	-2,500E-03	1,147	1437	1435	-2,635E-03	1,205
4 - coach	144	1008	12400	1,187	897	13000	1,238	110000	1317	1315	-2,050E-03	1,220	1275	1273	-2,100E-03	1,243
5 - freight	144	1000	18500	1,108	910	22600	1,353	148000	1470	1475	-2,985E-03	1,106	1287	1285	-3,220E-03	1,193
6 - freight	144	800	8600	1,504	890	9060	1,584	67900	1317	1315	-1,510E-03	1,641	1443	1463	-1,450E-03	1,576

Table 10-1 Results of simulations

		Max Nodal Vertical Acceleration LEFT Side				Max Nodal Vertical Acceleration RIGHT Side				Max Vertical Railway Girder Acceleration		Body Vertical Acceleration	Non-Compensated Acceleration
RFI type	Speed [km/h]	Rail Node #	Acceleration [m/s^2]	T beam Node #	Acceleration [m/s^2]	Rail Node #	Acceleration [m/s^2]	T beam Node #	Acceleration [m/s^2]	Node #	Acceleration [m/s^2]	Acceleration [m/s^2]	Acceleration [m/s^2]
1 - loco	144	1122	53,237	1286	5,218	1438	41,492	1285	2,824	1311	2,277	0,222	0,098
1 - coach	144	1116	49,884	1302	5,322	1275	50,669	1314	2,625	1311	2,543	0,131	0,22
2 - loco	144	1276	41,683	1286	5,77	1297	42,402	1285	3,146	1311	2,931	0,162	0,091
2 - coach	144	1276	42,754	1302	5,54	1287	43,264	1301	2,508	1311	2,294	0,192	0,088
3 - loco	144	1122	47,706	1302	5,78	1438	49,891	1314	4,649	1311	4,076	0,259	0,217
	120	1437	34,167	1286	4,103	1121	37,032	1285	2,758	1311	2,171	0,248	0,179
	110	1317	26,732	1315	2,62	1444	36,419	1314	1,858	1311	1,757	0,222	0,174
	100	1122	22,254	1286	2,806	1297	23,76	1285	2,119	1270	1,744	0,219	0,18
	90	1148	15,96	1274	2,835	1297	20,95	1314	2,044	1311	1,823	0,257	0,169
	80	1469	18,814	1286	2,152	1115	12,464	1273	1,603	1270	1,221	0,329	0,138
	70	1122	12,551	1286	1,851	1121	11,893	1314	1,527	1311	1,324	0,315	0,16
	60	1148	9,877	1302	1,129	1275	9,266	1285	0,932	1311	0,815	0,209	0,167
	50	1148	7,877	1302	0,929	1275	7,226	1285	0,722	1311	0,51	0,131	0,138
3 - coach	144	1116	64,233	1302	5,987	1275	51,892	1314	3,387	1311	3,254	0,229	0,201
4 - loco	144	1122	57,426	1286	5,755	1297	41,913	1301	4,165	1270	3,511	0,207	0,115
4 - coach	144	1122	52,673	1286	6,324	1297	52,054	1314	3,841	1311	3,699	0,229	0,113
5 - freight	144	1122	47,672	1302	5,167	1297	45,751	1285	2,299	1311	1,713	0,385	0,316
6 - freight	144	1437	64,895	1315	2,332	1297	41,633	1314	1,718	1311	1,562	1,579	4,858

Table 10-2 Results of simulations

The complete set of results are shown in Appendix 2, Local simulation results

10.4 Vehicle accelerations analysis

Table 10-3 presents vertical and non-compensated accelerations peaks of all RFI vehicles taken into consideration.

			Speed [km/h]	Body Vertical Acceleration [m/s^2]	Non-compensated Acceleration [m/s^2]
RFI 1	ETR 500	Locomotive	144	0,222	0,098
	ETR 500	Coach	144	0,131	0,220
RFI 2	ETR470	Locomotive	144	0,162	0,091
	ETR470	Coach	144	0,192	0,088
RFI 3	E 402 B	Locomotive	144	0,259	0,217
			120	0,248	0,179
			110	0,222	0,174
			100	0,219	0,180
			90	0,257	0,169
			80	0,329	0,138
			70	0,315	0,160
			60	0,209	0,167
			50	0,131	0,138
	Semipilota MD	Coach	144	0,229	0,201
RFI 4	TAF	Locomotive	144	0,207	0,115
	TAF	Coach	144	0,229	0,113
RFI 5	Freight Full Load	Coach	144	0,385	0,316
RFI 6	Freight Empty	Coach	144	1,579	4,858

Table 10-3 Vehicle body vertical and non-compensated accelerations.

10.5 Vehicle vertical wheel load analyses

Table 10-4 shows Impact Factors of the vertical wheel load measured on the front wheelset of each vehicle moving at a speed of 144 km/h.

	144 km/h		Static Vertical Load [N]	Dynamic Vertical Load [N]	Impact Factor
RFI 1	ETR 500	Locomotive	8,50E+04	1,15E+05	1,3529
	ETR 500	Coach	3,80E+04	5,80E+04	1,5263
RFI 2	ETR470	Locomotive	6,80E+04	8,80E+04	1,2941
	ETR470	Coach	5,90E+04	8,00E+04	1,3559
RFI 3	E 402 B	Locomotive	1,14E+05	1,50E+05	1,3193
	Semipilota MD	Coach	4,70E+04	8,10E+04	1,7234
RFI 4	TAF	Locomotive	9,90E+04	1,35E+05	1,3636
	TAF	Coach	7,80E+04	1,10E+05	1,4103
RFI 5	Freight Full Load	Coach	1,20E+05	1,48E+05	1,2333
RFI 6	Freight Empty	Coach	3,50E+04	6,79E+04	1,9386

Table 10-4 Impact Factors of the vertical wheel load for the front wheelset of each rail vehicle speeding at 144 km/h.

Table 10-5 shows Impact Factors of the vertical wheel load measured on the front wheelset of the locomotive E402B for a speed range between 50 km/h and 144 km/h with a step size of 10 km/h.

E402B locomotive	Speed [km/h]	Static Vertical Load [N]	Dynamic Vertical Load [N]	Impact Factor
	144	1,137E+05	1,50E+005	1,31889618
	120	1,137E+05	1,42E+005	1,24855505
	110	1,137E+05	1,40E+005	1,230969768
	100	1,137E+05	1,35E+005	1,187006562
	90	1,137E+05	1,30E+005	1,143043356
	80	1,137E+05	1,31E+005	1,151835997
	70	1,137E+05	1,27E+005	1,112269112
	60	1,137E+05	1,28E+005	1,125458074
	50	1,137E+05	1,23E+005	1,081494868

Table 10-5 Impact Factors of the vertical wheel load for the front wheelset of the locomotive E402B for a speed range between 50 km/h and 144 km/h.

			Vehicle speed [km/h]	Vehicle Mass [kg]	Vehicle total length [m]	Max bed Impact Factor	Max vertical wheel load [N]
RFI 1	ETR 500	Locomotive	144	68200	21,5	1,35	1,15E+05
	ETR 500	Coach	144	29675	27,5	1,45	5,80E+04
RFI 2	ETR470	Locomotive	144	55049	26,5	1,22	8,80E+04
	ETR470	Coach	144	49442	26,5	1,19	8,00E+04
RFI 3	E 402 B	Locomotive	144	88968	20,4	1,2	1,50E+05
			120			1,16	1,42E+05
			110			1,18	1,40E+05
			100			1,13	1,35E+05
			90			1,15	1,30E+05
			80			1,09	1,31E+05
			70			1,1	1,27E+05
			60			1,08	1,28E+05
			50			1,13	1,23E+05
	Semipilota MD	Coach	144	38440	27,5	1,76	8,10E+04
RFI 4	TAF	Locomotive	144	75090	27,4	1,18	1,25E+05
	TAF	Coach	144	62165	25,6	1,23	1,10E+05
RFI 5	Freight Full Load	Coach	144	99312	14	1,35	1,48E+05
RFI 6	Freight Empty	Coach	144	27125	23,2	1,58	6,79E+04

10.6 Comparison with Design Loads (Instructions from RFI)

With reference to table 10-3, the maximum vertical dynamic load is observed for E402B Locomotive, when runs at 144 km/h, and the calculated value is 150 kN x 2 = 300 kN for the front wheel-set. This value is used for the comparison with the worst load case in the static case.

The worst load case used for local verification in the static case is taken from the RFI instruction labelled as “ISTRUZIONI PER LA PROGETTAZIONE E L’ESECUZIONE DEI PONTI FERROVIARI - RFIDTC-ICI-POSPINF001A”. The train selected for purpose is the so called LM71, that is a theoretic train model defined by lumped and unlimited distributed forces as in the figure 10-20. The selected train rules the static local verifications for lengths were the lumped forces instead of the distributed give the greater influence. This is our case if the used length for local verifications is the distance between two transversal diaphragms i.e. 3.75 m.

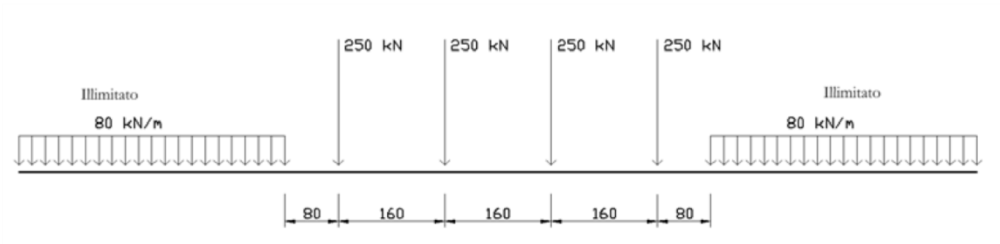

Figure 10-20 Figure at page 27 of RFIDTC-ICI-POSPINF001A instruction

The static verification can be made by considering a lumped load, or a distribution of lumped loads, that is amplified by two coefficients. The former is called α and represents an adapting coefficient that depends on the bridge type. In our case category A have to be considered and the coefficient is α = 1.1 as reported in table 10-6

MODELLO DI CARICO	COEFFICIENTE "α"	
	CATEGORIA "A"	CATEGORIA "B"
LM71	1.1	0.83(1)
SW/0	1.1	0.83(1)
SW/2	1.0	0.83(1)

Table 10-6 Table at page 27 of RFIDTC-ICI-POSPINF001A instruction

The second is a dynamic amplification coefficient and is calculated from the following formula (see page 37 of the RFI instructions):

$$\Phi_2 = \frac{1,44}{\sqrt{L_\phi} - 0,2} + 0,82 \qquad 1.00 \le \Phi_2 \le 1.67$$

being L_ϕ the characteristic length (in meters) defined for simply supported beams and that can be extended to other structure categories by proper scale factors.

In our case the governing length is the distance between two diaphragms: 3.75 m and the characteristic length is given by multiplying it by a factor of 3, that is the factor used for local tension verifications in the case of a steel grillage without ballast (see page 41 of the RFI instructions).

In this case $\Phi_2 = 1.277$.

By considering the associated simply supported scheme, the worst case scenario in the case of lumped forces is given by the scheme in 10-21 (distances measured in meters).

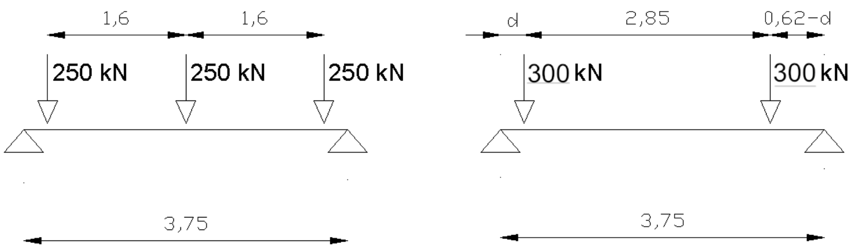

Figure 10-21 Left) static loads (LM71); right) dynamic loads (E402B from multibeam).

From figure 10-21 appears clear that the forces considered in the left scheme give greater effects than the forces in the right scheme, independently from the “d” value.

For this reason a simplified and worst case load comparison is given, by comparing the single wheel-set load:

static load: 250x1.1x1.277 = 351.175 kN > 300 kN.

In order to give a complete picture of the comparison the LM71 static load model is calculated for the 30 m characteristic length (1) (that is the length between two hangers) and the whole 300 m local model length (2).

1 When 30 m of characteristic length is considered the load model in fighure 9.x.x applies and the total static load is given by the expression: 250x4 + 80x(30-6.4) = 2888 kN. This load value is amplified by the adapting coeff. $\alpha = 1.1$ and the dynamic factor Φ_2 that is calculated by considering 4 times the characteristic length of 30 m (see page 47 of the RFI instructions, point 5.7). In this case $\Phi_2 < 1$ and then is posed $\Phi_2 = 1$. The resulting amplified static load is: 3177 kN

   The dynamic load is calculated by considering the full dynamic load from the locomotive and the dynamic load from the part of the coach required to fill up the 30 m length.

With reference to table 10-3, the resulting dynamic force is: 150x8 + 81x8x(30-20.4)/27.5 = 1426.2 kN < 3177.0 kN

2 When 300 m of characteristic length is considered, again the load model in fighure 10-20 applies and the total static load is given by the expression: 250x4 + 80x(300-6.4) = 24488 kN. This load value is amplified by the adapting coeff. α = 1.1 and the dynamic factor Φ_2, that is now calculated by considering 1.5 times the characteristic length of 30 m (see page 47 of the RFI instructions, point 5.2), when the considered model is a continuous beam with ten spans of 30 m each. In this case Φ_2 = 1.04. The resulting amplified static load is: 28048 kN

The dynamic load is calculated by considering the full dynamic load from the locomotive and the dynamic load from the number the coaches required to fill up the 300 m length.

With reference to table 10-3, the resulting dynamic force is: 150x8 + 81x8x(300-20.4)/27.5 = 7789 kN < 28048 kN

In case (2) the grater dynamic load value is taken from the simulation of the RFI4, that have a greater amplification from the coach with respect to the RFI3 (i.e. E402B). For the RFI4 the resulting dynamic force is again less than the amplified static load and is: 135x8 + 110x8x(300-27.4)/25.6 = 10451 kN

As train properties have been updated, now train RFI5 shall be considered as the worst case, hence the dynamic forces are 150x8+148x8x(30-20.4)/14=2012 kN and 150x8+148x8x(300-20.4)/14=24850 kN for 30m / 300m respectively.

From the comparison analyses follows that the ADTreS calculated dynamic forces never exceed the amplified RFI static worst case loads. For this reason no further analysis is required.

11 ADTRES Global Model and Analyses

In this section the ADTRES results concerning four Global IBDAS runability worst cases are provided. The IBDAS results are summarized in the following Table 11-1:

Limit state	Load combination	Train combination case	Track no.	WJ type	Meeting point	Train speed [km/h]	Wind speed [m/s]	Thermal load	Reduction of wind speed due to shielding [%]	Number of eigen frequencies in analysis	Seismic peak ground acc. [m/s^2]	Transition slope [m/m]	Change of cant [m/m]	Non-compensated lateral acc. [m/s^2]	Roll speed [rad/s]	Derailment ratio incl. wind [-]	Derailment ratio excl. wind [-]	Overturning ratio incl. wind [-]	Sperling Ride Index, WI (unweighted) [-]	Sperling Ride Index, WI (weighted) [-]	Peak vertical acc. (unweighted) [m/s^2]	Peak vertical acc. (weighted) [m/s^2]	RMS vertical acc. (1.0 s) (unweighted) [m/s^2]	RMS vertical acc. (1.0 s) (weighted) [m/s^2]	Mean (based on 1.0 s RMS coach acc.) [m/s^3]	Vertical peak acc., trackbed (unweighted) [m/s^2]	Vertical peak acc., trackbed (weighted) [m/s^2]
Limit												0.08	0.0025	0.6	0.033	0.8	0.8	0.9	2.2	2.2	2.00	2.00	0.75	0.75	0.25	0.70	0.70
SLS1	2	1	1	1		144	44	No	40	250	0.0	0.0003	0.0000	0.051	0.060	0.334	0.166	0.556								0.024	0.010
SLS1	2	1	1	1		120	44	No	40	250	0.0								0.58	0.47	0.97	0.57	0.52	0.36	0.44		
SLS1	2	4	1	4		144	44	No	40	250	0.0	0.0004	0.0000	0.046	0.021	0.188	0.114	0.356								0.037	0.014
SLS1	2	4	1	4		120	44	No	40	250	0.0								0.72	0.62	1.71	1.01	0.87	0.52	0.69		

Table 11-1 Worst case analyses

11.1 Global FE Model

An ADTRES version of the Global Model of the bridge has been implemented on purpose, as depicted in Fig. 11-1

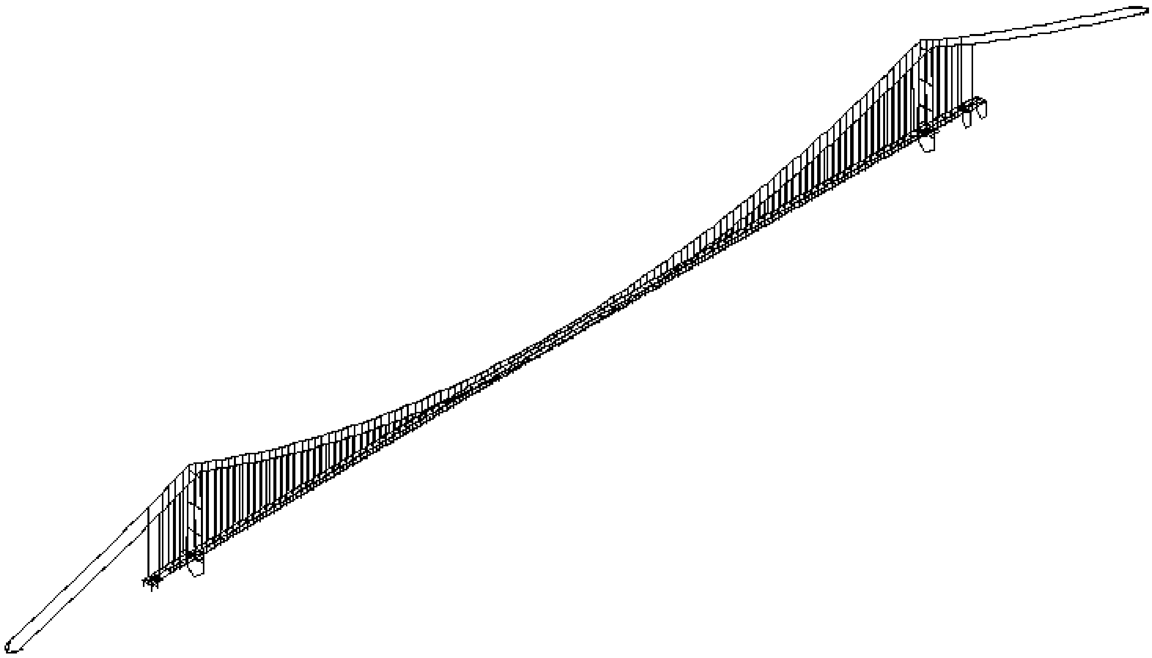

Fig. 11-1 – ADTRES Global Model

The finite element model is a beam model. The used finite elements are 3D Euler-Bernoulli formulation beams, considering also the effect of normal force in the geometric stiffness. The

ADTRES implementation uses a reduced mesh with respect to the IBDAS model, as the full runability analyses could be unstable otherwise, but the model characteristics fit the IBDAS model.

The train model is the same as described in section 9.1.1. The embedded rail is not explicitly modelled, but it is considered the rail imperfection according to "ORE B 176 Cahier des charges pour un bogie a caracteristiques ameliorees pour la circulation en courbe, Annex A. 6" with the following parameters:

- small irregularities
- number of harmonics: 1024
- fundamental harmonic: 0.00614 Hz
- sampling dx: 0.25 m
- total length: 1024 m

The following figures show rail irregularity input in vertical, roll, and lateral direction:

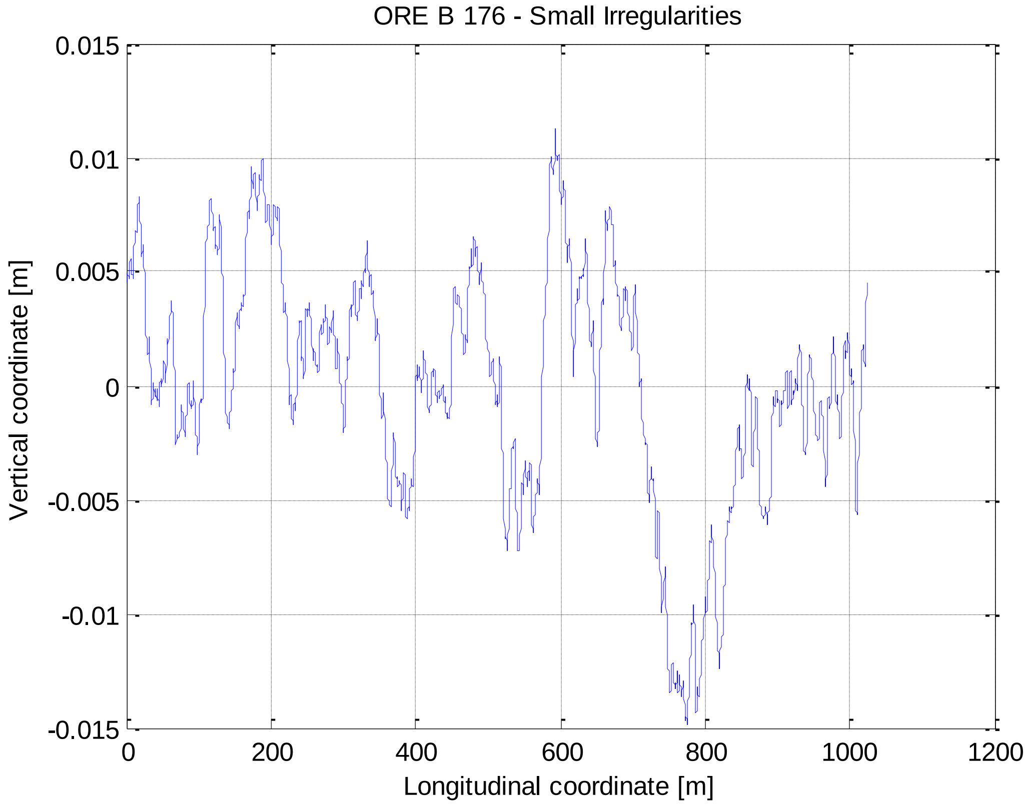

Vertical rail irregularity

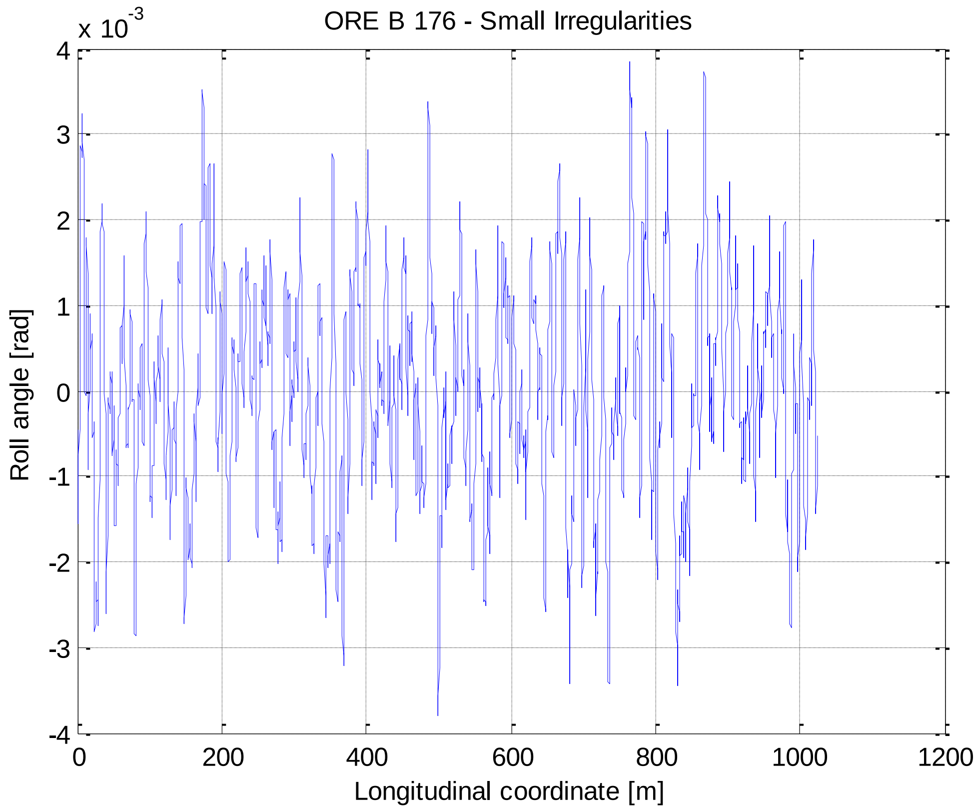

Roll angle rail irregularity

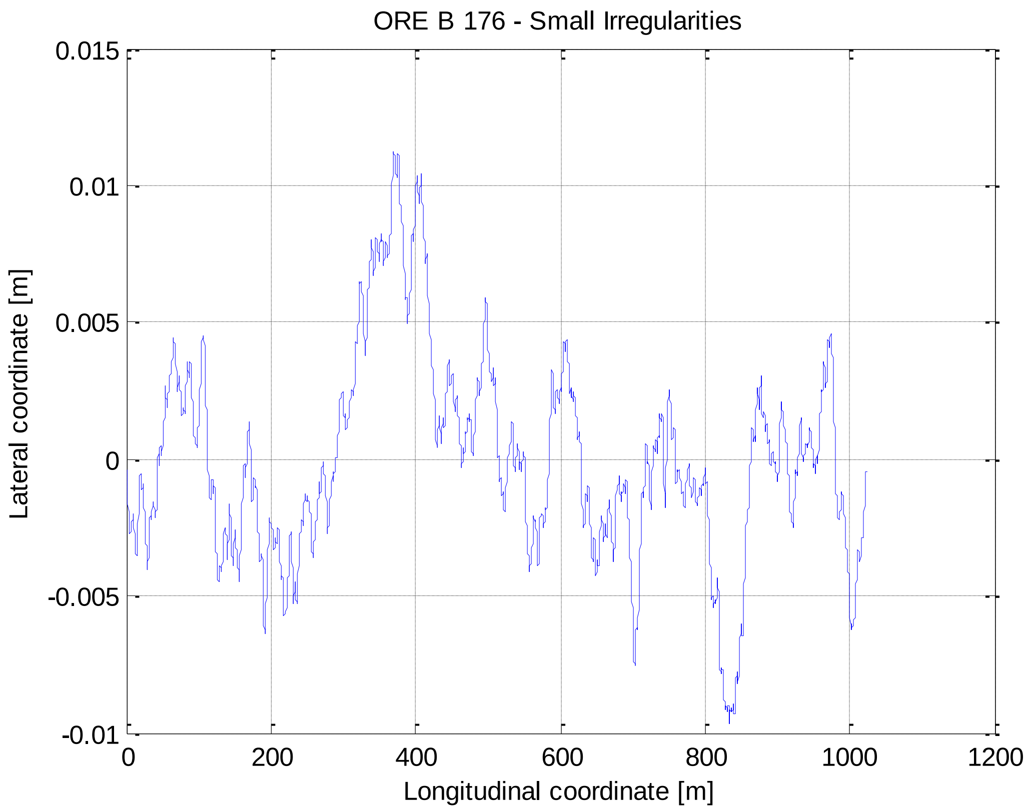

Lateral rail irregularity

Global analyses are performed according to the worst runnability cases pointed out in Table 11-1. Static wind load is applied to the structure (roadways and railway girders, towers, cables, hangers) using parameters as they are described in the documents "CG1000-P-RG-D-P-SV-00-00-00-00-00-01_A-01_IBDAS_App_G" and "CG1000-P-CL-D-P-SB-S3-00-00-00-00-03_A". Turbulent wind load is, instead, applied to the train.

11.2 Modal analysis

To verify the ADTRES implementation and to have a comparison with the IBDAS model, a modal analysis has been conducted. The first ten computed frequencies are listed in the following table.

Mode	1	2	3	4	5	6	7	8	9	10
Frequency [Hz]	0.0308	0.0573	0.0662	0.0796	0.0859	0.0935	0.0986	0.1024	0.1028	0.1063

Set of the first ten frequencies

The first modeshape is shown in the following figure:

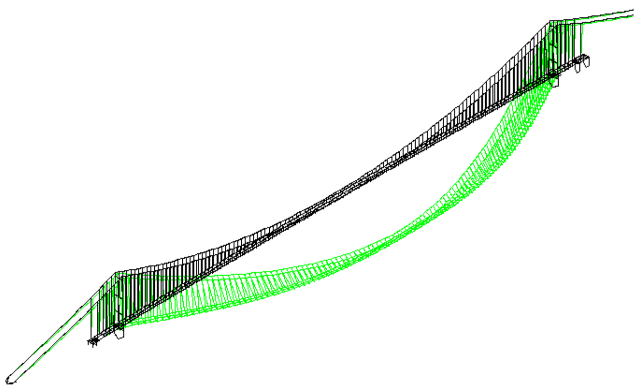

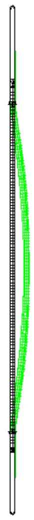

Isometric view   Top view

The second modeshape is shown in the following figure:

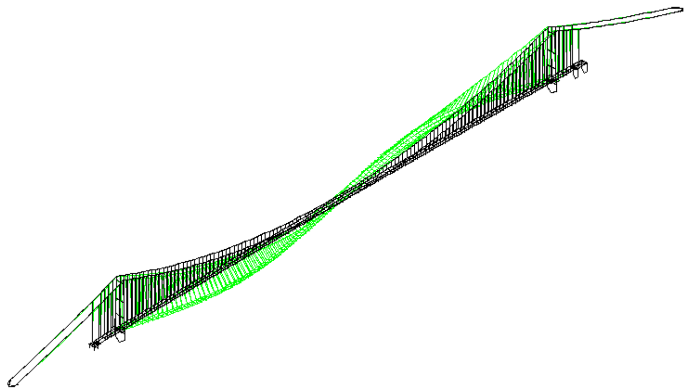

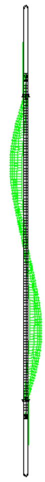

Isometric view   Top view

The third modeshape is shown in the following figure:

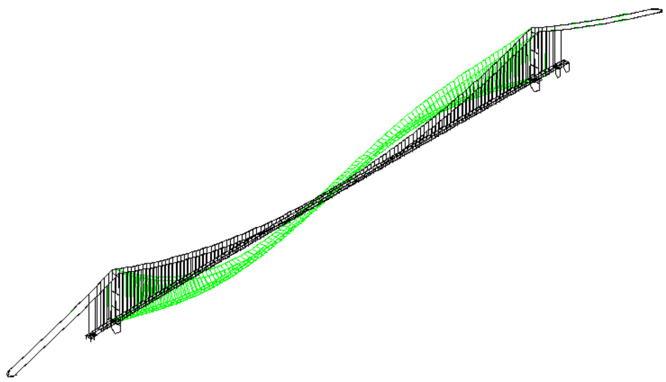

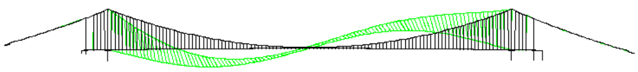

Isometric view

Side view

11.3 ADTreS global runnability analyses: results of critical cases

Railways runnability global analyses are performed using the software ADTreS. The assumptions adopted for the numerical simulations are as follows:

- Terminal structures and access viaducts are not included in the finite element model of the bridge
- Full length train running on the bridge is set at constant speeds, as reported in following Table

RFI Type	Train Speed [km/h]	Train Length [m]
1	120	353
	144	
4	120	208
	144	

Table – Train input data

- Static wind load is applied on the structure: roadways and railway girders, towers, cables, hangers. Aerodynamic coefficients and characteristic lengths are set according to Document no. A09055-NOT-3-027 titled “Wind input for IBDAS”.
- Road traffic static load is set equal to 3,75 kN/m on the first half of the downwind roadway girder.
- Turbulent wind load is applied to the train, whose turbulence specifications are reported in the following Table

Turbulence Intensity Iu	Integral Length Scale
14%	177

Table – Turbulent wind specifications

- Rail irregularity, called “Piccole lunghe”, is also included.

In particular, two different sets of global analyses are performed:

1) A preliminary set of global analyses
2) A final set of global analyses

The preliminary set of global analyses consist of static wind on the structure (roadways and railway girders, towers, cables, hangers) using parameters as they are described in the documents

"CG1000-P-RG-D-P-SV-00-00-00-00-00-01_A-01_IBDAS_App_G" and "CG1000-P-CL-D-P-SB-S3-00-00-00-00-03_A" and the wind speed is set equal to 30 m/s. Turbulent wind load is applied only to the first vehicle (locomotive) of the entire simulated train, where the wind speed is set equal to 18 m/s using a wind reduction factor equal to 0.6.

Results of the preliminary global analyses are shown in the following tables:

RFI 1						
Runnability Performance			CF (SLS1)	CF (SLS1)	CF (SLS1)	CF (SLS1)
Train Speed			120 km/h locomotive	120 km/h coach wagon	144 km/h locomotive	144 km/h coach wagon
Runnability Performance and Traffic Safety	Change of Cant (Short base: between 1,3 and 4,5 m)	< 0,250% (0,065% for rail irregularity + 0,185% for static and dynamic actions on the structure)	2,167E-04	2,142E-04	2,434E-04	2,311E-04
	Change of Cant (Long base: between 4,5 and 20 m)	< 0,250% (0,030% for rail irregularity + 0,170% for static and dynamic actions on the structure)	2,185E-04	2,056E-04	1,757E-04	2,009E-04
	Non-compensated Lateral Acceleration	< 0,6 m/s2	0,388	0,101	0,371	0,140

	Roll speed	< 0,033 rad/s	0,032	0,0149	0,0225	0,0197
	Jerk	< 0,25 m/s2	0,17	0,1316	0,1885	0,1541
	Bridge vertical acceleration	< 0,70 m/s2	0,114		0,21	
	Derailment check	< 0,8	0,249	0,096	0,269	0,113
	Overturning check	< 0,9	0,426	0,049	0,46	0,06

RFI 1						
Comfort Performance			**CF (SLS1)**	**CF (SLS1)**	**CF (SLS1)**	**CF (SLS1)**
Train Speed			**120 km/h** **locomotive**	**120 km/h** **coach wagon**	**144 km/h** **locomotive**	**144 km/h** **coach wagon**
Comfort and vehicle-structure interaction Performance	Wz comfort index	< 2,2	0,756	0,722	0,838	0,762
	Car Body Vertical Acceleration Peak	<=2 m/s2	0,242	0,209	0,276	0,201
	RMS Vertical Acceleration (passengers trains)	< 0,5 m/s2	0,069	0,059	0,0891	0,061
	RMS Lateral Acceleration (passengers trains)	< 0,75 m/s2	0,076	0,030	0,075	0,039

RFI 4						
Runnability Performance			**CF (SLS1)**	**CF (SLS1)**	**CF (SLS1)**	**CF (SLS1)**
Train Speed			**120 km/h locomotive**	**120 km/h coach wagon**	**144 km/h locomotive**	**144 km/h coach wagon**
Runnability Performance and Traffic Safety	Change of Cant (Short base: between 1,3 and 4,5 m)	< 0,250% (0,065% for rail irregularity + 0,185% for static and dynamic actions on the structure)	2,612E-04	2,218E-04	2,713E-04	2,454E-04
	Change of Cant (Long base: between 4,5 and 20 m)	< 0,250% (0,030% for rail irregularity + 0,170% for static and dynamic actions on the structure)	2,960E-04	2,204E-04	2,685E-04	2,444E-04
	Non-compensated Lateral	< 0,6 m/s2	0,578	0,141	0,704	0,218

	Acceleration					
	Roll speed	< 0,033 rad/s	0,026	0,0164	0,041	0,018
	Jerk	< 0,25 m/s2	0,268	0,133	0,300	0,192
	Bridge vertical acceleration	< 0,70 m/s2	0,131		0,178	
	Derailment check	a. < 0,8	b. 0,149	c. 0,086	d. 0,188	e. 0,093
	f. Overturning check	g. < 0,9	h. 0,401	i. 0,048	j. 0,424	k. 0,055

RFI 4						
Comfort Performance			**CF (SLS1)**	**CF (SLS1)**	**CF (SLS1)**	**CF (SLS1)**
Train Speed			**120 km/h locomotive**	**120 km/h coach wagon**	**144 km/h locomotive**	**144 km/h coach wagon**
Comfort and vehicle-structure interaction Performance	Wz comfort index	< 2,2	0,767	0,799	0,79192	0,800
	Car Body Vertical Acceleration Peak	<=2 m/s2	0,247	0,262	0,251	0,267
	RMS Vertical Acceleration (passengers trains)	< 0,5 m/s2	0,0748	0,086	0,072	0,0733
	RMS Lateral Acceleration (passengers trains)	< 0,75 m/s2	0,0684	0,0304	0,090	0,0425

A second set of global analyses is performed such that the wind speed is now set equal to 38 m/s on the structure (applied as a static load) and 24 m/s on both the first (locomotive) and the second (coach passengers) vehicles using a wind reduction factor of 0.65.

Results of these global analyses are shown in the following tables:

RFI 1						
Runnability Performance			**CF (SLS1)**	**CF (SLS1)**	**CF (SLS1)**	**CF (SLS1)**
Train Speed			**120 km/h** **locomotive**	**120 km/h** **coach wagon**	**144 km/h** **locomotive**	**144 km/h** **coach wagon**
Runnability Performance and Traffic Safety	Change of Cant (Short base: between 1,3 and 4,5 m)	< 0,250% (0,065% for rail irregularity + 0,185% for static and dynamic actions on the structure)	3,592E-04	2,125E-04	1,304E-04	2,301E-04
	Change of Cant (Long base: between 4,5 and 20 m)	< 0,250% (0,030% for rail irregularity + 0,170% for static and dynamic actions on the structure)	3,837E-04	2,047E-04	3,976E-04	2,259E-04
	Non-compensated Lateral Acceleration	< 0,6 m/s2	0,617	0,128	0,668	0,188

	Roll speed	< 0,033 rad/s	0,036	0,019	0,050	0,027
	Jerk	< 0,25 m/s2	0,211	0,184	0,275	0,228
	Bridge vertical acceleration	< 0,70 m/s2	0,12		0,21	
	Derailment check	< 0,8	0,369	0,266	0,371	0,270
	Overturning check	< 0,9	0,731	0,908	0,750	0,920

RFI 1						
Comfort Performance			**CF (SLS1)**	**CF (SLS1)**	**CF (SLS1)**	**CF (SLS1)**
Train Speed			**120 km/h locomotive**	**120 km/h coach wagon**	**144 km/h locomotive**	**144 km/h coach wagon**
Comfort and vehicle-structure interaction Performance	Wz comfort index	< 2,2	0,775	0,722	0,860	0,760
	Car Body Vertical Acceleration Peak	<=2 m/s2	0,296	0,209	0,290	0,199
	RMS Vertical Acceleration (passengers trains)	< 0,5 m/s2	0,076	0,059	0,097	0,061
	RMS Lateral Acceleration (passengers trains)	< 0,75 m/s2	0,131	0,034	0,154	0,047

RFI 4						
Runnability Performance			**CF (SLS1)**	**CF (SLS1)**	**CF (SLS1)**	**CF (SLS1)**
Train Speed			**120 km/h locomotive**	**120 km/h coach wagon**	**144 km/h locomotive**	**144 km/h coach wagon**
Runnability Performance and Traffic Safety	Change of Cant (Short base: between 1,3 and 4,5 m)	< 0,250% (0,065% for rail irregularity + 0,185% for static and dynamic actions on the structure)	2,652E-04	2,172E-04	1,306E-04	2,421E-04
	Change of Cant (Long base: between 4,5 and 20 m)	< 0,250% (0,030% for rail irregularity + 0,170% for static and dynamic actions on the structure)	2,645E-04	2,209E-04	3,204E-04	2,467E-04

	Non-compensated Lateral Acceleration	< 0,6 m/s2	0,928	0,194	1,070	0,293
	Roll speed	< 0,033 rad/s	0,070	0,019	0,094	0,022
	Jerk	< 0,25 m/s2	0,272	0,191	0,558	0,273
	Bridge vertical acceleration	< 0,70 m/s2	0,13		0,18	
	Derailment check	< 0,8	0,238	0,231	0,258	0,217
	Overturning check	< 0,9	0,569	0,490	0,591	0,573

RFI 4						
Comfort Performance			CF (SLS1)	CF (SLS1)	CF (SLS1)	CF (SLS1)
Train Speed			120 km/h locomotive	120 km/h coach wagon	144 km/h locomotive	144 km/h coach wagon
Comfort and vehicle-structure interaction Performance	Wz comfort index	< 2,2	0,766	0,800	0,794	0,800
	Car Body Vertical Acceleration Peak	<=2 m/s2	0,234	0,261	0,262	0,268
	RMS Vertical Acceleration (passengers trains)	< 0,5 m/s2	0,074	0,086	0,072	0,073
	RMS Lateral Acceleration (passengers trains)	< 0,75 m/s2	0,117	0,035	0,15224	0,050

Local analyses with wind load on the vehicle: RFI3 locomotive, 144 km/h

Local analyses are performed on the local multi beam model applying turbulent wind load on the right side of the vehicle. RFI 3 locomotive running at a speed of 144 km/h is chosen for the analyses.

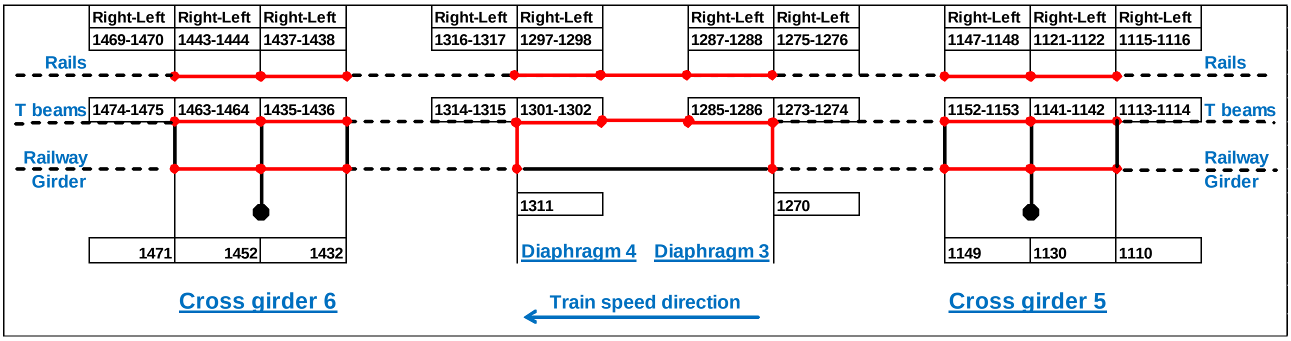

The following tables show a comparison between "Wind" and "No Wind" cases.

LEFT RAIL	Rail Node #	T Beam Node	Static Displacement [m]	WIND Dynamic Displacement [m]	WIND Impact Factor	NO WIND Dynamic Displacement [m]	NO WIND Impact Factor
Cross Girder # 5	1116	1114	-2,42E-03	-3,00E-03	1,24E+00	-2,65E-03	1,10E+00
	1122	1142	-2,42E-03	-2,87E-03	1,19E+00	-2,53E-03	1,05E+00
	1148	1153	-2,42E-03	-2,75E-03	1,14E+00	-2,42E-03	1,00E+00
Diaphragm 3 - 4	1276	1274	-2,42E-03	-2,90E-03	1,20E+00	-2,59E-03	1,07E+00
	1288	1286	-2,42E-03	-2,95E-03	1,22E+00	-2,62E-03	1,08E+00
	1298	1302	-2,41E-03	-2,76E-03	1,14E+00	-2,49E-03	1,03E+00
	1317	1315	-2,40E-03	-3,00E-03	1,25E+00	-2,69E-03	1,12E+00
Cross Girder # 6	1438	1436	-2,43E-03	-3,14E-03	1,29E+00	-2,83E-03	1,17E+00
	1444	1464	-2,42E-03	-2,79E-03	1,15E+00	-2,42E-03	9,99E-01
	1470	1475	-2,42E-03	-2,93E-03	1,21E+00	-2,63E-03	1,09E+00

Table – Impact factor evaluation from the nodal vertical displacement difference between rails and T beams on left hand side of the track. Impact factors are also shown from the ratio between static and dynamic quantities.

				WIND		NO WIND	
RIGHT RAIL	Rail Node #	T Beam Node	Static Displacement [m]	Dynamic Displacement [m]	Impact Factor	Dynamic Displacement [m]	Impact Factor
Cross Girder # 5	1115	1113	-2,42E-03	-2,01E-03	8,30E-01	-2,50E-03	1,03E+00
	1121	1141	-2,42E-03	-1,87E-03	7,73E-01	-2,32E-03	9,59E-01
	1147	1152	-2,42E-03	-2,04E-03	8,43E-01	-2,40E-03	9,92E-01
Diaphragm 3 - 4	1275	1273	-2,44E-03	-2,30E-03	9,43E-01	-2,68E-03	1,10E+00
	1287	1285	-2,42E-03	-2,24E-03	9,26E-01	-2,58E-03	1,06E+00
	1297	1301	-2,42E-03	-2,21E-03	9,15E-01	-2,54E-03	1,05E+00
	1316	1314	-2,43E-03	-2,39E-03	9,83E-01	-2,70E-03	1,11E+00
Cross Girder # 6	1437	1435	-2,42E-03	-2,20E-03	9,07E-01	-2,66E-03	1,10E+00
	1443	1463	-2,42E-03	-2,14E-03	8,84E-01	-2,68E-03	1,11E+00
	1469	1474	-2,42E-03	-2,10E-03	8,68E-01	-2,52E-03	1,04E+00

Table – Impact factor evaluation from the nodal vertical displacement difference between rails and T beams on right hand side of the track. Impact factors are also shown from the ratio between static and dynamic quantities.

		WIND	NO WIND
	Node #	Displacement [m]	Displacement [m]
Cross Girder # 5	1110	-3,6E-03	-3,6E-03
	1130	-3,6E-03	-3,6E-03
	1149	-3,6E-03	-3,6E-03
Diaphragm # 3	1270	-4,6E-03	-4,6E-03
Diaphragm # 4	1311	-4,6E-03	-4,6E-03
Cross Girder # 6	1432	-3,6E-03	-3,6E-03
	1452	-3,6E-03	-3,6E-03
	1471	-3,6E-03	-3,6E-03

Table – Vertical displacements of the railway girder nodes.

			WIND		NO WIND	
LEFT RAIL	Bed #	Static Force [N]	Dynamic Force [N]	Impact Factor	Dynamic Force [N]	Impact Factor
	795	15000	18900	1,26E+00	16800	1,12E+00
	800	14950	17930	1,20E+00	15870	1,06E+00
	803	14950	17800	1,19E+00	15700	1,05E+00
	808	14950	16746	1,12E+00	14750	9,87E-01
	892	15000	15850	1,06E+00	13500	9,00E-01
	899	14950	18140	1,21E+00	16000	1,07E+00
	912	15000	16000	1,07E+00	14600	9,73E-01
	995	15000	19650	1,31E+00	17730	1,18E+00
	1000	14950	17120	1,15E+00	14800	9,90E-01
	1003	14950	17200	1,15E+00	14925	9,98E-01
	1008	14900	18150	1,22E+00	16300	1,09E+00

Table – Impact factor evaluation from static and dynamic loads at specific beds locations positioned underneath the left rail.

			WIND		NO WIND	
RIGHT RAIL	Bed #	Static Force [N]	Dynamic Force [N]	Impact Factor	Dynamic Force [N]	Impact Factor
	793	15000	12550	8,37E-01	15750	1,05E+00
	798	14950	11154	7,46E-01	13690	9,16E-01
	801	14950	11878	7,95E-01	14970	1,00E+00
	806	14990	12710	8,48E-01	14930	9,96E-01
	890	15000	15280	1,02E+00	17600	1,17E+00
	897	14950	14000	9,36E-01	16100	1,08E+00
	910	15000	16000	1,07E+00	18000	1,20E+00
	993	14950	13870	9,28E-01	16670	1,12E+00
	998	14950	13235	8,85E-01	16500	1,10E+00
	1001	14940	13000	8,70E-01	16300	1,09E+00
	1006	15000	14000	9,33E-01	16800	1,12E+00

Table – Impact factor evaluation from static and dynamic loads at specific beds locations positioned underneath the right rail.

	NO WIND							
	T beam Right Node #	Vertical Acceleration Peak [m/s^2]	T beam Left Node #	Vertical Acceleration Peak [m/s^2]	Right Rail Node #	Vertical Acceleration Peak [m/s^2]	Left Rail Node #	Vertical Acceleration Peak [m/s^2]
Cross girder # 5	1113	1,782	1114	2,257	1115	38,323	1116	34,945
	1141	1,814	1142	2,183	1121	33,843	1122	47,706
	1152	1,903	1153	2,185	1147	31,929	1148	42,309
Diaphragms # 3 – 4	1273	3,655	1274	4,749	1275	28,901	1276	41,525
	1285	4,249	1286	5,666	1287	33,231	1288	43,647
	1301	4,604	1302	5,78	1297	32,066	1298	29,881
	1314	4,649	1315	5,395	1316	38,051	1317	38,994
Cross girder # 6	1435	2,238	1436	2,364	1438	49,891	1437	27,322
	1463	2,186	1464	2,304	1444	26,726	1443	35,381
	1474	2,173	1475	2,589	1470	27,419	1469	36,262
	WIND							
	T beam Right Node #	Vertical Acceleration Peak [m/s^2]	T beam Left Node #	Vertical Acceleration Peak [m/s^2]	Right Rail Node #	Vertical Acceleration Peak [m/s^2]	Left Rail Node #	Vertical Acceleration Peak [m/s^2]
Cross girder # 5	1113	1,749	1114	2,233	1115	37,118	1116	36,331
	1141	1,786	1142	2,162	1121	33,631	1122	53,795
	1152	1,874	1153	2,146	1147	27,858	1148	49,297
Diaphragms # 3 – 4	1273	3,658	1274	4,738	1275	26,228	1276	40,547
	1285	4,231	1286	5,68	1287	37,049	1288	39,472
	1301	4,591	1302	5,754	1297	33,018	1298	32,033
	1314	4,656	1315	5,489	1316	38,135	1317	45,439
Cross girder # 6	1435	2,24	1436	2,442	1438	43,98	1437	27,131
	1463	2,179	1464	2,312	1444	30,604	1443	35,398
	1474	2,184	1475	2,593	1470	27,504	1469	37,396

Table - Nodal vertical acceleration peaks of right and left rails and T beams.

		NO WIND	WIND
	Railway Girder Node #	Vertical Acceleration Peak [m/s^2]	Vertical Acceleration Peak [m/s^2]
Cross girder # 5	1110	1,652	1,641
	1130	1,749	1,732
	1149	1,766	1,755
Diaphragm # 3	1270	3,279	3,308
Diaphragm # 4	1311	4,076	4,104
Cross girder # 6	1432	2,15	2,148
	1452	2,116	2,107
	1471	2,025	2,019

Table - Nodal vertical acceleration peaks of the railway girder.

	RFI type	Speed [km/h]	Max Visco-Elastic Bed Force						Max Contact Force	Max Nodal Dynamic Vertical Displacement LEFT Rail-Tbeam				Max Nodal Dynamic Vertical Displacement RIGHT Rail-Tbeam			
			Bed #	Left Bed [N]	I.F.	Bed #	Right Bed [N]	I.F.	Force [N]	Rail Node #	Tbeam Node #	Displacement [m]	I.F.	Rail Node #	Tbeam Node #	Displacement [m]	I.F.
NO WIND	3 - loco	144	995	17730	1,18	890	17600	1,17	1,50E+05	1438	1436	-2,83E-03	1,17	1316	1314	-2,70E-03	1,11
WIND	3 - loco	144	995	19650	1,31	890	15280	1,02	1,68E+05	1438	1436	-3,14E-03	1,29	1316	1314	-2,39E-03	0,98

Table - Visco-elastic beds maximum vertical forces and nodal rails and stringers maximum vertical displacements at all simulated vehicles speeds.

	RFI type	Speed [km/h]	Max Nodal Vertical Acceleration LEFT Side				Max Nodal Vertical Acceleration RIGHT Side				Max Vertical Railway Girder Acceleration		Body Vertical Acceleration [m/s^2]	Non-compensated Acceleration [m/s^2]
			Rail Node #	Acceleration [m/s^2]	Tbeam Node #	Acceleration [m/s^2]	Rail Node #	Acceleration [m/s^2]	Tbeam Node #	Acceleration [m/s^2]	Node #	Acceleration [m/s^2]		
NO WIND	3 - loco	144	1122	47,706	1302	5,78	1438	49,891	1314	4,649	1311	4,076	0,259	0,217
WIND	3 - loco	144	1122	53,795	1302	5,754	1438	43,98	1314	4,656	1311	4,104	0,316	0,355

Table - Nodal rails, stringers, and rail car-bodies maximum vertical accelerations at all simulated vehicles speeds.

FREQUENCY ANALYSES RAIL, T-beam ACCELERATIONS

Frequency analyses of rails and T beams vertical accelerations are carried out in order to check results shown in Table 10-2. In this table, the reported peak values of vertical accelerations time histories, result in large discrepancies between right and left hand sides of rails and T beams. Spectral analyses show that energy levels of the two signals (left and right, rails and T beams) are reasonably similar.

RFI 1 locomotive:

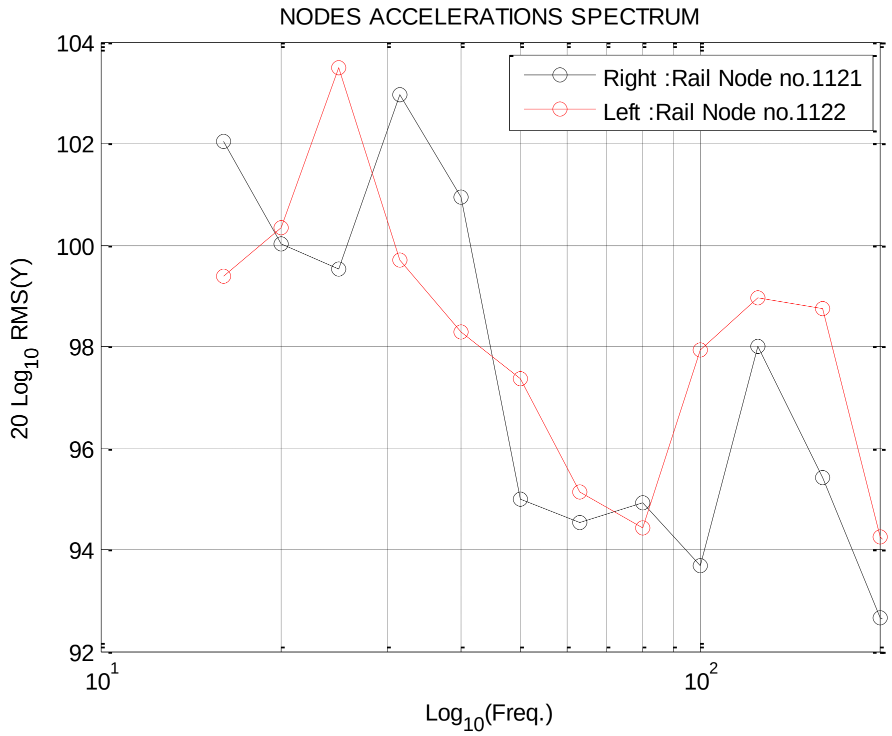

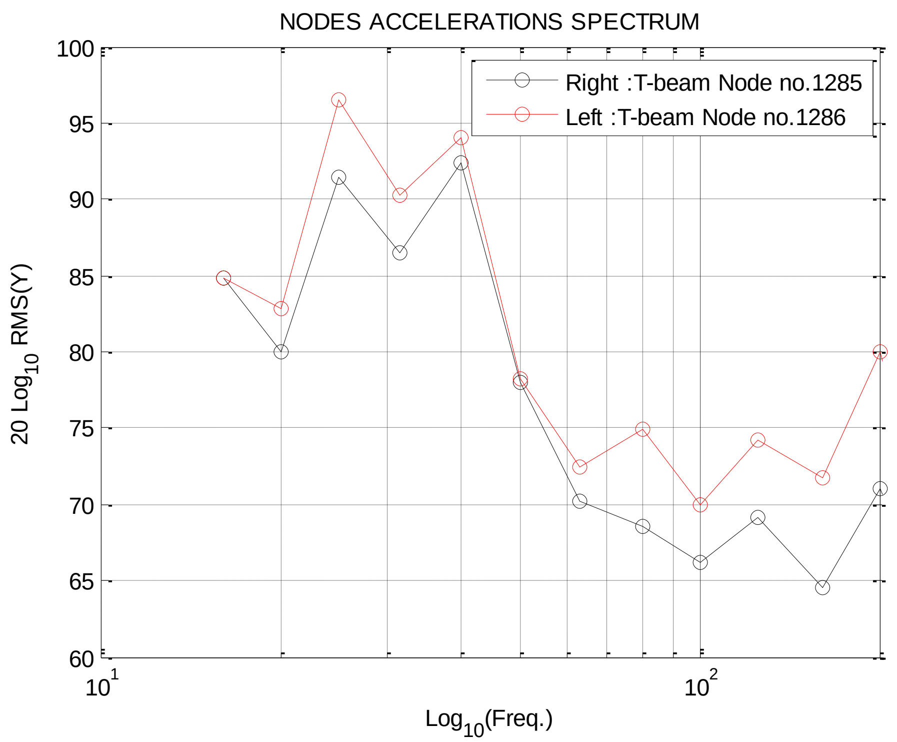
NODES ACCELERATIONS SPECTRUM
Right :T-beam Node no.1285
Left :T-beam Node no.1286
20 Log10 RMS(Y)
Log10(Freq.)

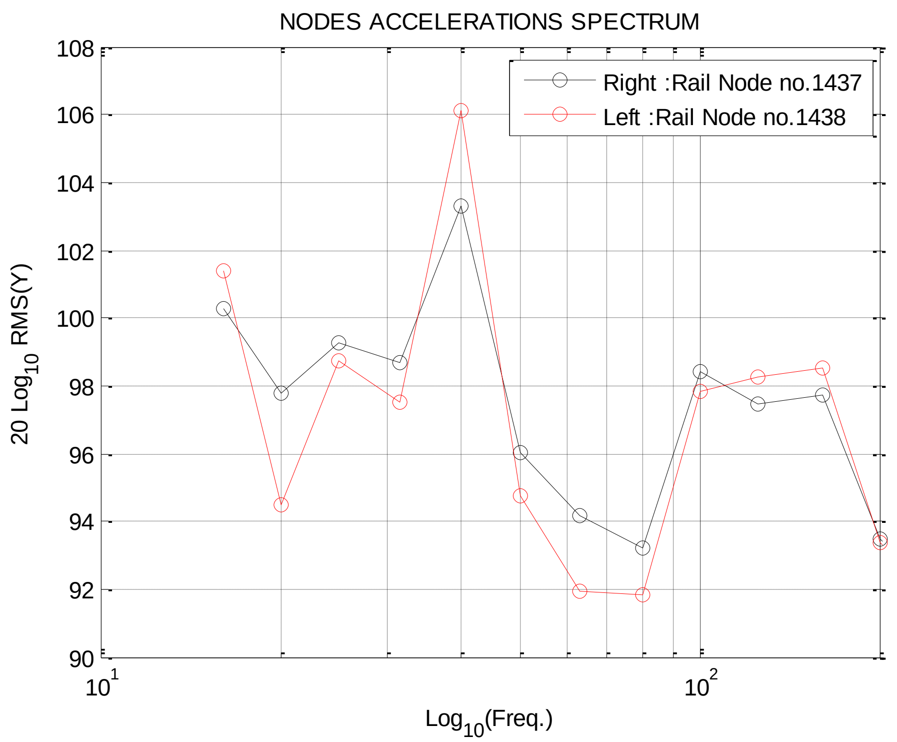
NODES ACCELERATIONS SPECTRUM
Right :Rail Node no.1437
Left :Rail Node no.1438
20 Log10 RMS(Y)
Log10(Freq.)

RFI 1 coach:

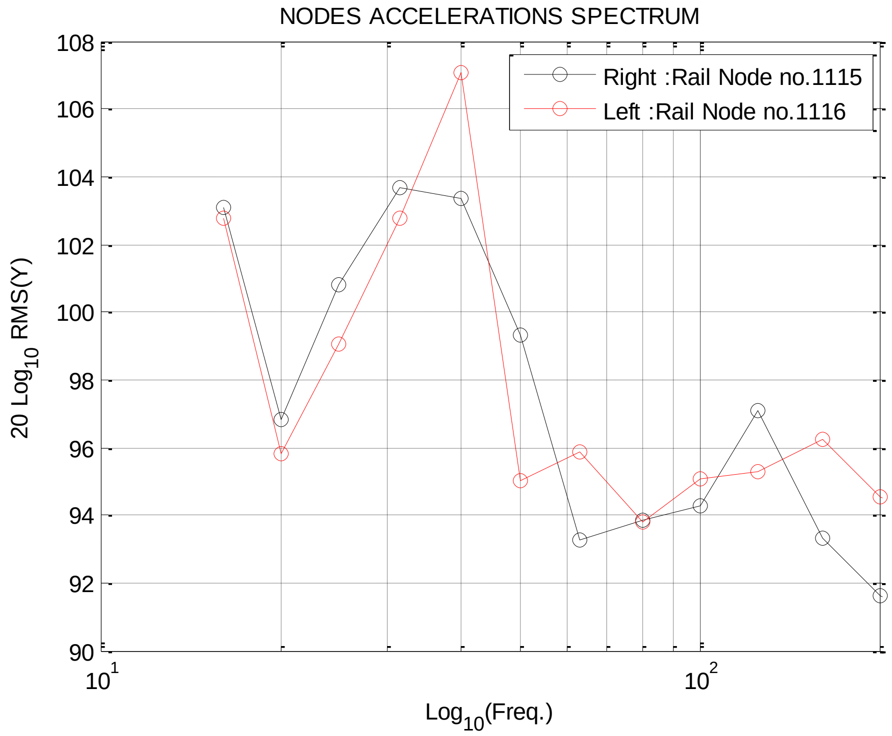
NODES ACCELERATIONS SPECTRUM
Right :Rail Node no.1115
Left :Rail Node no.1116
108
106
104
102
100
98
96
94
92
90
20 Log10 RMS(Y)
10^1
10^2
Log10(Freq.)

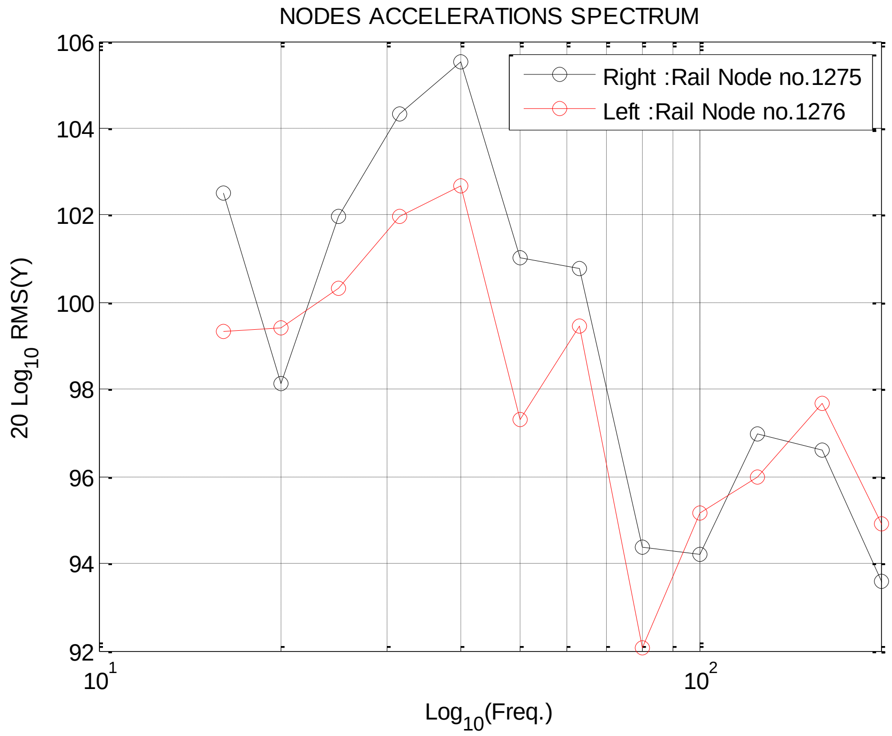
NODES ACCELERATIONS SPECTRUM
Right :Rail Node no.1275
Left :Rail Node no.1276
106
104
102
100
98
96
94
92
20 Log10 RMS(Y)
10^1
10^2
Log10(Freq.)

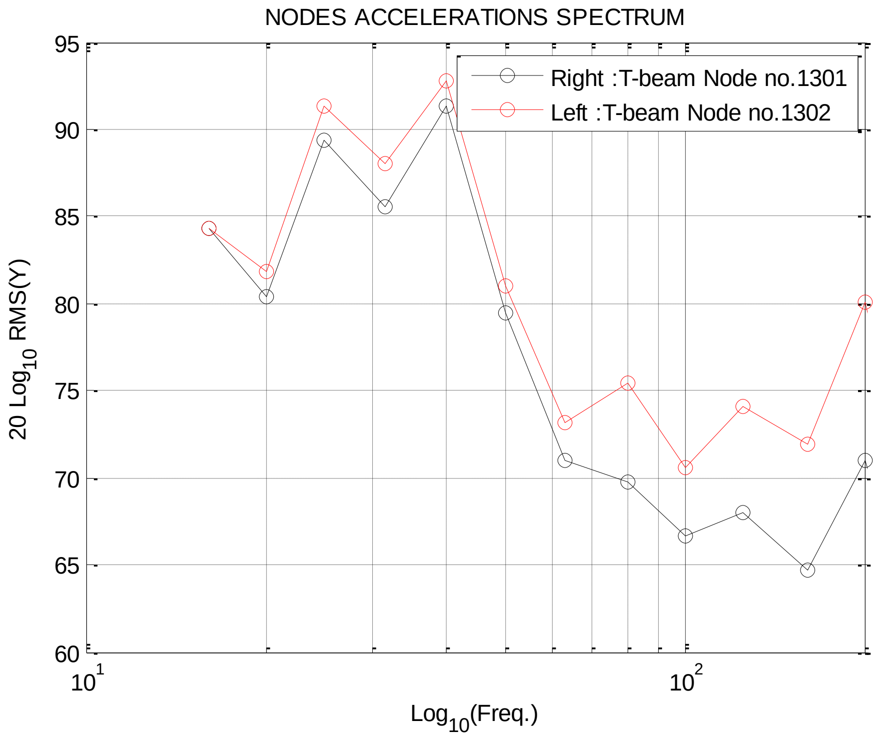
NODES ACCELERATIONS SPECTRUM
Right :T-beam Node no.1301
Left :T-beam Node no.1302
20 Log10 RMS(Y)
Log10(Freq.)
95
90
85
80
75
70
65
60
10^1
10^2

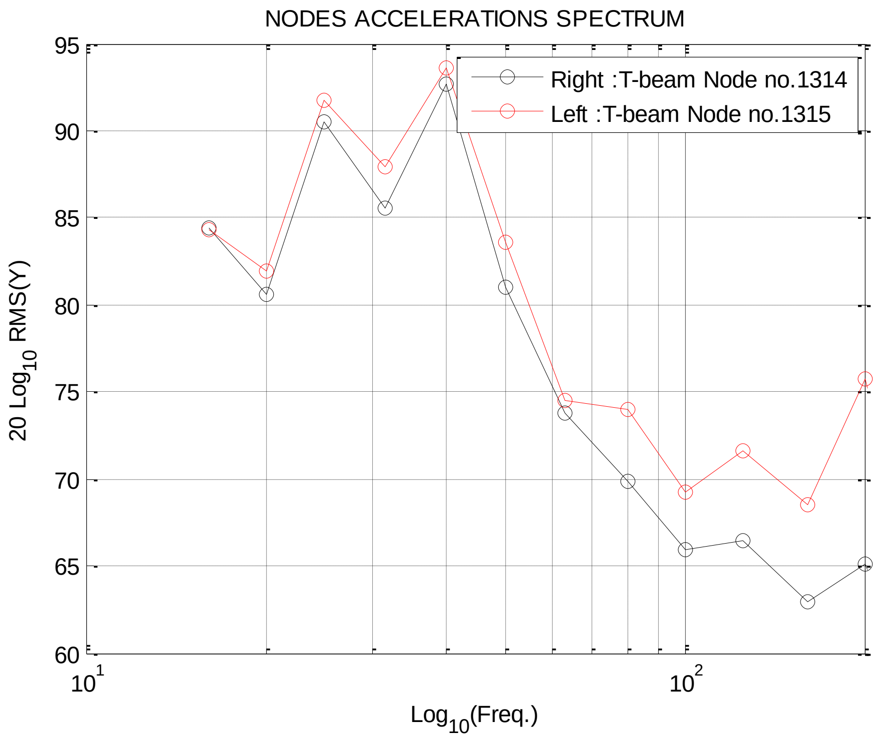
NODES ACCELERATIONS SPECTRUM
Right :T-beam Node no.1314
Left :T-beam Node no.1315
20 Log10 RMS(Y)
Log10(Freq.)
95
90
85
80
75
70
65
60
10^1
10^2

RFI 2 locomotive:

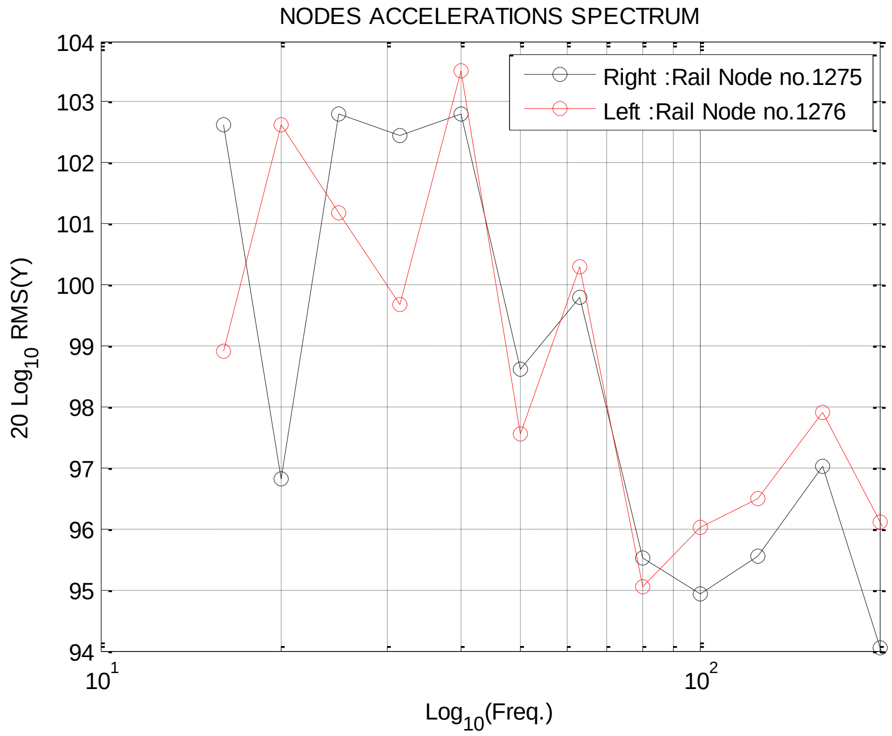

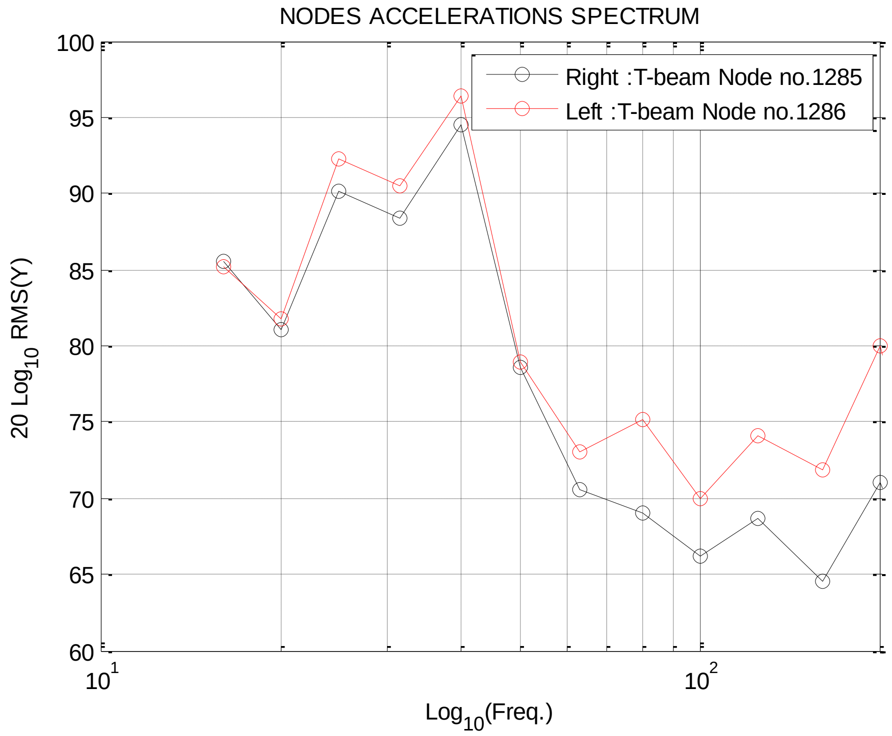

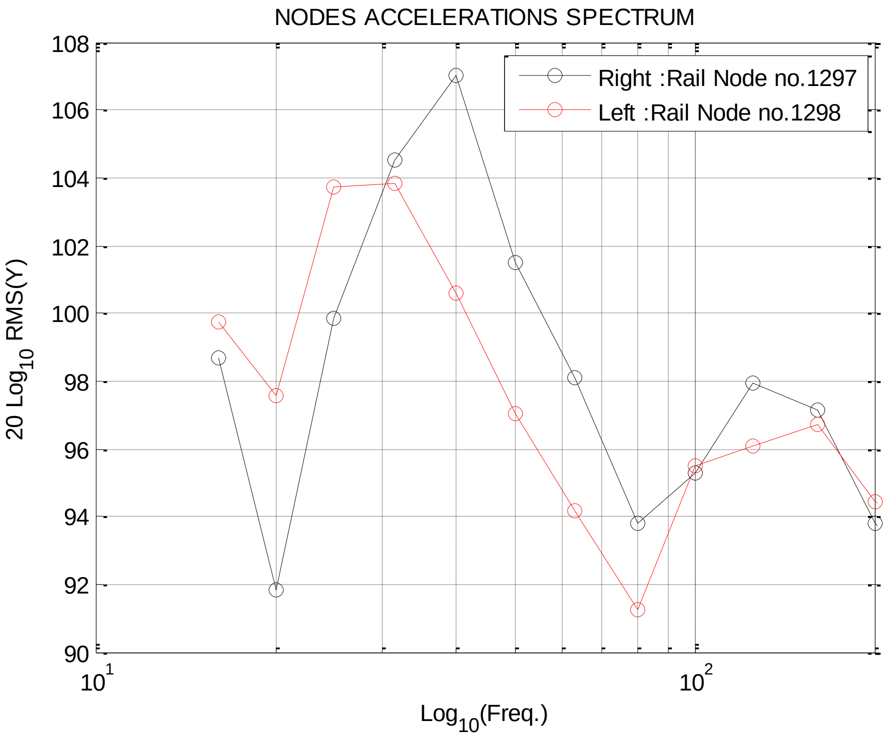

NODES ACCELERATIONS SPECTRUM
Right :Rail Node no.1297
Left :Rail Node no.1298
108
106
104
102
100
98
96
94
92
90
20 Log10 RMS(Y)
10^1
10^2
Log10(Freq.)

RFI 2 coach:

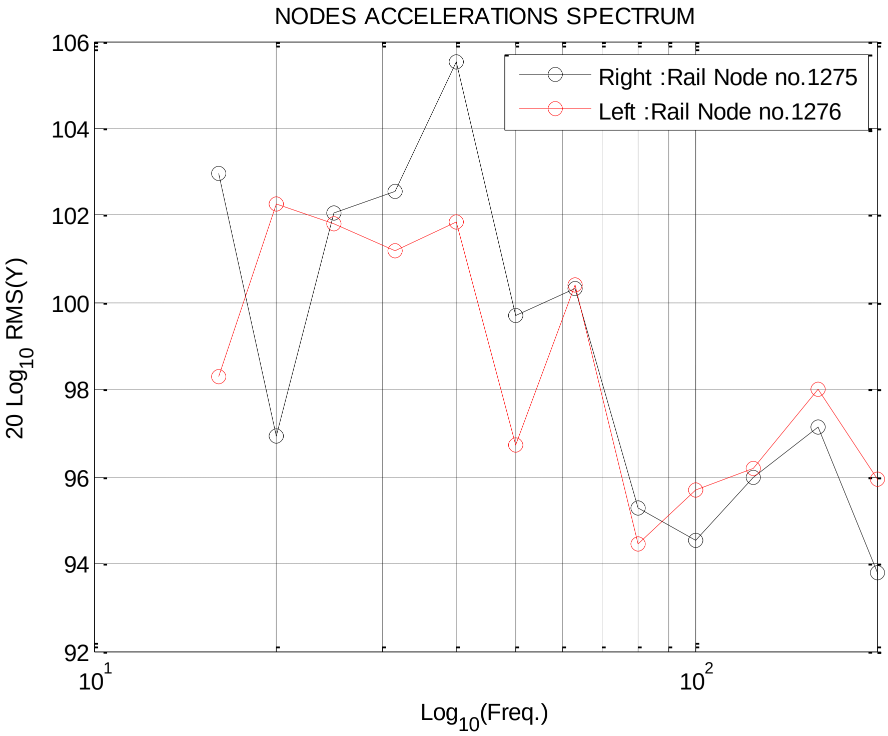
NODES ACCELERATIONS SPECTRUM
Right :Rail Node no.1275
Left :Rail Node no.1276
20 Log10 RMS(Y)
106
104
102
100
98
96
94
92
10^1
10^2
Log10(Freq.)

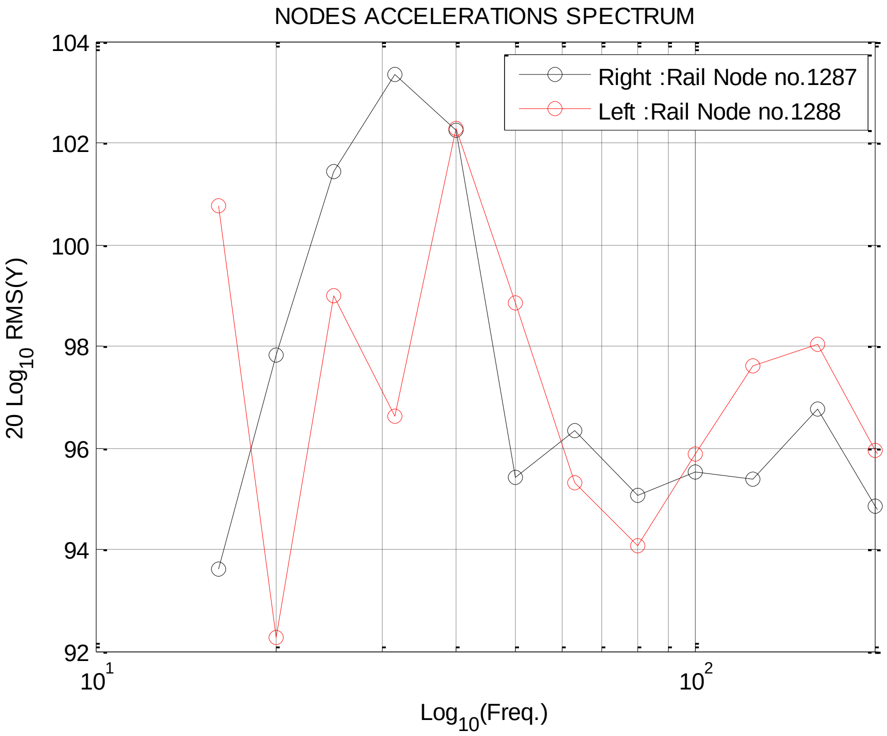
NODES ACCELERATIONS SPECTRUM
Right :Rail Node no.1287
Left :Rail Node no.1288
20 Log10 RMS(Y)
104
102
100
98
96
94
92
10^1
10^2
Log10(Freq.)

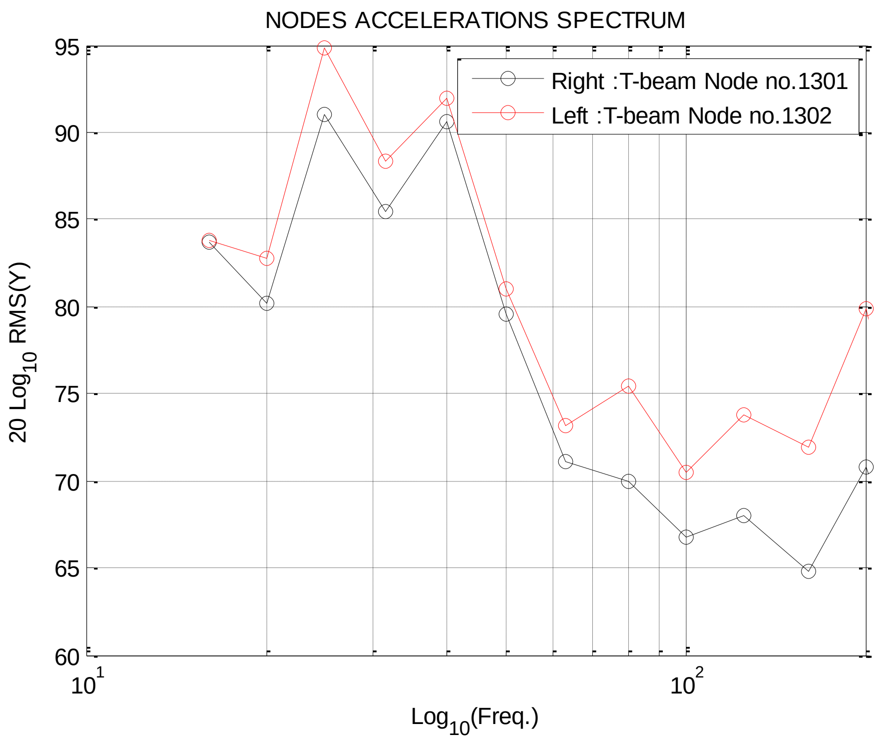
NODES ACCELERATIONS SPECTRUM
95
90
85
80
75
70
65
60
Right :T-beam Node no.1301
Left :T-beam Node no.1302
20 Log10 RMS(Y)
10^1
10^2
Log10(Freq.)

RFI 3 loco 144 km/h:

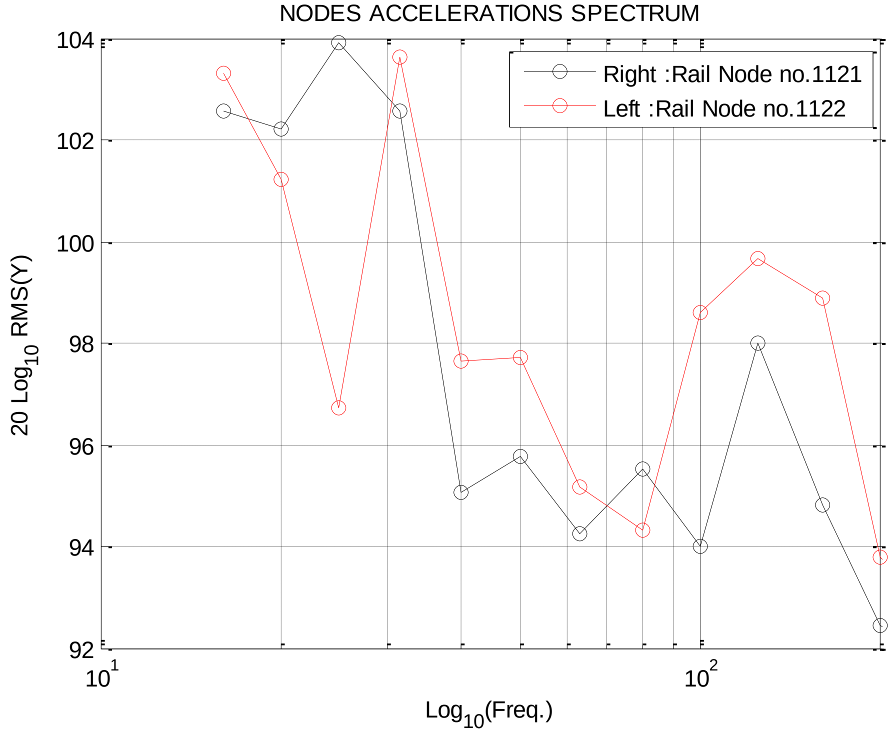

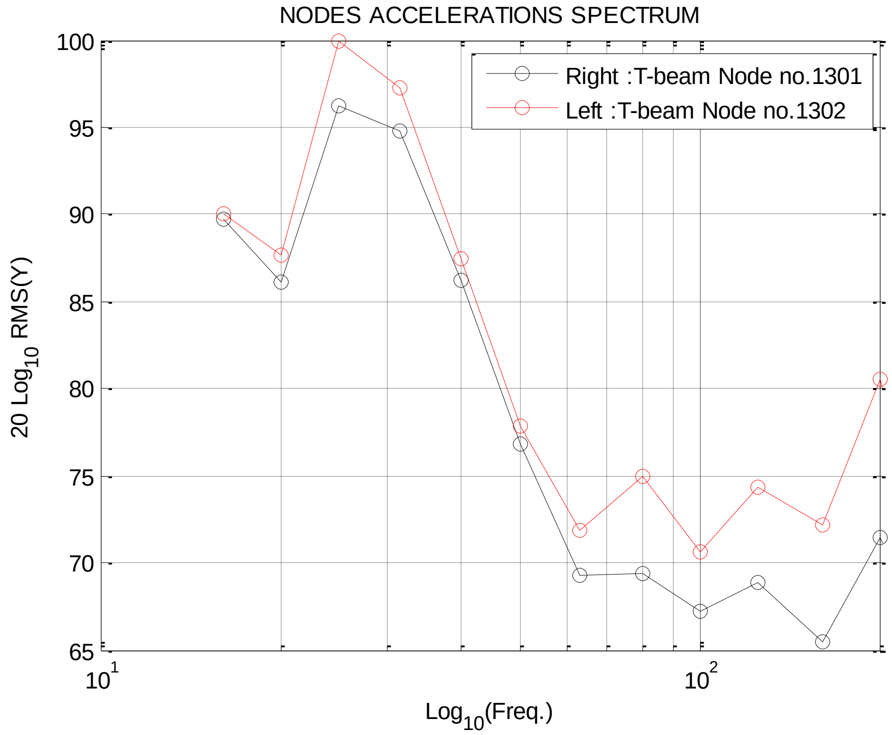

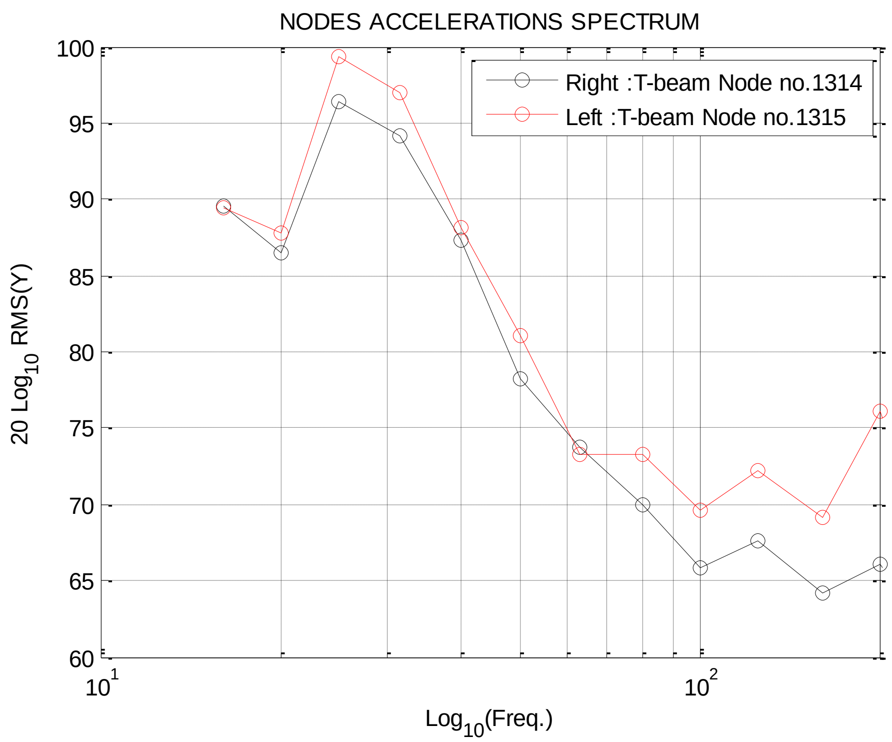
NODES ACCELERATIONS SPECTRUM
Right :T-beam Node no.1314
Left :T-beam Node no.1315
20 Log10 RMS(Y)
Log10(Freq.)

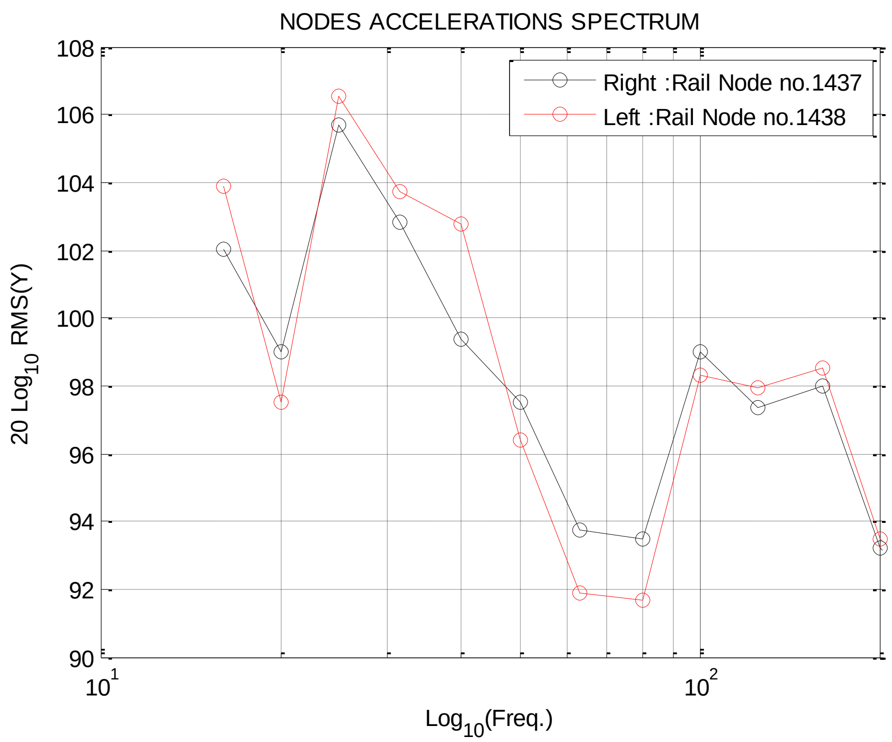
NODES ACCELERATIONS SPECTRUM
Right :Rail Node no.1437
Left :Rail Node no.1438
20 Log10 RMS(Y)
Log10(Freq.)

RFI 3 coach MD:

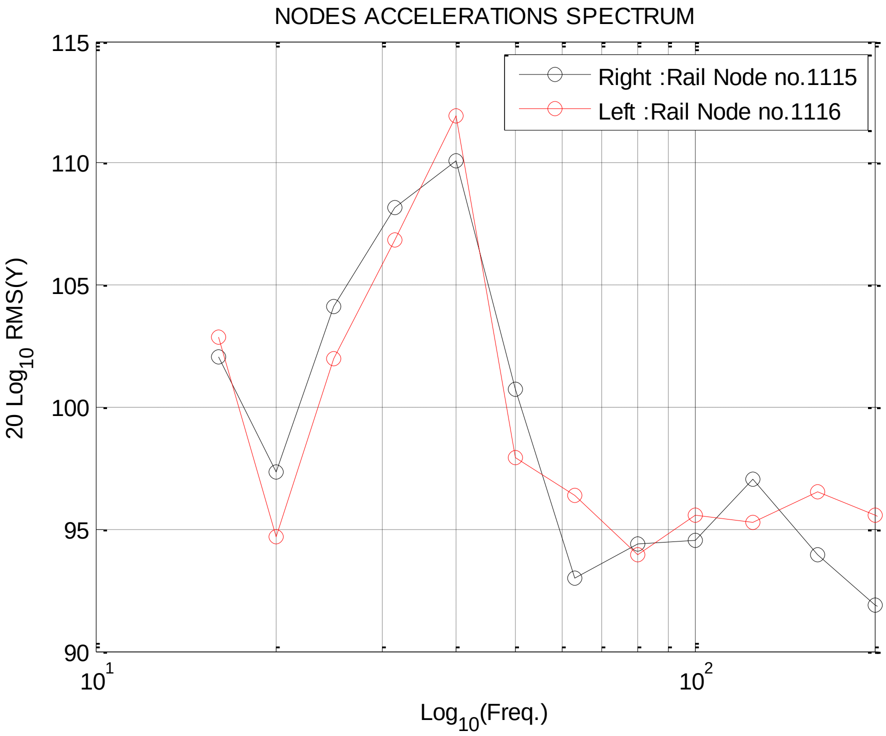

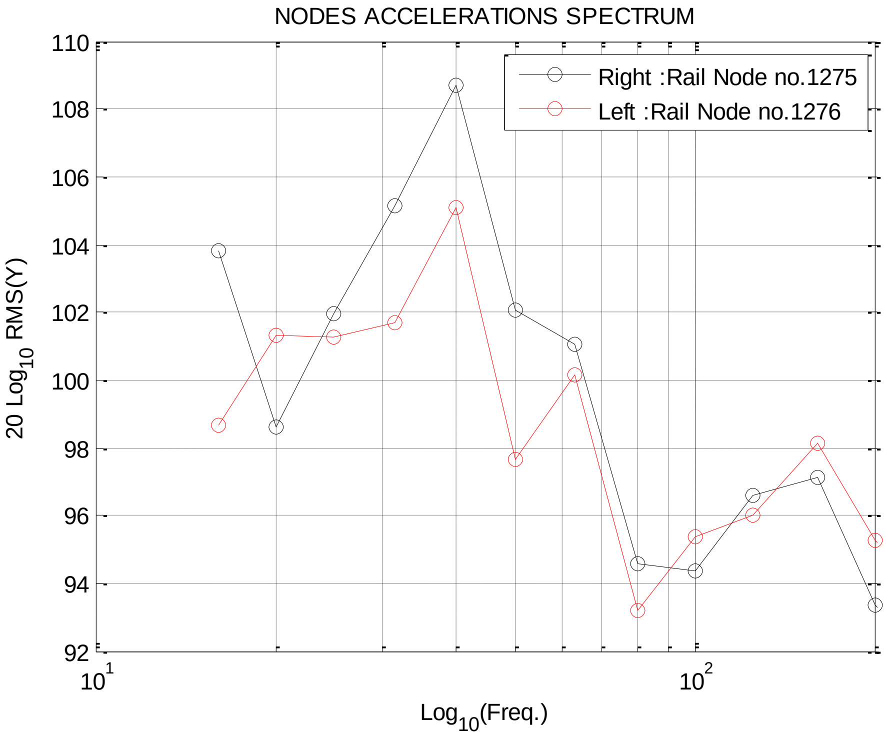

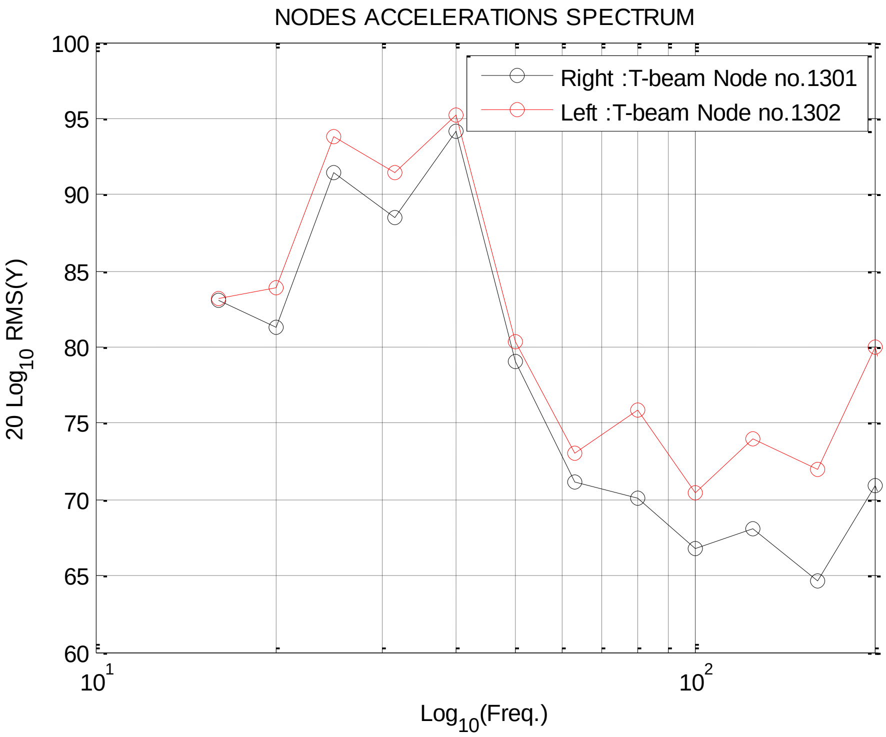

NODES ACCELERATIONS SPECTRUM
Right :T-beam Node no.1301
Left :T-beam Node no.1302
20 Log10 RMS(Y)
Log10(Freq.)
100
95
90
85
80
75
70
65
60
10^1
10^2

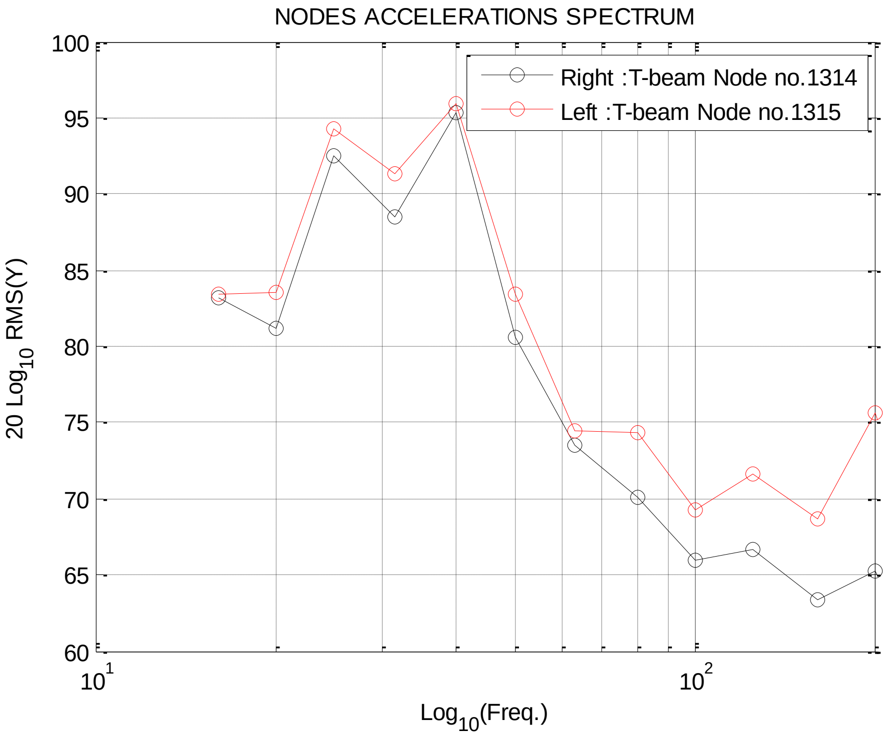

NODES ACCELERATIONS SPECTRUM
Right :T-beam Node no.1314
Left :T-beam Node no.1315
20 Log10 RMS(Y)
Log10(Freq.)
100
95
90
85
80
75
70
65
60
10^1
10^2

RFI 4 locomotive:

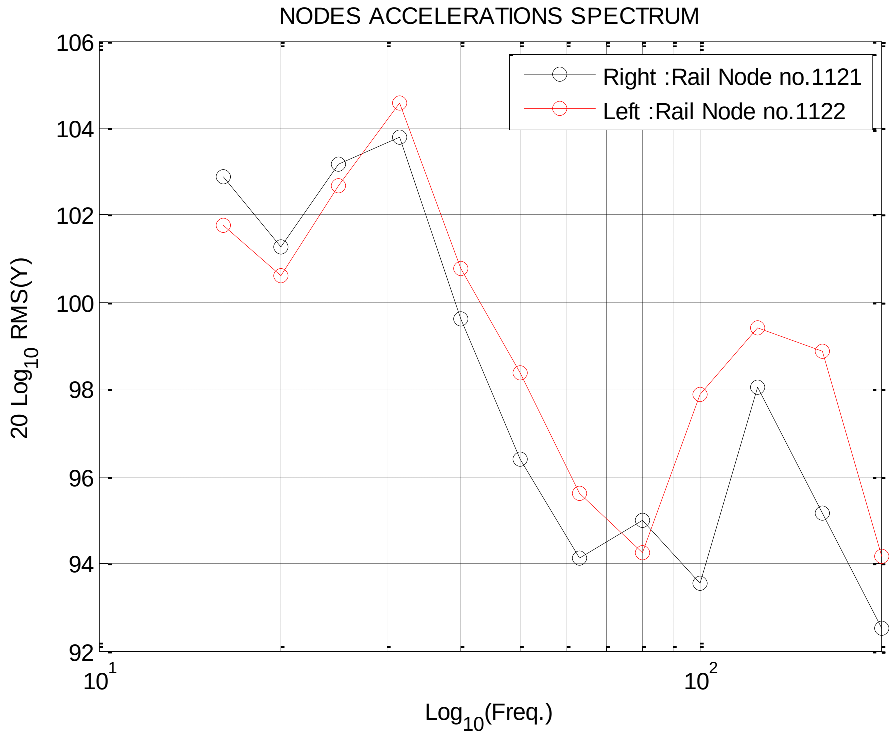

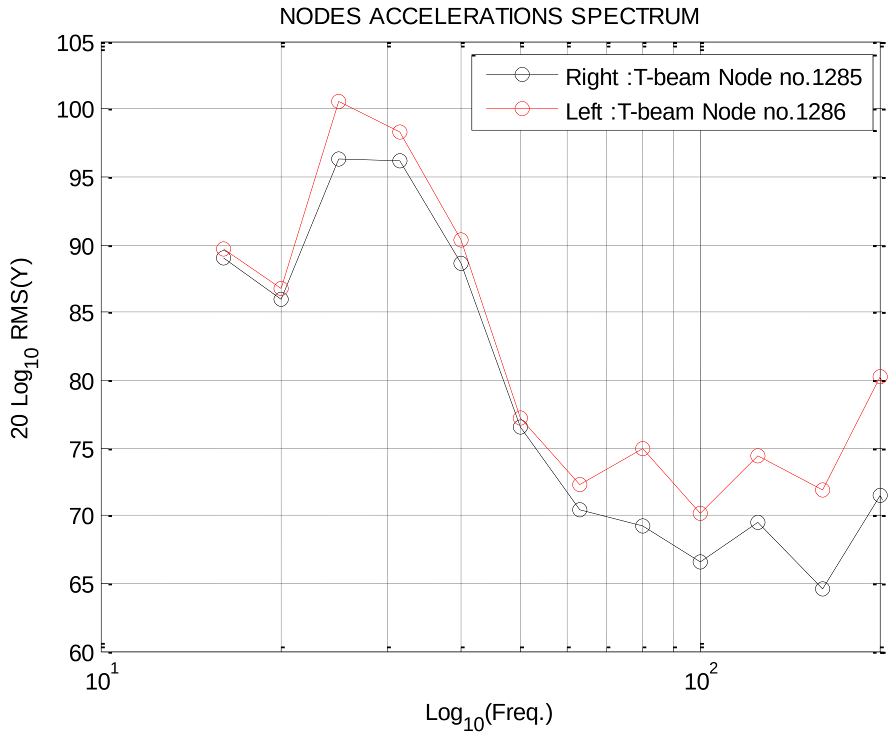

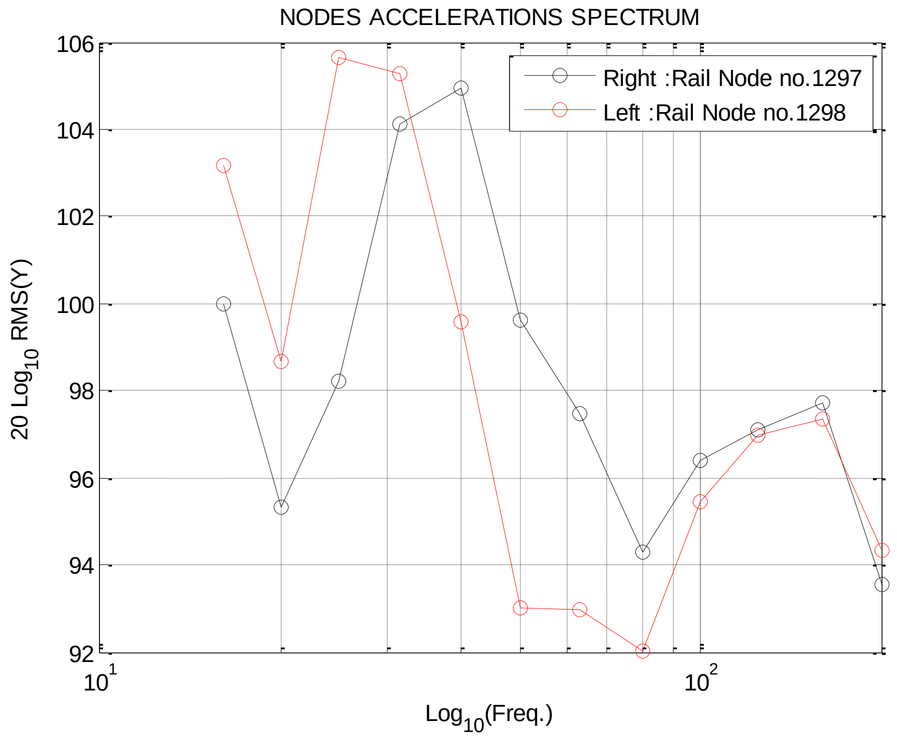
NODES ACCELERATIONS SPECTRUM
Right :Rail Node no.1297
Left :Rail Node no.1298
20 Log10 RMS(Y)
Log10(Freq.)
106
104
102
100
98
96
94
92
10^1
10^2

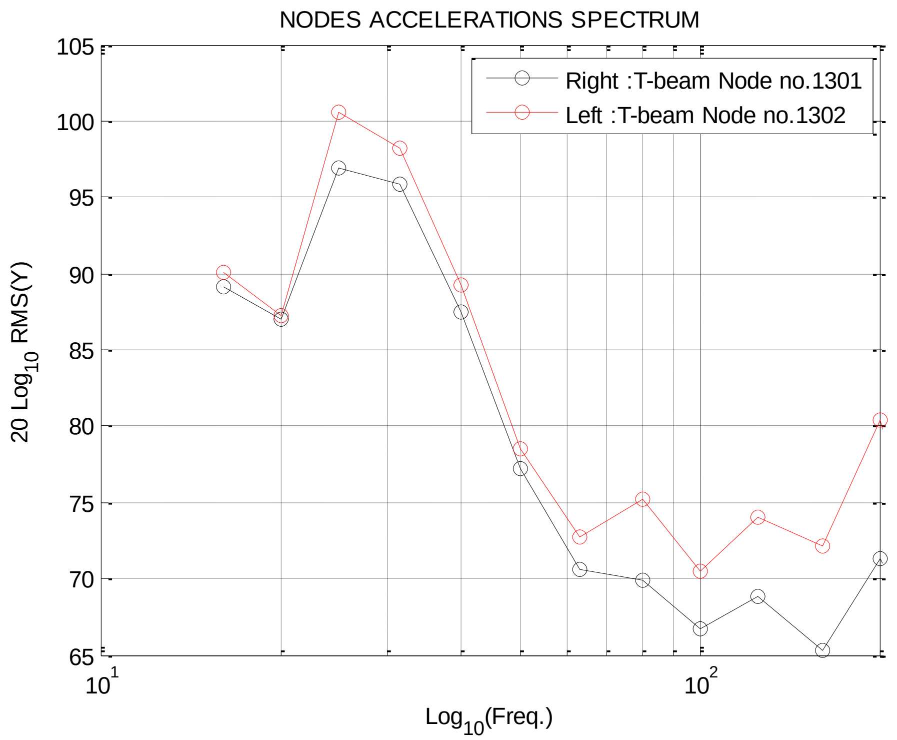
NODES ACCELERATIONS SPECTRUM
Right :T-beam Node no.1301
Left :T-beam Node no.1302
20 Log10 RMS(Y)
Log10(Freq.)
105
100
95
90
85
80
75
70
65
10^1
10^2

RFI 4 coach:

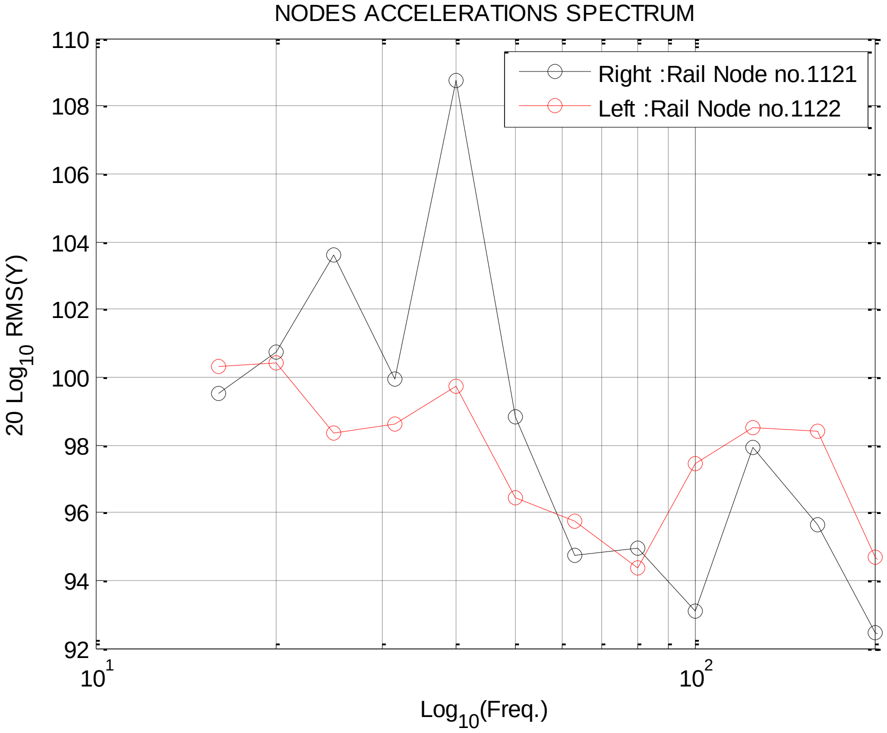
NODES ACCELERATIONS SPECTRUM
Right :Rail Node no.1121
Left :Rail Node no.1122
110
108
106
104
102
100
98
96
94
92
20 Log10 RMS(Y)
10^1
10^2
Log10(Freq.)

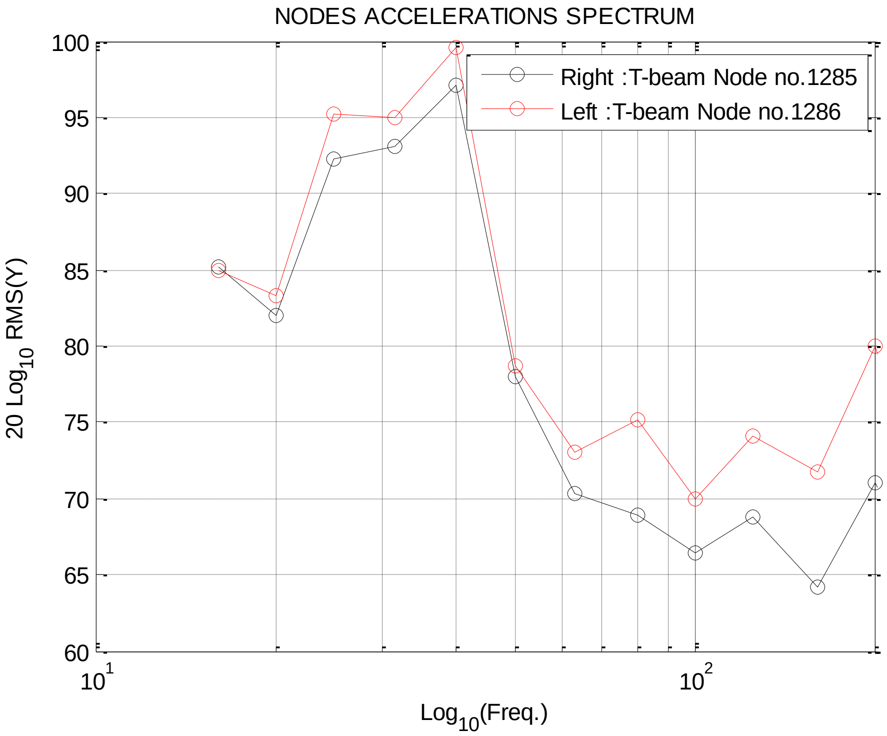
NODES ACCELERATIONS SPECTRUM
Right :T-beam Node no.1285
Left :T-beam Node no.1286
100
95
90
85
80
75
70
65
60
20 Log10 RMS(Y)
10^1
10^2
Log10(Freq.)

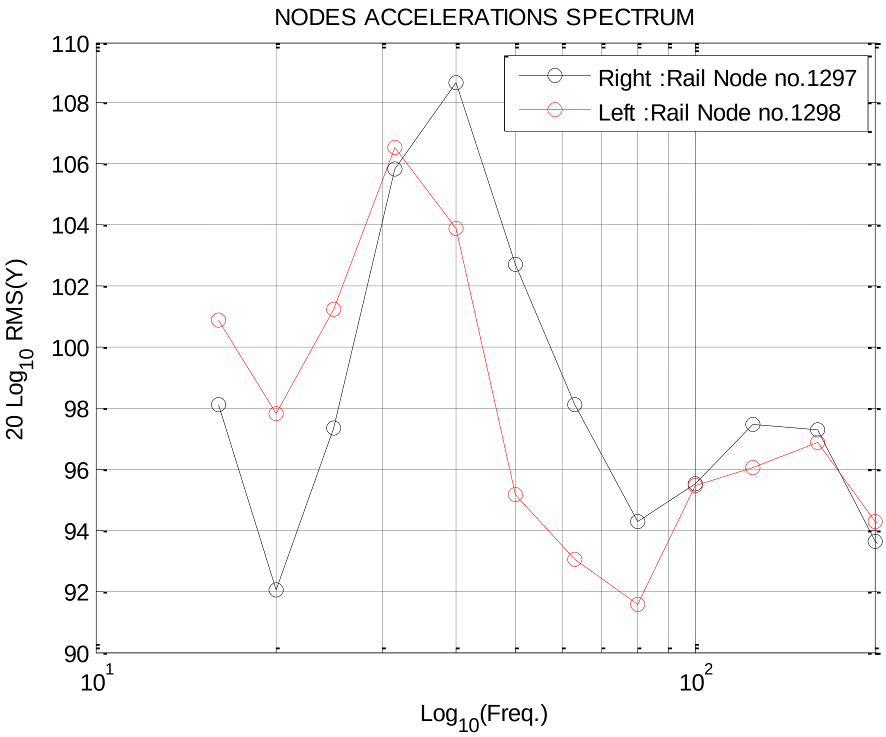

NODES ACCELERATIONS SPECTRUM
Right :Rail Node no.1297
Left :Rail Node no.1298
20 Log10 RMS(Y)
Log10(Freq.)
110
108
106
104
102
100
98
96
94
92
90
10^1
10^2

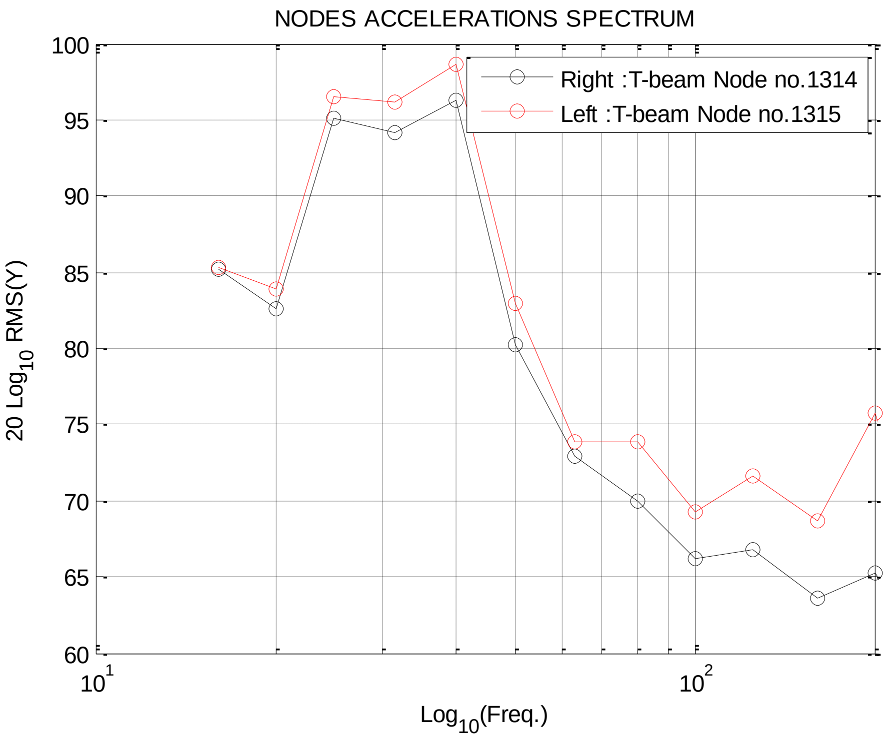

NODES ACCELERATIONS SPECTRUM
Right :T-beam Node no.1314
Left :T-beam Node no.1315
20 Log10 RMS(Y)
Log10(Freq.)
100
95
90
85
80
75
70
65
60
10^1
10^2

RFI 5 Full Load Freight Coach:

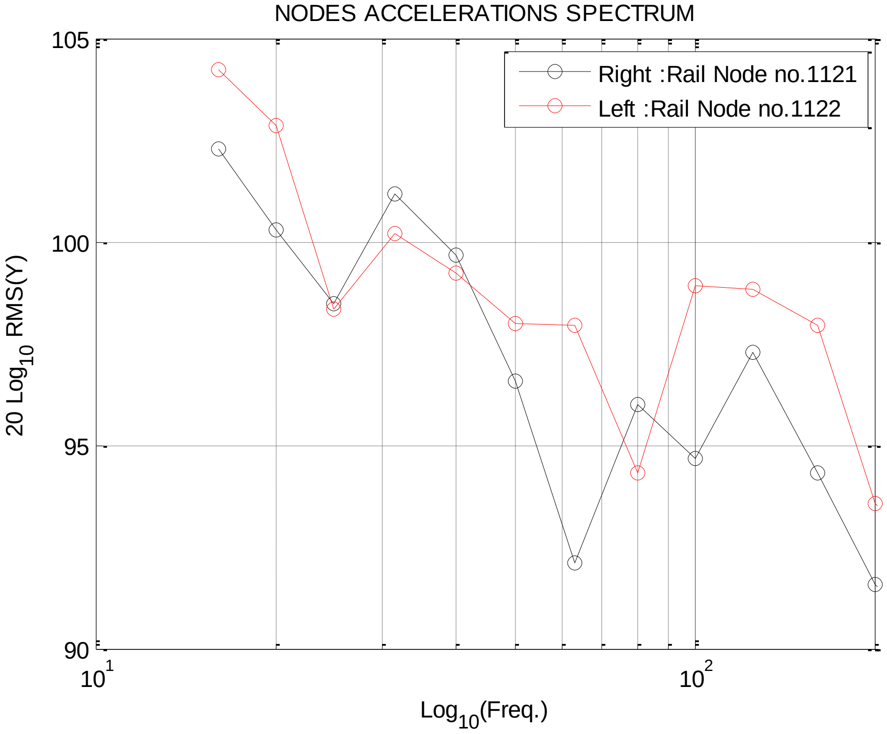

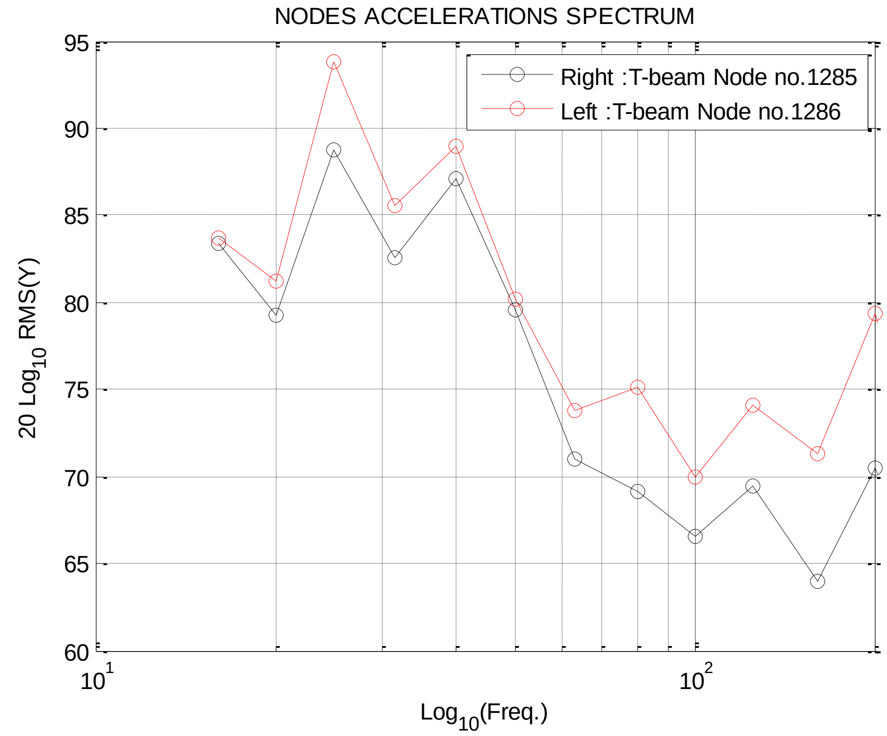

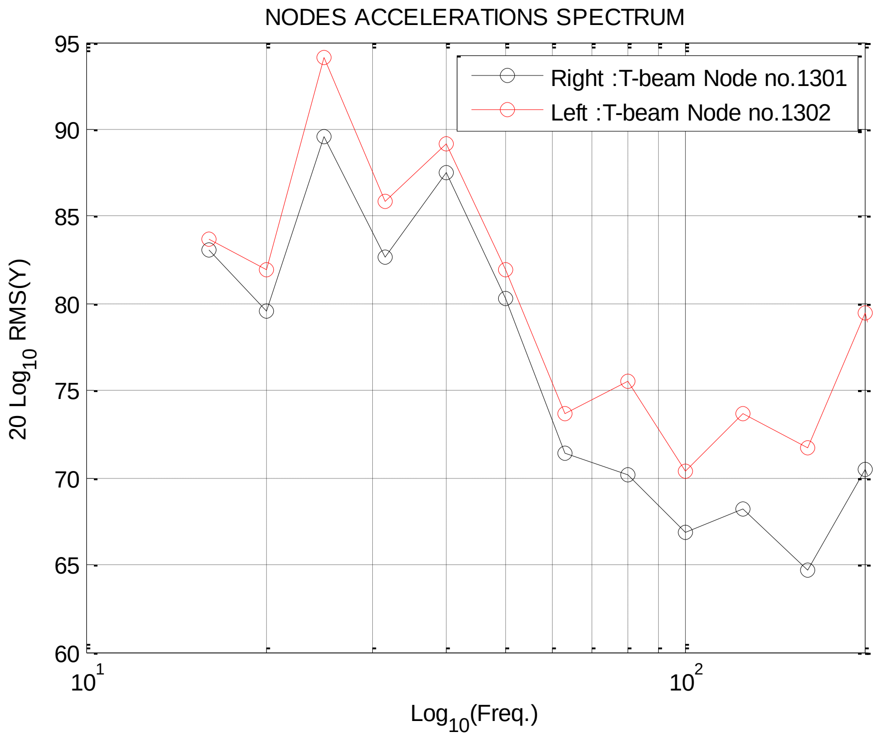
NODES ACCELERATIONS SPECTRUM
Right :T-beam Node no.1301
Left :T-beam Node no.1302
95
90
85
80
75
70
65
60
20 Log10 RMS(Y)
10^1
10^2
Log10(Freq.)

RFI 6 Empty Freight Coach:

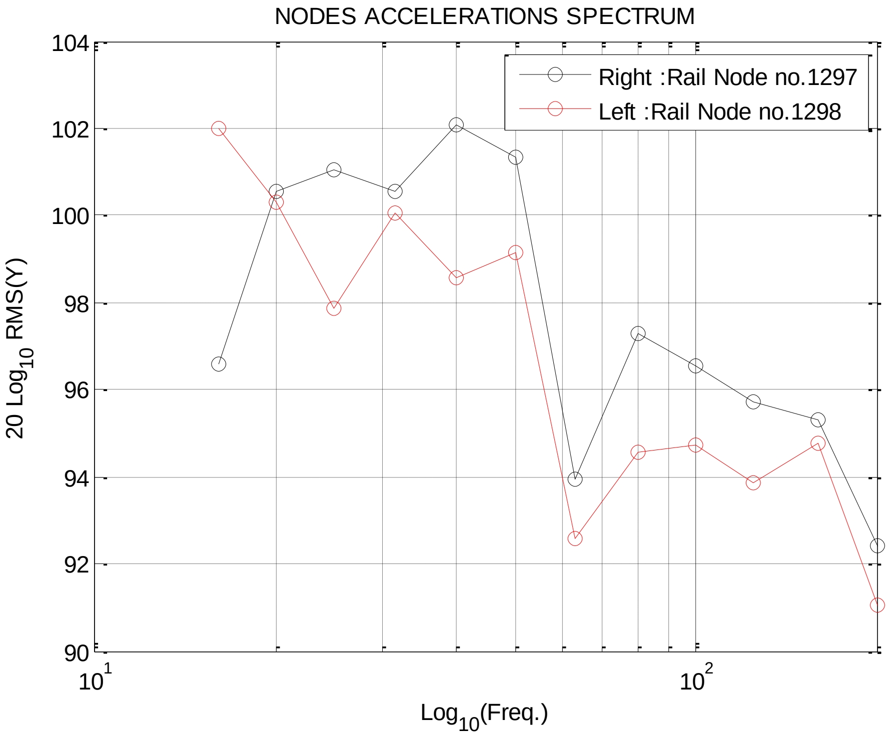

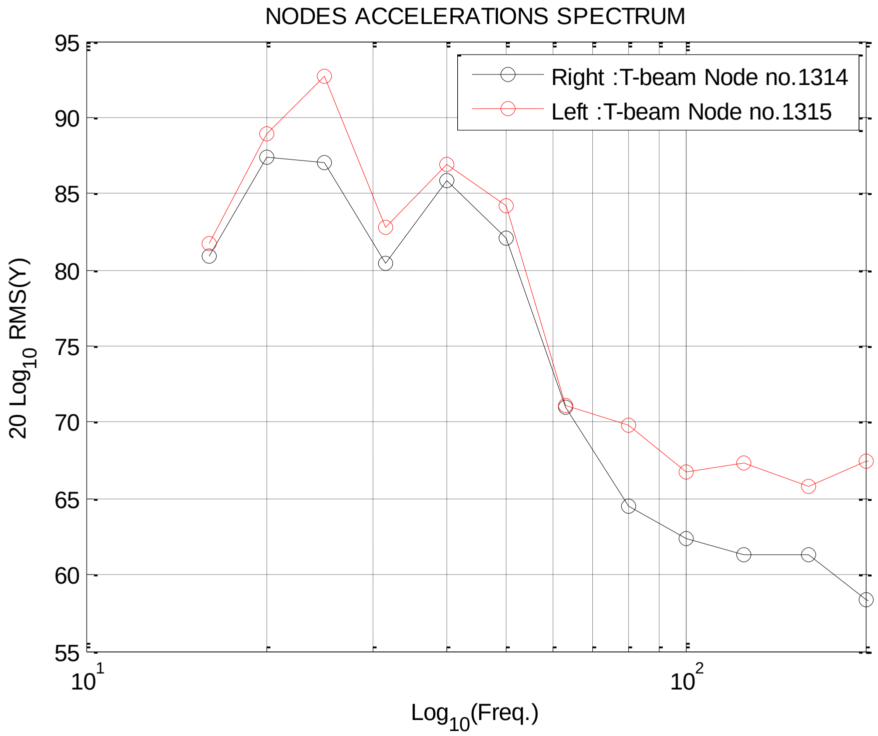

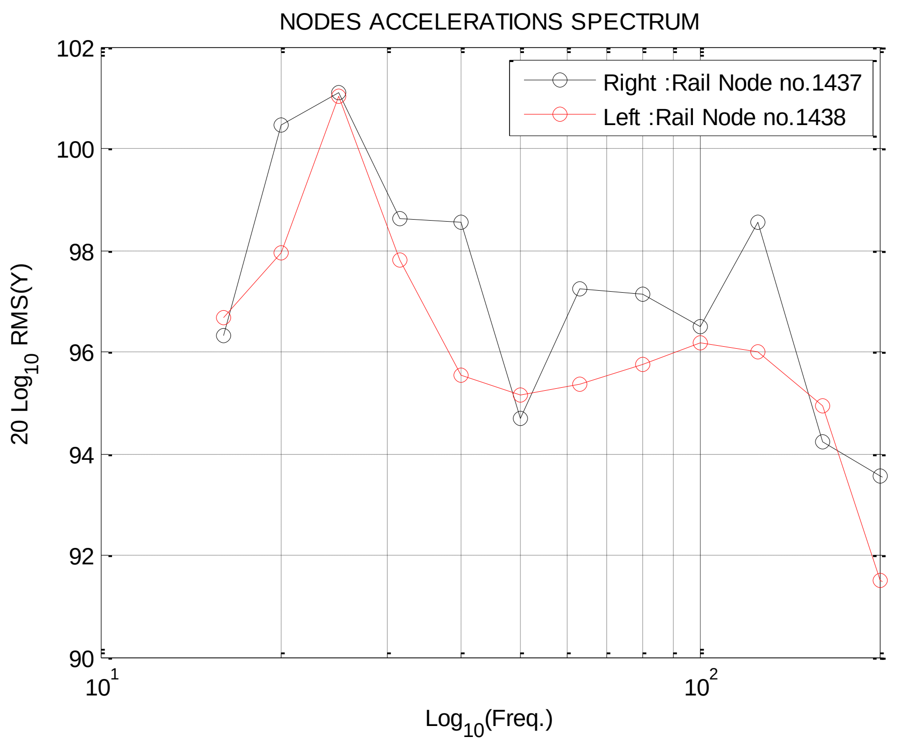

12 References

1 Stretto di Messina, DT.ISP.F.E.R3.001, "*Treni "Reali" Di Riferimento RFI. Caratteristiche Dinamiche Per Le Simulazioni Numeriche*"

2 Stretto di Messina, GCG.F.04.01 *Basis of Design and Expected Performance Levels for the Bridge.*

3 PG 2R B0-001 N03 p1 (GLOBAL MODEL)

4 ORE C 138 report 8: "Permissible maximum levels for the Y- and Q-forces and derailment criteria", Utrecht, September 1984

5 Esveld, Modern Railway Track, 1989, ISBN 90-800324-1-7.

6 Esveld, Interacton between Moving Vehicles and Railway Track at High Speed, REI / Edition 1998, no. 3, 1998.

7 Janin, Maintaining track geometry decision making for levelling and lining, French Railway Review, Vol. 1, No. 1, 1983.

8 TDC Report 59012B-DC-0201

9 Stretto di Messina, DT.ISP.A.E.R1.003, Approfondimento Del Comportamento Aerodinamico E Aeroelastico Del L'impalcato, III Fase, 30 Marzo 2004.

10 Esveld, Modern Railway Track 2nd Editino, ISBN 90-800324-3-3

11 J.J Kalker, "Computational contact mechanics of the wheel-rail system", Rail Quality and Maintenance for Modern Railway Operation, pp. 151-164

12 Shen, Z.Y., Hendrick J.K., Elkins J.A., (1983) "A comparison of alternative creep force models for rail vehicle dynamic analysis", 8th IAVSD Symposium Cambridge, MA

13 Diana G., Cheli F., Bruni S., Collina A., Viganò R., Di Bianco R., Traini G., A.D.Tre.S.: a software for bridge runnability analysis - World Congress on Railway Research WCRR'97, Firenze, Italy November 16-19 1997.

14 Diana G., Cheli F., Bruni S., Collina A., Modelli matematici per lo studio della interazione veicolo-struttura-armamento - Ingegneria Ferroviaria N. 12, Anno 1995.

15 Giorgio Diana, Bruno Pizzigoni, Federico Cheli, Sulla Dinamica dei Veicoli Ferroviari: Carrozza Gran Comfort (Modello a 23 g.d.l.), Politecnico di Milano, Dipartimento di Ingegneria Meccanica.

13 Appendix 1 (Full IBDAS results)

13.1 SLS1 load combination 2 - No thermal load

Limit state	Load combination	Train combination case	Track no.	RFI type	Meeting point	Train speed [km/h]	10 min mean wind speed [m/s]	Gust wind speed (incl. mean wind) [m/s]	Location for gust wind peak ("Chinese hat")	Thermal load	Seismic peak ground acc. [m/s^2]	Transverse slope [m/m]	Change of cant [m/m]	Non-compensated lateral acc. [m/s^2]	Roll speed [rad/s]	Derailment ratio incl. wind [-]	Derailment ratio excl. wind [-]	Overturning ratio incl. wind [-]	Sperling Ride index, Wz (unweighted) [-]	Sperling Ride index, Wz (weighted) [-]	Peak vertical acc. (unweighted) [m/s^2]	Peak vertical acc. (weighted) [m/s^2]	RMS vertical acc. (2.0 s.) (unweighted) [m/s^2]	RMS vertical acc. (2.0 s.) (weighted) [m/s^2]	Recoil (based on 2.0 s. RMS coach acc.) [m/s^3]	Vertical peak acc., trackbed (unweighted) [m/s^2]	Vertical peak acc., trackbed (weighted) [m/s^2]
Limit												0.08	0.0025	0.6	0.033	0.8	0.8	0.9	2.2	2.2	2.00	2.00	0.75	0.75	0.25	0.70	0.70
SLS1	2	1	1	1		144	0	0		No	0.0	0.0095	0.0000	0.134	0.006	0.105	0.105	0.192								0.040	0.025
SLS1	2	1	1	1		120	0	0		No	0.0								0.61	0.51	1.37	0.84	0.60	0.33	0.84		
SLS1	2	2	1	2		144	0	0		No	0.0	0.0098	0.0001	0.138	0.009	0.068	0.068	0.119								0.038	0.018
SLS1	2	2	1	2		120	0	0		No	0.0								0.61	0.52	1.40	0.87	0.60	0.34	0.87		
SLS1	2	3	1	3		144	0	0		No	0.0	0.0099	0.0001	0.139	0.017	0.100	0.100	0.241								0.050	0.033
SLS1	2	3	1	3		120	0	0		No	0.0								0.63	0.55	1.84	1.22	0.77	0.51	1.22		
SLS1	2	4	1	4		144	0	0		No	0.0	0.0094	0.0000	0.132	0.003	0.022	0.022	0.195								0.060	0.043
SLS1	2	4	1	4		120	0	0		No	0.0								0.70	0.60	1.81	1.07	0.91	0.54	0.97		
SLS1	2	5	1	5		144	0	0		No	0.0	0.0201	0.0001	0.281	0.019	0.124	0.124	0.284								0.110	0.043
SLS1	2	6	1	6		144	0	0		No	0.0	0.0099	0.0001	0.138	0.016	0.097	0.097	0.450								0.041	0.027
SLS1	2	7	1	1	Middle of bridge	144	0	0		No	0.0	0.0095	0.0000	0.134	0.006	0.105	0.105	0.192								0.042	0.026
			2	1								0.0080	0.0000	0.113	0.006	0.104	0.104	0.189									
SLS1	2	7	1	1	S+ tower	144	0	0		No	0.0	0.0095	0.0000	0.134	0.006	0.105	0.105	0.192								0.047	0.026
			2	1								0.0064	0.0000	0.090	0.006	0.091	0.091	0.189									
SLS1	2	7	1	1	S+ expansion joint	144	0	0		No	0.0	0.0095	0.0001	0.134	0.006	0.105	0.105	0.192								0.047	0.026
			2	1								0.0064	0.0000	0.090	0.006	0.091	0.091	0.189									
SLS1	2	7	1	1	Middle of bridge	120	0	0		No	0.0								0.61	0.51	1.37	0.84	0.60	0.33	0.83		
			2	1															0.61	0.51	1.37	0.84	0.60	0.34	1.10		
SLS1	2	7	1	1	S+ tower	120	0	0		No	0.0								0.56	0.47	1.37	0.84	0.60	0.33	0.83		
			2	1															0.56	0.47	1.37	0.84	0.60	0.34	1.10		
SLS1	2	7	1	1	S+ expansion joint	120	0	0		No	0.0								0.56	0.47	1.37	0.84	0.60	0.33	0.83		
			2	1															0.56	0.47	1.37	0.84	0.60	0.34	1.10		
SLS1	2	8	1	1	Middle of bridge	144	0	0		No	0.0	0.0096	0.0000	0.134	0.006	0.105	0.105	0.192								0.042	0.025
			2	2								0.0078	0.0000	0.110	0.009	0.083	0.083	0.122									
SLS1	2	8	1	1	S+ tower	144	0	0		No	0.0	0.0095	0.0000	0.134	0.006	0.105	0.105	0.192								0.052	0.025
			2	2								0.0062	0.0000	0.087	0.009	0.084	0.084	0.122									
SLS1	2	8	1	1	S+ expansion joint	144	0	0		No	0.0	0.0095	0.0000	0.134	0.006	0.105	0.105	0.192								0.047	0.025
			2	2								0.0062	0.0000	0.087	0.009	0.084	0.084	0.122									
SLS1	2	8	1	1	Middle of bridge	120	0	0		No	0.0								0.61	0.51	1.37	0.84	0.60	0.33	0.83		
			2	2															0.61	0.52	1.40	0.87	0.61	0.36	1.20		
SLS1	2	8	1	1	S+ tower	120	0	0		No	0.0								0.56	0.47	1.37	0.84	0.60	0.33	0.83		
			2	2															0.56	0.47	1.40	0.87	0.61	0.36	1.20		
SLS1	2	8	1	1	S+ expansion joint	120	0	0		No	0.0								0.56	0.47	1.37	0.84	0.60	0.33	0.83		
			2	2															0.56	0.47	1.40	0.87	0.61	0.36	1.20		
SLS1	2	9	1	1	Middle of bridge	144	0	0		No	0.0	0.0096	0.0001	0.134	0.006	0.105	0.105	0.192								0.047	0.031
			2	3								0.0080	0.0000	0.113	0.016	0.112	0.112	0.244									
SLS1	2	9	1	1	S+ tower	144	0	0		No	0.0	0.0095	0.0000	0.134	0.006	0.105	0.105	0.192								0.050	0.031
			2	3								0.0064	0.0000	0.089	0.016	0.112	0.112	0.244									
SLS1	2	9	1	1	S+ expansion joint	144	0	0		No	0.0	0.0095	0.0001	0.134	0.006	0.105	0.105	0.192								0.047	0.031
			2	3								0.0063	0.0000	0.089	0.016	0.112	0.112	0.244									
SLS1	2	9	1	1	Middle of bridge	120	0	0		No	0.0								0.60	0.51	1.37	0.84	0.60	0.33	0.83		
			2	3															0.63	0.55	1.82	1.34	0.77	0.51	2.09		
SLS1	2	9	1	1	S+ tower	120	0	0		No	0.0								0.56	0.47	1.37	0.84	0.60	0.33	0.83		
			2	3															0.58	0.51	1.82	1.34	0.77	0.51	2.09		
SLS1	2	9	1	1	S+ expansion joint	120	0	0		No	0.0								0.55	0.47	1.37	0.84	0.60	0.33	0.83		
			2	3															0.58	0.51	1.82	1.34	0.77	0.51	2.09		
SLS1	2	10	1	1	Middle of bridge	144	0	0		No	0.0	0.0095	0.0000	0.134	0.006	0.106	0.106	0.192								0.060	0.042
			2	4								0.0081	0.0000	0.113	0.002	0.027	0.027	0.209									
SLS1	2	10	1	1	S+ tower	144	0	0		No	0.0	0.0095	0.0000	0.134	0.006	0.105	0.105	0.192								0.060	0.042
			2	4								0.0065	0.0001	0.091	0.002	0.026	0.026	0.209									
SLS1	2	10	1	1	S+ expansion joint	144	0	0		No	0.0	0.0095	0.0001	0.134	0.006	0.105	0.105	0.192								0.060	0.042
			2	4								0.0065	0.0001	0.091	0.002	0.026	0.026	0.209									
SLS1	2	10	1	1	Middle of bridge	120	0	0		No	0.0								0.61	0.51	1.37	0.84	0.60	0.33	0.84		
			2	4															0.70	0.60	1.80	1.06	0.92	0.55	1.23		
SLS1	2	10	1	1	S+ tower	120	0	0		No	0.0								0.56	0.47	1.37	0.84	0.60	0.33	0.83		
			2	4															0.64	0.55	1.79	1.05	0.92	0.56	1.23		
SLS1	2	10	1	1	S+ expansion joint	120	0	0		No	0.0								0.56	0.47	1.37	0.84	0.60	0.33	0.83		
			2	4															0.64	0.55	1.79	1.05	0.92	0.56	1.23		
SLS1	2	11	1	1	Middle of bridge	144	0	0		No	0.0	0.0128	0.0001	0.179	0.006	0.106	0.106	0.191								0.107	0.041
			2	5								0.0013	0.0001	0.111	0.016	0.107	0.107	0.299									
SLS1	2	11	1	1	S+ tower	144	0	0		No	0.0	0.0095	0.0000	0.134	0.006	0.094	0.094	0.192								0.110	0.041
			2	5								0.0012	0.0001	0.105	0.015	0.107	0.107	0.299									
SLS1	2	11	1	1	S+ expansion joint	144	0	0		No	0.0	0.0095	0.0001	0.134	0.006	0.094	0.094	0.192								0.116	0.044
			2	5								0.0009	0.0001	0.105	0.015	0.107	0.107	0.299									
SLS1	2	11	1	1	Middle of bridge	120	0	0		No	0.0								0.60	0.51	1.37	0.84	0.60	0.33	0.84		
SLS1	2	11	1	1	S+ tower	120	0	0		No	0.0								0.56	0.47	1.37	0.84	0.60	0.33	0.83		
SLS1	2	11	1	1	S+ expansion joint	120	0	0		No	0.0								0.55	0.47	1.37	0.84	0.60	0.33	0.83		
SLS1	2	12	1	1	Middle of bridge	144	0	0		No	0.0	0.0095	0.0000	0.134	0.006	0.104	0.104	0.191								0.041	0.025
			2	6								0.0082	0.0000	0.115	0.016	0.113	0.113	0.432									
SLS1	2	12	1	1	S+ tower	144	0	0		No	0.0	0.0095	0.0000	0.134	0.006	0.103	0.103	0.192								0.050	0.025
			2	6								0.0065	0.0000	0.091	0.016	0.113	0.113	0.432									
SLS1	2	12	1	1	S+ expansion joint	144	0	0		No	0.0	0.0095	0.0001	0.134	0.006	0.103	0.103	0.192								0.045	0.025
			2	6								0.0065	0.0000	0.091	0.016	0.113	0.113	0.432									
SLS1	2	12	1	1	Middle of bridge	120	0	0		No	0.0								0.60	0.51	1.37	0.84	0.60	0.33	0.84		
SLS1	2	12	1	1	S+ tower	120	0	0		No	0.0								0.55	0.47	1.37	0.84	0.60	0.33	0.83		
SLS1	2	12	1	1	S+ expansion joint	120	0	0		No	0.0								0.55	0.47	1.37	0.84	0.60	0.33	0.83		
SLS1	2	13	1	2	Middle of bridge	144	0	0		No	0.0	0.0099	0.0001	0.139	0.009	0.067	0.067	0.120								0.048	0.022
			2	2								0.0081	0.0000	0.114	0.009	0.083	0.083	0.121									
SLS1	2	13	1	2	S+ tower	144	0	0		No	0.0	0.0098	0.0001	0.138	0.009	0.067	0.067	0.120								0.049	0.022
			2	2								0.0062	0.0001	0.087	0.009	0.077	0.077	0.122									
SLS1	2	13	1	2	S+ expansion joint	144	0	0		No	0.0	0.0098	0.0001	0.138	0.009	0.067	0.067	0.120								0.049	0.020
			2	2								0.0062	0.0001	0.087	0.009	0.077	0.077	0.122									
SLS1	2	13	1	2	Middle of bridge	120	0	0		No	0.0								0.61	0.52	1.40	0.87	0.60	0.34	0.87		
			2	2															0.61	0.52	1.40	0.87	0.61	0.36	1.20		
SLS1	2	13	1	2	S+ tower	120	0	0		No	0.0								0.56	0.47	1.40	0.87	0.60	0.34	0.87		
			2	2															0.56	0.47	1.40	0.87	0.61	0.36	1.20		
SLS1	2	13	1	2	S+ expansion joint	120	0	0		No	0.0								0.56	0.47	1.40	0.87	0.60	0.34	0.87		
			2	2															0.56	0.47	1.40	0.87	0.61	0.36	1.20		

Limit state	Load combination	Train combination case	Track no.	RFI type	Meeting point	Train speed [km/h]	10 min mean wind speed [m/s]	Gust wind speed (incl. mean wind) [m/s]	Location for gust wind peak ("Chinese hat")	Thermal load	Seismic peak ground acc. [m/s^2]	Transverse slope [m/m]	Change of cant [m/m]	Non-compensated lateral acc. [m/s^2]	Roll speed [rad/s]	Derailment ratio incl. wind [-]	Derailment ratio excl. wind [-]	Overturning ratio incl. wind [-]	Sperling Ride index, Wz (unweighted) [-]	Sperling Ride index, Wz (weighted) [-]	Peak vertical acc. (unweighted) [m/s^2]	Peak vertical acc. (weighted) [m/s^2]	RMS vertical acc. (2.0 s.) (unweighted) [m/s^2]	RMS vertical acc. (2.0 s.) (weighted) [m/s^2]	Recoil (based on 2.0 s. RMS coach acc.) [m/s^3]	Vertical peak acc., trackbed (unweighted) [m/s^2]	Vertical peak acc., trackbed (weighted) [m/s^2]
Limit												0.08	0.0025	0.6	0.033	0.8	0.8	0.9	2.2	2.2	2.00	2.00	0.75	0.75	0.25	0.70	0.70
SLS1	2	14	1	2	Middle of bridge	144	0	0		No	0.0	0.0099	0.0001	0.139	0.009	0.067	0.067	0.120								0.051	0.031
			2	3								0.0083	0.0000	0.117	0.016	0.112	0.112	0.244									
SLS1	2	14	1	2	S+ tower	144	0	0		No	0.0	0.0098	0.0001	0.138	0.009	0.066	0.066	0.120								0.049	0.031
			2	3								0.0064	0.0001	0.089	0.016	0.112	0.112	0.244									
SLS1	2	14	1	2	S+ expansion joint	144	0	0		No	0.0	0.0098	0.0001	0.138	0.009	0.066	0.066	0.120								0.048	0.031
			2	3								0.0063	0.0001	0.089	0.016	0.112	0.112	0.244									
SLS1	2	14	1	2	Middle of bridge	120	0	0		No	0.0								0.60	0.51	1.40	0.87	0.60	0.34	0.87		
			2	3															0.63	0.55	1.82	1.34	0.77	0.51	2.09		
SLS1	2	14	1	2	S+ tower	120	0	0		No	0.0								0.56	0.47	1.40	0.87	0.60	0.34	0.87		
			2	3															0.58	0.51	1.82	1.34	0.77	0.51	2.09		
SLS1	2	14	1	2	S+ expansion joint	120	0	0		No	0.0								0.55	0.47	1.40	0.87	0.60	0.34	0.87		
			2	3															0.58	0.51	1.82	1.34	0.77	0.51	2.09		
SLS1	2	15	1	2	Middle of bridge	144	0	0		No	0.0	0.0099	0.0001	0.138	0.009	0.067	0.067	0.120								0.060	0.042
			2	4								0.0084	0.0000	0.117	0.002	0.027	0.027	0.209									
SLS1	2	15	1	2	S+ tower	144	0	0		No	0.0	0.0098	0.0001	0.138	0.009	0.067	0.067	0.120								0.062	0.042
			2	4								0.0065	0.0001	0.091	0.002	0.026	0.026	0.209									
SLS1	2	15	1	2	S+ expansion joint	144	0	0		No	0.0	0.0098	0.0001	0.138	0.009	0.067	0.067	0.120								0.060	0.042
			2	4								0.0065	0.0001	0.091	0.002	0.026	0.026	0.209									
SLS1	2	15	1	2	Middle of bridge	120	0	0		No	0.0								0.61	0.52	1.40	0.87	0.60	0.34	0.87		
			2	4															0.70	0.60	1.79	1.05	0.92	0.55	1.23		
SLS1	2	15	1	2	S+ tower	120	0	0		No	0.0								0.56	0.48	1.40	0.87	0.60	0.34	0.87		
			2	4															0.64	0.55	1.79	1.05	0.92	0.56	1.23		
SLS1	2	15	1	2	S+ expansion joint	120	0	0		No	0.0								0.56	0.47	1.40	0.87	0.60	0.34	0.87		
			2	4															0.64	0.55	1.79	1.05	0.92	0.56	1.23		
SLS1	2	16	1	2	Middle of bridge	144	0	0		No	0.0	0.0131	0.0001	0.184	0.009	0.067	0.067	0.119								0.107	0.041
			2	5								0.0017	0.0001	0.112	0.016	0.107	0.107	0.299									
SLS1	2	16	1	2	S+ tower	144	0	0		No	0.0	0.0098	0.0001	0.138	0.009	0.062	0.062	0.120								0.108	0.041
			2	5								0.0013	0.0001	0.105	0.015	0.107	0.107	0.299									
SLS1	2	16	1	2	S+ expansion joint	144	0	0		No	0.0	0.0098	0.0001	0.138	0.009	0.062	0.062	0.120								0.116	0.043
			2	5								0.0009	0.0001	0.105	0.015	0.107	0.107	0.299									
SLS1	2	16	1	2	Middle of bridge	120	0	0		No	0.0								0.60	0.51	1.40	0.87	0.60	0.34	0.87		
SLS1	2	16	1	2	S+ tower	120	0	0		No	0.0								0.56	0.47	1.40	0.87	0.60	0.34	0.87		
SLS1	2	16	1	2	S+ expansion joint	120	0	0		No	0.0								0.56	0.47	1.40	0.87	0.60	0.34	0.87		
SLS1	2	17	1	2	Middle of bridge	144	0	0		No	0.0	0.0098	0.0001	0.138	0.009	0.067	0.067	0.119								0.041	0.024
			2	6								0.0085	0.0000	0.119	0.016	0.113	0.113	0.432									
SLS1	2	17	1	2	S+ tower	144	0	0		No	0.0	0.0098	0.0001	0.138	0.009	0.065	0.065	0.120								0.055	0.027
			2	6								0.0065	0.0000	0.091	0.016	0.113	0.113	0.432									
SLS1	2	17	1	2	S+ expansion joint	144	0	0		No	0.0	0.0098	0.0001	0.138	0.009	0.065	0.065	0.120								0.046	0.024
			2	6								0.0065	0.0001	0.091	0.016	0.113	0.113	0.432									
SLS1	2	17	1	2	Middle of bridge	120	0	0		No	0.0								0.60	0.51	1.40	0.87	0.60	0.34	0.87		
SLS1	2	17	1	2	S+ tower	120	0	0		No	0.0								0.56	0.47	1.40	0.87	0.60	0.34	0.87		
SLS1	2	17	1	2	S+ expansion joint	120	0	0		No	0.0								0.55	0.47	1.40	0.87	0.60	0.34	0.87		
SLS1	2	18	1	3	Middle of bridge	144	0	0		No	0.0	0.0100	0.0001	0.141	0.016	0.098	0.098	0.241								0.059	0.033
			2	3								0.0084	0.0000	0.118	0.016	0.113	0.113	0.244									
SLS1	2	18	1	3	S+ tower	144	0	0		No	0.0	0.0099	0.0000	0.139	0.016	0.097	0.097	0.241								0.065	0.033
			2	3								0.0064	0.0001	0.089	0.016	0.112	0.112	0.244									
SLS1	2	18	1	3	S+ expansion joint	144	0	0		No	0.0	0.0099	0.0001	0.139	0.016	0.097	0.097	0.241								0.054	0.033
			2	3								0.0063	0.0001	0.089	0.016	0.112	0.112	0.244									
SLS1	2	18	1	3	Middle of bridge	120	0	0		No	0.0								0.63	0.55	1.84	1.22	0.77	0.51	1.22		
			2	3															0.63	0.55	1.82	1.34	0.77	0.51	2.09		
SLS1	2	18	1	3	S+ tower	120	0	0		No	0.0								0.58	0.51	1.84	1.22	0.77	0.51	1.22		
			2	3															0.58	0.51	1.82	1.34	0.77	0.51	2.09		
SLS1	2	18	1	3	S+ expansion joint	120	0	0		No	0.0								0.58	0.51	1.84	1.22	0.77	0.51	1.22		
			2	3															0.58	0.51	1.82	1.34	0.77	0.51	2.09		
SLS1	2	19	1	3	Middle of bridge	144	0	0		No	0.0	0.0100	0.0001	0.141	0.016	0.098	0.098	0.241								0.065	0.042
			2	4								0.0083	0.0000	0.117	0.002	0.027	0.027	0.209									
SLS1	2	19	1	3	S+ tower	144	0	0		No	0.0	0.0099	0.0000	0.139	0.016	0.097	0.097	0.241								0.083	0.045
			2	4								0.0065	0.0001	0.091	0.002	0.026	0.026	0.209									
SLS1	2	19	1	3	S+ expansion joint	144	0	0		No	0.0	0.0099	0.0001	0.139	0.016	0.097	0.097	0.241								0.075	0.042
			2	4								0.0065	0.0001	0.091	0.002	0.026	0.026	0.209									
SLS1	2	19	1	3	Middle of bridge	120	0	0		No	0.0								0.63	0.55	1.84	1.22	0.77	0.51	1.22		
			2	4															0.70	0.60	1.79	1.05	0.92	0.56	1.23		
SLS1	2	19	1	3	S+ tower	120	0	0		No	0.0								0.59	0.51	1.84	1.22	0.77	0.51	1.22		
			2	4															0.64	0.55	1.79	1.05	0.92	0.56	1.23		
SLS1	2	19	1	3	S+ expansion joint	120	0	0		No	0.0								0.58	0.51	1.84	1.22	0.77	0.51	1.22		
			2	4															0.64	0.55	1.79	1.05	0.92	0.56	1.23		
SLS1	2	20	1	3	Middle of bridge	144	0	0		No	0.0	0.0132	0.0001	0.185	0.017	0.101	0.101	0.241								0.107	0.041
			2	5								0.0016	0.0001	0.113	0.016	0.108	0.108	0.299									
SLS1	2	20	1	3	S+ tower	144	0	0		No	0.0	0.0099	0.0001	0.139	0.016	0.097	0.097	0.240								0.108	0.044
			2	5								0.0015	0.0001	0.105	0.015	0.107	0.107	0.299									
SLS1	2	20	1	3	S+ expansion joint	144	0	0		No	0.0	0.0099	0.0001	0.139	0.016	0.097	0.097	0.240								0.112	0.044
			2	5								0.0012	0.0001	0.106	0.015	0.107	0.107	0.299									
SLS1	2	20	1	3	Middle of bridge	120	0	0		No	0.0								0.63	0.55	1.84	1.22	0.77	0.51	1.21		
SLS1	2	20	1	3	S+ tower	120	0	0		No	0.0								0.58	0.51	1.84	1.22	0.77	0.51	1.21		
SLS1	2	20	1	3	S+ expansion joint	120	0	0		No	0.0								0.58	0.51	1.84	1.22	0.77	0.51	1.21		
SLS1	2	21	1	3	Middle of bridge	144	0	0		No	0.0	0.0100	0.0001	0.140	0.016	0.099	0.099	0.238								0.050	0.033
			2	6								0.0085	0.0000	0.120	0.016	0.114	0.114	0.432									
SLS1	2	21	1	3	S+ tower	144	0	0		No	0.0	0.0099	0.0000	0.139	0.016	0.097	0.097	0.241								0.060	0.033
			2	6								0.0065	0.0000	0.091	0.016	0.113	0.113	0.432									
SLS1	2	21	1	3	S+ expansion joint	144	0	0		No	0.0	0.0099	0.0001	0.139	0.016	0.097	0.097	0.241								0.051	0.033
			2	6								0.0065	0.0001	0.091	0.016	0.113	0.113	0.432									
SLS1	2	21	1	3	Middle of bridge	120	0	0		No	0.0								0.63	0.55	1.84	1.22	0.77	0.51	1.22		
SLS1	2	21	1	3	S+ tower	120	0	0		No	0.0								0.58	0.51	1.84	1.22	0.77	0.51	1.21		
SLS1	2	21	1	3	S+ expansion joint	120	0	0		No	0.0								0.58	0.51	1.84	1.22	0.77	0.51	1.21		
SLS1	2	22	1	4	Middle of bridge	144	0	0		No	0.0	0.0093	0.0000	0.131	0.003	0.022	0.022	0.195								0.060	0.043
			2	4								0.0079	0.0000	0.111	0.002	0.026	0.026	0.209									
SLS1	2	22	1	4	S+ tower	144	0	0		No	0.0	0.0094	0.0000	0.132	0.003	0.022	0.022	0.195								0.062	0.043
			2	4								0.0065	0.0000	0.091	0.002	0.026	0.026	0.209									
SLS1	2	22	1	4	S+ expansion joint	144	0	0		No	0.0	0.0094	0.0001	0.132	0.003	0.022	0.022	0.195								0.060	0.043
			2	4								0.0065	0.0000	0.091	0.002	0.026	0.026	0.209									
SLS1	2	22	1	4	Middle of bridge	120	0	0		No	0.0								0.70	0.61	1.81	1.07	0.91	0.54	0.97		
			2	4															0.70	0.60	1.80	1.06	0.92	0.56	1.23		
SLS1	2	22	1	4	S+ tower	120	0	0		No	0.0								0.64	0.55	1.81	1.07	0.91	0.54	0.97		
			2	4															0.64	0.55	1.80	1.06	0.92	0.56	1.23		
SLS1	2	22	1	4	S+ expansion joint	120	0	0		No	0.0								0.64	0.55	1.81	1.07	0.91	0.54	0.97		
			2	4															0.64	0.55	1.80	1.06	0.92	0.56	1.23		

Limit state	Load combination	Train combination case	Track no.	RFI type	Meeting point	Train speed [km/h]	10 min mean wind speed [m/s]	Gust wind speed (incl. mean wind) [m/s]	Location for gust wind peak ("Chinese hat")	Thermal load	Seismic peak ground acc. [m/s^2]	Transverse slope [m/m]	Change of cant [m/m]	Non-compensated lateral acc. [m/s^2]	Roll speed [rad/s]	Derailment ratio incl. wind [-]	Derailment ratio excl. wind [-]	Overturning ratio incl. wind [-]	Sperling Ride index, Wz (unweighted) [-]	Sperling Ride index, Wz (weighted) [-]	Peak vertical acc. (unweighted) [m/s^2]	Peak vertical acc. (weighted) [m/s^2]	RMS vertical acc. (2.0 s.) (unweighted) [m/s^2]	RMS vertical acc. (2.0 s.) (weighted) [m/s^2]	Recoil (based on 2.0 s. RMS coach acc.) [m/s^3]	Vertical peak acc., trackbed (unweighted) [m/s^2]	Vertical peak acc., trackbed (weighted) [m/s^2]
Limit												0.08	0.0025	0.6	0.033	0.8	0.8	0.9	2.2	2.2	2.00	2.00	0.75	0.75	0.25	0.70	0.70
SLS1	2	23	1	4	Middle of bridge	144	0	0		No	0.0	0.0125	0.0001	0.176	0.003	0.024	0.024	0.194								0.105	0.043
			2	5								0.0012	0.0001	0.110	0.016	0.108	0.108	0.299									
SLS1	2	23	1	4	S+ tower	144	0	0		No	0.0	0.0094	0.0000	0.132	0.003	0.023	0.023	0.195								0.113	0.043
			2	5								0.0011	0.0001	0.105	0.015	0.107	0.107	0.299									
SLS1	2	23	1	4	S+ expansion joint	144	0	0		No	0.0	0.0094	0.0001	0.132	0.003	0.023	0.023	0.195								0.108	0.043
			2	5								0.0006	0.0001	0.106	0.015	0.107	0.107	0.299									
SLS1	2	23	1	4	Middle of bridge	120	0	0		No	0.0								0.69	0.60	1.81	1.06	0.91	0.54	0.97		
SLS1	2	23	1	4	S+ tower	120	0	0		No	0.0								0.64	0.55	1.81	1.06	0.91	0.54	0.97		
SLS1	2	23	1	4	S+ expansion joint	120	0	0		No	0.0								0.64	0.55	1.81	1.06	0.91	0.54	0.97		
SLS1	2	24	1	4	Middle of bridge	144	0	0		No	0.0	0.0093	0.0000	0.130	0.003	0.022	0.022	0.194								0.060	0.043
			2	6								0.0080	0.0000	0.112	0.016	0.113	0.113	0.432									
SLS1	2	24	1	4	S+ tower	144	0	0		No	0.0	0.0094	0.0000	0.132	0.003	0.023	0.023	0.195								0.060	0.043
			2	6								0.0065	0.0000	0.091	0.016	0.113	0.113	0.432									
SLS1	2	24	1	4	S+ expansion joint	144	0	0		No	0.0	0.0094	0.0001	0.132	0.003	0.023	0.023	0.195								0.060	0.043
			2	6								0.0065	0.0000	0.091	0.016	0.113	0.113	0.432									
SLS1	2	24	1	4	Middle of bridge	120	0	0		No	0.0								0.69	0.59	1.81	1.06	0.91	0.54	0.97		
SLS1	2	24	1	4	S+ tower	120	0	0		No	0.0								0.64	0.55	1.81	1.06	0.91	0.54	0.97		
SLS1	2	24	1	4	S+ expansion joint	120	0	0		No	0.0								0.64	0.55	1.81	1.06	0.91	0.54	0.97		
SLS1	2	25	1	5	Middle of bridge	144	0	0		No	0.0	0.0238	0.0002	0.333	0.018	0.138	0.138	0.284								0.132	0.050
			2	5								0.0119	0.0001	0.166	0.015	0.102	0.102	0.299									
SLS1	2	25	1	5	S+ tower	144	0	0		No	0.0	0.0201	0.0001	0.281	0.015	0.118	0.118	0.284								0.157	0.065
			2	5								0.0063	0.0001	0.105	0.016	0.107	0.107	0.299									
SLS1	2	25	1	5	S+ expansion joint	144	0	0		No	0.0	0.0201	0.0001	0.281	0.015	0.118	0.118	0.284								0.185	0.072
			2	5								0.0045	0.0001	0.107	0.017	0.117	0.117	0.299									
SLS1	2	26	1	5	Middle of bridge	144	0	0		No	0.0	0.0203	0.0001	0.285	0.020	0.123	0.123	0.284								0.109	0.043
			2	6								0.0186	0.0000	0.261	0.015	0.107	0.107	0.432									
SLS1	2	26	1	5	S+ tower	144	0	0		No	0.0	0.0201	0.0001	0.281	0.015	0.118	0.118	0.284								0.116	0.048
			2	6								0.0078	0.0001	0.109	0.016	0.113	0.113	0.432									
SLS1	2	26	1	5	S+ expansion joint	144	0	0		No	0.0	0.0201	0.0001	0.281	0.015	0.118	0.118	0.284								0.112	0.046
			2	6								0.0065	0.0001	0.091	0.016	0.113	0.113	0.432									
SLS1	2	27	1	6	Middle of bridge	144	0	0		No	0.0	0.0100	0.0001	0.141	0.016	0.096	0.096	0.451								0.044	0.027
			2	6								0.0085	0.0000	0.119	0.016	0.111	0.111	0.432									
SLS1	2	27	1	6	S+ tower	144	0	0		No	0.0	0.0099	0.0000	0.138	0.016	0.097	0.097	0.451								0.044	0.027
			2	6								0.0065	0.0000	0.091	0.016	0.113	0.113	0.432									
SLS1	2	27	1	6	Middle of bridge	144	0	0		No	0.0	0.0099	0.0001	0.138	0.016	0.097	0.097	0.451								0.057	0.028
			2	6								0.0046	0.0001	0.065	0.006	0.043	0.043	0.069									

13.2 SLS1 load combination 2 - Thermal load

Limit state	Load combination	Train combination case	Track no.	RFI type	Meeting point	Train speed [km/h]	10 min mean wind speed [m/s]	Gust wind speed (incl. mean wind) [m/s]	Location for gust wind peak ("Chinese hat")	Thermal load	Seismic peak ground acc. [m/s^2]	Transverse slope [m/m]	Change of cant [m/m]	Non-compensated lateral acc. [m/s^2]	Roll speed [rad/s]	Derailment ratio incl. wind [-]	Derailment ratio excl. wind [-]	Overturning ratio incl. wind [-]	Sperling Ride index, Wz (unweighted) [-]	Sperling Ride index, Wz (weighted) [-]	Peak vertical acc. (unweighted) [m/s^2]	Peak vertical acc. (weighted) [m/s^2]	RMS vertical acc. (2.0 s.) (unweighted) [m/s^2]	RMS vertical acc. (2.0 s.) (weighted) [m/s^2]	Recoil (based on 2.0 s. RMS coach acc.) [m/s^3]	Vertical peak acc., trackbed (unweighted) [m/s^2]	Vertical peak acc., trackbed (weighted) [m/s^2]
Limit												0.08	0.0025	0.6	0.033	0.8	0.8	0.9	2.2	2.2	2.00	2.00	0.75	0.75	0.25	0.70	0.70
SLS1	2	1	1	1		144	0	0		Yes	0.0	0.0095	0.0001	0.134	0.005	0.081	0.081	0.192								0.040	0.026
SLS1	2	1	1	1		120	0	0		Yes	0.0								0.61	0.51	1.37	0.84	0.60	0.33	0.83		
SLS1	2	2	1	2		144	0	0		Yes	0.0	0.0098	0.0001	0.138	0.007	0.053	0.053	0.119								0.038	0.018
SLS1	2	2	1	2		120	0	0		Yes	0.0								0.61	0.52	1.40	0.87	0.60	0.34	0.86		
SLS1	2	3	1	3		144	0	0		Yes	0.0	0.0099	0.0001	0.139	0.012	0.075	0.075	0.241								0.050	0.033
SLS1	2	3	1	3		120	0	0		Yes	0.0								0.63	0.55	1.84	1.22	0.74	0.49	1.22		
SLS1	2	4	1	4		144	0	0		Yes	0.0	0.0094	0.0001	0.132	0.002	0.018	0.018	0.195								0.060	0.043
SLS1	2	4	1	4		120	0	0		Yes	0.0								0.70	0.60	1.79	1.06	0.90	0.53	0.95		
SLS1	2	5	1	5		144	0	0		Yes	0.0	0.0201	0.0001	0.281	0.022	0.136	0.136	0.284								0.111	0.044
SLS1	2	6	1	6		144	0	0		Yes	0.0	0.0099	0.0001	0.139	0.012	0.074	0.074	0.450								0.040	0.027
SLS1	2	7	1	1	Middle of bridge	144	0	0		Yes	0.0	0.0095	0.0001	0.134	0.005	0.080	0.080	0.192								0.042	0.026
			2	1								0.0080	0.0000	0.113	0.005	0.079	0.079	0.189									
SLS1	2	7	1	1	S+ tower	144	0	0		Yes	0.0	0.0095	0.0001	0.134	0.005	0.080	0.080	0.192								0.048	0.026
			2	1								0.0064	0.0001	0.090	0.005	0.070	0.070	0.189									
SLS1	2	7	1	1	S+ expansion joint	144	0	0		Yes	0.0	0.0095	0.0001	0.134	0.005	0.080	0.080	0.192								0.047	0.026
			2	1								0.0064	0.0001	0.090	0.005	0.070	0.070	0.189									
SLS1	2	7	1	1	Middle of bridge	120	0	0		Yes	0.0								0.61	0.51	1.37	0.84	0.60	0.33	0.83		
			2	1															0.61	0.51	1.37	0.84	0.60	0.34	1.12		
SLS1	2	7	1	1	S+ tower	120	0	0		Yes	0.0								0.56	0.47	1.37	0.84	0.60	0.33	0.83		
			2	1															0.56	0.47	1.37	0.84	0.60	0.34	1.12		
SLS1	2	7	1	1	S+ expansion joint	120	0	0		Yes	0.0								0.56	0.47	1.37	0.84	0.60	0.33	0.83		
			2	1															0.56	0.47	1.37	0.84	0.60	0.34	1.12		
SLS1	2	8	1	1	Middle of bridge	144	0	0		Yes	0.0	0.0096	0.0001	0.135	0.005	0.081	0.081	0.191								0.042	0.026
			2	2								0.0078	0.0000	0.110	0.007	0.061	0.061	0.120									
SLS1	2	8	1	1	S+ tower	144	0	0		Yes	0.0	0.0095	0.0001	0.134	0.005	0.080	0.080	0.192								0.051	0.026
			2	2								0.0062	0.0001	0.087	0.007	0.059	0.059	0.120									
SLS1	2	8	1	1	S+ expansion joint	144	0	0		Yes	0.0	0.0095	0.0001	0.134	0.005	0.080	0.080	0.192								0.048	0.026
			2	2								0.0062	0.0001	0.087	0.007	0.059	0.059	0.120									
SLS1	2	8	1	1	Middle of bridge	120	0	0		Yes	0.0								0.61	0.51	1.37	0.84	0.60	0.33	0.83		
			2	2															0.61	0.52	1.40	0.87	0.61	0.35	1.23		
SLS1	2	8	1	1	S+ tower	120	0	0		Yes	0.0								0.56	0.47	1.37	0.84	0.60	0.33	0.83		
			2	2															0.56	0.47	1.40	0.87	0.61	0.35	1.23		
SLS1	2	8	1	1	S+ expansion joint	120	0	0		Yes	0.0								0.56	0.47	1.37	0.84	0.60	0.33	0.83		
			2	2															0.56	0.47	1.40	0.87	0.61	0.35	1.23		
SLS1	2	9	1	1	Middle of bridge	144	0	0		Yes	0.0	0.0096	0.0001	0.134	0.005	0.081	0.081	0.192								0.047	0.031
			2	3								0.0080	0.0000	0.113	0.012	0.086	0.086	0.244									
SLS1	2	9	1	1	S+ tower	144	0	0		Yes	0.0	0.0095	0.0001	0.134	0.005	0.079	0.079	0.192								0.050	0.031
			2	3								0.0064	0.0001	0.089	0.012	0.086	0.086	0.244									
SLS1	2	9	1	1	S+ expansion joint	144	0	0		Yes	0.0	0.0095	0.0001	0.134	0.005	0.079	0.079	0.192								0.047	0.031
			2	3								0.0064	0.0001	0.089	0.012	0.086	0.086	0.244									
SLS1	2	9	1	1	Middle of bridge	120	0	0		Yes	0.0								0.60	0.51	1.37	0.84	0.60	0.33	0.83		
			2	3															0.63	0.55	1.82	1.23	0.74	0.49	2.11		
SLS1	2	9	1	1	S+ tower	120	0	0		Yes	0.0								0.56	0.47	1.37	0.84	0.60	0.33	0.83		
			2	3															0.58	0.51	1.82	1.23	0.74	0.49	2.11		
SLS1	2	9	1	1	S+ expansion joint	120	0	0		Yes	0.0								0.55	0.47	1.37	0.84	0.60	0.33	0.83		
			2	3															0.58	0.51	1.82	1.23	0.74	0.49	2.11		
SLS1	2	10	1	1	Middle of bridge	144	0	0		Yes	0.0	0.0095	0.0001	0.134	0.005	0.081	0.081	0.192								0.060	0.042
			2	4								0.0081	0.0000	0.113	0.002	0.020	0.020	0.209									
SLS1	2	10	1	1	S+ tower	144	0	0		Yes	0.0	0.0095	0.0001	0.134	0.005	0.080	0.080	0.192								0.060	0.042
			2	4								0.0065	0.0001	0.091	0.002	0.020	0.020	0.209									
SLS1	2	10	1	1	S+ expansion joint	144	0	0		Yes	0.0	0.0095	0.0001	0.134	0.005	0.080	0.080	0.192								0.060	0.042
			2	4								0.0065	0.0001	0.091	0.002	0.020	0.020	0.209									
SLS1	2	10	1	1	Middle of bridge	120	0	0		Yes	0.0								0.61	0.51	1.37	0.84	0.60	0.33	0.83		
			2	4															0.70	0.60	1.80	1.06	0.90	0.54	1.27		
SLS1	2	10	1	1	S+ tower	120	0	0		Yes	0.0								0.56	0.47	1.37	0.84	0.60	0.33	0.83		
			2	4															0.64	0.55	1.79	1.05	0.90	0.54	1.27		
SLS1	2	10	1	1	S+ expansion joint	120	0	0		Yes	0.0								0.56	0.47	1.37	0.84	0.60	0.33	0.83		
			2	4															0.64	0.55	1.79	1.05	0.90	0.54	1.27		
SLS1	2	11	1	1	Middle of bridge	144	0	0		Yes	0.0	0.0128	0.0001	0.179	0.005	0.082	0.082	0.191								0.107	0.041
			2	5								0.0013	0.0001	0.111	0.012	0.082	0.082	0.300									
SLS1	2	11	1	1	S+ tower	144	0	0		Yes	0.0	0.0095	0.0001	0.134	0.004	0.072	0.072	0.192								0.111	0.042
			2	5								0.0012	0.0001	0.105	0.012	0.081	0.081	0.300									
SLS1	2	11	1	1	S+ expansion joint	144	0	0		Yes	0.0	0.0095	0.0001	0.134	0.004	0.072	0.072	0.192								0.118	0.045
			2	5								0.0009	0.0001	0.105	0.012	0.081	0.081	0.300									
SLS1	2	11	1	1	Middle of bridge	120	0	0		Yes	0.0								0.60	0.51	1.37	0.84	0.60	0.33	0.83		
SLS1	2	11	1	1	S+ tower	120	0	0		Yes	0.0								0.56	0.47	1.37	0.84	0.60	0.33	0.83		
SLS1	2	11	1	1	S+ expansion joint	120	0	0		Yes	0.0								0.55	0.47	1.37	0.84	0.60	0.33	0.83		
SLS1	2	12	1	1	Middle of bridge	144	0	0		Yes	0.0	0.0095	0.0001	0.134	0.005	0.080	0.080	0.191								0.041	0.026
			2	6								0.0082	0.0000	0.115	0.012	0.087	0.087	0.432									
SLS1	2	12	1	1	S+ tower	144	0	0		Yes	0.0	0.0095	0.0001	0.134	0.004	0.072	0.072	0.192								0.050	0.026
			2	6								0.0065	0.0001	0.091	0.012	0.086	0.086	0.432									
SLS1	2	12	1	1	S+ expansion joint	144	0	0		Yes	0.0	0.0095	0.0001	0.134	0.004	0.072	0.072	0.192								0.045	0.026
			2	6								0.0065	0.0001	0.091	0.012	0.086	0.086	0.432									
SLS1	2	12	1	1	Middle of bridge	120	0	0		Yes	0.0								0.60	0.51	1.37	0.84	0.60	0.33	0.83		
SLS1	2	12	1	1	S+ tower	120	0	0		Yes	0.0								0.55	0.47	1.37	0.84	0.60	0.33	0.83		
SLS1	2	12	1	1	S+ expansion joint	120	0	0		Yes	0.0								0.55	0.47	1.37	0.84	0.60	0.33	0.83		
SLS1	2	13	1	2	Middle of bridge	144	0	0		Yes	0.0	0.0099	0.0001	0.139	0.007	0.051	0.051	0.121								0.048	0.022
			2	2								0.0081	0.0000	0.114	0.007	0.059	0.059	0.120									
SLS1	2	13	1	2	S+ tower	144	0	0		Yes	0.0	0.0098	0.0001	0.138	0.007	0.051	0.051	0.121								0.049	0.022
			2	2								0.0062	0.0001	0.087	0.007	0.059	0.059	0.120									
SLS1	2	13	1	2	S+ expansion joint	144	0	0		Yes	0.0	0.0098	0.0001	0.138	0.007	0.051	0.051	0.121								0.049	0.020
			2	2								0.0062	0.0001	0.087	0.007	0.059	0.059	0.120									
SLS1	2	13	1	2	Middle of bridge	120	0	0		Yes	0.0								0.61	0.52	1.40	0.87	0.60	0.34	0.86		
			2	2															0.61	0.52	1.40	0.87	0.61	0.35	1.23		
SLS1	2	13	1	2	S+ tower	120	0	0		Yes	0.0								0.56	0.47	1.40	0.87	0.60	0.34	0.86		
			2	2															0.56	0.47	1.40	0.87	0.61	0.35	1.23		
SLS1	2	13	1	2	S+ expansion joint	120	0	0		Yes	0.0								0.56	0.47	1.40	0.87	0.60	0.34	0.86		
			2	2															0.56	0.47	1.40	0.87	0.61	0.35	1.23		

Limit state	Load combination	Train combination case	Track no.	RFI type	Meeting point	Train speed [km/h]	10 min mean wind speed [m/s]	Gust wind speed (incl. mean wind) [m/s]	Location for gust wind peak ("Chinese hat")	Thermal load	Seismic peak ground acc. [m/s^2]	Transverse slope [m/m]	Change of cant [m/m]	Non-compensated lateral acc. [m/s^2]	Roll speed [rad/s]	Derailment ratio incl. wind [-]	Derailment ratio excl. wind [-]	Overturning ratio incl. wind [-]	Sperling Ride index, Wz (unweighted) [-]	Sperling Ride index, Wz (weighted) [-]	Peak vertical acc. (unweighted) [m/s^2]	Peak vertical acc. (weighted) [m/s^2]	RMS vertical acc. (2.0 s.) (unweighted) [m/s^2]	RMS vertical acc. (2.0 s.) (weighted) [m/s^2]	Recoil (based on 2.0 s. RMS coach acc.) [m/s^3]	Vertical peak acc., trackbed (unweighted) [m/s^2]	Vertical peak acc., trackbed (weighted) [m/s^2]
Limit												0.08	0.0025	0.6	0.033	0.8	0.8	0.9	2.2	2.2	2.00	2.00	0.75	0.75	0.25	0.70	0.70
SLS1	2	14	1	2	Middle of bridge	144	0	0		Yes	0.0	0.0099	0.0001	0.139	0.007	0.050	0.050	0.121								0.051	0.031
			2	3								0.0083	0.0000	0.117	0.012	0.086	0.086	0.244									
SLS1	2	14	1	2	S+ tower	144	0	0		Yes	0.0	0.0098	0.0001	0.138	0.007	0.051	0.051	0.121								0.049	0.031
			2	3								0.0064	0.0001	0.089	0.012	0.086	0.086	0.244									
SLS1	2	14	1	2	S+ expansion joint	144	0	0		Yes	0.0	0.0098	0.0001	0.138	0.007	0.051	0.051	0.121								0.049	0.031
			2	3								0.0064	0.0001	0.089	0.012	0.086	0.086	0.244									
SLS1	2	14	1	2	Middle of bridge	120	0	0		Yes	0.0								0.60	0.51	1.40	0.87	0.60	0.34	0.86		
			2	3															0.63	0.55	1.82	1.23	0.74	0.49	2.11		
SLS1	2	14	1	2	S+ tower	120	0	0		Yes	0.0								0.56	0.47	1.40	0.87	0.60	0.34	0.86		
			2	3															0.58	0.51	1.82	1.23	0.74	0.49	2.11		
SLS1	2	14	1	2	S+ expansion joint	120	0	0		Yes	0.0								0.55	0.47	1.40	0.87	0.60	0.34	0.86		
			2	3															0.58	0.51	1.82	1.23	0.74	0.49	2.11		
SLS1	2	15	1	2	Middle of bridge	144	0	0		Yes	0.0	0.0099	0.0001	0.138	0.007	0.052	0.052	0.121								0.060	0.042
			2	4								0.0084	0.0000	0.117	0.002	0.020	0.020	0.209									
SLS1	2	15	1	2	S+ tower	144	0	0		Yes	0.0	0.0098	0.0001	0.138	0.007	0.051	0.051	0.121								0.061	0.042
			2	4								0.0065	0.0001	0.091	0.002	0.020	0.020	0.209									
SLS1	2	15	1	2	S+ expansion joint	144	0	0		Yes	0.0	0.0098	0.0001	0.138	0.007	0.051	0.051	0.121								0.060	0.042
			2	4								0.0065	0.0001	0.091	0.002	0.020	0.020	0.209									
SLS1	2	15	1	2	Middle of bridge	120	0	0		Yes	0.0								0.61	0.52	1.40	0.87	0.60	0.34	0.86		
			2	4															0.70	0.60	1.79	1.04	0.90	0.54	1.27		
SLS1	2	15	1	2	S+ tower	120	0	0		Yes	0.0								0.56	0.48	1.40	0.87	0.60	0.34	0.86		
			2	4															0.64	0.55	1.79	1.05	0.90	0.54	1.27		
SLS1	2	15	1	2	S+ expansion joint	120	0	0		Yes	0.0								0.56	0.47	1.40	0.87	0.60	0.34	0.86		
			2	4															0.64	0.55	1.79	1.05	0.90	0.54	1.27		
SLS1	2	16	1	2	Middle of bridge	144	0	0		Yes	0.0	0.0131	0.0001	0.184	0.007	0.053	0.053	0.119								0.107	0.041
			2	5								0.0017	0.0001	0.112	0.012	0.082	0.082	0.300									
SLS1	2	16	1	2	S+ tower	144	0	0		Yes	0.0	0.0098	0.0001	0.138	0.007	0.048	0.048	0.120								0.108	0.041
			2	5								0.0013	0.0001	0.105	0.012	0.081	0.081	0.300									
SLS1	2	16	1	2	S+ expansion joint	144	0	0		Yes	0.0	0.0098	0.0001	0.138	0.007	0.048	0.048	0.120								0.118	0.044
			2	5								0.0009	0.0001	0.105	0.012	0.081	0.081	0.300									
SLS1	2	16	1	2	Middle of bridge	120	0	0		Yes	0.0								0.60	0.51	1.40	0.87	0.60	0.34	0.86		
SLS1	2	16	1	2	S+ tower	120	0	0		Yes	0.0								0.56	0.47	1.40	0.87	0.60	0.34	0.86		
SLS1	2	16	1	2	S+ expansion joint	120	0	0		Yes	0.0								0.55	0.47	1.40	0.87	0.60	0.34	0.86		
SLS1	2	17	1	2	Middle of bridge	144	0	0		Yes	0.0	0.0098	0.0001	0.138	0.007	0.051	0.051	0.119								0.041	0.024
			2	6								0.0085	0.0000	0.119	0.012	0.087	0.087	0.432									
SLS1	2	17	1	2	S+ tower	144	0	0		Yes	0.0	0.0098	0.0001	0.138	0.007	0.050	0.050	0.120								0.055	0.027
			2	6								0.0065	0.0001	0.091	0.012	0.086	0.086	0.432									
SLS1	2	17	1	2	S+ expansion joint	144	0	0		Yes	0.0	0.0098	0.0001	0.138	0.007	0.050	0.050	0.120								0.046	0.024
			2	6								0.0065	0.0001	0.091	0.012	0.086	0.086	0.432									
SLS1	2	17	1	2	Middle of bridge	120	0	0		Yes	0.0								0.60	0.51	1.40	0.87	0.60	0.34	0.86		
SLS1	2	17	1	2	S+ tower	120	0	0		Yes	0.0								0.55	0.47	1.40	0.87	0.60	0.34	0.86		
SLS1	2	17	1	2	S+ expansion joint	120	0	0		Yes	0.0								0.55	0.47	1.40	0.87	0.60	0.34	0.86		
SLS1	2	18	1	3	Middle of bridge	144	0	0		Yes	0.0	0.0100	0.0001	0.141	0.013	0.076	0.076	0.241								0.059	0.033
			2	3								0.0084	0.0000	0.118	0.012	0.087	0.087	0.244									
SLS1	2	18	1	3	S+ tower	144	0	0		Yes	0.0	0.0099	0.0001	0.139	0.012	0.075	0.075	0.241								0.066	0.033
			2	3								0.0064	0.0001	0.089	0.012	0.086	0.086	0.244									
SLS1	2	18	1	3	S+ expansion joint	144	0	0		Yes	0.0	0.0099	0.0001	0.139	0.012	0.075	0.075	0.241								0.053	0.033
			2	3								0.0063	0.0001	0.089	0.012	0.086	0.086	0.244									
SLS1	2	18	1	3	Middle of bridge	120	0	0		Yes	0.0								0.63	0.55	1.84	1.22	0.74	0.49	1.22		
			2	3															0.63	0.55	1.82	1.23	0.74	0.49	2.11		
SLS1	2	18	1	3	S+ tower	120	0	0		Yes	0.0								0.58	0.51	1.84	1.22	0.74	0.49	1.22		
			2	3															0.58	0.51	1.82	1.23	0.74	0.49	2.11		
SLS1	2	18	1	3	S+ expansion joint	120	0	0		Yes	0.0								0.58	0.51	1.84	1.22	0.74	0.49	1.22		
			2	3															0.58	0.51	1.82	1.23	0.74	0.49	2.11		
SLS1	2	19	1	3	Middle of bridge	144	0	0		Yes	0.0	0.0100	0.0001	0.141	0.013	0.076	0.076	0.241								0.065	0.042
			2	4								0.0083	0.0000	0.117	0.002	0.020	0.020	0.209									
SLS1	2	19	1	3	S+ tower	144	0	0		Yes	0.0	0.0099	0.0001	0.139	0.012	0.075	0.075	0.241								0.083	0.045
			2	4								0.0065	0.0001	0.091	0.002	0.020	0.020	0.209									
SLS1	2	19	1	3	S+ expansion joint	144	0	0		Yes	0.0	0.0099	0.0001	0.139	0.012	0.075	0.075	0.241								0.074	0.042
			2	4								0.0065	0.0001	0.091	0.002	0.020	0.020	0.209									
SLS1	2	19	1	3	Middle of bridge	120	0	0		Yes	0.0								0.63	0.55	1.84	1.22	0.74	0.49	1.22		
			2	4															0.69	0.60	1.79	1.05	0.90	0.54	1.27		
SLS1	2	19	1	3	S+ tower	120	0	0		Yes	0.0								0.59	0.51	1.84	1.22	0.74	0.49	1.22		
			2	4															0.64	0.55	1.79	1.05	0.90	0.54	1.27		
SLS1	2	19	1	3	S+ expansion joint	120	0	0		Yes	0.0								0.58	0.51	1.84	1.22	0.74	0.49	1.22		
			2	4															0.64	0.55	1.79	1.05	0.90	0.54	1.27		
SLS1	2	20	1	3	Middle of bridge	144	0	0		Yes	0.0	0.0132	0.0001	0.185	0.013	0.078	0.078	0.241								0.107	0.041
			2	5								0.0016	0.0001	0.113	0.012	0.083	0.083	0.300									
SLS1	2	20	1	3	S+ tower	144	0	0		Yes	0.0	0.0099	0.0001	0.139	0.012	0.075	0.075	0.240								0.107	0.043
			2	5								0.0015	0.0001	0.105	0.012	0.081	0.081	0.300									
SLS1	2	20	1	3	S+ expansion joint	144	0	0		Yes	0.0	0.0099	0.0001	0.139	0.012	0.075	0.075	0.240								0.112	0.044
			2	5								0.0012	0.0001	0.106	0.012	0.081	0.081	0.300									
SLS1	2	20	1	3	Middle of bridge	120	0	0		Yes	0.0								0.63	0.55	1.84	1.22	0.74	0.49	1.22		
SLS1	2	20	1	3	S+ tower	120	0	0		Yes	0.0								0.58	0.51	1.84	1.22	0.74	0.49	1.22		
SLS1	2	20	1	3	S+ expansion joint	120	0	0		Yes	0.0								0.58	0.51	1.84	1.22	0.74	0.49	1.22		
SLS1	2	21	1	3	Middle of bridge	144	0	0		Yes	0.0	0.0100	0.0001	0.140	0.013	0.076	0.076	0.238								0.050	0.033
			2	6								0.0085	0.0000	0.120	0.012	0.088	0.088	0.432									
SLS1	2	21	1	3	S+ tower	144	0	0		Yes	0.0	0.0099	0.0001	0.139	0.012	0.075	0.075	0.241								0.060	0.033
			2	6								0.0065	0.0001	0.091	0.012	0.086	0.086	0.432									
SLS1	2	21	1	3	S+ expansion joint	144	0	0		Yes	0.0	0.0099	0.0001	0.139	0.012	0.075	0.075	0.241								0.052	0.033
			2	6								0.0065	0.0001	0.091	0.012	0.086	0.086	0.432									
SLS1	2	21	1	3	Middle of bridge	120	0	0		Yes	0.0								0.63	0.55	1.83	1.20	0.74	0.49	1.22		
SLS1	2	21	1	3	S+ tower	120	0	0		Yes	0.0								0.58	0.51	1.84	1.22	0.74	0.49	1.22		
SLS1	2	21	1	3	S+ expansion joint	120	0	0		Yes	0.0								0.58	0.50	1.84	1.22	0.74	0.49	1.22		
SLS1	2	22	1	4	Middle of bridge	144	0	0		Yes	0.0	0.0093	0.0001	0.131	0.002	0.018	0.018	0.195								0.060	0.043
			2	4								0.0079	0.0000	0.111	0.002	0.020	0.020	0.209									
SLS1	2	22	1	4	S+ tower	144	0	0		Yes	0.0	0.0094	0.0001	0.132	0.002	0.018	0.018	0.195								0.061	0.043
			2	4								0.0065	0.0001	0.091	0.002	0.020	0.020	0.209									
SLS1	2	22	1	4	S+ expansion joint	144	0	0		Yes	0.0	0.0094	0.0001	0.132	0.002	0.018	0.018	0.195								0.060	0.043
			2	4								0.0065	0.0001	0.091	0.002	0.020	0.020	0.209									
SLS1	2	22	1	4	Middle of bridge	120	0	0		Yes	0.0								0.70	0.60	1.79	1.06	0.90	0.53	0.95		
			2	4															0.70	0.60	1.80	1.06	0.90	0.54	1.27		
SLS1	2	22	1	4	S+ tower	120	0	0		Yes	0.0								0.64	0.55	1.79	1.06	0.90	0.53	0.95		
			2	4															0.64	0.55	1.80	1.06	0.90	0.54	1.27		
SLS1	2	22	1	4	S+ expansion joint	120	0	0		Yes	0.0								0.64	0.55	1.79	1.06	0.90	0.53	0.95		
			2	4															0.64	0.55	1.80	1.06	0.90	0.54	1.27		

Limit state	Load combination	Train combination case	Track no.	RFI type	Meeting point	Train speed [km/h]	10 min mean wind speed [m/s]	Gust wind speed (incl. mean wind) [m/s]	Location for gust wind peak ("Chinese hat")	Thermal load	Seismic peak ground acc. [m/s^2]	Transverse slope [m/m]	Change of cant [m/m]	Non-compensated lateral acc. [m/s^2]	Roll speed [rad/s]	Derailment ratio incl. wind [-]	Derailment ratio excl. wind [-]	Overturning ratio incl. wind [-]	Sperling Ride index, Wz (unweighted) [-]	Sperling Ride index, Wz (weighted) [-]	Peak vertical acc. (unweighted) [m/s^2]	Peak vertical acc. (weighted) [m/s^2]	RMS vertical acc. (2.0 s.) (unweighted) [m/s^2]	RMS vertical acc. (2.0 s.) (weighted) [m/s^2]	Recoil (based on 2.0 s. RMS coach acc.) [m/s^3]	Vertical peak acc., trackbed (unweighted) [m/s^2]	Vertical peak acc., trackbed (weighted) [m/s^2]
Limit												0.08	0.0025	0.6	0.033	0.8	0.8	0.9	2.2	2.2	2.00	2.00	0.75	0.75	0.25	0.70	0.70
SLS1	2	23	1	4	Middle of bridge	144	0	0		Yes	0.0	0.0125	0.0001	0.176	0.002	0.024	0.024	0.194								0.105	0.043
			2	5								0.0012	0.0001	0.110	0.012	0.082	0.082	0.300									
SLS1	2	23	1	4	S+ tower	144	0	0		Yes	0.0	0.0094	0.0001	0.132	0.002	0.018	0.018	0.195								0.113	0.043
			2	5								0.0011	0.0001	0.105	0.012	0.081	0.081	0.300									
SLS1	2	23	1	4	S+ expansion joint	144	0	0		Yes	0.0	0.0094	0.0001	0.132	0.002	0.018	0.018	0.195								0.109	0.044
			2	5								0.0006	0.0001	0.106	0.012	0.081	0.081	0.300									
SLS1	2	23	1	4	Middle of bridge	120	0	0		Yes	0.0								0.69	0.60	1.79	1.06	0.90	0.53	0.95		
SLS1	2	23	1	4	S+ tower	120	0	0		Yes	0.0								0.64	0.55	1.79	1.06	0.90	0.53	0.95		
SLS1	2	23	1	4	S+ expansion joint	120	0	0		Yes	0.0								0.64	0.55	1.79	1.06	0.90	0.53	0.95		
SLS1	2	24	1	4	Middle of bridge	144	0	0		Yes	0.0	0.0093	0.0001	0.130	0.002	0.018	0.018	0.194								0.060	0.043
			2	6								0.0080	0.0000	0.113	0.012	0.087	0.087	0.432									
SLS1	2	24	1	4	S+ tower	144	0	0		Yes	0.0	0.0094	0.0001	0.132	0.002	0.018	0.018	0.195								0.060	0.043
			2	6								0.0065	0.0001	0.091	0.012	0.086	0.086	0.432									
SLS1	2	24	1	4	S+ expansion joint	144	0	0		Yes	0.0	0.0094	0.0001	0.132	0.002	0.018	0.018	0.195								0.060	0.043
			2	6								0.0065	0.0001	0.091	0.012	0.086	0.086	0.432									
SLS1	2	24	1	4	Middle of bridge	120	0	0		Yes	0.0								0.69	0.59	1.79	1.06	0.90	0.53	0.95		
SLS1	2	24	1	4	S+ tower	120	0	0		Yes	0.0								0.64	0.55	1.79	1.06	0.90	0.53	0.95		
SLS1	2	24	1	4	S+ expansion joint	120	0	0		Yes	0.0								0.64	0.55	1.79	1.06	0.90	0.53	0.95		
SLS1	2	25	1	5	Middle of bridge	144	0	0		Yes	0.0	0.0238	0.0002	0.333	0.020	0.147	0.147	0.284								0.133	0.050
			2	5								0.0119	0.0001	0.166	0.011	0.076	0.076	0.300									
SLS1	2	25	1	5	S+ tower	144	0	0		Yes	0.0	0.0201	0.0001	0.281	0.017	0.127	0.127	0.284								0.158	0.065
			2	5								0.0063	0.0001	0.105	0.019	0.123	0.123	0.300									
SLS1	2	25	1	5	S+ expansion joint	144	0	0		Yes	0.0	0.0201	0.0001	0.281	0.017	0.127	0.127	0.284								0.185	0.072
			2	5								0.0045	0.0001	0.107	0.020	0.133	0.133	0.300									
SLS1	2	26	1	5	Middle of bridge	144	0	0		Yes	0.0	0.0203	0.0001	0.286	0.023	0.140	0.140	0.284								0.110	0.043
			2	6								0.0186	0.0000	0.261	0.011	0.081	0.081	0.432									
SLS1	2	26	1	5	S+ tower	144	0	0		Yes	0.0	0.0201	0.0001	0.281	0.017	0.127	0.127	0.284								0.115	0.048
			2	6								0.0078	0.0001	0.109	0.018	0.116	0.116	0.432									
SLS1	2	26	1	5	S+ expansion joint	144	0	0		Yes	0.0	0.0201	0.0001	0.281	0.017	0.127	0.127	0.284								0.112	0.046
			2	6								0.0065	0.0001	0.091	0.019	0.125	0.125	0.432									
SLS1	2	27	1	6	Middle of bridge	144	0	0		Yes	0.0	0.0100	0.0001	0.141	0.012	0.073	0.073	0.451								0.044	0.027
			2	6								0.0085	0.0000	0.119	0.012	0.084	0.084	0.432									
SLS1	2	27	1	6	S+ tower	144	0	0		Yes	0.0	0.0099	0.0001	0.139	0.012	0.074	0.074	0.451								0.044	0.027
			2	6								0.0065	0.0001	0.091	0.012	0.086	0.086	0.432									
SLS1	2	27	1	6	Middle of bridge	144	0	0		Yes	0.0	0.0099	0.0001	0.139	0.012	0.074	0.074	0.451								0.057	0.028
			2	6								0.0065	0.0001	0.091	0.012	0.086	0.086	0.432									

13.3 SLS1 Load combination 4 - No thermal load

13.3.1 44 m/s 10 min mean wind speed (SLS1 wind time record) - Runability and safety results

Limit state	Load combination	Train combination case	Track no.	RFI type	Meeting point	Train speed [km/h]	Wind load type	Mean wind speed [m/s]	Maximum gust wind speed in time series [m/s]	Thermal load	Seismic peak ground acc. [m/s^2]	Transverse slope [m/m]	Change of cant [m/m]	Non-compensated lateral acc. [m/s^2]	Roll speed [rad/s]	Derailment ratio [-]	Overturning ratio [-]	Vertical peak acc., trackbed (unweighted) [m/s^2]	Vertical peak acc., trackbed (weighted) [m/s^2]
Limit												0.08	0.0025	0.6	0.033	0.8	0.9	0.70	0.70
SLS1	4	1	1	1	One train only	144	Dynamic time series	44	58.5	No	0.0	0.0161	0.0001	0.226	0.044	0.536	0.529	1.383	0.924
SLS1	4	2	1	2	One train only	144	Dynamic time series	44	58.5	No	0.0	0.0165	0.0001	0.231	0.085	0.655	0.538	8.777	2.357
SLS1	4	3	1	3	One train only	144	Dynamic time series	44	58.5	No	0.0	0.0181	0.0001	0.254	0.107	0.511	0.684	1.383	0.932
SLS1	4	4	1	4	One train only	144	Dynamic time series	44	58.5	No	0.0	0.0162	0.0001	0.227	0.034	0.208	0.471	1.359	0.881
SLS1	4	5	1	5	One train only	144	Dynamic time series	44	58.5	No	0.0	0.0282	0.0001	0.396	0.090	0.422	0.424	1.424	0.994
SLS1	4	6	1	6	One train only	144	Dynamic time series	44	58.5	No	0.0	0.0185	0.0001	0.260	0.093	0.517	1.029	1.383	0.941
SLS1	4	7	1	1	Middle of bridge	144	Dynamic time series	44	58.5	No	0.0	0.0161	0.0001	0.226	0.046	0.474	0.527	1.384	0.914
			2	1								0.0137	0.0001	0.193	0.040	0.590	0.570		
SLS1	4	8	1	1	Middle of bridge	144	Dynamic time series	44	58.5	No	0.0	0.0164	0.0001	0.230	0.046	0.471	0.528	8.592	2.307
			2	2								0.0136	0.0001	0.191	0.049	0.541	0.466		
SLS1	4	9	1	1	Middle of bridge	144	Dynamic time series	44	58.5	No	0.0	0.0165	0.0001	0.231	0.047	0.484	0.527	1.384	0.909
			2	3								0.0139	0.0001	0.195	0.064	0.474	0.732		
SLS1	4	10	1	1	Middle of bridge	144	Dynamic time series	44	58.5	No	0.0	0.0160	0.0001	0.224	0.045	0.485	0.532	1.384	0.920
			2	4								0.0139	0.0001	0.196	0.047	0.222	0.504		
SLS1	4	11	1	1	Middle of bridge	144	Dynamic time series	44	58.5	No	0.0	0.0213	0.0001	0.299	0.045	0.485	0.528	1.401	0.949
			2	5								0.0089	0.0002	0.250	0.079	0.321	0.440		
SLS1	4	12	1	1	Middle of bridge	144	Dynamic time series	44	58.5	No	0.0	0.0166	0.0001	0.232	0.046	0.485	0.527	1.384	0.914
			2	6								0.0146	0.0001	0.204	0.062	0.520	1.047		
SLS1	4	13	1	2	Middle of bridge	144	Dynamic time series	44	58.5	No	0.0	0.0169	0.0001	0.237	0.084	0.661	0.543	1.384	0.913
			2	2								0.0137	0.0001	0.192	0.048	0.544	0.503		
SLS1	4	14	1	2	Middle of bridge	144	Dynamic time series	44	58.5	No	0.0	0.0171	0.0001	0.240	0.078	0.680	0.561	1.384	0.908
			2	3								0.0142	0.0001	0.199	0.058	0.475	0.733		
SLS1	4	15	1	2	Middle of bridge	144	Dynamic time series	44	58.5	No	0.0	0.0165	0.0001	0.232	0.085	0.656	0.539	1.384	0.919
			2	4								0.0141	0.0001	0.198	0.047	0.221	0.515		
SLS1	4	16	1	2	Middle of bridge	144	Dynamic time series	44	58.5	No	0.0	0.0219	0.0001	0.308	0.078	0.682	0.562	1.452	0.951
			2	5								0.0091	0.0002	0.251	0.079	0.319	0.441		
SLS1	4	17	1	2	Middle of bridge	144	Dynamic time series	44	58.5	No	0.0	0.0172	0.0001	0.241	0.078	0.679	0.560	1.384	0.912
			2	6								0.0148	0.0001	0.208	0.064	0.520	1.047		
SLS1	4	18	1	3	Middle of bridge	144	Dynamic time series	44	58.5	No	0.0	0.0190	0.0001	0.266	0.106	0.355	0.834	1.384	0.913
			2	3								0.0142	0.0001	0.200	0.062	0.475	0.733		
SLS1	4	19	1	3	Middle of bridge	144	Dynamic time series	44	58.5	No	0.0	0.0185	0.0001	0.259	0.106	0.354	0.834	1.384	0.926
			2	4								0.0140	0.0001	0.196	0.047	0.222	0.515		
SLS1	4	20	1	3	Middle of bridge	144	Dynamic time series	44	58.5	No	0.0	0.0232	0.0001	0.325	0.106	0.348	0.833	1.456	0.953
			2	5								0.0090	0.0002	0.252	0.079	0.320	0.440		
SLS1	4	21	1	3	Middle of bridge	144	Dynamic time series	44	58.5	No	0.0	0.0191	0.0001	0.268	0.106	0.352	0.833	1.384	0.917
			2	6								0.0147	0.0001	0.206	0.064	0.520	1.047		
SLS1	4	22	1	4	Middle of bridge	144	Dynamic time series	44	58.5	No	0.0	0.0160	0.0001	0.225	0.034	0.207	0.471	1.372	0.883
			2	4								0.0140	0.0001	0.196	0.047	0.222	0.515		
SLS1	4	23	1	4	Middle of bridge	144	Dynamic time series	44	58.5	No	0.0	0.0196	0.0001	0.275	0.035	0.206	0.471	11.637	3.125
			2	5								0.0091	0.0002	0.250	0.079	0.319	0.440		
SLS1	4	24	1	4	Middle of bridge	144	Dynamic time series	44	58.5	No	0.0	0.0148	0.0001	0.207	0.034	0.208	0.471	1.384	0.909
			2	6								0.0146	0.0001	0.205	0.065	0.520	1.047		
SLS1	4	25	1	5	Middle of bridge	144	Dynamic time series	44	58.5	No	0.0	0.0333	0.0002	0.467	0.087	0.408	0.453	1.384	0.931
			2	5								0.0175	0.0002	0.303	0.079	0.292	0.435		
SLS1	4	26	1	5	Middle of bridge	144	Dynamic time series	44	58.5	No	0.0	0.0292	0.0001	0.409	0.091	0.428	0.454	1.384	0.965
			2	6								0.0246	0.0001	0.344	0.062	0.520	1.045		
SLS1	4	27	1	6	Middle of bridge	144	Dynamic time series	44	58.5	No	0.0	0.0194	0.0001	0.272	0.093	0.517	1.033	1.384	0.929
			2	6								0.0145	0.0001	0.203	0.065	0.523	1.046		

13.3.2 38 m/s 10 min mean wind speed (scaled SLS1 wind time record) - Runability and safety results

Limit state	Load combination	Train combination case	Track no.	RFI type	Meeting point	Train speed [km/h]	Wind load type	Mean wind speed [m/s]	Maximum gust wind speed in time series [m/s]	Thermal load	Seismic peak ground acc. [m/s^2]	Transverse slope [m/m]	Change of cant [m/m]	Non-compensated lateral acc. [m/s^2]	Roll speed [rad/s]	Derailment ratio [-]	Overturning ratio [-]	Vertical peak acc., trackbed (unweighted) [m/s^2]	Vertical peak acc., trackbed (weighted) [m/s^2]
Limit												0.08	0.0025	0.6	0.033	0.8	0.9	0.70	0.70
SLS1	4	1	1	1	One train only	144	Dynamic time series	38	50.5	No	0.0	0.0144	0.0001	0.202	0.034	0.388	0.418	1.036	0.713
SLS1	4	2	1	2	One train only	144	Dynamic time series	38	50.5	No	0.0	0.0151	0.0001	0.211	0.064	0.540	0.414	7.851	5.083
SLS1	4	3	1	3	One train only	144	Dynamic time series	38	50.5	No	0.0	0.0164	0.0001	0.229	0.082	0.405	0.675	1.027	0.718
SLS1	4	4	1	4	One train only	144	Dynamic time series	38	50.5	No	0.0	0.0141	0.0001	0.199	0.026	0.164	0.401	1.025	0.718
SLS1	4	5	1	5	One train only	144	Dynamic time series	38	50.5	No	0.0	0.0265	0.0001	0.371	0.069	0.338	0.412	1.088	0.710
SLS1	4	6	1	6	One train only	144	Dynamic time series	38	50.5	No	0.0	0.0166	0.0001	0.233	0.073	0.430	0.879	1.039	0.714

13.3.3 38 m/s 10 min mean wind speed (scaled SLS1 wind time record) - Comfort results

Limit state	Load combination	Train combination case	Track no.	RFI type	Meeting point	Train speed [km/h]	Wind load type	Mean wind speed [m/s]	Maximum gust wind speed in time series [m/s]	Thermal load	Seismic peak ground acc. [m/s^2]	Sperling Ride index, Wz (unweighted) [-]	Sperling Ride index, Wz (weighted) [-]	Peak vertical acc. (unweighted) [m/s^2]	Peak vertical acc. (weighted) [m/s^2]	RMS vertical acc. (2.0 s.) (unweighted) [m/s^2]	RMS vertical acc. (2.0 s.) (weighted) [m/s^2]	Recoil (based on 2.0 s. RMS coach acc.) [m/s^3]
Limit												2.2	2.2	2.00	2.00	0.75	0.75	0.25
SLS1	4	1	1	1	One train only	120	Dynamic time series	38	50.5	No	0.0	0.68	0.55	1.44	0.74	0.78	0.41	1.11
SLS1	4	2	1	2	One train only	120	Dynamic time series	38	50.5	No	0.0	0.68	0.55	1.45	0.74	0.74	0.38	1.01
SLS1	4	3	1	3	One train only	120	Dynamic time series	38	50.5	No	0.0	0.72	0.62	1.90	1.11	0.88	0.54	1.33
SLS1	4	4	1	4	One train only	120	Dynamic time series	38	50.5	No	0.0	0.75	0.62	1.89	1.04	1.07	0.59	1.24
SLS1	4	7	1	1	Middle of bridge	120	Dynamic time series	38	50.5	No	0.0	0.68	0.55	1.45	0.75	0.78	0.41	1.07
			2	1								0.68	0.55	1.53	0.69	0.72	0.36	1.16
SLS1	4	8	1	1	Middle of bridge	120	Dynamic time series	38	50.5	No	0.0	0.68	0.55	1.46	0.75	0.79	0.41	1.07
			2	2								0.68	0.55	1.47	0.70	0.67	0.36	1.20
SLS1	4	9	1	1	Middle of bridge	120	Dynamic time series	38	50.5	No	0.0	0.68	0.55	1.46	0.76	0.79	0.42	1.07
			2	3								0.71	0.60	1.96	1.22	0.88	0.55	2.21
SLS1	4	10	1	1	Middle of bridge	120	Dynamic time series	38	50.5	No	0.0	0.68	0.55	1.45	0.75	0.78	0.41	1.07
			2	4								0.76	0.63	1.85	0.95	1.05	0.58	1.26
SLS1	4	11	1	1	Middle of bridge	120	Dynamic time series	38	50.5	No	0.0	0.68	0.55	1.46	0.75	0.77	0.40	1.16
SLS1	4	12	1	1	Middle of bridge	120	Dynamic time series	38	50.5	No	0.0	0.68	0.55	1.46	0.75	0.79	0.42	1.08
SLS1	4	13	1	2	Middle of bridge	120	Dynamic time series	38	50.5	No	0.0	0.68	0.55	1.45	0.75	0.75	0.39	1.01
			2	2								0.68	0.55	1.47	0.70	0.67	0.36	1.20
SLS1	4	14	1	2	Middle of bridge	120	Dynamic time series	38	50.5	No	0.0	0.68	0.55	1.45	0.76	0.75	0.39	1.00
			2	3								0.71	0.60	1.96	1.22	0.89	0.55	2.21
SLS1	4	15	1	2	Middle of bridge	120	Dynamic time series	38	50.5	No	0.0	0.68	0.55	1.45	0.75	0.74	0.39	1.01
			2	4								0.76	0.63	1.85	0.95	1.06	0.58	1.26
SLS1	4	16	1	2	Middle of bridge	120	Dynamic time series	38	50.5	No	0.0	0.68	0.55	1.45	0.74	0.74	0.38	1.13
SLS1	4	17	1	2	Middle of bridge	120	Dynamic time series	38	50.5	No	0.0	0.68	0.55	1.45	0.75	0.75	0.39	0.99
SLS1	4	18	1	3	Middle of bridge	120	Dynamic time series	38	50.5	No	0.0	0.72	0.62	1.90	1.11	0.89	0.54	1.32
			2	3								0.71	0.60	1.96	1.22	0.89	0.55	2.21
SLS1	4	19	1	3	Middle of bridge	120	Dynamic time series	38	50.5	No	0.0	0.72	0.61	1.90	1.11	0.88	0.54	1.32
			2	4								0.76	0.63	1.85	0.95	1.06	0.58	1.26
SLS1	4	20	1	3	Middle of bridge	120	Dynamic time series	38	50.5	No	0.0	0.72	0.62	1.90	1.10	0.88	0.54	1.45
SLS1	4	21	1	3	Middle of bridge	120	Dynamic time series	38	50.5	No	0.0	0.72	0.61	1.90	1.11	0.90	0.54	1.32
SLS1	4	22	1	4	Middle of bridge	120	Dynamic time series	38	50.5	No	0.0	0.75	0.62	1.87	1.02	1.08	0.60	1.22
			2	4								0.76	0.63	1.85	0.95	1.05	0.57	1.26
SLS1	4	23	1	4	Middle of bridge	120	Dynamic time series	38	50.5	No	0.0	0.76	0.63	1.87	1.01	1.06	0.59	1.26
SLS1	4	24	1	4	Middle of bridge	120	Dynamic time series	38	50.5	No	0.0	0.75	0.62	1.89	1.03	1.09	0.60	1.25

13.3.4 47 m/s 10 min mean wind speed (SLS2 wind time record) - Runability and safety results

Limit state	Load combination	Train combination case	Track no.	RFI type	Meeting point	Train speed [km/h]	Wind load type	Mean wind speed [m/s]	Maximum gust wind speed in time series [m/s]	Thermal load	Seismic peak ground acc. [m/s^2]	Transverse slope [m/m]	Change of cant [m/m]	Non-compensated lateral acc. [m/s^2]	Roll speed [rad/s]	Derailment ratio [-]	Overturning ratio [-]	Vertical peak acc., trackbed (unweighted) [m/s^2]	Vertical peak acc., trackbed (weighted) [m/s^2]
Limit												0.10	0.0040	0.8	0.036	0.8	0.9	1.00	1.00
SLS2	4	1	1	1	One train only	144	Dynamic time series	47	62.1	No	0.0	0.0195	0.0001	0.273	0.049	0.325	0.713	1.600	1.042
SLS2	4	2	1	2	One train only	144	Dynamic time series	47	62.1	No	0.0	0.0197	0.0001	0.277	0.034	0.302	0.586	1.600	1.042
SLS2	4	3	1	3	One train only	144	Dynamic time series	47	62.1	No	0.0	0.0198	0.0001	0.278	0.059	0.317	0.788	7.876	5.099
SLS2	4	4	1	4	One train only	144	Dynamic time series	47	62.1	No	0.0	0.0195	0.0001	0.273	0.042	0.255	0.604	1.610	1.040

13.4 SLS1 Load combination 4 - Thermal load

13.4.1 38 m/s 10 min mean wind speed (scaled SLS1 wind time record) - Runability and safety results

Limit state	Load combination	Train combination case	Track no.	RFI type	Meeting point	Train speed [km/h]	Wind load type	Mean wind speed [m/s]	Maximum gust wind speed in time series [m/s]	Thermal load	Seismic peak ground acc. [m/s^2]	Transverse slope [m/m]	Change of cant [m/m]	Non-compensated lateral acc. [m/s^2]	Roll speed [rad/s]	Derailment ratio [-]	Overturning ratio [-]	Vertical peak acc., trackbed (unweighted) [m/s^2]	Vertical peak acc., trackbed (weighted) [m/s^2]
Limit												0.08	0.0025	0.6	0.033	0.8	0.9	0.70	0.70
SLS1	4	1	1	1	One train only	144	Dynamic time series	38	50.5	Yes	0.0	0.0142	0.0001	0.199	0.029	0.213	0.377	0.993	0.683
SLS1	4	2	1	2	One train only	144	Dynamic time series	38	50.5	Yes	0.0	0.0149	0.0001	0.209	0.022	0.188	0.311	7.650	4.953
SLS1	4	3	1	3	One train only	144	Dynamic time series	38	50.5	Yes	0.0	0.0161	0.0001	0.226	0.039	0.210	0.451	0.986	0.688
SLS1	4	4	1	4	One train only	144	Dynamic time series	38	50.5	Yes	0.0	0.0139	0.0001	0.195	0.024	0.158	0.319	0.985	0.688
SLS1	4	5	1	5	One train only	144	Dynamic time series	38	50.5	Yes	0.0	0.0262	0.0001	0.368	0.048	0.123	0.210	1.047	0.680
SLS1	4	6	1	6	One train only	144	Dynamic time series	38	50.5	Yes	0.0	0.0163	0.0001	0.229	0.030	0.267	0.539	0.999	0.684

13.5 Appendix 2: Local model simulation results

13.5.1 Simulation 1 - RFI 1: ETR500 locomotive (speed 144 km/h)

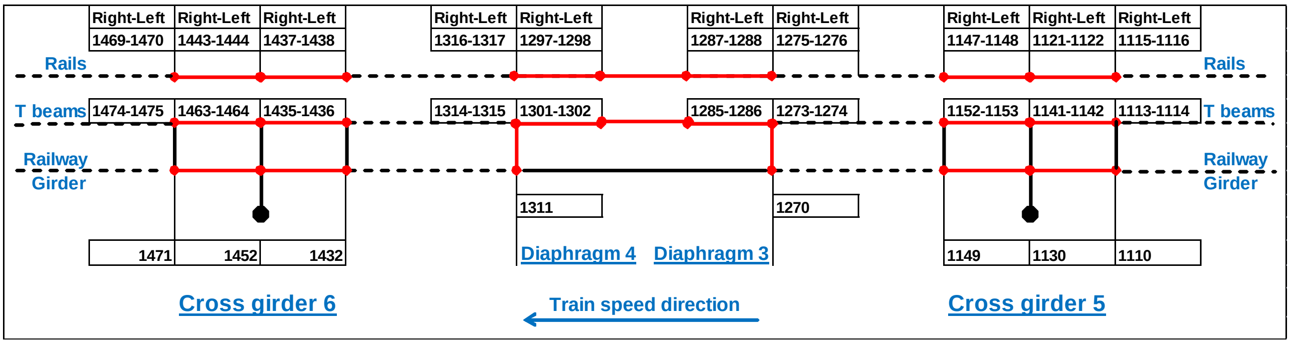

Tables A2-6 and A2-7 present the maximum vertical force transmitted to the listed visco-elastic beds located underneath the left and right rails and computed from static and dynamic simulations. Impact Factors are also listed in the same tables.

LEFT RAIL	Bed #	Static Force [N]	Dynamic Force [N]	Impact Factor
	795	11500	13400	1,165217391
	800	11400	12200	1,070175439
	803	11450	11150	0,973799127
	808	11490	12600	1,096605744
	892	11470	11680	1,018308631
	899	11435	12030	1,052033231
	912	11470	12320	1,074106364
	995	11480	11420	0,994773519
	1000	11450	13000	1,135371179
	1003	11468	11800	1,028950122
	1008	14500	13250	0,913793103

Table A2-6 – Impact factor evaluation from static and dynamic loads at specific beds locations

positioned underneath the left rail.

RIGHT RAIL	Bed #	Static Force [N]	Dynamic Force [N]	Impact Factor
	793	11450	11620	1,014847162
	798	11400	12100	1,061403509
	801	11450	12620	1,102183406
	806	11490	11600	1,009573542
	890	11470	12350	1,076721883
	897	11440	12880	1,125874126
	910	11470	13650	1,190061029
	993	11500	11850	1,030434783
	998	11460	13060	1,139616056
	1001	11450	11770	1,027947598
	1006	11460	15500	1,352530541

Table A2-7 – Impact factor evaluation from static and dynamic loads at specific beds locations positioned underneath the right rail.

Table A2-8 presents vertical displacements of selected railway girder nodes located at cross girders 5 and 6 and diaphragms 3 and 4.

	Node #	Displacement [m]
Cross Girder # 5	1110	-2,7700E-03
	1130	-2,7600E-03
	1149	-2,7800E-03
Diaphragm # 3	1270	-3,5000E-03
Diaphragm # 4	1311	-3,5000E-03
Cross Girder # 6	1432	-2,7900E-03
	1452	-2,7850E-03
	1471	-2,7800E-03

Table A2-8 – Vertical displacements of the railway girder nodes.

Tables A2-9 and A2-10 presents the vertical displacement difference between the listed rails and T beams for both static and dynamic simulations on both left and right hand side of the track. Impact Factors are also listed in the same tables.

LEFT RAIL	Rail Node #	T Beam Node #	Static Displacement [m]	Dynamic Displacement [m]	Impact Factor
Cross Girder # 5	1116	1114	-1,8600E-03	-2,1720E-03	1,167741935
	1122	1142	1,8550E-03	1,8950E-03	1,021563342
	1148	1153	1,8550E-03	2,1000E-03	1,132075472
Diaphragm 3 - 4	1276	1274	1,8600E-03	2,0000E-03	1,075268817
	1288	1286	1,8550E-03	2,0120E-03	1,084636119
	1298	1302	1,8500E-03	2,1175E-03	1,144594595
	1317	1315	1,8500E-03	2,2500E-03	1,216216216
Cross Girder # 6	1438	1436	1,8550E-03	1,8300E-03	0,986522911
	1444	1464	1,8500E-03	2,0200E-03	1,091891892
	1470	1475	1,8600E-03	2,2000E-03	1,182795699

Table A2-9 – Impact factor evaluation from the nodal vertical displacement difference between rails and T beams on left hand side of the track. Impact factors are also shown from the ratio between static and dynamic quantities.

RIGHT RAIL	Rail Node #	T Beam Node #	Static Displacement [m]	Dynamic Displacement [m]	Impact Factor
Cross Girder # 5	1115	1113	-0,001855	-0,0018345	0,988948787
	1121	1141	-0,00186	-0,00202	1,086021505
	1147	1152	1,8550E-03	1,8200E-03	0,981132075
Diaphragm 3 - 4	1275	1273	1,8600E-03	2,1800E-03	1,172043011
	1287	1285	1,8550E-03	2,0360E-03	1,097574124
	1297	1301	1,8550E-03	1,9550E-03	1,053908356
	1316	1314	1,8600E-03	1,8850E-03	1,01344086
Cross Girder # 6	1437	1435	1,8550E-03	1,9500E-03	1,051212938
	1443	1463	1,8600E-03	2,0500E-03	1,102150538
	1469	1474	1,8500E-03	1,9100E-03	1,032432432

Table A2-10 – Impact factor evaluation from the nodal vertical displacement difference between *rails and T beams on right hand side of the track. Impact factors are also shown from the ratio between static and dynamic quantities.*

Table A2-11 presents nodal vertical acceleration peaks of right and left rails and T beams.

	T beam Right Node #	Vertical Acceleration Peak [m/s^2]	T beam Left Node #	Vertical Acceleration Peak [m/s^2]	Right Rail Node #	Vertical Acceleration Peak [m/s^2]	Left Rail Node #	Vertical Acceleration Peak [m/s^2]
Cross girder # 5	1113	1.760	1114	1.840	1115	29.600	1116	35.645
	1141	1.472	1142	1.616	1121	35.001	1122	53.237
	1152	1.673	1153	1.869	1147	28.045	1148	28.815
Diaphragms # 3 – 4	1273	2.483	1274	4.367	1275	31.673	1276	39.152
	1285	2.824	1286	5.218	1287	32.324	1288	31.877
	1301	2.790	1302	5.059	1297	36.233	1298	36.475
	1314	2.806	1315	3.949	1316	34.185	1317	33.578
Cross girder # 6	1435	1.244	1436	1.913	1438	41.492	1437	29.126
	1463	1.166	1464	1.533	1444	27.932	1443	33.770
	1474	1.264	1475	1.755	1470	37.235	1469	40.936

Table A2-11 - Nodal vertical acceleration peaks of right and left rails and T beams.

Table A2-12 presents nodal vertical acceleration peaks of the railway girder.

	Railway Girder Node #	Vertical Acceleration Peak [m/s^2]
Cross girder # 5	1110	1.496
	1130	1.442
	1149	1.602
Diaphragm # 3	1270	2.217
Diaphragm # 4	1311	2.277
Cross girder # 6	1432	1.249
	1452	1.037
	1471	1.069

Table A2-12 - Nodal vertical acceleration peaks of the railway girder.

13.5.2 Simulation 2 - RFI 1: ETR500 coach (speed 144 km/h)

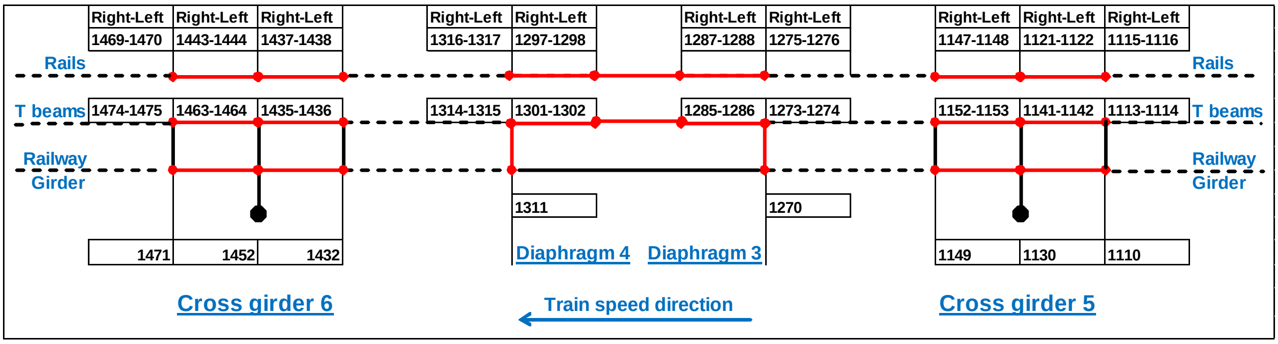

Tables A2-13 and A2-14 present the maximum vertical force transmitted to the listed visco-elastic beds located underneath the left and right rails and computed from static and dynamic simulations. Impact Factors are also listed in the same tables.

LEFT RAIL	Bed #	Static Force [N]	Dynamic Force [N]	Impact Factor
	795	5000	7250	1,4500E+00
	800	5000	6350	1,2700E+00
	803	5000	5762	1,1524E+00
	808	5000	6000	1,2000E+00
	892	5000	6370	1,2740E+00
	899	5000	5570	1,1140E+00
	912	5000	5980	1,1960E+00
	995	5000	5828	1,1656E+00
	1000	5000	5920	1,1840E+00
	1003	5000	6000	1,2000E+00
	1008	5000	5900	1,1800E+00

Table A2-13 – Impact factor evaluation from static and dynamic loads at specific beds locations positioned underneath the left rail.

RIGHT RAIL	Bed #	Static Force [N]	Dynamic Force [N]	Impact Factor
	793	5000	5800	1,1600E+00
	798	5000	6380	1,2760E+00
	801	5000	6084	1,2168E+00
	806	5000	6889	1,3778E+00
	890	5000	6165	1,2330E+00
	897	5000	6252	1,2504E+00
	910	5000	6290	1,2580E+00
	993	5000	6000	1,2000E+00
	998	5000	5800	1,1600E+00
	1001	5000	5400	1,0800E+00
	1006	5000	5800	1,1600E+00

Table A2-14 – Impact factor evaluation from static and dynamic loads at specific beds locations positioned underneath the right rail.

Table A2-15 presents vertical displacements of selected railway girder nodes located at cross girders 5 and 6 and diaphragms 3 and 4.

	Node #	Displacement [m]
Cross Girder # 5	1110	-1,2100E-03
	1130	-1,2000E-03
	1149	-1,2200E-03
Diaphragm # 3	1270	-1,6000E-03
Diaphragm # 4	1311	-1,6000E-03
Cross Girder # 6	1432	-1,2200E-03
	1452	-1,2200E-03
	1471	-1,2300E-03

Table A2-15 – Vertical displacements of the railway girder nodes.

Tables A2-16 and A2-17 presents the vertical displacement difference between the listed rails and T beams for both static and dynamic simulations on both left and right hand side of the track. Impact Factors are also listed in the same tables.

LEFT RAIL	Rail	T Beam	Static	Dynamic	Impact
	Node #	Node #	Displacement [m]	Displacement [m]	Factor
Cross Girder # 5	1116	1114	-8,0700E-04	-1,0785E-03	1,3364E+00
	1122	1142	-8,0740E-04	-9,8740E-04	1,2229E+00
	1148	1153	-8,0750E-04	-1,0100E-03	1,2508E+00
Diaphragm 3 - 4	1276	1274	-8,0930E-04	-9,7000E-04	1,1986E+00
	1288	1286	-8,0525E-04	-9,6840E-04	1,2026E+00
	1298	1302	-8,0500E-04	-9,5000E-04	1,1801E+00
	1317	1315	-8,0265E-04	-1,0250E-03	1,2770E+00
Cross Girder # 6	1438	1436	-8,0850E-04	-1,0000E-03	1,2369E+00
	1444	1464	-8,0760E-04	-9,1200E-04	1,1293E+00
	1470	1475	-8,0700E-04	-1,0190E-03	1,2627E+00

Table A2-16 – Impact factor evaluation from the nodal vertical displacement difference between rails and T beams on left hand side of the track. Impact factors are also shown from the ratio between static and dynamic quantities.

RIGHT RAIL	Rail	T Beam	Static	Dynamic	Impact
	Node #	Node #	Displacement [m]	Displacement [m]	Factor
Cross Girder # 5	1115	1113	-8,0700E-04	-8,7000E-04	1,0781E+00
	1121	1141	-8,0700E-04	-1,0200E-03	1,2639E+00
	1147	1152	-8,0800E-04	-1,1250E-03	1,3923E+00
Diaphragm 3 - 4	1275	1273	-8,0800E-04	-1,1524E-03	1,4262E+00
	1287	1285	-8,0640E-04	-9,8320E-04	1,2192E+00
	1297	1301	-8,0530E-04	-9,3000E-04	1,1548E+00
	1316	1314	-8,1000E-04	-8,5000E-04	1,0494E+00
Cross Girder # 6	1437	1435	-8,0800E-04	-1,0300E-03	1,2748E+00
	1443	1463	-8,0750E-04	-8,5000E-04	1,0526E+00
	1469	1474	-8,1000E-04	-8,8000E-04	1,0864E+00

Table A2-17 – Impact factor evaluation from the nodal vertical displacement difference between rails and T beams on right hand side of the track. Impact factors are also shown from the ratio between static and dynamic quantities.

Table A2-18 presents nodal vertical acceleration peaks of right and left rails and T beams.

	T beam Right Node #	Vertical Acceleration Peak [m/s^2]	T beam Left Node #	Vertical Acceleration Peak [m/s^2]	Right Rail Node #	Vertical Acceleration Peak [m/s^2]	Left Rail Node #	Vertical Acceleration Peak [m/s^2]
Cross girder # 5	1113	1.305	1114	1.712	1115	34.281	1116	49.884
	1141	1.424	1142	1.673	1121	28.367	1122	39.189
	1152	1.605	1153	1.893	1147	34.759	1148	37.310
Diaphragms # 3 – 4	1273	2.514	1274	3.262	1275	50.669	1276	38.472
	1285	2.371	1286	5.133	1287	27.708	1288	25.780
	1301	2.500	1302	5.322	1297	35.753	1298	33.656
	1314	2.625	1315	4.187	1316	27.977	1317	29.698
Cross girder # 6	1435	1.242	1436	1.557	1438	34.585	1437	27.183
	1463	1.090	1464	1.443	1444	28.050	1443	42.265
	1474	1.209	1475	1.641	1470	34.482	1469	38.205

Table A2-18 - Nodal vertical acceleration peaks of right and left rails and T beams.

Table A2-19 presents nodal vertical acceleration peaks of the railway girder.

	Railway Girder Node #	Vertical Acceleration Peak [m/s^2]
Cross girder # 5	1110	1.439
	1130	1.432
	1149	1.669
Diaphragm # 3	1270	2.302
Diaphragm # 4	1311	2.543
Cross girder # 6	1432	1.107
	1452	0.897
	1471	1.004

Table A2-19 - Nodal vertical acceleration peaks of the railway girder.

13.5.3 Simulation 3 - RFI 2: ETR470 locomotive (speed 144 km/h)

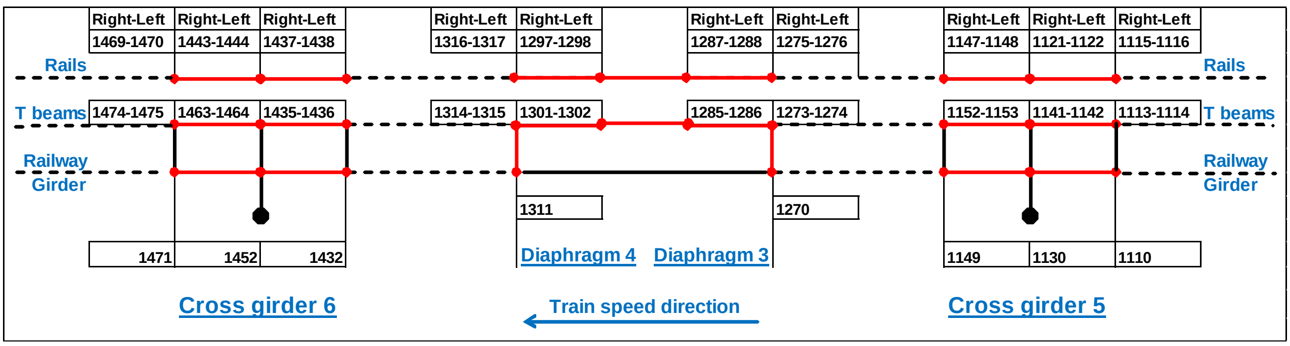

Tables A2-20 and A2-21 present the maximum vertical force transmitted to the listed visco-elastic beds located underneath the left and right rails and computed from static and dynamic simulations. Impact Factors are also listed in the same tables.

LEFT RAIL	Bed #	Static Force [N]	Dynamic Force [N]	Impact Factor
	795	9250	10360	1,1200E+00
	800	9250	9353	1,0111E+00
	803	9258	9460	1,0218E+00
	808	9245	9250	1,0005E+00
	892	9259	10048	1,0852E+00
	899	9230	9900	1,0726E+00
	912	9265	10700	1,1549E+00
	995	9266	9820	1,0598E+00
	1000	9250	11283	1,2198E+00
	1003	9250	10000	1,0811E+00
	1008	9236	10820	1,1715E+00

Table A2-20 – Impact factor evaluation from static and dynamic loads at specific beds locations positioned underneath the left rail.

RIGHT RAIL	Bed #	Static Force [N]	Dynamic Force [N]	Impact Factor
	793	9246	10160	1,0989E+00
	798	9250	10080	1,0897E+00
	801	9255	10340	1,1172E+00
	806	9274	10200	1,0998E+00
	890	9255	10100	1,0913E+00
	897	9233	11140	1,2065E+00
	910	9240	11249	1,2174E+00
	993	9280	9865	1,0630E+00
	998	9250	11260	1,2173E+00
	1001	9250	10000	1,0811E+00
	1006	9242	10650	1,1523E+00

Table A2-21 – Impact factor evaluation from static and dynamic loads at specific beds locations positioned underneath the right rail.

Table A2-22 presents vertical displacements of selected railway girder nodes located at cross girders 5 and 6 and diaphragms 3 and 4.

	Node #	Displacement [m]
Cross Girder # 5	1110	-2,2000E-03
	1130	-2,2500E-03
	1149	-2,2300E-03
Diaphragm # 3	1270	-2,9000E-03
Diaphragm # 4	1311	-2,9000E-03
Cross Girder # 6	1432	-2,2500E-03
	1452	-2,2500E-03
	1471	-2,2000E-03

Table A2-22 – Vertical displacements of the railway girder nodes.

Tables A2-23 and A2-24 presents the vertical displacement difference between the listed rails and

T beams for both static and dynamic simulations on both left and right hand side of the track. Impact Factors are also listed in the same tables.

LEFT RAIL	Rail	T Beam	Static	Dynamic	Impact
	Node #	Node #	Displacement [m]	Displacement [m]	Factor
Cross Girder # 5	1116	1114	-1,5000E-03	-1,6800E-03	1,1200E+00
	1122	1142	-1,4980E-03	-1,4885E-03	9,9366E-01
	1148	1153	-1,4960E-03	-1,5290E-03	1,0221E+00
Diaphragm 3 - 4	1276	1274	-1,5000E-03	-1,7330E-03	1,1553E+00
	1288	1286	-1,4940E-03	-1,6625E-03	1,1128E+00
	1298	1302	-1,4940E-03	-1,7000E-03	1,1379E+00
	1317	1315	-1,4889E-03	-1,7685E-03	1,1878E+00
Cross Girder # 6	1438	1436	-1,5000E-03	-1,5900E-03	1,0600E+00
	1444	1464	-1,4980E-03	-1,7282E-03	1,1537E+00
	1470	1475	-1,4950E-03	-1,7900E-03	1,1973E+00

Table A2-23 – Impact factor evaluation from the nodal vertical displacement difference between rails and T beams on left hand side of the track. Impact factors are also shown from the ratio between static and dynamic quantities.

RIGHT RAIL	Rail	T Beam	Static	Dynamic	Impact
	Node #	Node #	Displacement [m]	Displacement [m]	Factor
Cross Girder # 5	1115	1113	-1,5000E-03	-1,6380E-03	1,0920E+00
	1121	1141	-1,5000E-03	-1,6715E-03	1,1143E+00
	1147	1152	-1,4970E-03	-1,6300E-03	1,0888E+00
Diaphragm 3 - 4	1275	1273	-1,5000E-03	-1,7500E-03	1,1667E+00
	1287	1285	-1,4960E-03	-1,7750E-03	1,1865E+00
	1297	1301	-1,4950E-03	-1,7940E-03	1,2000E+00
	1316	1314	-1,4900E-03	-1,6230E-03	1,0893E+00
Cross Girder # 6	1437	1435	-1,5000E-03	-1,5650E-03	1,0433E+00
	1443	1463	-1,5000E-03	-1,7480E-03	1,1653E+00
	1469	1474	-1,4980E-03	-1,7689E-03	1,1808E+00

Table A2-24 – Impact factor evaluation from the nodal vertical displacement difference between rails and T beams on right hand side of the track. Impact factors are also shown from the ratio between static and dynamic quantities.

Table A2-25 presents nodal vertical acceleration peaks of right and left rails and T beams.

	T beam Right Node #	Vertical Acceleration Peak [m/s^2]	T beam Left Node #	Vertical Acceleration Peak [m/s^2]	Right Rail Node #	Vertical Acceleration Peak [m/s^2]	Left Rail Node #	Vertical Acceleration Peak [m/s^2]
Cross girder # 5	1113	1.705	1114	1.904	1115	30.348	1116	37.436
	1141	1.610	1142	1.705	1121	32.732	1122	47.720
	1152	1.836	1153	1.916	1147	27.125	1148	26.872
Diaphragms # 3 – 4	1273	2.800	1274	5.034	1275	32.188	1276	41.683
	1285	3.146	1286	5.770	1287	40.559	1288	30.840
	1301	3.036	1302	5.436	1297	42.402	1298	27.460
	1314	3.027	1315	4.321	1316	31.122	1317	31.285
Cross girder # 6	1435	1.348	1436	1.606	1438	40.332	1437	25.245
	1463	1.239	1464	1.633	1444	31.443	1443	32.744
	1474	1.282	1475	1.718	1470	36.188	1469	37.674

Table A2-25 - Nodal vertical acceleration peaks of right and left rails and T beams.

Table A2-26 presents nodal vertical acceleration peaks of the railway girder.

	Railway Girder Node #	Vertical Acceleration Peak [m/s^2]
Cross girder # 5	1110	1.890
	1130	1.606
	1149	1.846
Diaphragm # 3	1270	2.602
Diaphragm # 4	1311	2.931
Cross girder # 6	1432	1.293
	1452	1.135
	1471	1.165

Table A2-26 - Nodal vertical acceleration peaks of the railway girder.

13.5.4 Simulation 4 - RFI 2: ETR470 coach (speed 144 km/h)

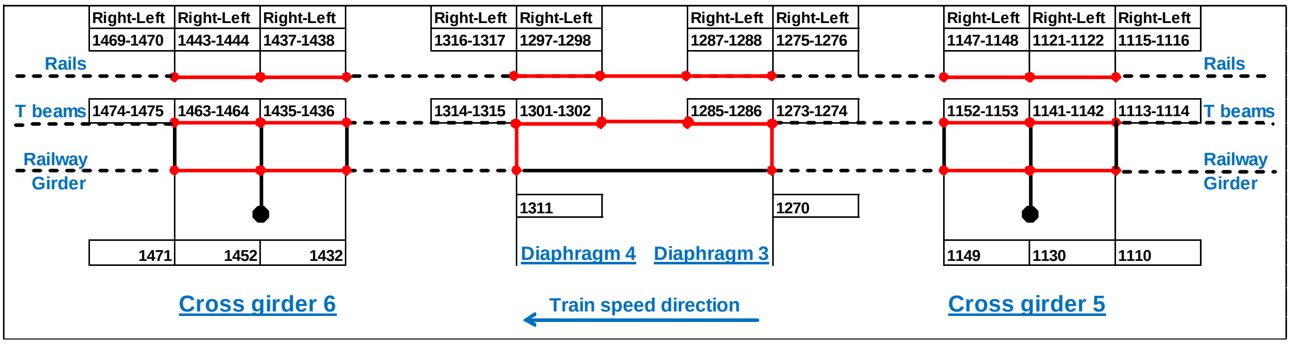

Tables A2-27 and A2-28 each the left and right rails and computed from static and dynamic simulations. Impact Factors are also listed in the same tables.

LEFT RAIL	Bed #	Static Force [N]	Dynamic Force [N]	Impact Factor
	795	8170	9755	1,1940E+00
	800	8160	9600	1,1765E+00
	803	8165	8720	1,0680E+00
	808	8165	9140	1,1194E+00
	892	8167	9466	1,1591E+00
	899	8140	8240	1,0123E+00
	912	8170	8600	1,0526E+00
	995	8200	8600	1,0488E+00
	1000	8160	9120	1,1176E+00
	1003	8163	8638	1,0582E+00
	1008	8165	8913	1,0916E+00

Table A2-27 – Impact factor evaluation from static and dynamic loads at specific beds locations positioned underneath the left rail.

RIGHT RAIL	Bed #	Static Force [N]	Dynamic Force [N]	Impact Factor
	793	8155	8660	1,0619E+00
	798	8155	8891	1,0903E+00
	801	8165	8710	1,0667E+00
	806	8180	9200	1,1247E+00
	890	8163	9231	1,1308E+00
	897	8150	9375	1,1503E+00
	910	8166	9670	1,1842E+00
	993	8200	8800	1,0732E+00
	998	8160	8750	1,0723E+00
	1001	8160	8400	1,0294E+00
	1006	8150	8680	1,0650E+00

Table A2-28 – Impact factor evaluation from static and dynamic loads at specific beds locations positioned underneath the right rail.

Table A2-29 presents vertical displacements of selected railway girder nodes located at cross girders 5 and 6 and diaphragms 3 and 4.

	Node #	Displacement [m]
Cross Girder # 5	1110	-1,9700E-03
	1130	-1,9700E-03
	1149	-1,9700E-03
Diaphragm # 3	1270	-2,5000E-03
Diaphragm # 4	1311	-2,5000E-03
Cross Girder # 6	1432	-1,9800E-03
	1452	-1,9800E-03
	1471	-1,9800E-03

Table A2-29 – Vertical displacements of the railway girder nodes.

Tables A2-30 and A2-31 presents the vertical displacement difference between the listed rails and T beams for both static and dynamic simulations on both left and right hand side of the track. Impact Factors are also listed in the same tables.

LEFT RAIL	Rail	T Beam	Static	Dynamic	Impact
	Node #	Node #	Displacement [m]	Displacement [m]	Factor
Cross Girder # 5	1116	1114	-1,3208E-03	-1,4588E-03	1,1045E+00
	1122	1142	-1,3200E-03	-1,4950E-03	1,1326E+00
	1148	1153	-1,3214E-03	-1,5400E-03	1,1654E+00
Diaphragm 3 - 4	1276	1274	-1,3243E-03	-1,4550E-03	1,0987E+00
	1288	1286	-1,3176E-03	-1,4276E-03	1,0835E+00
	1298	1302	-1,3174E-03	-1,4123E-03	1,0720E+00
	1317	1315	-1,3134E-03	-1,5000E-03	1,1421E+00
Cross Girder # 6	1438	1436	-1,3230E-03	-1,4650E-03	1,1073E+00
	1444	1464	-1,3213E-03	-1,4000E-03	1,0596E+00
	1470	1475	-1,3214E-03	-1,5000E-03	1,1352E+00

Table A2-30 – Impact factor evaluation from the nodal vertical displacement difference between rails and T beams on left hand side of the track. Impact factors are also shown from the ratio between static and dynamic quantities.

RIGHT RAIL	Rail Node #	T Beam Node #	Static Displacement [m]	Dynamic Displacement [m]	Impact Factor
Cross Girder # 5	1115	1113	-1,3227E-03	-1,3565E-03	1,0256E+00
	1121	1141	-1,3200E-03	-1,4369E-03	1,0886E+00
	1147	1152	-1,3225E-03	-1,4900E-03	1,1267E+00
Diaphragm 3 - 4	1275	1273	-1,3227E-03	-1,5542E-03	1,1750E+00
	1287	1285	-1,3200E-03	-1,4712E+00	1,1145E+03
	1297	1301	-1,3196E-03	-1,4685E-03	1,1128E+00
	1316	1314	-1,3143E-03	-1,3440E-03	1,0226E+00
Cross Girder # 6	1437	1435	-1,3200E-03	-1,5000E-04	1,1364E-01
	1443	1463	-1,3210E-03	-1,3474E-03	1,0200E+00
	1469	1474	-1,3210E-03	-1,3700E-03	1,0371E+00

Table A2-31 – Impact factor evaluation from the nodal vertical displacement difference between rails and T beams on right hand side of the track. Impact factors are also shown from the ratio between static and dynamic quantities.

Table A2-32 presents nodal vertical acceleration peaks of right and left rails and T beams.

	T beam Right Node #	Vertical Acceleration Peak [m/s^2]	T beam Left Node #	Vertical Acceleration Peak [m/s^2]	Right Rail Node #	Vertical Acceleration Peak [m/s^2]	Left Rail Node #	Vertical Acceleration Peak [m/s^2]
Cross girder # 5	1113	1.316	1114	1.739	1115	27.574	1116	45.621
	1141	1.425	1142	1.657	1121	35.421	1122	55.469
	1152	1.593	1153	1.868	1147	26.602	1148	33.086
Diaphragms # 3 – 4	1273	2.240	1274	3.530	1275	36.484	1276	42.754
	1285	2.350	1286	5.417	1287	43.264	1288	28.755
	1301	2.508	1302	5.540	1297	39.204	1298	27.472
	1314	2.313	1315	4.484	1316	35.361	1317	30.478
Cross girder # 6	1435	1.227	1436	1.442	1438	29.735	1437	24.761
	1463	1.016	1464	1.389	1444	28.791	1443	34.908
	1474	1.206	1475	1.685	1470	31.483	1469	34.986

Table A2-32 - Nodal vertical acceleration peaks of right and left rails and T beams.

Table A2-33 presents nodal vertical acceleration peaks of the railway girder.

	Railway Girder Node #	Vertical Acceleration Peak [m/s^2]
Cross girder # 5	1110	1.308
	1130	1.405
	1149	1.584
Diaphragm # 3	1270	1.925
Diaphragm # 4	1311	2.294
Cross girder # 6	1432	1.063
	1452	0.843
	1471	0.976

Table A2-33 - Nodal vertical acceleration peaks of the railway girder.

13.5.5 Simulation 5.1 - RFI 3: E402B locomotive (speed 144 km/h)

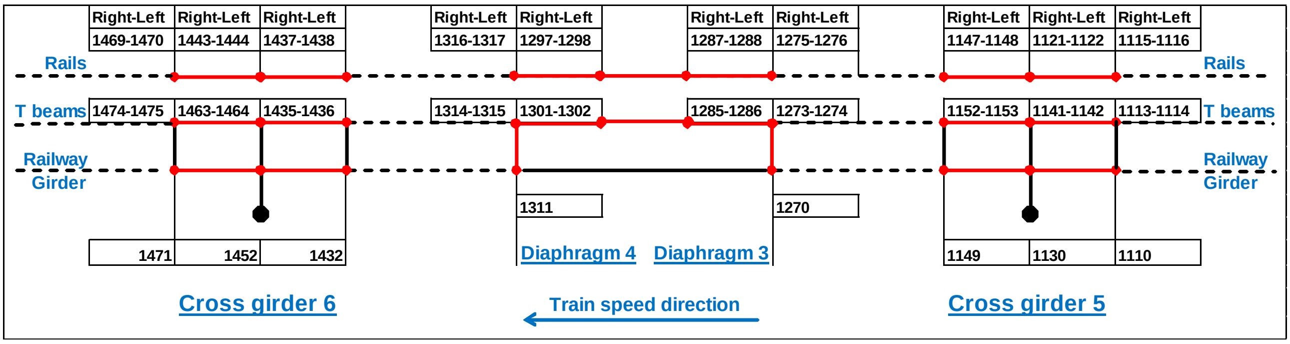

Tables A2-34 and A2-35 present the maximum vertical force transmitted to the listed visco-elastic beds located underneath the left and right rails and computed from static and dynamic simulations. Impact Factors are also listed in the same tables.

LEFT RAIL	Bed #	Static Force [N]	Dynamic Force [N]	Impact Factor
	795	15000	16800	1,1200E+00
	800	14950	15870	1,0615E+00
	803	14950	15700	1,0502E+00
	808	14950	14750	9,8662E-01
	892	15000	13500	9,0000E-01
	899	14950	16000	1,0702E+00
	912	15000	14600	9,7333E-01
	995	15000	17730	1,1820E+00
	1000	14950	14800	9,8997E-01
	1003	14950	14925	9,9833E-01
	1008	14900	16300	1,0940E+00

Table A2-34 – Impact factor evaluation from static and dynamic loads at specific beds locations positioned underneath the left rail.

RIGHT RAIL	Bed #	Static Force [N]	Dynamic Force [N]	Impact Factor
	793	15000	15750	1,0500E+00
	798	14950	13690	9,1572E-01
	801	14950	14970	1,0013E+00
	806	14990	14930	9,9600E-01
	890	15000	17600	1,1733E+00
	897	14950	16100	1,0769E+00
	910	15000	17000	1,1333E+00
	993	14950	16670	1,1151E+00
	998	14950	16500	1,1037E+00
	1001	14940	16300	1,0910E+00
	1006	15000	16800	1,1200E+00

Table A2-35 – Impact factor evaluation from static and dynamic loads at specific beds locations

positioned underneath the right rail.

Table A2-36 presents vertical displacements of selected railway girder nodes located at cross girders 5 and 6 and diaphragms 3 and 4.

	Node #	Displacement [m]
Cross Girder # 5	1110	-3,6000E-03
	1130	-3,6000E-03
	1149	-3,6000E-03
Diaphragm # 3	1270	-4,5500E-03
Diaphragm # 4	1311	-4,5500E-03
Cross Girder # 6	1432	-3,6000E-03
	1452	-3,6000E-03
	1471	-3,6000E-03

Table A2-36 – Vertical displacements of the railway girder nodes.

Tables A2-37 and A2-38 presents the vertical displacement difference between the listed rails and T beams for both static and dynamic simulations on both left and right hand side of the track. Impact Factors are also listed in the same tables.

LEFT RAIL	Rail	T Beam	Static	Dynamic	Impact
	Node #	Node #	Displacement [m]	Displacement [m]	Factor
Cross Girder # 5	1116	1114	-2,4200E-03	-2,6500E-03	1,0950E+00
	1122	1142	-2,4200E-03	-2,5330E-03	1,0467E+00
	1148	1153	-2,4180E-03	-2,4220E-03	1,0017E+00
Diaphragm 3 - 4	1276	1274	-2,4200E-03	-2,59E-03	1,0694E+00
	1288	1286	-2,4200E-03	-2,6150E-03	1,0806E+00
	1298	1302	-2,4140E-03	-2,4850E-03	1,0294E+00
	1317	1315	-2,4000E-03	-2,6900E-03	1,1208E+00
Cross Girder # 6	1438	1436	-2,4250E-03	-2,8300E-03	1,1670E+00
	1444	1464	-2,4210E-03	-2,4180E-03	9,9876E-01
	1470	1475	-2,42E-03	-2,6300E-03	1,0863E+00

Table A2-37 – Impact factor evaluation from the nodal vertical displacement difference between rails and T beams on left hand side of the track. Impact factors are also shown from the ratio between static and dynamic quantities.

RIGHT RAIL	Rail Node #	T Beam Node #	Static Displacement [m]	Dynamic Displacement [m]	Impact Factor
Cross Girder # 5	1115	1113	-2,4220E-03	-2,5000E-03	1,0322E+00
	1121	1141	-2,4200E-03	-2,3200E-03	9,5868E-01
	1147	1152	-2,4200E-03	-2,4000E-03	9,9174E-01
Diaphragm 3 - 4	1275	1273	-2,4350E-03	-2,68E-03	1,1006E+00
	1287	1285	-2,4180E-03	-2,5750E-03	1,0649E+00
	1297	1301	-2,4150E-03	-2,5360E-03	1,0501E+00
	1316	1314	-2,4300E-03	-2,7000E-03	1,1111E+00
Cross Girder # 6	1437	1435	-2,4200E-03	-2,6550E-03	1,0971E+00
	1443	1463	-2,4200E-03	-2,6760E-03	1,1058E+00
	1469	1474	-2,42E-03	-2,5230E-03	1,0426E+00

Table A2-38 – Impact factor evaluation from the nodal vertical displacement difference between rails and T beams on right hand side of the track. Impact factors are also shown from the ratio between static and dynamic quantities.

Table A2-39 presents nodal vertical acceleration peaks of right and left rails and T beams.

	T beam Right Node #	Vertical Acceleration Peak [m/s^2]	T beam Left Node #	Vertical Acceleration Peak [m/s^2]	Right Rail Node #	Vertical Acceleration Peak [m/s^2]	Left Rail Node #	Vertical Acceleration Peak [m/s^2]
Cross girder # 5	1113	1.782	1114	2.257	1115	38.323	1116	34.945
	1141	1.814	1142	2.183	1121	33.843	1122	47.706
	1152	1.903	1153	2.185	1147	31.929	1148	42.309
Diaphragms # 3 – 4	1273	3.655	1274	4.749	1275	28.901	1276	41.525
	1285	4.249	1286	5.666	1287	33.231	1288	43.647
	1301	4.604	1302	5.780	1297	32.066	1298	29.881
	1314	4.649	1315	5.395	1316	38.051	1317	38.994
Cross girder # 6	1435	2.238	1436	2.364	1438	49.891	1437	27.322
	1463	2.186	1464	2.304	1444	26.726	1443	35.381
	1474	2.173	1475	2.589	1470	27.419	1469	36.262

Table A2-39 - Nodal vertical acceleration peaks of right and left rails and T beams.

Table A2-40 presents nodal vertical acceleration peaks of the railway girder.

	Railway Girder Node #	Vertical Acceleration Peak [m/s^2]
Cross girder # 5	1110	1.652
	1130	1.749
	1149	1.766
Diaphragm # 3	1270	3.279
Diaphragm # 4	1311	4.076
Cross girder # 6	1432	2.150
	1452	2.116
	1471	2.025

Table A2-40 - Nodal vertical acceleration peaks of the railway girder.

13.5.6 Simulation 5.2 - RFI 3: E402B locomotive (speed 120 km/h)

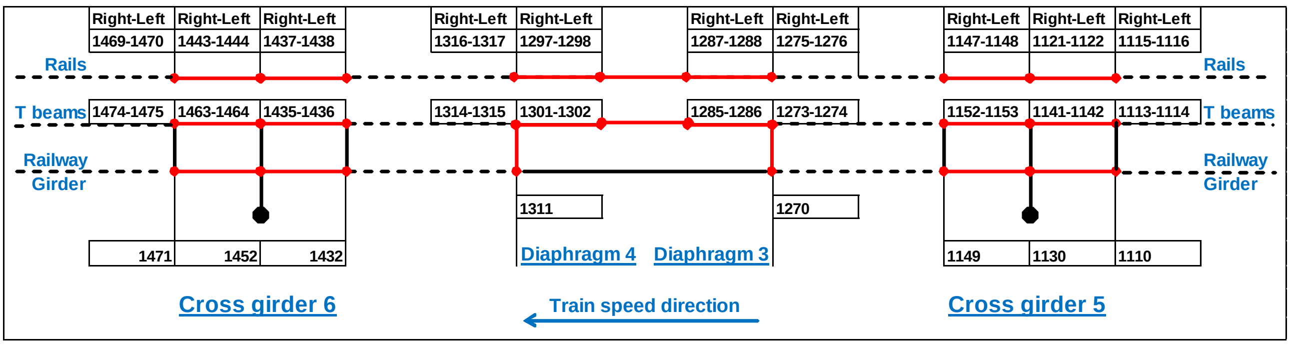

Tables A2-41 and A2-42 present the maximum vertical force transmitted to the listed visco-elastic beds located underneath the left and right rails and computed from static and dynamic simulations. Impact Factors are also listed in the same tables.

LEFT RAIL	Bed #	Static Force [N]	Dynamic Force [N]	Impact Factor
	795	15000	17500	1,1667E+00
	800	15000	16000	1,0667E+00
	803	19500	15150	7,7692E-01
	808	15000	16300	1,0867E+00
	892	14950	14400	9,6321E-01
	899	14900	15150	1,0168E+00
	912	15000	16000	1,0667E+00
	995	14950	15150	1,0134E+00
	1000	14900	16400	1,1007E+00
	1003	14950	15350	1,0268E+00
	1008	15000	17400	1,1600E+00

Table A2-41 – Impact factor evaluation from static and dynamic loads at specific beds locations positioned underneath the left rail.

RIGHT RAIL	Bed #	Static Force [N]	Dynamic Force [N]	Impact Factor
	793	14950	15400	1,0301E+00
	798	14900	15600	1,0470E+00
	801	14900	16500	1,1074E+00
	806	15000	15300	1,0200E+00
	890	15000	16700	1,1133E+00
	897	14950	17400	1,1639E+00
	910	15000	17400	1,1600E+00
	993	14950	16000	1,0702E+00
	998	14950	17500	1,1706E+00
	1001	14900	15900	1,0671E+00
	1006	14950	15100	1,0100E+00

Table A2-42 – Impact factor evaluation from static and dynamic loads at specific beds locations positioned underneath the right rail.

Table A2-43 presents vertical displacements of selected railway girder nodes located at cross girders 5 and 6 and diaphragms 3 and 4.

	Node #	Displacement [m]
Cross Girder # 5	1110	-3,5500E-03
	1130	-3,5500E-03
	1149	-3,5500E-03
Diaphragm # 3	1270	-4,5000E-03
Diaphragm # 4	1311	-4,5000E-03
Cross Girder # 6	1432	-3,5500E-03
	1452	-3,5500E-03
	1471	-3,6000E-03

Table A2-43 – Vertical displacements of the railway girder nodes.

Tables A2-44 and A2-45 presents the vertical displacement difference between the listed rails and T beams for both static and dynamic simulations on both left and right hand side of the track. Impact Factors are also listed in the same tables.

LEFT RAIL	Rail	T Beam	Static	Dynamic	Impact
	Node #	Node #	Displacement [m]	Displacement [m]	Factor
Cross Girder # 5	1116	1114	-2,4200E-03	-2,8600E-03	1,1818E+00
	1122	1142	-2,4200E-03	-2,4800E-03	1,0248E+00
	1148	1153	-2,4250E-03	-2,7000E-03	1,1134E+00
Diaphragm 3 - 4	1276	1274	-2,4270E-03	-2,44E-03	1,0033E+00
	1288	1286	-2,4150E-03	-2,5000E-03	1,0352E+00
	1298	1302	-2,4000E-03	-2,9000E-03	1,2083E+00
	1317	1315	-2,4500E-03	-2,9500E-03	1,2041E+00
Cross Girder # 6	1438	1436	2,4250E-03	2,3400E-03	9,6495E-01
	1444	1464	-2,4200E-03	-2,5850E-03	1,0682E+00
	1470	1475	-2,42E-03	-2,8200E-03	1,1653E+00

Table A2-44 – Impact factor evaluation from the nodal vertical displacement difference between rails and T beams on left hand side of the track. Impact factors are also shown from the ratio between static and dynamic quantities.

RIGHT RAIL	Rail Node #	T Beam Node #	Static Displacement [m]	Dynamic Displacement [m]	Impact Factor
Cross Girder # 5	1115	1113	-2,4200E-03	-2,4500E-03	1,0124E+00
	1121	1141	-2,4200E-03	-2,6250E-03	1,0847E+00
	1147	1152	-2,4200E-03	-2,3800E-03	9,8347E-01
Diaphragm 3 - 4	1275	1273	-2,4250E-03	-2,80E-03	1,1546E+00
	1287	1285	-2,4200E-03	-2,7200E-03	1,1240E+00
	1297	1301	-2,4100E-03	-2,5100E-03	1,0415E+00
	1316	1314	-2,4300E-03	-2,3900E-03	9,8354E-01
Cross Girder # 6	1437	1435	-2,4200E-03	-2,4700E-03	1,0207E+00
	1443	1463	-2,4200E-03	-2,7000E-03	1,1157E+00
	1469	1474	-2,42E-03	-2,5000E-03	1,0314E+00

Table A2-45 – Impact factor evaluation from the nodal vertical displacement difference between rails and T beams on right hand side of the track. Impact factors are also shown from the ratio between static and dynamic quantities.

Table A2-46 presents nodal vertical acceleration peaks of right and left rails and T beams.

	T beam Right Node #	Vertical Acceleration Peak [m/s^2]	T beam Left Node #	Vertical Acceleration Peak [m/s^2]	Right Rail Node #	Vertical Acceleration Peak [m/s^2]	Left Rail Node #	Vertical Acceleration Peak [m/s^2]
Cross girder # 5	1113	1.723	1114	1.866	1115	22.860	1116	36.380
	1141	1.666	1142	1.833	1121	37.032	1122	26.091
	1152	1.598	1153	1.809	1147	33.154	1148	24.453
Diaphragms # 3 – 4	1273	2.546	1274	3.874	1275	35.079	1276	26.970
	1285	2.758	1286	4.103	1287	30.595	1288	32.778
	1301	2.346	1302	3.698	1297	32.434	1298	28.211
	1314	2.227	1315	2.625	1316	26.457	1317	28.706
Cross girder # 6	1435	1.492	1436	1.734	1438	24.273	1437	34.167
	1463	1.528	1464	1.650	1444	24.060	1443	23.269
	1474	1.505	1475	1.655	1470	22.441	1469	23.230

Table A2-46 - Nodal vertical acceleration peaks of right and left rails and T beams.

Table A2-47 presents nodal vertical acceleration peaks of the railway girder.

	Railway Girder Node #	Vertical Acceleration Peak [m/s^2]
Cross girder # 5	1110	1.637
	1130	1.568
	1149	1.635
Diaphragm # 3	1270	2.147
Diaphragm # 4	1311	2.171
Cross girder # 6	1432	1.469
	1452	1.487
	1471	1.519

Table A2-47 - Nodal vertical acceleration peaks of the railway girder.

13.5.7 Simulation 5.3 - RFI 3: E402B110 locomotive (speed 110 km/h)

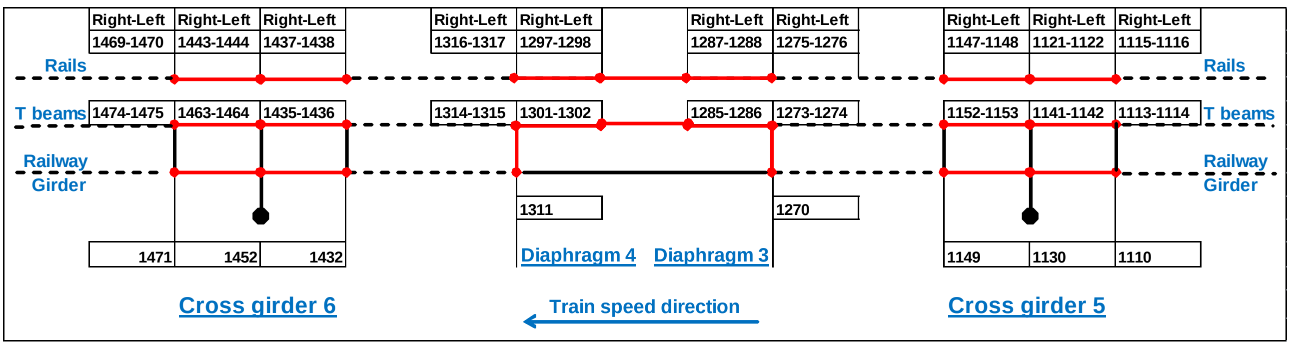

Tables A2-48 and A2-49 present the maximum vertical force transmitted to the listed visco-elastic beds located underneath the left and right rails and computed from static and dynamic simulations. Impact Factors are also listed in the same tables.

LEFT RAIL	Bed #	Static Force [N]	Dynamic Force [N]	Impact Factor
	795	15000	17800	1,1867E+00
	800	14900	15800	1,0604E+00
	803	14900	15900	1,0671E+00
	808	14900	15700	1,0537E+00
	892	14950	14700	9,8328E-01
	899	14900	15050	1,0101E+00
	912	14900	15800	1,0604E+00
	995	14950	14650	9,7993E-01
	1000	14900	15700	1,0537E+00
	1003	14960	14950	9,9933E-01
	1008	15000	16500	1,1000E+00

Table A2-48 – Impact factor evaluation from static and dynamic loads at specific beds locations positioned underneath the left rail.

RIGHT RAIL	Bed #	Static Force [N]	Dynamic Force [N]	Impact Factor
	793	14900	15300	1,0268E+00
	798	14900	16100	1,0805E+00
	801	14900	15600	1,0470E+00
	806	15000	16400	1,0933E+00
	890	14900	16200	1,0872E+00
	897	14900	16400	1,1007E+00
	910	15000	16700	1,1133E+00
	993	15000	15600	1,0400E+00
	998	15000	16550	1,1033E+00
	1001	14950	15000	1,0033E+00
	1006	14950	15000	1,0033E+00

Table A2-49 – Impact factor evaluation from static and dynamic loads at specific beds locations

positioned underneath the right rail.

Table A2-50 presents vertical displacements of selected railway girder nodes located at cross girders 5 and 6 and diaphragms 3 and 4.

	Node #	Displacement [m]
Cross Girder # 5	1110	-3,6000E-03
	1130	-3,6000E-03
	1149	-3,6000E-03
Diaphragm # 3	1270	-4,5500E-03
Diaphragm # 4	1311	-4,5500E-03
Cross Girder # 6	1432	-3,6000E-03
	1452	-3,6000E-03
	1471	-3,6000E-03

Table A2-50 – Vertical displacements of the railway girder nodes.

Tables A2-51 and A2-52 presents the vertical displacement difference between the listed rails and T beams for both static and dynamic simulations on both left and right hand side of the track. Impact Factors are also listed in the same tables.

LEFT RAIL	Rail	T Beam	Static	Dynamic	Impact
	Node #	Node #	Displacement [m]	Displacement [m]	Factor
Cross Girder # 5	1116	1114	-2,4200E-03	-2,8900E-03	1,1942E+00
	1122	1142	-2,4200E-03	-2,5500E-03	1,0537E+00
	1148	1153	-2,4300E-03	-2,6300E-03	1,0823E+00
Diaphragm 3 - 4	1276	1274	-2,4200E-03	-2,37E-03	9,7934E-01
	1288	1286	2,4200E-03	-2,4900E-03	1,0289E+00
	1298	1302	-2,4300E-03	-2,7500E-03	1,1317E+00
	1317	1315	-2,4400E-03	-2,7000E-03	1,1066E+00
Cross Girder # 6	1438	1436	-2,4200E-03	-2,3700E-03	9,7934E-01
	1444	1464	-2,4200E-03	-2,4300E-03	1,0041E+00
	1470	1475	-2,43E-03	-2,7300E-03	1,1235E+00

Table A2-51 – Impact factor evaluation from the nodal vertical displacement difference between rails and T beams on left hand side of the track. Impact factors are also shown from the ratio between static and dynamic quantities.

RIGHT RAIL	Rail	T Beam	Static	Dynamic	Impact
	Node #	Node #	Displacement [m]	Displacement [m]	Factor
Cross Girder # 5	1115	1113	-2,4200E-03	-2,3200E-03	9,5868E-01
	1121	1141	-2,4200E-03	-2,5700E-03	1,0620E+00
	1147	1152	-2,4200E-03	-2,6300E-03	1,0868E+00
Diaphragm 3 - 4	1275	1273	-2,4300E-03	-2,70E-03	1,1111E+00
	1287	1285	-2,4200E-03	-2,6500E-03	1,0950E+00
	1297	1301	-2,4200E-03	-2,5600E-03	1,0579E+00
	1316	1314	-2,4300E-03	-2,4200E-03	9,9588E-01
Cross Girder # 6	1437	1435	-2,4200E-03	-2,6800E-03	1,1074E+00
	1443	1463	-2,4200E-03	-2,5700E-03	1,0620E+00
	1469	1474	-2,42E-03	-2,4800E-03	1,0248E+00

Table A2-52 – Impact factor evaluation from the nodal vertical displacement difference between rails and T beams on right hand side of the track. Impact factors are also shown from

the ratio between static and dynamic quantities.

Table A2-53 presents nodal vertical acceleration peaks of right and left rails and T beams.

	T beam Right Node #	Vertical Acceleration Peak [m/s^2]	T beam Left Node #	Vertical Acceleration Peak [m/s^2]	Right Rail Node #	Vertical Acceleration Peak [m/s^2]	Left Rail Node #	Vertical Acceleration Peak [m/s^2]
Cross girder # 5	1113	1.087	1114	1.499	1115	22.698	1116	24.890
	1141	1.191	1142	1.449	1121	26.125	1122	24.720
	1152	1.063	1153	1.389	1147	26.074	1148	27.910
Diaphragms # 3 – 4	1273	1.638	1274	2.149	1275	33.929	1276	21.343
	1285	1.628	1286	2.377	1287	32.009	1288	27.925
	1301	1.792	1302	2.474	1297	23.941	1298	26.737
	1314	1.858	1315	2.620	1316	29.711	1317	26.732
Cross girder # 6	1435	1.214	1436	1.345	1438	23.830	1437	22.201
	1463	1.189	1464	1.374	1444	36.419	1443	21.076
	1474	1.242	1475	1.473	1470	19.389	1469	19.362

Table A2-53 - Nodal vertical acceleration peaks of right and left rails and T beams.

Table A2-54 presents nodal vertical acceleration peaks of the railway girder.

	Railway Girder Node #	Vertical Acceleration Peak [m/s^2]
Cross girder # 5	1110	1.145
	1130	1.084
	1149	1.069
Diaphragm # 3	1270	1.634
Diaphragm # 4	1311	1.757
Cross girder # 6	1432	1.145
	1452	1.160
	1471	1.238

Table A2-54 - Nodal vertical acceleration peaks of the railway girder.

13.5.8 Simulation 5.4 - RFI 3: E402B100 locomotive (speed 100 km/h)

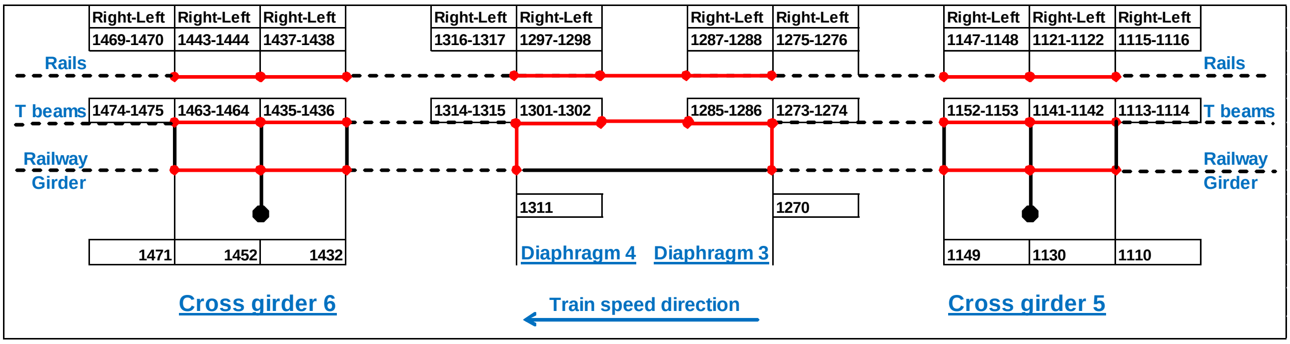

Tables A2-55 and A2-56 present the maximum vertical force transmitted to the listed visco-elastic beds located underneath the left and right rails and computed from static and dynamic simulations. Impact Factors are also listed in the same tables.

LEFT RAIL	Bed #	Static Force [N]	Dynamic Force [N]	Impact Factor
	795	15000	17000	1,1333E+00
	800	15000	16700	1,1133E+00
	803	14950	15650	1,0468E+00
	808	14900	15900	1,0671E+00
	892	14960	14955	9,9967E-01
	899	14900	15250	1,0235E+00
	912	15000	15700	1,0467E+00
	995	14950	14800	9,8997E-01
	1000	15000	15800	1,0533E+00
	1003	15000	15200	1,0133E+00
	1008	15000	16100	1,0733E+00

Table A2-55 Impact factor evaluation from static and dynamic loads at specific beds locationspositioned underneath the left rail.

RIGHT RAIL	Bed #	Static Force [N]	Dynamic Force [N]	Impact Factor
	793	14900	14100	9,4631E-01
	798	14950	15000	1,0033E+00
	801	14950	14900	9,9666E-01
	806	15000	16000	1,0667E+00
	890	15000	17000	1,1333E+00
	897	15000	17000	1,1333E+00
	910	15000	16250	1,0833E+00
	993	15000	15650	1,0433E+00
	998	15000	15850	1,0567E+00
	1001	14950	15200	1,0167E+00
	1006	14900	15700	1,0537E+00

Table A2-56 – Impact factor evaluation from static and dynamic loads at specific beds locations positioned underneath the right rail.

Table A2-57 presents vertical displacements of selected railway girder nodes located at cross girders 5 and 6 and diaphragms 3 and 4.

	Node #	Displacement [m]
Cross Girder # 5	1110	-3,5800E-03
	1130	-3,5600E-03
	1149	-3,5800E-03
Diaphragm # 3	1270	-4,5000E-03
Diaphragm # 4	1311	-4,5000E-03
Cross Girder # 6	1432	-3,6000E-03
	1452	-3,6000E-03
	1471	-3,6000E-03

Table A2-57 – Vertical displacements of the railway girder nodes.

Tables A2-58 and A2-59 presents the vertical displacement difference between the listed rails and T beams for both static and dynamic simulations on both left and right hand side of the track. Impact Factors are also listed in the same tables.

LEFT RAIL	Rail	T Beam	Static	Dynamic	Impact
	Node #	Node #	Displacement [m]	Displacement [m]	Factor
Cross Girder # 5	1116	1114	-2,4200E-03	-2,7000E-03	1,1157E+00
	1122	1142	-2,4200E-03	-2,6250E-03	1,0847E+00
	1148	1153	-2,4400E-03	-2,6600E-03	1,0902E+00
Diaphragm 3 - 4	1276	1274	-2,4400E-03	-2,49E-03	1,0205E+00
	1288	1286	-2,4100E-03	-2,4400E-03	1,0124E+00
	1298	1302	-2,4200E-03	-2,7400E-03	1,1322E+00
	1317	1315	-2,4500E-03	-2,6000E-03	1,0612E+00
Cross Girder # 6	1438	1436	-2,4200E-03	-2,3400E-03	9,6694E-01
	1444	1464	-2,4200E-03	-2,4450E-03	1,0103E+00
	1470	1475	-2,44E-03	-2,6700E-03	1,0943E+00

Table A2-58 – Impact factor evaluation from the nodal vertical displacement difference between rails and T beams on left hand side of the track. Impact factors are also shown from the ratio between static and dynamic quantities.

RIGHT RAIL	Rail	T Beam	Static	Dynamic	Impact
	Node #	Node #	Displacement [m]	Displacement [m]	Factor
Cross Girder # 5	1115	1113	-2,4200E-03	-2,3000E-03	9,5041E-01
	1121	1141	-2,4200E-03	-2,4300E-03	1,0041E+00
	1147	1152	-2,4200E+00	-2,6200E-03	1,0826E-03
Diaphragm 3 - 4	1275	1273	-2,4400E-03	-2,60E-03	1,0656E+00
	1287	1285	-2,4400E-03	-2,6700E-03	1,0943E+00
	1297	1301	-2,4200E-03	-2,5400E-03	1,0496E+00
	1316	1314	-2,4000E-03	-2,5500E-03	1,0625E+00
Cross Girder # 6	1437	1435	-2,4400E-03	-2,6500E-03	1,0861E+00
	1443	1463	-2,4200E-03	-2,4700E-03	1,0207E+00
	1469	1474	-2,42E-03	-2,3600E-03	9,7521E-01

Table A2-59 – Impact factor evaluation from the nodal vertical displacement difference between rails and T beams on right hand side of the track. Impact factors are also shown from the ratio between static and dynamic quantities.

Table A2-60 presents nodal vertical acceleration peaks of right and left rails and T beams.

	T beam Right Node #	Vertical Acceleration Peak [m/s^2]	T beam Left Node #	Vertical Acceleration Peak [m/s^2]	Right Rail Node #	Vertical Acceleration Peak [m/s^2]	Left Rail Node #	Vertical Acceleration Peak [m/s^2]
Cross girder # 5	1113	1.555	1114	1.670	1115	20.303	1116	15.281
	1141	1.412	1142	1.477	1121	17.560	1122	22.254
	1152	1.314	1153	1.351	1147	23.124	1148	21.026
Diaphragms # 3 – 4	1273	2.092	1274	2.741	1275	22.165	1276	16.600
	1285	2.119	1286	2.806	1287	18.412	1288	13.824
	1301	2.095	1302	2.767	1297	23.760	1298	18.642
	1314	1.963	1315	2.701	1316	22.507	1317	17.619
Cross girder # 6	1435	1.012	1436	1.506	1438	14.648	1437	18.496
	1463	1.055	1464	1.462	1444	20.440	1443	15.081
	1474	0.958	1475	1.213	1470	15.083	1469	20.407

Table A2-60 - Nodal vertical acceleration peaks of right and left rails and T beams.

Table A2-61 presents nodal vertical acceleration peaks of the railway girder.

	Railway Girder Node #	Vertical Acceleration Peak [m/s^2]
Cross girder # 5	1110	1.483
	1130	1.382
	1149	1.286
Diaphragm # 3	1270	1.744
Diaphragm # 4	1311	1.677
Cross girder # 6	1432	1.110
	1452	1.034
	1471	0.926

Table A2-61 - Nodal vertical acceleration peaks of the railway girder.

13.5.9 Simulation 5.5 - RFI 3: E402B90 locomotive (speed 90 km/h)

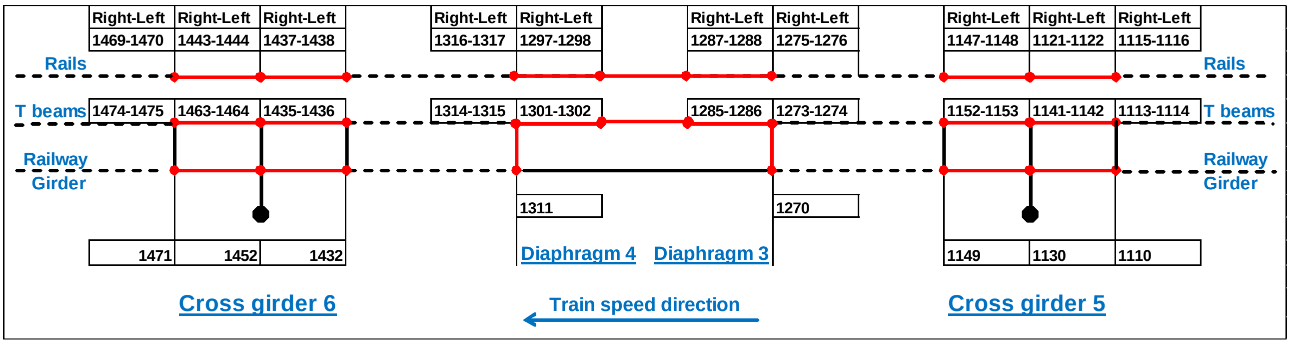

Tables A2-62 and A2-63 present the maximum vertical force transmitted to the listed visco-elastic beds located underneath the left and right rails and computed from static and dynamic simulations. Impact Factors are also listed in the same tables.

LEFT RAIL	Bed #	Static Force [N]	Dynamic Force [N]	Impact Factor
	795	15000	16400	1,0933E+00
	800	14900	16900	1,1342E+00
	803	14950	15100	1,0100E+00
	808	14900	15700	1,0537E+00
	892	14950	15400	1,0301E+00
	899	14900	16000	1,0738E+00
	912	14950	15100	1,0100E+00
	995	15000	14500	9,6667E-01
	1000	14950	14640	9,7926E-01
	1003	14950	15200	1,0167E+00
	1008	15000	16000	1,0667E+00

Table A2-62 – Impact factor evaluation from static and dynamic loads at specific beds locations positioned underneath the left rail.

RIGHT RAIL	Bed #	Static Force [N]	Dynamic Force [N]	Impact Factor
	793	14900	15300	1,0268E+00
	798	14950	15100	1,0100E+00
	801	14950	15700	1,0502E+00
	806	15000	15900	1,0600E+00
	890	15000	17300	1,1533E+00
	897	14900	16800	1,1275E+00
	910	14950	15700	1,0502E+00
	993	15000	16200	1,0800E+00
	998	15000	16000	1,0667E+00
	1001	14900	15200	1,0201E+00
	1006	14900	15900	1,0671E+00

Table A2-63 – Impact factor evaluation from static and dynamic loads at specific beds locations

positioned underneath the right rail.

Table A2-64 presents vertical displacements of selected railway girder nodes located at cross girders 5 and 6 and diaphragms 3 and 4.

	Node #	Displacement [m]
Cross Girder # 5	1110	-3,6000E-03
	1130	-3,6000E-03
	1149	-3,6000E-03
Diaphragm # 3	1270	-4,5000E-03
Diaphragm # 4	1311	-4,5000E-03
Cross Girder # 6	1432	-3,5800E-03
	1452	-3,5800E-03
	1471	-3,6000E-03

Table A2-64 – Vertical displacements of the railway girder nodes.

Tables A2-65 and A2-66 presents the vertical displacement difference between the listed rails and T beams for both static and dynamic simulations on both left and right hand side of the track. Impact Factors are also listed in the same tables.

LEFT RAIL	Rail	T Beam	Static	Dynamic	Impact
	Node #	Node #	Displacement [m]	Displacement [m]	Factor
Cross Girder # 5	1116	1114	-2,4200E-03	-2,6000E-03	1,0744E+00
	1122	1142	-2,4200E-03	-2,6000E-03	1,0744E+00
	1148	1153	-2,4300E-03	-2,6600E-03	1,0947E+00
Diaphragm 3 - 4	1276	1274	-2,4400E-03	-2,53E-03	1,0369E+00
	1288	1286	-2,4200E-03	-2,5000E-03	1,0331E+00
	1298	1302	-2,4200E-03	-2,7500E-03	1,1364E+00
	1317	1315	-2,4400E-03	-2,7000E-03	1,1066E+00
Cross Girder # 6	1438	1436	-2,4200E-03	-2,4400E-03	1,0083E+00
	1444	1464	-2,4200E-03	-2,4300E-03	1,0041E+00
	1470	1475	-2,43E-03	-2,6300E-03	1,0823E+00

Table A2-65 – Impact factor evaluation from the nodal vertical displacement difference between rails and T beams on left hand side of the track. Impact factors are also shown from the ratio between static and dynamic quantities.

RIGHT RAIL	Rail	T Beam	Static	Dynamic	Impact
	Node #	Node #	Displacement [m]	Displacement [m]	Factor
Cross Girder # 5	1115	1113	-2,4200E-03	-2,5000E-03	1,0331E+00
	1121	1141	-2,4200E-03	-2,5200E-03	1,0413E+00
	1147	1152	-2,4200E-03	-2,5600E-03	1,0579E+00
Diaphragm 3 - 4	1275	1273	-2,4200E-03	-2,60E-03	1,0744E+00
	1287	1285	-2,4200E-03	-2,6700E-03	1,1033E+00
	1297	1301	-2,4200E-03	-2,6000E-03	1,0744E+00
	1316	1314	-2,4000E-03	-2,5700E-03	1,0708E+00
Cross Girder # 6	1437	1435	-2,4200E-03	-2,6500E-03	1,0950E+00
	1443	1463	-2,4200E-03	-2,5000E-03	1,0331E+00
	1469	1474	-2,42E-03	-2,3400E-03	9,6694E-01

Table A2-66 – Impact factor evaluation from the nodal vertical displacement difference between rails and T beams on right hand side of the track. Impact factors are also shown from

the ratio between static and dynamic quantities.

Table A2-67 presents nodal vertical acceleration peaks of right and left rails and T beams.

	T beam Right Node #	Vertical Acceleration Peak [m/s^2]	T beam Left Node #	Vertical Acceleration Peak [m/s^2]	Right Rail Node #	Vertical Acceleration Peak [m/s^2]	Left Rail Node #	Vertical Acceleration Peak [m/s^2]
Cross girder # 5	1113	1.365	1114	1.466	1115	10.779	1116	14.990
	1141	1.347	1142	1.437	1121	15.043	1122	15.746
	1152	1.346	1153	1.351	1147	15.741	1148	15.960
Diaphragms # 3 – 4	1273	1.879	1274	2.835	1275	18.915	1276	13.769
	1285	1.954	1286	2.512	1287	14.072	1288	13.843
	1301	1.955	1302	2.494	1297	20.950	1298	14.268
	1314	2.044	1315	2.376	1316	14.001	1317	16.219
Cross girder # 6	1435	1.293	1436	1.394	1438	16.329	1437	16.711
	1463	1.271	1464	1.332	1444	13.499	1443	13.703
	1474	1.341	1475	1.265	1470	14.585	1469	14.837

Table A2-67 - Nodal vertical acceleration peaks of right and left rails and T beams.

Table A2-68 presents nodal vertical acceleration peaks of the railway girder.

	Railway Girder Node #	Vertical Acceleration Peak [m/s^2]
Cross girder # 5	1110	1.336
	1130	1.346
	1149	1.331
Diaphragm # 3	1270	1.692
Diaphragm # 4	1311	1.823
Cross girder # 6	1432	1.374
	1452	1.238
	1471	1.388

Table A2-69 - Nodal vertical acceleration peaks of the railway girder.

13.5.10 Simulation 5.6 - RFI 3: E402B80 locomotive (speed 80 km/h)

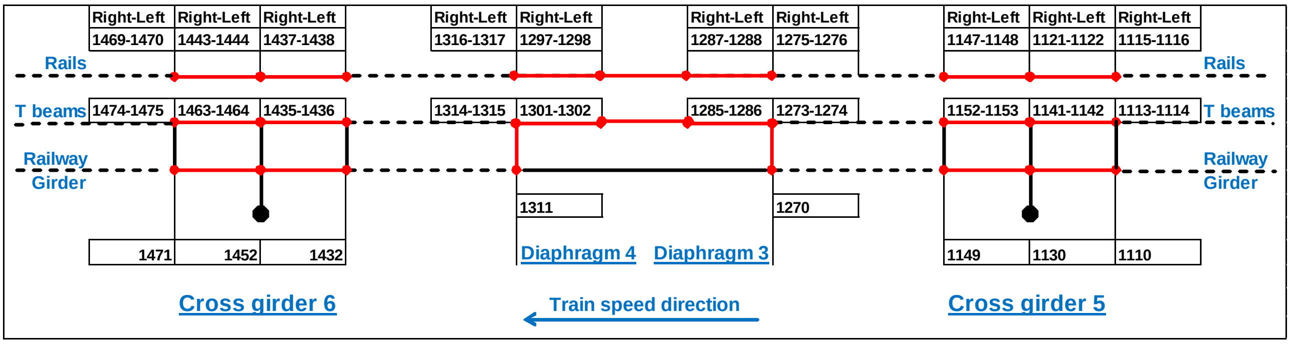

Tables A2-70 and A2-71 present the maximum vertical force transmitted to the listed visco-elastic beds located underneath the left and right rails and computed from static and dynamic simulations. Impact Factors are also listed in the same tables.

LEFT RAIL	Bed #	Static Force [N]	Dynamic Force [N]	Impact Factor
	795	15000	16350	1,0900E+00
	800	15000	16400	1,0933E+00
	803	14950	15200	1,0167E+00
	808	14950	15500	1,0368E+00
	892	14950	15150	1,0134E+00
	899	14900	15100	1,0134E-04
	912	14950	14900	9,9666E-01
	995	14950	14750	9,8662E-01
	1000	14950	15200	1,0167E+00
	1003	15000	15300	1,0200E+00
	1008	15000	16000	1,0667E+00

Table A2-70 – Impact factor evaluation from static and dynamic loads at specific beds locations positioned underneath the left rail.

RIGHT RAIL	Bed #	Static Force [N]	Dynamic Force [N]	Impact Factor
	793	14900	16250	1,0906E+00
	798	14950	15500	1,0368E+00
	801	14950	15100	1,0100E+00
	806	15000	16000	1,0667E+00
	890	15000	16300	1,0867E+00
	897	14900	16300	1,0940E+00
	910	15000	15800	1,0533E+00
	993	15000	16500	1,1000E+00
	998	14950	16100	1,0769E+00
	1001	14950	15250	1,0201E+00
	1006	14950	15500	1,0368E+00

Table A2-71 – Impact factor evaluation from static and dynamic loads at specific beds locations positioned underneath the right rail.

Table A2-72 presents vertical displacements of selected railway girder nodes located at cross girders 5 and 6 and diaphragms 3 and 4.

	Node #	Displacement [m]
Cross Girder # 5	1110	-3,6000E-03
	1130	-3,6000E-03
	1149	-3,6000E-03
Diaphragm # 3	1270	-4,5000E-03
Diaphragm # 4	1311	-4,5000E-03
Cross Girder # 6	1432	-3,6000E-03
	1452	-3,6000E-03
	1471	-3,6000E-03

Table A2-72 – Vertical displacements of the railway girder nodes.

Tables A2-73 and A2-74 presents the vertical displacement difference between the listed rails and T beams for both static and dynamic simulations on both left and right hand side of the track. Impact Factors are also listed in the same tables.

LEFT RAIL	Rail	T Beam	Static	Dynamic	Impact
	Node #	Node #	Displacement [m]	Displacement [m]	Factor
Cross Girder # 5	1116	1114	-2,4200E-03	-2,6500E-03	1,0950E+00
	1122	1142	-2,4200E-03	-2,5500E-03	1,0537E+00
	1148	1153	-2,4250E-03	-2,5500E-03	1,0515E+00
Diaphragm 3 - 4	1276	1274	-2,4400E-03	-2,54E-03	1,0410E+00
	1288	1286	-2,4200E-03	-2,4400E-03	1,0083E+00
	1298	1302	-2,4100E-03	-2,5500E-03	1,0581E+00
	1317	1315	-2,4250E-03	-2,6000E-03	1,0722E+00
Cross Girder # 6	1438	1436	-2,4200E-03	-2,4450E-03	1,0103E+00
	1444	1464	-2,4200E-03	-2,4600E-03	1,0165E+00
	1470	1475	-2,42E-03	-2,6120E-03	1,0793E+00

Table A2-73 – Impact factor evaluation from the nodal vertical displacement difference between rails and T beams on left hand side of the track. Impact factors are also shown from the ratio between static and dynamic quantities.

RIGHT RAIL	Rail	T Beam	Static	Dynamic	Impact
	Node #	Node #	Displacement [m]	Displacement [m]	Factor
Cross Girder # 5	1115	1113	-2,4250E-03	-2,6000E-03	1,0722E+00
	1121	1141	-2,4200E-03	-2,5000E-03	1,0331E+00
	1147	1152	-2,4200E-03	-2,5800E-03	1,0661E+00
Diaphragm 3 - 4	1275	1273	-2,4200E-03	-2,60E-03	1,0744E+00
	1287	1285	-2,4150E-03	-2,6000E-03	1,0766E+00
	1297	1301	-2,4200E-03	-2,6000E-03	1,0744E+00
	1316	1314	-2,4280E-03	-2,4800E-03	1,0214E+00
Cross Girder # 6	1437	1435	-2,4250E-03	-2,6550E-03	1,0948E+00
	1443	1463	-2,4200E-03	-2,5600E-03	1,0579E+00
	1469	1474	-2,39E-03	-2,4260E-03	1,0151E+00

Table A2-74 – Impact factor evaluation from the nodal vertical displacement difference between rails and T beams on right hand side of the track. Impact factors are also shown from the ratio between static and dynamic quantities.

Table A2-75 presents nodal vertical acceleration peaks of right and left rails and T beams.

	T beam Right Node #	Vertical Acceleration Peak [m/s^2]	T beam Left Node #	Vertical Acceleration Peak [m/s^2]	Right Rail Node #	Vertical Acceleration Peak [m/s^2]	Left Rail Node #	Vertical Acceleration Peak [m/s^2]
Cross girder # 5	1113	0.956	1114	1.030	1115	12.464	1116	14.778
	1141	0.858	1142	0.988	1121	9.308	1122	14.496
	1152	0.944	1153	0.851	1147	8.370	1148	11.744
Diaphragms # 3 – 4	1273	1.603	1274	2.111	1275	12.008	1276	10.487
	1285	1.567	1286	2.152	1287	11.337	1288	7.930
	1301	1.558	1302	2.126	1297	11.530	1298	13.303
	1314	1.535	1315	2.039	1316	9.584	1317	10.961
Cross girder # 6	1435	0.934	1436	0.989	1438	13.614	1437	10.658
	1463	0.889	1464	1.068	1444	12.208	1443	13.616
	1474	0.968	1475	1.024	1470	11.368	1469	18.814

Table A2-75 - Nodal vertical acceleration peaks of right and left rails and T beams.

Table A2-76 presents nodal vertical acceleration peaks of the railway girder.

	Railway Girder Node #	Vertical Acceleration Peak [m/s^2]
Cross girder # 5	1110	0.894
	1130	0.852
	1149	0.851
Diaphragm # 3	1270	1.221
Diaphragm # 4	1311	1.188
Cross girder # 6	1432	0.923
	1452	0.837
	1471	0.956

Table A2-76 - Nodal vertical acceleration peaks of the railway girder.

13.5.11 Simulation 5.7 - RFI 3: E402B70 locomotive (speed 70 km/h)

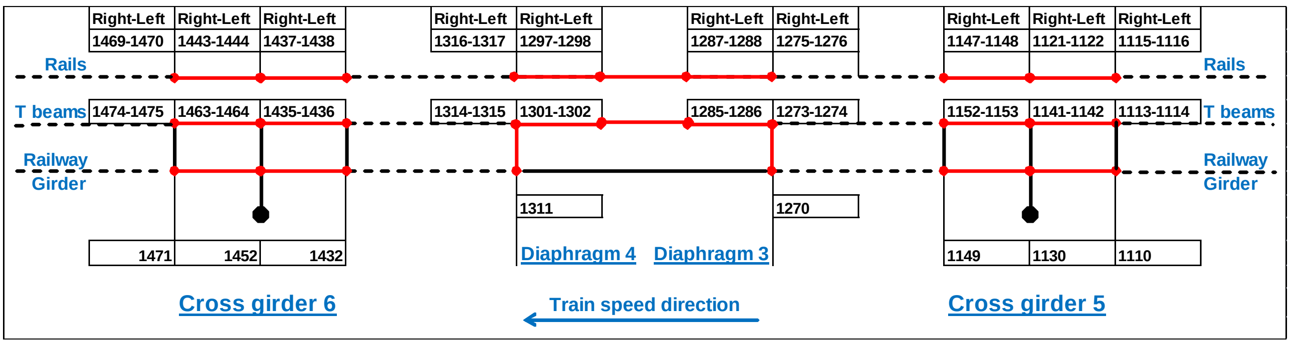

Tables A2-77 and A2-78 present the maximum vertical force transmitted to the listed visco-elastic beds located underneath the left and right rails and computed from static and dynamic simulations. Impact Factors are also listed in the same tables.

LEFT RAIL	Bed #	Static Force [N]	Dynamic Force [N]	Impact Factor
	795	15000	16500	1,1000E+00
	800	15000	16400	1,0933E+00
	803	15000	16200	9,2593E-01
	808	15000	16200	1,0800E+00
	892	14950	15250	1,0201E+00
	899	14900	15200	1,0201E+00
	912	15000	15600	1,0400E+00
	995	14950	14650	9,7993E-01
	1000	14950	15100	1,0100E+00
	1003	15000	15800	1,0533E+00
	1008	15000	15800	1,0533E+00

Table A2-77 – Impact factor evaluation from static and dynamic loads at specific beds locations positioned underneath the left rail.

RIGHT RAIL	Bed #	Static Force [N]	Dynamic Force [N]	Impact Factor
	793	14940	15700	1,0509E+00
	798	15000	15500	1,0333E+00
	801	14950	15350	9,7394E-01
	806	15000	15250	1,0167E+00
	890	14950	15350	1,0268E+00
	897	14900	15800	1,0604E+00
	910	15000	15800	1,0533E+00
	993	15000	16500	1,1000E+00
	998	15000	15820	1,0547E+00
	1001	14950	15300	1,0234E+00
	1006	15000	15600	1,0400E+00

Table A2-78 – Impact factor evaluation from static and dynamic loads at specific beds locations

positioned underneath the right rail.

Table A2-79 presents vertical displacements of selected railway girder nodes located at cross girders 5 and 6 and diaphragms 3 and 4.

	Node #	Displacement [m]
Cross Girder # 5	1110	-3,6000E-03
	1130	-3,6000E-03
	1149	-3,6000E-03
Diaphragm # 3	1270	-4,5000E-03
Diaphragm # 4	1311	-4,5000E-03
Cross Girder # 6	1432	-3,6000E-03
	1452	-3,6000E-03
	1471	-3,6000E-03

Table A2-79 – Vertical displacements of the railway girder nodes.

Tables A2-80 and A2-81 presents the vertical displacement difference between the listed rails and T beams for both static and dynamic simulations on both left and right hand side of the track. Impact Factors are also listed in the same tables.

LEFT RAIL	Rail	T Beam	Static	Dynamic	Impact
	Node #	Node #	Displacement [m]	Displacement [m]	Factor
Cross Girder # 5	1116	1114	-2,4200E-03	-2,6500E-03	1,0950E+00
	1122	1142	-2,4200E-03	-2,5500E-03	1,0537E+00
	1148	1153	-2,4200E-03	-2,5800E-03	1,0661E+00
Diaphragm 3 - 4	1276	1274	-2,4400E-03	-2,58E-03	1,0574E+00
	1288	1286	-2,4200E-03	-2,4700E-03	1,0207E+00
	1298	1302	-2,4180E-03	-2,4220E-03	1,0017E+00
	1317	1315	-2,4250E-03	-2,4400E-03	1,0062E+00
Cross Girder # 6	1438	1436	-2,4220E-03	-2,3700E-03	9,7853E-01
	1444	1464	-2,4200E-03	-2,5000E-03	1,0331E+00
	1470	1475	-2,42E-03	-2,5600E-03	1,0579E+00

Table A2-80 – Impact factor evaluation from the nodal vertical displacement difference between rails and T beams on left hand side of the track. Impact factors are also shown from the ratio between static and dynamic quantities.

RIGHT RAIL	Rail	T Beam	Static	Dynamic	Impact
	Node #	Node #	Displacement [m]	Displacement [m]	Factor
Cross Girder # 5	1115	1113	-2,4200E-03	-2,4900E-03	1,0289E+00
	1121	1141	-2,4200E-03	-2,4000E-03	9,9174E-01
	1147	1152	-2,4220E-03	-2,5000E-03	1,0322E+00
Diaphragm 3 - 4	1275	1273	-2,4200E-03	-2,55E-03	1,0537E+00
	1287	1285	-2,4200E-03	-2,5600E-03	1,0579E+00
	1297	1301	-2,4200E-03	-2,5800E-03	1,0661E+00
	1316	1314	-2,4400E-03	-2,5100E-03	1,0287E+00
Cross Girder # 6	1437	1435	-2,4200E-03	-2,6000E-03	1,0744E+00
	1443	1463	-2,4200E-03	-2,4500E-03	1,0124E+00
	1469	1474	-2,42E-03	-2,4350E-03	1,0062E+00

Table A2-81 – Impact factor evaluation from the nodal vertical displacement difference between rails and T beams on right hand side of the track. Impact factors are also shown from

the ratio between static and dynamic quantities.

Table A2-82 presents nodal vertical acceleration peaks of right and left rails and T beams.

	T beam Right Node #	Vertical Acceleration Peak [m/s^2]	T beam Left Node #	Vertical Acceleration Peak [m/s^2]	Right Rail Node #	Vertical Acceleration Peak [m/s^2]	Left Rail Node #	Vertical Acceleration Peak [m/s^2]
Cross girder # 5	1113	0.846	1114	0.963	1115	10.433	1116	12.494
	1141	0.840	1142	0.981	1121	11.893	1122	12.551
	1152	1.056	1153	0.984	1147	8.472	1148	8.316
Diaphragms # 3 – 4	1273	1.402	1274	1.819	1275	9.852	1276	8.706
	1285	1.389	1286	1.851	1287	7.498	1288	9.984
	1301	1.408	1302	1.843	1297	10.175	1298	8.520
	1314	1.527	1315	1.821	1316	8.617	1317	10.493
Cross girder # 6	1435	0.910	1436	0.963	1438	9.011	1437	8.951
	1463	0.824	1464	0.914	1444	8.995	1443	9.205
	1474	0.758	1475	0.900	1470	8.710	1469	7.39

Table A2-82 - Nodal vertical acceleration peaks of right and left rails and T beams.

Table A2-83 presents nodal vertical acceleration peaks of the railway girder.

	Railway Girder Node #	Vertical Acceleration Peak [m/s^2]
Cross girder # 5	1110	0.927
	1130	0.847
	1149	0.881
Diaphragm # 3	1270	1.179
Diaphragm # 4	1311	1.324
Cross girder # 6	1432	0.901
	1452	0.744
	1471	0.787

Table A2-83 - Nodal vertical acceleration peaks of the railway girder.

13.5.12 Simulation 5.8 - RFI 3: E402B60 locomotive (speed 60 km/h)

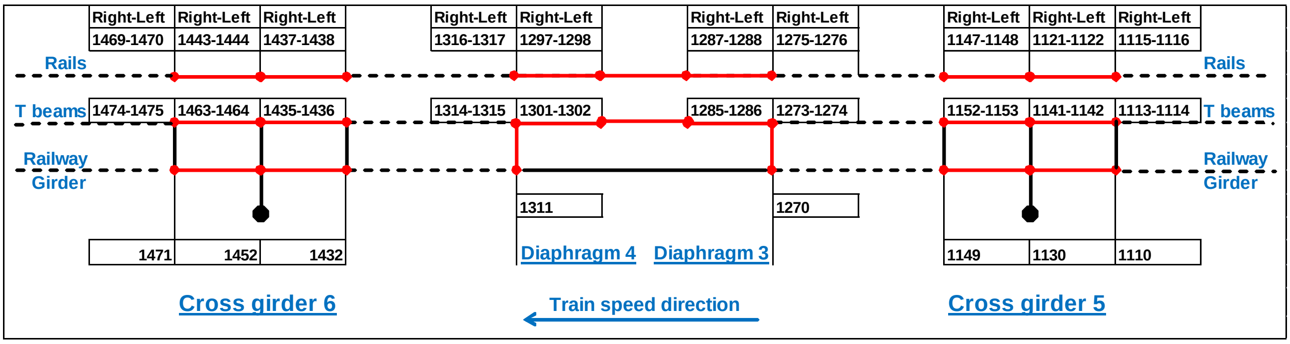

Tables A2-84 and A2-85 present the maximum vertical force transmitted to the listed visco-elastic beds located underneath the left and right rails and computed from static and dynamic simulations. Impact Factors are also listed in the same tables.

LEFT RAIL	Bed #	Static Force [N]	Dynamic Force [N]	Impact Factor
	795	15000	16300	1,0867E+00
	800	15000	15700	1,0467E+00
	803	15000	16200	9,2593E-01
	808	15000	16300	1,0867E+00
	892	14950	15200	1,0167E+00
	899	14900	15500	1,0403E+00
	912	14600	15000	1,0274E+00
	995	15000	14500	9,6667E-01
	1000	14950	15250	1,0201E+00
	1003	15000	15600	1,0400E+00
	1008	15000	15600	1,0400E+00

Table A2-84 – Impact factor evaluation from static and dynamic loads at specific beds locations positioned underneath the left rail.

RIGHT RAIL	Bed #	Static Force [N]	Dynamic Force [N]	Impact Factor
	793	14950	15400	1,0301E+00
	798	14950	15300	1,0234E+00
	801	15000	15800	9,4937E-01
	806	14950	14900	9,9666E-01
	890	15000	15400	1,0267E+00
	897	14900	15500	1,0403E+00
	910	15000	16100	1,0733E+00
	993	15000	15300	1,0200E+00
	998	14950	15300	1,0234E+00
	1001	14950	15000	1,0033E+00
	1006	14950	15450	1,0334E+00

Table A2-85 – Impact factor evaluation from static and dynamic loads at specific beds locations positioned underneath the right rail.

Table A2-86 presents vertical displacements of selected railway girder nodes located at cross girders 5 and 6 and diaphragms 3 and 4.

	Node #	Displacement [m]
Cross Girder # 5	1110	-3,6000E-03
	1130	-3,6000E-03
	1149	-3,6000E-03
Diaphragm # 3	1270	-4,5000E-03
Diaphragm # 4	1311	-4,5000E-03
Cross Girder # 6	1432	-3,6000E-03
	1452	-3,6000E-03
	1471	-3,6000E-03

Table A2-86 – Vertical displacements of the railway girder nodes.

Tables A2-87 and A2-88 presents the vertical displacement difference between the listed rails and T beams for both static and dynamic simulations on both left and right hand side of the track. Impact Factors are also listed in the same tables.

LEFT RAIL	Rail	T Beam	Static	Dynamic	Impact
	Node #	Node #	Displacement [m]	Displacement [m]	Factor
Cross Girder # 5	1116	1114	-2,4200E-03	-2,6000E-03	1,0744E+00
	1122	1142	-2,4200E-03	-2,6200E-03	1,0826E+00
	1148	1153	-2,4200E-03	-2,6000E-03	1,0744E+00
Diaphragm 3 - 4	1276	1274	-2,4250E-03	-2,56E-03	1,0557E+00
	1288	1286	-2,4200E-03	-2,4800E-03	1,0248E+00
	1298	1302	-2,4170E-03	-2,4250E-03	1,0033E+00
	1317	1315	-2,4400E-03	-2,5300E-03	1,0369E+00
Cross Girder # 6	1438	1436	-2,4200E-03	-2,3900E-03	9,8760E-01
	1444	1464	-2,4200E-03	-2,5000E-03	1,0331E+00
	1470	1475	-2,42E-03	-2,5200E-03	1,0413E+00

Table A2-87 – Impact factor evaluation from the nodal vertical displacement difference between rails and T beams on left hand side of the track. Impact factors are also shown from the ratio between static and dynamic quantities.

RIGHT RAIL	Rail Node #	T Beam Node #	Static Displacement [m]	Dynamic Displacement [m]	Impact Factor
Cross Girder # 5	1115	1113	-2,4200E-03	-2,3920E-03	9,8843E-01
	1121	1141	-2,4200E-03	-2,5600E-03	1,0579E+00
	1147	1152	-2,4200E-03	-2,5000E-03	1,0331E+00
Diaphragm 3 - 4	1275	1273	-2,4300E-03	-2,46E-03	1,0123E+00
	1287	1285	-2,4200E-03	-2,5600E-03	1,0579E+00
	1297	1301	-2,4200E-03	-2,5100E-03	1,0372E+00
	1316	1314	-2,4300E-03	-2,5800E-03	1,0617E+00
Cross Girder # 6	1437	1435	-2,4200E-03	-2,5400E-03	1,0496E+00
	1443	1463	-2,4200E-03	-2,4500E-03	1,0124E+00
	1469	1474	-2,42E-03	-2,4800E-03	1,0248E+00

Table A2-88 – Impact factor evaluation from the nodal vertical displacement difference between rails and T beams on right hand side of the track. Impact factors are also shown from the ratio between static and dynamic quantities.

Table A2-89 presents nodal vertical acceleration peaks of right and left rails and T beams.

	T beam Right Node #	Vertical Acceleration Peak [m/s^2]	T beam Left Node #	Vertical Acceleration Peak [m/s^2]	Right Rail Node #	Vertical Acceleration Peak [m/s^2]	Left Rail Node #	Vertical Acceleration Peak [m/s^2]
Cross girder # 5	1113	0.647	1114	0.631	1115	6.253	1116	9.358
	1141	0.640	1142	0.752	1121	7.137	1122	6.078
	1152	0.753	1153	0.660	1147	7.137	1148	9.877
Diaphragms # 3 – 4	1273	0.878	1274	1.072	1275	9.266	1276	7.246
	1285	0.932	1286	1.103	1287	5.587	1288	7.292
	1301	0.883	1302	1.129	1297	6.620	1298	9.185
	1314	0.789	1315	1.078	1316	5.526	1317	6.855
Cross girder # 6	1435	0.568	1436	0.598	1438	7.171	1437	6.099
	1463	0.627	1464	0.644	1444	5.632	1443	8.487
	1474	0.645	1475	0.717	1470	6.154	1469	6.845

Table A2-89 - Nodal vertical acceleration peaks of right and left rails and T beams.

Table A2-90 presents nodal vertical acceleration peaks of the railway girder.

	Railway Girder Node #	Vertical Acceleration Peak [m/s^2]
Cross girder # 5	1110	0.677
	1130	0.642
	1149	0.660
Diaphragm # 3	1270	0.746
Diaphragm # 4	1311	0.815
Cross girder # 6	1432	0.550
	1452	0.607
	1471	0.636

Table A2-90 - Nodal vertical acceleration peaks of the railway girder.

13.5.13 Simulation 5.9 - RFI 3: E402B50 locomotive (speed 50 km/h)

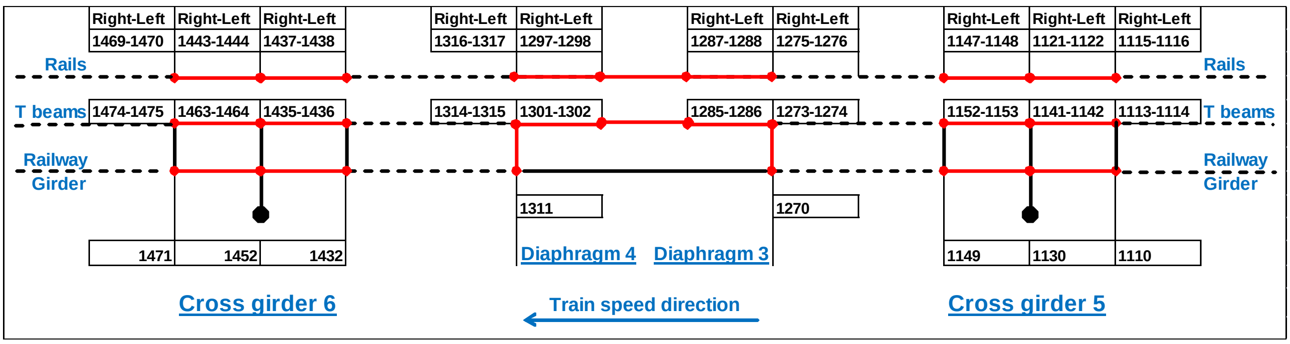

Tables A2-91 and A2-92 present the maximum vertical force transmitted to the listed visco-elastic beds located underneath the left and right rails and computed from static and dynamic simulations. Impact Factors are also listed in the same tables.

LEFT RAIL	Bed #	Static Force [N]	Dynamic Force [N]	Impact Factor
	795	15000	16400	1,0933E+00
	800	15000	16200	1,0800E+00
	803	15000	16500	1,1000E+00
	808	15000	17000	1,1333E+00
	892	14950	15300	1,0234E+00
	899	14900	15500	1,0403E+00
	912	15000	15100	1,0067E+00
	995	14980	15020	1,0027E+00
	1000	15000	15400	1,0267E+00
	1003	15000	16000	1,0667E+00
	1008	15000	15500	1,0333E+00

Table A2-91 – Impact factor evaluation from static and dynamic loads at specific beds locations positioned underneath the left rail.

RIGHT RAIL	Bed #	Static Force [N]	Dynamic Force [N]	Impact Factor
	793	14950	15750	1,0535E+00
	798	14950	15000	1,0033E+00
	801	14950	15100	1,0100E+00
	806	15000	14600	9,7333E-01
	890	15000	15300	1,0200E+00
	897	14900	15600	1,0470E+00
	910	15000	16100	1,0733E+00
	993	15000	15700	1,0467E+00
	998	15000	15800	1,0533E+00
	1001	15000	15500	1,0333E+00
	1006	15000	15300	1,0200E+00

Table A2-92 – Impact factor evaluation from static and dynamic loads at specific beds locations

positioned underneath the right rail.

Table A2-93 presents vertical displacements of selected railway girder nodes located at cross girders 5 and 6 and diaphragms 3 and 4.

	Node #	Displacement [m]
Cross Girder # 5	1110	-3,6000E-03
	1130	-3,6000E-03
	1149	-3,6000E-03
Diaphragm # 3	1270	-4,5000E-03
Diaphragm # 4	1311	-4,5000E-03
Cross Girder # 6	1432	-3,6000E-03
	1452	-3,6000E-03
	1471	-3,6000E-03

Table A2-93 – Vertical displacements of the railway girder nodes.

Tables A2-94 and A2-95 presents the vertical displacement difference between the listed rails and T beams for both static and dynamic simulations on both left and right hand side of the track. Impact Factors are also listed in the same tables.

LEFT RAIL	Rail	T Beam	Static	Dynamic	Impact
	Node #	Node #	Displacement [m]	Displacement [m]	Factor
Cross Girder # 5	1116	1114	-2,4200E-03	-2,6500E-03	1,0950E+00
	1122	1142	-2,4200E-03	-2,7000E-03	1,1157E+00
	1148	1153	-2,4200E-03	-2,70E-03	9,7521E-01
Diaphragm 3 - 4	1276	1274	-2,4300E-03	-2,56E-03	1,0535E+00
	1288	1286	-2,4200E-03	-2,5600E-03	1,0579E+00
	1298	1302	-2,4200E-03	-2,4800E-03	1,0248E+00
	1317	1315	-2,4400E-03	-2,4850E-03	1,0184E+00
Cross Girder # 6	1438	1436	-2,4250E-03	-2,4900E-03	1,0268E+00
	1444	1464	-2,4200E-03	-2,5600E-03	1,0579E+00
	1470	1475	-2,42E-03	-2,6000E-03	1,0744E+00

Table A2-94 – Impact factor evaluation from the nodal vertical displacement difference between rails and T beams on left hand side of the track. Impact factors are also shown from the ratio between static and dynamic quantities.

RIGHT RAIL	Rail	T Beam	Static	Dynamic	Impact
	Node #	Node #	Displacement [m]	Displacement [m]	Factor
Cross Girder # 5	1115	1113	-2,4200E-03	-2,5000E-03	1,0331E+00
	1121	1141	-2,4200E-03	-2,4700E-03	1,0207E+00
	1147	1152	-2,4200E-03	-2,36E-03	9,7521E-01
Diaphragm 3 - 4	1275	1273	-2,4300E-03	-2,46E-03	1,0103E+00
	1287	1285	-2,4200E-03	-2,5200E-03	1,0413E+00
	1297	1301	-2,4200E-03	-2,5000E-03	1,0331E+00
	1316	1314	-2,4000E-03	-2,6000E-03	1,0833E+00
Cross Girder # 6	1437	1435	-2,4200E-03	-2,5200E-03	1,0413E+00
	1443	1463	-2,4200E-03	-2,4700E-03	1,0207E+00
	1469	1474	-2,42E-03	-2,5500E-03	1,0537E+00

Table A2-95 – Impact factor evaluation from the nodal vertical displacement difference between rails and T beams on right hand side of the track. Impact factors are also shown from

the ratio between static and dynamic quantities.

13.5.14 Simulation 5.10 - RFI 3: E402B locomotive (speed 144 km/h)

The design of rails, fittings and rail box girder is realized according to conventional static loads specified by Code RFI DTC-ICI-PO SP INF 001 A. As such, the dynamic load distribution on the visco-elastic beds due to the vehicle transit is needed for comparison purposes. This more detailed analysis is performed for the locomotive E402B, being the most critical vehicle at the speed of 144 km/h. Tables A2-34 and A2-35 show that the largest impact factor is 1.18 on the left rail, thus, this rail is chosen for the detailed analysis.

Figure A2-46 shows the total load distribution on the visco-elastic beds located underneath the left rail between cross-girders 5 and 6. The maximum load is 3.5 x 105 N and occurs at the time t0 equal to 4.04 seconds.

The load of each bed at this time t0 is then plotted through the longitudinal location of the visco-elastic bed along the railway girder. Figures A2-47 and A2-48 show how the vertical load on each bed varies along the left rail and the Impact Factor of right and left rail plotted vs. the vehicle speed, respectively.

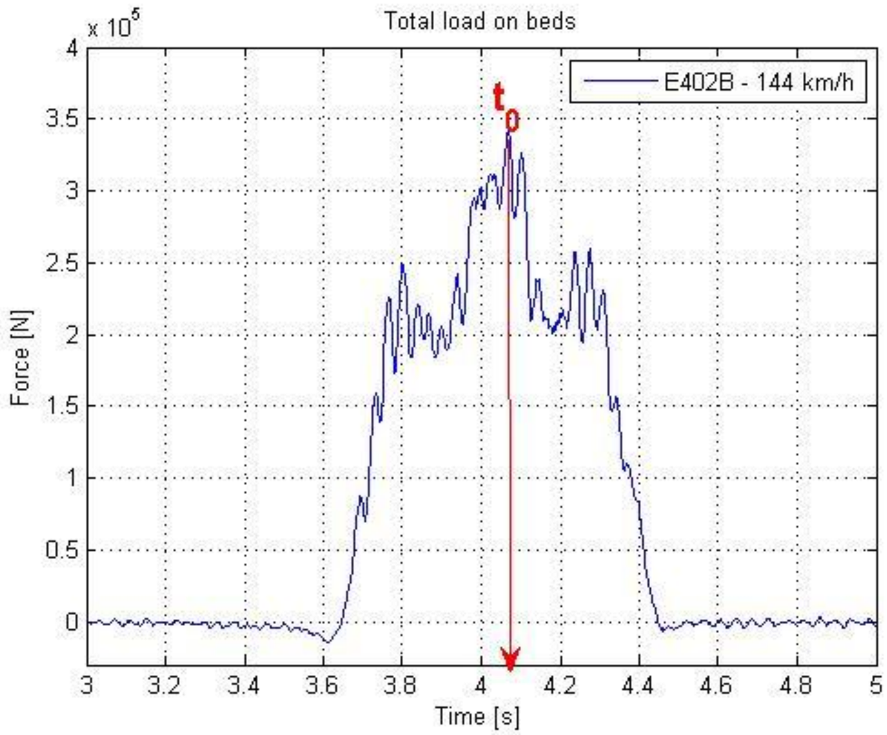

Figure A2-46 – Total load distribution on the visco-elastic beds located underneath the left rail between cross-girders 5 and 6. The maximum load is 3.5 x 105 N and occur at the time t0 equal to 4.04 seconds.

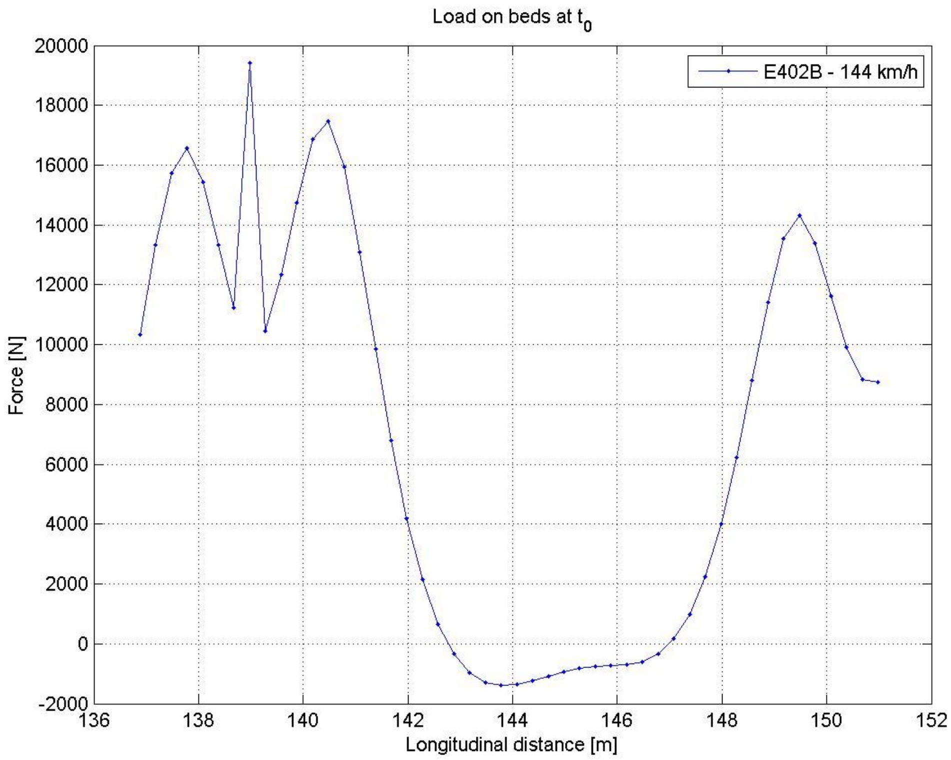

Figure A2-47 - Vertical load variation on each bed along the left rail.

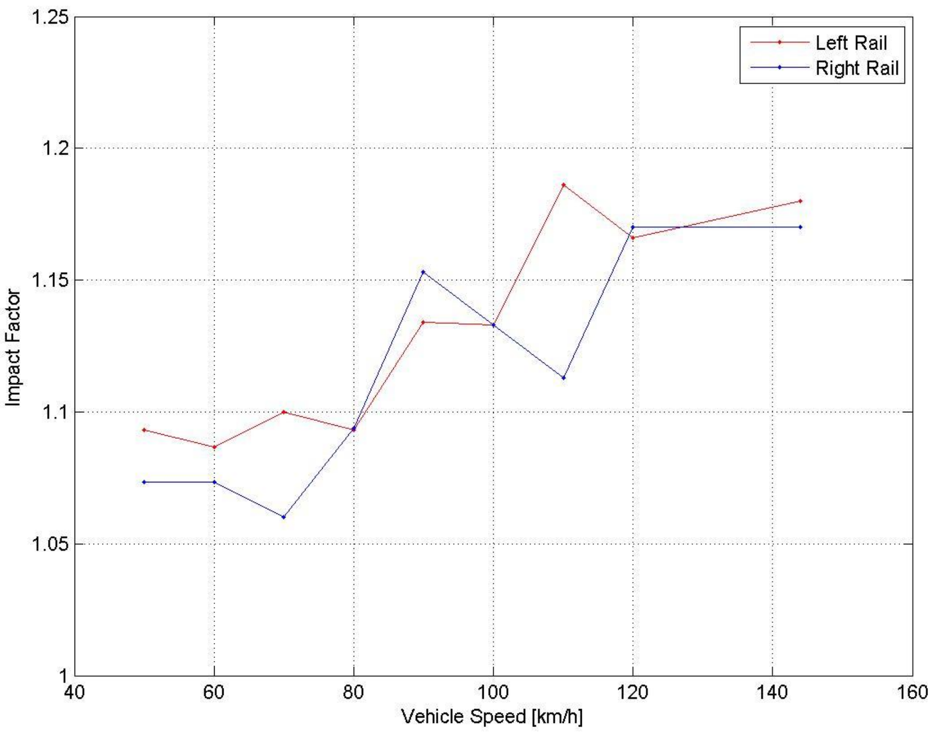

Figure A2-48 - Impact Factor of right and left rail plotted vs. the vehicle speed.

13.5.15 Simulation 6 - RFI 3: Semipilota MD (speed 144 km/h)

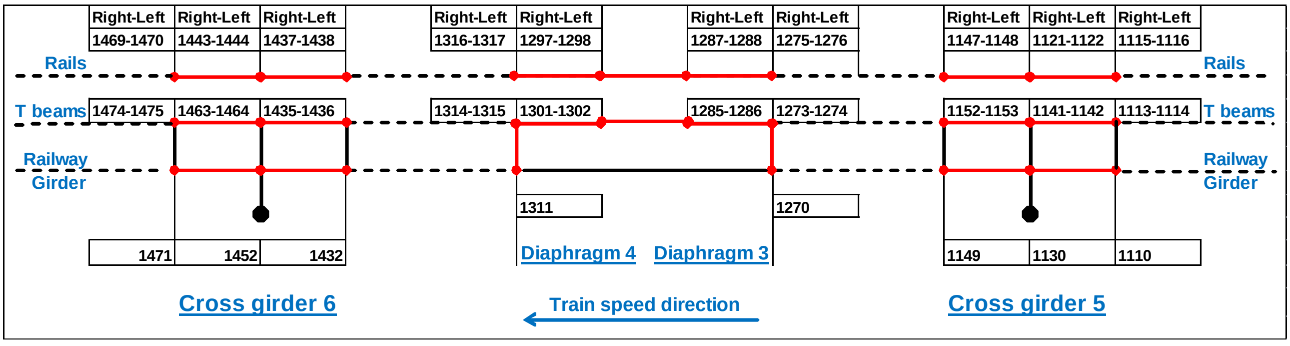

Tables A2-96 and A2-97 present the maximum vertical force transmitted to the listed visco-elastic beds located underneath the left and right rails and computed from static and dynamic simulations. Impact Factors are also listed in the same tables.

LEFT RAIL	Bed #	Static Force [N]	Dynamic Force [N]	Impact Factor
	795	6468	9750	1,5074E+00
	800	6458	8970	1,3890E+00
	803	6465	9027	1,3963E+00
	808	6470	11415	1,7643E+00
	892	6460	9800	1,5170E+00
	899	6445	10300	1,5981E+00
	912	6444	6920	1,0739E+00
	995	6460	8867	1,3726E+00
	1000	6458	9120	1,4122E+00
	1003	6465	8730	1,3503E+00
	1008	6474	8930	1,3794E+00

Table A2-96 – Impact factor evaluation from static and dynamic loads at specific beds locations positioned underneath the left rail.

RIGHT RAIL	Bed #	Static Force [N]	Dynamic Force [N]	Impact Factor
	793	6457	9100	1,4093E+00
	798	6450	9400	1,4574E+00
	801	6460	8800	1,3622E+00
	806	6467	9265	1,4327E+00
	890	6462	9000	1,3928E+00
	897	6466	8000	1,2372E+00
	910	6460	8000	1,2384E+00
	993	6450	7650	1,1860E+00
	998	6455	7940	1,2301E+00
	1001	6465	7750	1,1988E+00
	1006	6460	8682	1,3440E+00

Table A2-97 – Impact factor evaluation from static and dynamic loads at specific beds locations positioned underneath the right rail.

Table A2-98 presents vertical displacements of selected railway girder nodes located at cross girders 5 and 6 and diaphragms 3 and 4.

	Node #	Displacement [m]
Cross Girder # 5	1110	-1,5800E-03
	1130	-1,5800E-03
	1149	-1,5800E-03
Diaphragm # 3	1270	-2,0000E-03
Diaphragm # 4	1311	-2,0000E-03
Cross Girder # 6	1432	-1,5800E-03
	1452	-1,5700E-03
	1471	-1,5800E-03

Table A2-98 – Vertical displacements of the railway girder nodes.

Tables A2-99 and A2-100 presents the vertical displacement difference between the listed rails and T beams for both static and dynamic simulations on both left and right hand side of the track. Impact Factors are also listed in the same tables.

LEFT RAIL	Rail Node #	T Beam Node #	Static Displacement [m]	Dynamic Displacement [m]	Impact Factor
Cross Girder # 5	1116	1114	-1,0455E-03	-1,5000E-03	1,4347E+00
	1122	1142	-1,0450E-03	-1,4000E-03	1,3397E+00
	1148	1153	-1,0500E-03	-1,8950E-03	1,8048E+00
Diaphragm 3 - 4	1276	1274	-1,0500E-02	-1,19E-03	1,1333E-01
	1288	1286	-1,0430E-03	-1,2000E-03	1,1505E+00
	1298	1302	-1,0430E-03	-1,1820E-03	1,1333E+00
	1317	1315	-1,0545E-03	-1,4200E-03	1,3466E+00
Cross Girder # 6	1438	1436	-1,0480E-03	-1,5300E-03	1,4599E+00
	1444	1464	-1,0500E-03	-1,3618E-03	1,2970E+00
	1470	1475	-1,0500E-03	-1,5400E-03	1,4667E+00

Table A2-99 – Impact factor evaluation from the nodal vertical displacement difference between rails and T beams on left hand side of the track. Impact factors are also shown from the ratio between static and dynamic quantities.

RIGHT RAIL	Rail	T Beam	Static	Dynamic	Impact
	Node #	Node #	Displacement [m]	Displacement [m]	Factor
Cross Girder # 5	1115	1113	-1,0470E-03	-1,4440E-03	1,3792E+00
	1121	1141	-1,0457E-03	-1,4800E-03	1,4153E+00
	1147	1152	-1,0500E-03	-1,5000E-03	1,4286E+00
Diaphragm 3 - 4	1275	1273	-1,0500E-02	-1,40E-03	1,3333E-01
	1287	1285	-1,0440E-03	-1,5880E-03	1,5211E+00
	1297	1301	-1,0430E-03	-1,5100E-03	1,4477E+00
	1316	1314	-1,0430E-03	-1,5000E-03	1,4382E+00
Cross Girder # 6	1437	1435	-1,0480E-03	-1,2848E-03	1,2260E+00
	1443	1463	-1,0460E-03	-1,3600E-03	1,3002E+00
	1469	1474	-1,0500E-03	-1,3216E-03	1,2587E+00

Table A2-100 – Impact factor evaluation from the nodal vertical displacement difference between rails and T beams on right hand side of the track. Impact factors are also shown from the ratio between static and dynamic quantities.

Table A2-101 presents nodal vertical acceleration peaks of right and left rails and T beams.

	T beam Right Node #	Vertical Acceleration Peak [m/s^2]	T beam Left Node #	Vertical Acceleration Peak [m/s^2]	Right Rail Node #	Vertical Acceleration Peak [m/s^2]	Left Rail Node #	Vertical Acceleration Peak [m/s^2]
Cross girder # 5	1113	1.723	1114	2.160	1115	72.058	1116	56.267
	1141	1.929	1142	2.084	1121	83.725	1122	47.964
	1152	2.130	1153	2.493	1147	43.277	1148	46.944
Diaphragms # 3 – 4	1273	2.969	1274	4.129	1275	55.776	1276	45.999
	1285	3.181	1286	5.272	1287	93.837	1288	60.183
	1301	3.394	1302	5.337	1297	41.679	1298	37.525
	1314	3.399	1315	4.374	1316	41.710	1317	58.089
Cross girder # 6	1435	1.634	1436	2.531	1438	40.827	1437	32.985
	1463	1.393	1464	2.004	1444	47.848	1443	63.862
	1474	1.449	1475	2.082	1470	35.337	1469	50.223

Table A2-101 - Nodal vertical acceleration peaks of right and left rails and T beams.

Table A2-102 presents nodal vertical acceleration peaks of the railway girder.

	Railway Girder Node #	Vertical Acceleration Peak [m/s^2]
Cross girder # 5	1110	1.725
	1130	1.861
	1149	2.065
Diaphragm # 3	1270	2.858
Diaphragm # 4	1311	3.427
Cross girder # 6	1432	1.517
	1452	1.278
	1471	1.379

Table A2-102 - Nodal vertical acceleration peaks of the railway girder.

A more detailed analysis is performed for the locomotive SemipilotaMD, for Impact Factors are found to be quite critical. Tables A2-96 and A2-97 show that the largest impact factor is 1.76 on the left rail, thus, this rail is chosen for the detailed analysis.

Figure A2-49 shows the total load distribution on the visco-elastic beds located underneath the left rail between cross-girders 5 and 6. The maximum load is 17.5 x 104 N and occurs at the time t0 equal to 3.63 seconds.

The load of each bed at this time t0 is then plotted through the longitudinal location of the visco-elastic bed along the railway girder. Figures A2-50 shows how the vertical load on each bed varies along the left rail.

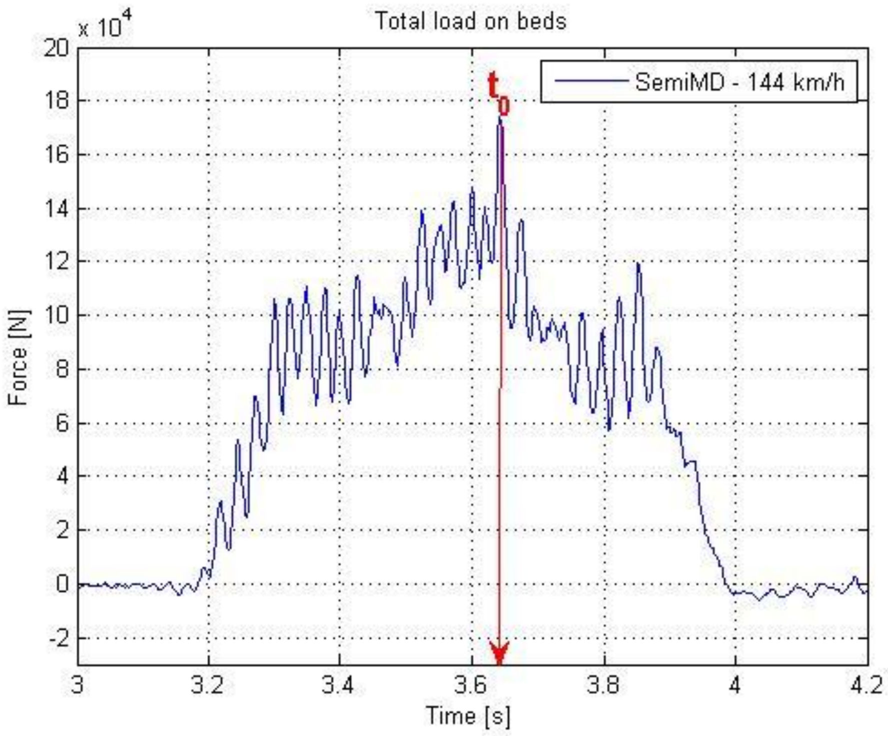

Figure A2-49 - Total load distribution on the visco-elastic beds located underneath the left rail between cross-girders 5 and 6. The maximum load is 17.5 x 104 N and occurs at the time t0 equal to 3.63 seconds.

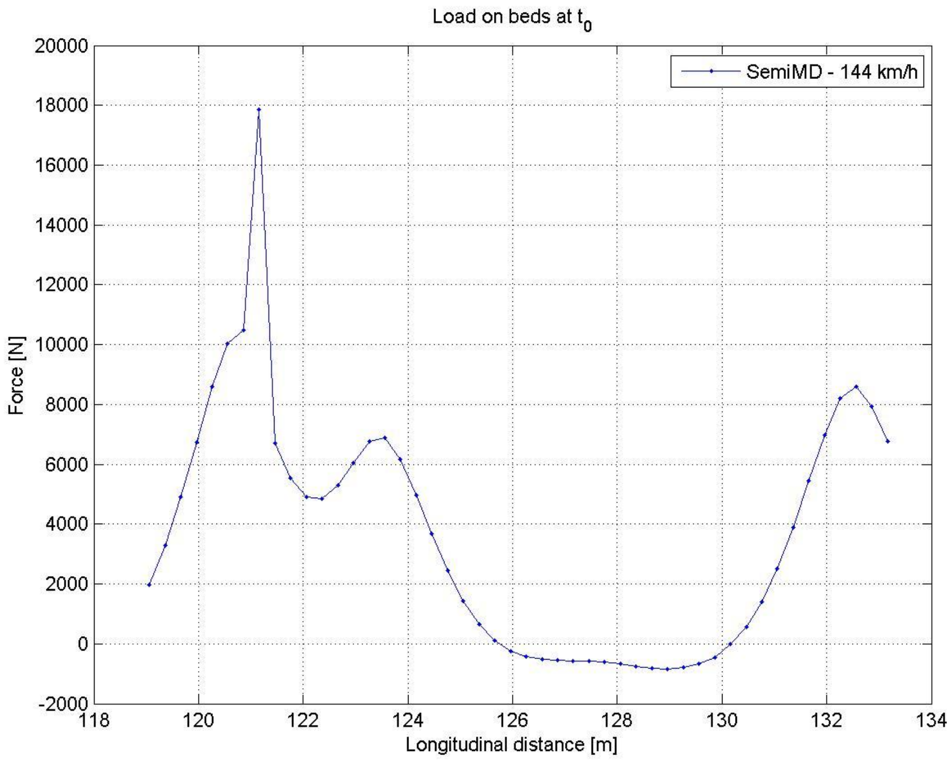

Figure A2-50 - Vertical load variation on each bed along the left rail.

13.5.16 Simulation 7 - RFI 4: TAF locomotive (speed 144 km/h)

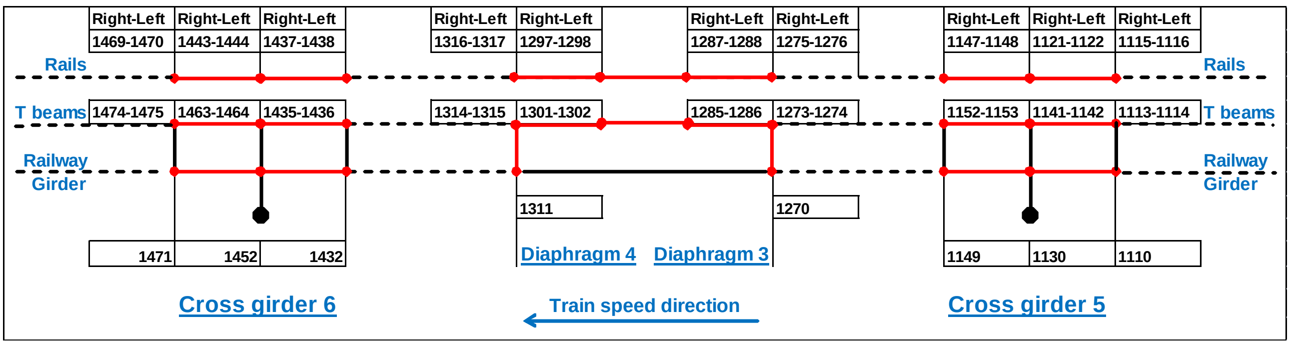

Tables A2-103 and A2-104 present the maximum vertical force transmitted to the listed visco-elastic beds located underneath the left and right rails and computed from static and dynamic simulations. Impact Factors are also listed in the same tables.

LEFT RAIL	Bed #	Static Force [N]	Dynamic Force [N]	Impact Factor
	795	13500	15600	1,1556E+00
	800	13480	13520	1,0030E+00
	803	13500	13900	1,0296E+00
	808	13500	14100	1,0444E+00
	892	13500	14200	1,0519E+00
	899	13450	13700	1,0186E+00
	912	13500	13580	1,0059E+00
	995	13500	16000	1,1852E+00
	1000	13500	15200	1,1259E+00
	1003	13500	15200	1,1259E+00
	1008	13500	15100	1,1185E+00

Table A2-103 – Impact factor evaluation from static and dynamic loads at specific beds locations positioned underneath the left rail.

RIGHT RAIL	Bed #	Static Force [N]	Dynamic Force [N]	Impact Factor
	793	13470	15290	1,1351E+00
	798	13500	14200	1,0519E+00
	801	13480	14840	1,1009E+00
	806	13500	12900	9,5556E-01
	890	13500	14700	1,0889E+00
	897	13400	15400	1,1493E+00
	910	13500	14600	1,0815E+00
	993	13500	17000	1,2593E+00
	998	13500	15200	1,1259E+00
	1001	13500	15500	1,1481E+00
	1006	13500	16000	1,1852E+00

Table A2-104 – Impact factor evaluation from static and dynamic loads at specific beds locations positioned underneath the right rail.

Table A2-105 presents vertical displacements of selected railway girder nodes located at cross girders 5 and 6 and diaphragms 3 and 4.

	Node #	Displacement [m]
Cross Girder # 5	1110	-3,3000E-03
	1130	-3,3000E-03
	1149	-3,3000E-03
Diaphragm # 3	1270	-4,1600E-03
Diaphragm # 4	1311	-4,1800E-03
Cross Girder # 6	1432	3,2800E-03
	1452	3,2500E-03
	1471	3,2500E-03

Table A2-105 – Vertical displacements of the railway girder nodes.

Tables A2-106 and A2-107 presents the vertical displacement difference between the listed rails and T beams for both static and dynamic simulations on both left and right hand side of the track. Impact Factors are also listed in the same tables.

LEFT RAIL	Rail Node #	T Beam Node #	Static Displacement [m]	Dynamic Displacement [m]	Impact Factor
Cross Girder # 5	1116	1114	-2,1850E-03	-2,5000E-03	1,1442E+00
	1122	1142	-2,1900E-03	-2,1000E-03	9,5890E-01
	1148	1153	-2,1800E-03	-2,4000E-03	1,1009E+00
Diaphragm 3 - 4	1276	1274	-2,1860E-03	-2,43E-03	1,1116E+00
	1288	1286	-2,1787E-03	-2,2670E-03	1,0405E+00
	1298	1302	-2,1750E-03	-2,3000E-03	1,0575E+00
	1317	1315	-2,1700E-03	-2,3200E-03	1,0691E+00
Cross Girder # 6	1438	1436	-2,1870E-03	-2,5000E-03	1,1431E+00
	1444	1464	-2,1800E-03	-2,5000E-03	1,1468E+00
	1470	1475	-2,1780E-03	-2,4500E-03	1,1249E+00

Table A2-106 – Impact factor evaluation from the nodal vertical displacement difference between rails and T beams on left hand side of the track. Impact factors are also shown from the ratio between static and dynamic quantities.

RIGHT RAIL	Rail Node #	T Beam Node #	Static Displacement [m]	Dynamic Displacement [m]	Impact Factor
Cross Girder # 5	1115	1113	-2,1850E-03	-2,5000E-03	1,1442E+00
	1121	1141	-2,1817E-03	-2,3700E-03	1,0863E+00
	1147	1152	-2,1800E-03	-1,9200E-03	8,8073E-01
Diaphragm 3 - 4	1275	1273	-2,1900E-03	-2,30E-03	1,0502E+00
	1287	1285	-2,1760E-03	-2,3700E-03	1,0892E+00
	1297	1301	-2,1768E-03	-2,3135E-03	1,0628E+00
	1316	1314	-2,1900E-03	-2,3000E-03	1,0502E+00
Cross Girder # 6	1437	1435	-2,1870E-03	-2,6350E-03	1,2048E+00
	1443	1463	-2,1870E-03	-2,5000E-03	1,1431E+00
	1469	1474	-2,1800E-03	-2,4100E-03	1,1055E+00

Table A2-107 – Impact factor evaluation from the nodal vertical displacement difference between rails and T beams on right hand side of the track. Impact factors are also shown from the ratio between static and dynamic quantities.

Table A2-108 presents nodal vertical acceleration peaks of right and left rails and T beams.

	T beam Right Node #	Vertical Acceleration Peak [m/s^2]	T beam Left Node #	Vertical Acceleration Peak [m/s^2]	Right Rail Node #	Vertical Acceleration Peak [m/s^2]	Left Rail Node #	Vertical Acceleration Peak [m/s^2]
Cross girder # 5	1113	2.280	1114	2.482	1115	38.073	1116	38.442
	1141	2.191	1142	2.487	1121	35.077	1122	57.426
	1152	2.298	1153	2.649	1147	31.335	1148	31.217
Diaphragms # 3 – 4	1273	4.006	1274	5.333	1275	28.090	1276	40.059
	1285	3.869	1286	5.755	1287	36.980	1288	38.839
	1301	4.165	1302	5.394	1297	41.913	1298	28.903
	1314	4.062	1315	5.361	1316	37.193	1317	27.949
Cross girder # 6	1435	2.035	1436	2.226	1438	56.166	1437	37.647
	1463	1.803	1464	2.079	1444	25.683	1443	34.503
	1474	2.039	1475	2.356	1470	30.811	1469	38.698

Table A2-108 - Nodal vertical acceleration peaks of right and left rails and T beams.

Table A2-109 presents nodal vertical acceleration peaks of the railway girder.

	Railway Girder Node #	Vertical Acceleration Peak [m/s^2]
Cross girder # 5	1110	2.251
	1130	2.019
	1149	2.082
Diaphragm # 3	1270	3.511
Diaphragm # 4	1311	3.380
Cross girder # 6	1432	2.010
	1452	1.819
	1471	2.017

Table A2-109 - Nodal vertical acceleration peaks of the railway girder.

13.5.17 Simulation 8 - RFI 4: TAF coach (speed 144 km/h)

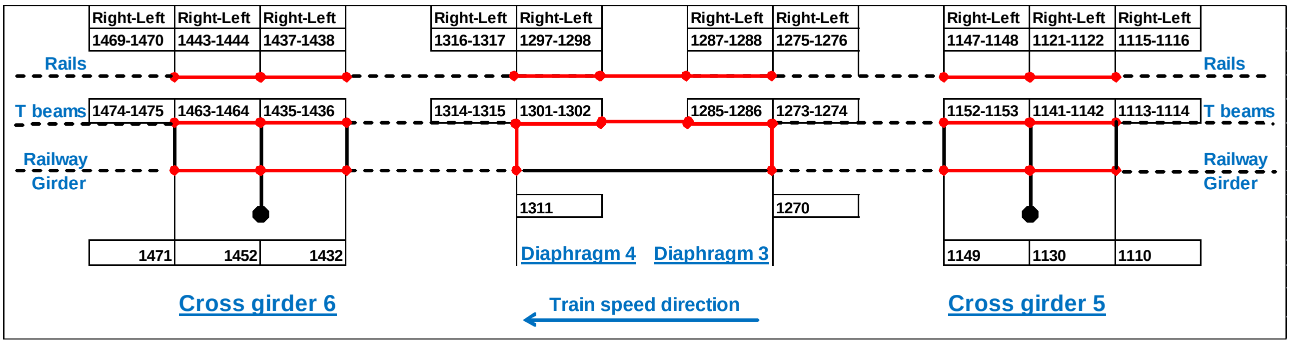

Tables A2-110 and A2-111 present the maximum vertical force transmitted to the listed visco-elastic beds located underneath the left and right rails and computed from static and dynamic simulations. Impact Factors are also listed in the same tables.

LEFT RAIL	Bed #	Static Force [N]	Dynamic Force [N]	Impact Factor
	795	10400	12100	1,1635E+00
	800	10450	12200	1,1675E+00
	803	10400	10800	1,0385E+00
	808	10400	12000	1,1538E+00
	892	10450	10800	1,0335E+00
	899	10400	11800	1,1346E+00
	912	10500	11800	1,1238E+00
	995	10460	11000	1,0516E+00
	1000	10460	12400	1,1855E+00
	1003	10450	11100	1,0622E+00
	1008	10450	12400	1,1866E+00

Table A2-110 – Impact factor evaluation from static and dynamic loads at specific beds locations positioned underneath the left rail.

RIGHT RAIL	Bed #	Static Force [N]	Dynamic Force [N]	Impact Factor
	793	10500	12200	1,1619E+00
	798	10400	12200	1,1731E+00
	801	10450	11800	1,1292E+00
	806	10400	12200	1,1731E+00
	890	10450	12500	1,1962E+00
	897	10500	13000	1,2381E+00
	910	10500	12200	1,1619E+00
	993	10480	11000	1,0496E+00
	998	10460	12500	1,1950E+00
	1001	10440	11300	1,0824E+00
	1006	10500	12000	1,1429E+00

Table A2-111 – Impact factor evaluation from static and dynamic loads at specific beds locations

positioned underneath the right rail.

Table A2-112 presents vertical displacements of selected railway girder nodes located at cross girders 5 and 6 and diaphragms 3 and 4.

	Node #	Displacement [m]
Cross Girder # 5	1110	2,5500E-03
	1130	2,5500E-03
	1149	2,5500E-03
Diaphragm # 3	1270	-3,2000E-03
Diaphragm # 4	1311	-3,2000E-03
Cross Girder # 6	1432	-2,5000E-03
	1452	-2,5000E-03
	1471	-2,5000E-03

Table A2-112 – Vertical displacements of the railway girder nodes.

Tables A2-113 and A2-114 presents the vertical displacement difference between the listed rails and T beams for both static and dynamic simulations on both left and right hand side of the track. Impact Factors are also listed in the same tables.

LEFT RAIL	Rail	T Beam	Static	Dynamic	Impact
	Node #	Node #	Displacement [m]	Displacement [m]	Factor
Cross Girder # 5	1116	1114	-1,6900E+03	-1,8200E-03	1,0769E-06
	1122	1142	-1,6900E-03	-1,8200E-03	1,0769E+00
	1148	1153	-1,6800E-03	-1,8700E-03	1,1131E+00
Diaphragm 3 - 4	1276	1274	-1,7000E-03	-1,98E-03	1,1647E+00
	1288	1286	-1,6900E-03	-1,8500E-03	1,0947E+00
	1298	1302	-1,6900E-03	-1,9300E-03	1,1420E+00
	1317	1315	-1,6800E-03	-2,0500E-03	1,2202E+00
Cross Girder # 6	1438	1436	-1,6900E-03	-1,7500E-03	1,0355E+00
	1444	1464	-1,6900E-03	-1,9000E-03	1,1243E+00
	1470	1475	-1,69E-03	-2,0500E-03	1,2130E+00

Table A2-113 – Impact factor evaluation from the nodal vertical displacement difference between rails and T beams on left hand side of the track. Impact factors are also shown from the ratio between static and dynamic quantities.

RIGHT RAIL	Rail	T Beam	Static	Dynamic	Impact
	Node #	Node #	Displacement [m]	Displacement [m]	Factor
Cross Girder # 5	1115	1113	-1,7000E-03	-1,9000E-03	1,1176E+00
	1121	1141	-1,7000E-03	-1,9500E-03	1,1471E+00
	1147	1152	-1,7000E-03	-1,9500E-03	1,1471E+00
Diaphragm 3 - 4	1275	1273	-1,6900E-03	-2,10E-03	1,2426E+00
	1287	1285	-1,6800E-03	-2,0500E-03	1,2202E+00
	1297	1301	-1,6900E-03	-2,0500E-03	1,2130E+00
	1316	1314	-1,6900E-03	-2,0000E-03	1,1834E+00
Cross Girder # 6	1437	1435	-1,7000E-03	-1,7500E-03	1,0294E+00
	1443	1463	-1,6900E-03	-1,9400E-03	1,1479E+00
	1469	1474	-1,68E-03	-1,9500E-03	1,1607E+00

Table A2-114 – Impact factor evaluation from the nodal vertical displacement difference between rails and T beams on right hand side of the track. Impact factors are also shown from

the ratio between static and dynamic quantities.

Table A2-115 presents nodal vertical acceleration peaks of right and left rails and T beams.

	T beam Right Node #	Vertical Acceleration Peak [m/s^2]	T beam Left Node #	Vertical Acceleration Peak [m/s^2]	Right Rail Node #	Vertical Acceleration Peak [m/s^2]	Left Rail Node #	Vertical Acceleration Peak [m/s^2]
Cross girder # 5	1113	2.146	1114	2.427	1115	32.287	1116	39.234
	1141	2.146	1142	2.268	1121	38.823	1122	52.673
	1152	2.293	1153	2.505	1147	32.017	1148	30.898
Diaphragms # 3 – 4	1273	3.610	1274	5.684	1275	31.233	1276	40.362
	1285	3.591	1286	6.324	1287	45.362	1288	36.802
	1301	3.699	1302	5.798	1297	52.054	1298	33.004
	1314	3.841	1315	4.877	1316	34.588	1317	30.273
Cross girder # 6	1435	1.599	1436	2.213	1438	46.059	1437	24.406
	1463	1.648	1464	2.019	1444	31.052	1443	36.158
	1474	1.868	1475	2.241	1470	36.976	1469	41.568

Table A2-115 - Nodal vertical acceleration peaks of right and left rails and T beams.

Table A2-116 presents nodal vertical acceleration peaks of the railway girder.

	Railway Girder Node #	Vertical Acceleration Peak [m/s^2]
Cross girder # 5	1110	2.143
	1130	2.165
	1149	2.085
Diaphragm # 3	1270	2.956
Diaphragm # 4	1311	3.699
Cross girder # 6	1432	1.583
	1452	1.489
	1471	1.706

Table A2-116 - Nodal vertical acceleration peaks of the railway girder.

Simulation 9 - RFI 5: Freight coach – Full Load (speed 144 km/h)

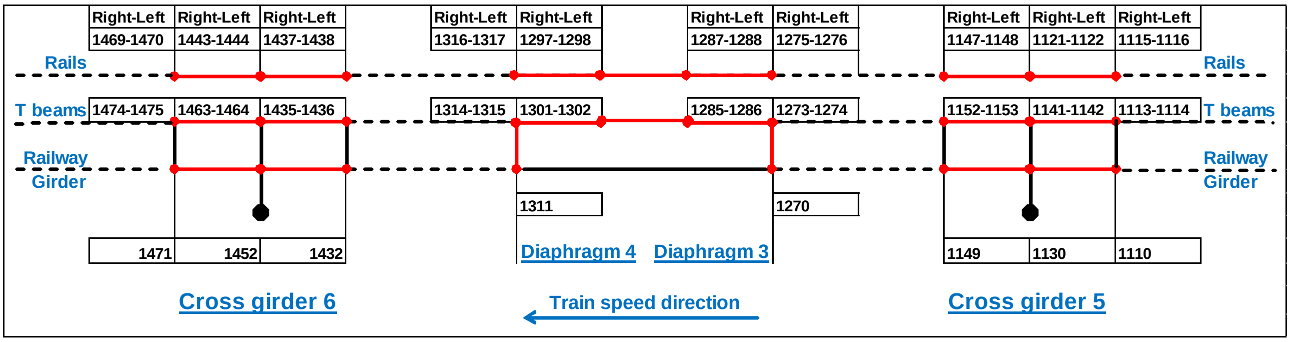

Tables 1 and 2 present the maximum vertical force transmitted to the listed visco-elastic beds located underneath the left and right rails and computed from static and dynamic simulations. Impact Factors are also listed in the same tables.

LEFT RAIL	Bed #	Static Force [N]	Dynamic Force [N]	Impact Factor
	795	1,6700E+04	1,7600E+04	1,0539E+00
	800	1,6700E+04	1,7160E+04	1,0275E+00
	803	1,6700E+04	1,7450E+04	1,0449E+00
	808	1,6700E+04	1,7230E+04	1,0317E+00
	892	1,6700E+04	1,7660E+04	1,0575E+00
	899	1,6700E+04	1,7240E+04	1,0323E+00
	912	1,6700E+04	1,7140E+04	1,0263E+00
	995	1,6700E+04	1,7950E+04	1,0749E+00
	1000	1,6700E+04	1,8500E+04	1,1078E+00
	1003	1,6700E+04	1,7690E+04	1,0593E+00
	1008	1,6700E+04	1,8100E+04	1,0838E+00

Table 1 – Impact factor evaluation from static and dynamic loads at specific beds locations positioned underneath the left rail.

RIGHT RAIL	Bed #	Static Force [N]	Dynamic Force [N]	Impact Factor
	793	1,6700E+04	1,6030E+04	9,5988E-01
	798	1,6700E+04	1,5320E+04	9,1737E-01
	801	1,6700E+04	1,5260E+04	9,1377E-01
	806	1,6700E+04	1,5650E+04	9,3713E-01
	890	1,6700E+04	2,0070E+04	1,2018E+00
	897	1,6700E+04	2,0200E+04	1,2096E+00
	910	1,6700E+04	2,2600E+04	1,3533E+00
	993	1,6700E+04	1,5565E+04	9,3204E-01
	998	1,6700E+04	1,6150E+04	9,6707E-01
	1001	1,6700E+04	1,5350E+04	9,1916E-01
	1006	1,6700E+04	1,6000E+04	9,5808E-01

Table 2 – Impact factor evaluation from static and dynamic loads at specific beds locations positioned underneath the right rail.

Table 3 presents vertical displacements of selected railway girder nodes located at cross girders 5 and 6 and diaphragms 3 and 4.

	Node #	Displacement [m]
Cross Girder # 5	1110	-3,9500E-03
	1130	-3,9500E-03
	1149	-3,9500E-03
Diaphragm # 3	1270	-5,1000E-03
Diaphragm # 4	1311	-5,1000E-03
Cross Girder # 6	1432	-3,9500E-03
	1452	-3,9500E-03
	1471	-4,0000E-03

Table 3 – Vertical displacements of the railway girder nodes.

Tables 4 and 5 presents the vertical displacement difference between the listed rails and T beams for both static and dynamic simulations on both left and right hand side of the track. Impact Factors are also listed in the same tables.

LEFT RAIL	Rail	T Beam	Static	Dynamic	Impact
	Node #	Node #	Displacement [m]	Displacement [m]	Factor
Cross Girder # 5	1116	1114	-2,7000E-03	-2,8650E-03	1,0611E+00
	1122	1142	-2,7000E-03	-2,7950E-03	1,0352E+00
	1148	1153	-2,7000E-03	-2,8200E-03	1,0444E+00
Diaphragm 3 - 4	1276	1274	-2,7000E-03	-2,8000E-03	1,0370E+00
	1288	1286	-2,7000E-03	-2,7100E-03	1,0037E+00
	1298	1302	-2,7000E-03	-2,8380E-03	1,0511E+00
	1317	1315	-2,7000E-03	-2,8175E-03	1,0435E+00
Cross Girder # 6	1438	1436	-2,7000E-03	-2,9800E-03	1,1037E+00
	1444	1464	-2,7000E-03	-2,8700E-03	1,0630E+00
	1470	1475	-2,7000E-03	-2,9850E-03	1,1056E+00

Table 4 – Impact factor evaluation from the nodal vertical displacement difference between rails and T beams on left hand side of the track. Impact factors are also shown from the ratio between static and dynamic quantities.

RIGHT RAIL	Rail	T Beam	Static	Dynamic	Impact
	Node #	Node #	Displacement [m]	Displacement [m]	Factor
Cross Girder # 5	1115	1113	-2,7000E-03	-2,5500E-03	9,4444E-01
	1121	1141	-2,7000E-03	-2,4950E-03	9,2407E-01
	1147	1152	-2,7000E-03	-2,5500E-03	9,4444E-01
Diaphragm 3 - 4	1275	1273	-2,7000E-03	-3,0800E-03	1,1407E+00
	1287	1285	-2,7000E-03	-3,2200E-03	1,1926E+00
	1297	1301	-2,7000E-03	-3,1700E-03	1,1741E+00
	1316	1314	-2,7000E-03	-3,1360E-03	1,1615E+00
Cross Girder # 6	1437	1435	-2,7000E-03	-2,5900E-03	9,5926E-01
	1443	1463	-2,7000E-03	-2,5350E-03	9,3889E-01
	1469	1474	-2,7000E-03	-2,4920E-03	9,2296E-01

Table 5 – Impact factor evaluation from the nodal vertical displacement difference between rails and T beams on right hand side of the track. Impact factors are also shown from the ratio between static and dynamic quantities.

Table 6 presents nodal vertical acceleration peaks of right and left rails and T beams.

	T beam Right Node #	Vertical Acceleration Peak [m/s^2]	T beam Left Node	Vertical Acceleration Peak [m/s^2]	Right Rail Node #	Vertical Acceleration Peak [m/s^2]	Left Rail Node #	Vertical Acceleration Peak [m/s^2]
Cross girder # 5	1113	1,328	1114	1,667	1115	33,121	1116	33,152
	1141	1,362	1142	1,644	1121	29,602	1122	47,672
	1152	1,479	1153	1,707	1147	37,757	1148	43,043
Diaphragms # 3 – 4	1273	1,978	1274	3,675	1275	30,303	1276	38,631
	1285	2,299	1286	4,857	1287	30,85	1288	37,102
	1301	2,216	1302	5,167	1297	45,751	1298	31,766
	1314	2,18	1315	4,274	1316	43,484	1317	34,636
Cross girder # 6	1435	1,031	1436	1,348	1438	27,753	1437	30,555
	1463	0,977	1464	1,574	1444	28,707	1443	34,096
	1474	1,092	1475	1,715	1470	24,393	1469	38,305

Table 6 - Nodal vertical acceleration peaks of right and left rails and T beams.

Table 7 presents nodal vertical acceleration peaks of the railway girder.

	Railway Girder Node #	Vertical Acceleration Peak [m/s^2]
Cross girder # 5	1110	1,105
	1130	1,239
	1149	1,351
Diaphragm # 3	1270	1,512
Diaphragm # 4	1311	1,713
Cross girder # 6	1432	0,812
	1452	0,793
	1471	0,898

Table 7 - Nodal vertical acceleration peaks of the railway girder.

Simulation 10 - RFI 6: Freight coach – Empty Wagon (speed 144 km/h)

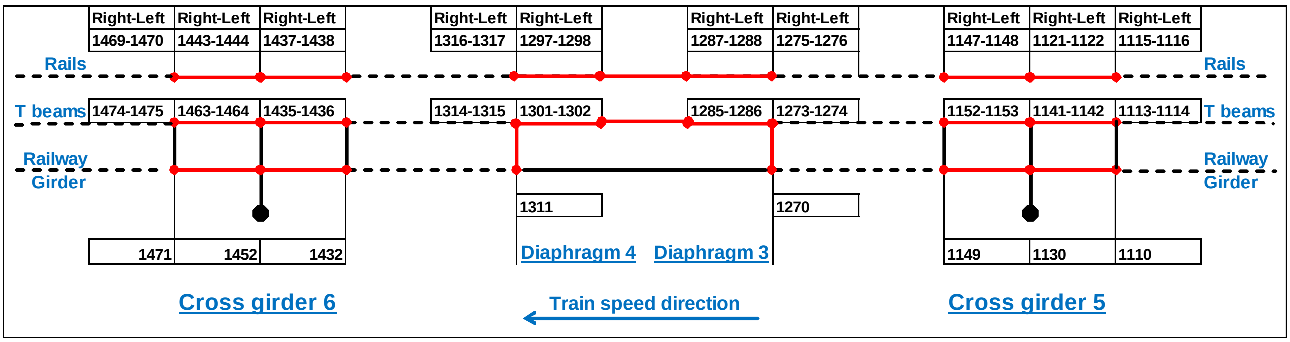

Tables 8 and 9 present the maximum vertical force transmitted to the listed visco-elastic beds located underneath the left and right rails and computed from static and dynamic simulations. Impact Factors are also listed in the same tables.

LEFT RAIL	Bed #	Static Force [N]	Dynamic Force [N]	Impact Factor
	795	5,7200E+03	8,7600E+03	1,5315E+00
	800	5,7200E+03	8,6000E+03	1,5035E+00
	803	5,7200E+03	8,7600E+03	1,5315E+00
	808	5,7200E+03	7,2000E+03	1,2587E+00
	892	5,7200E+03	8,2000E+03	1,4336E+00
	899	5,7200E+03	8,0000E+03	1,3986E+00
	912	5,7200E+03	8,4000E+03	1,4685E+00
	995	5,7200E+03	5,9300E+03	1,0367E+00
	1000	5,7200E+03	5,0400E+03	8,8112E-01
	1003	5,7200E+03	4,9000E+03	8,5664E-01
	1008	5,7200E+03	4,9200E+03	8,6014E-01

Table 8 – Impact factor evaluation from static and dynamic loads at specific beds locations positioned underneath the left rail.

RIGHT RAIL	Bed #	Static Force [N]	Dynamic Force [N]	Impact Factor
	793	5,7200E+03	5,6000E+03	9,7902E-01
	798	5,7200E+03	5,5200E+03	9,6503E-01
	801	5,7200E+03	5,7700E+03	1,0087E+00
	806	5,7200E+03	6,1500E+03	1,0752E+00
	890	5,7200E+03	9,0600E+03	1,5839E+00
	897	5,7200E+03	8,9100E+03	1,5577E+00
	910	5,7200E+03	5,8500E+03	1,0227E+00
	993	5,7200E+03	7,9700E+03	1,3934E+00
	998	5,7200E+03	8,9400E+03	1,5629E+00
	1001	5,7200E+03	8,9700E+03	1,5682E+00
	1006	5,7200E+03	8,5200E+03	1,4895E+00

Table 9 – Impact factor evaluation from static and dynamic loads at specific beds locations positioned underneath the right rail.

Table 10 presents vertical displacements of selected railway girder nodes located at cross girders 5 and 6 and diaphragms 3 and 4.

	Node #	Displacement [m]
Cross Girder # 5	1110	-1,15E-03
	1130	-1,15E-03
	1149	-1,15E-03
Diaphragm # 3	1270	-1,30E-03
Diaphragm # 4	1311	-1,30E-03
Cross Girder # 6	1432	-1,15E-03
	1452	-1,15E-03
	1471	-1,15E-03

Table 10 – Vertical displacements of the railway girder nodes.

Tables 11 and 12 presents the vertical displacement difference between the listed rails and T beams for both static and dynamic simulations on both left and right hand side of the track. Impact Factors are also listed in the same tables.

LEFT RAIL	Rail	T Beam	Static	Dynamic	Impact
	Node #	Node #	Displacement [m]	Displacement [m]	Factor
Cross Girder # 5	1116	1114	-9,2000E-04	-1,3950E-03	1,5163E+00
	1122	1142	-9,2000E-04	-1,3970E-03	1,5185E+00
	1148	1153	-9,2000E-04	-1,2570E-03	1,3663E+00
Diaphragm 3 - 4	1276	1274	-9,2000E-04	-1,3550E-03	1,4728E+00
	1288	1286	-9,2000E-04	-1,3080E-03	1,4217E+00
	1298	1302	-9,2000E-04	-1,3350E-03	1,4511E+00
	1317	1315	-9,2000E-04	-1,5100E-03	1,6413E+00
Cross Girder # 6	1438	1436	-9,2000E-04	-9,4000E-04	1,0217E+00
	1444	1464	-9,2000E-04	-7,8000E-04	8,4783E-01
	1470	1475	-9,2000E-04	-7,7400E-04	8,4130E-01

Table 11 – Impact factor evaluation from the nodal vertical displacement difference between rails and T beams on left hand side of the track. Impact factors are also shown from the ratio between static and dynamic quantities.

RIGHT RAIL	Rail	T Beam	Static	Dynamic	Impact
	Node #	Node #	Displacement [m]	Displacement [m]	Factor
Cross Girder # 5	1115	1113	-9,2000E-04	-9,1900E-04	9,9891E-01
	1121	1141	-9,2000E-04	-8,9400E-04	9,7174E-01
	1147	1152	-9,2000E-04	-9,8250E-04	1,0679E+00
Diaphragm 3 - 4	1275	1273	-9,2000E-04	-1,5200E-03	1,6522E+00
	1287	1285	-9,2000E-04	-1,4450E-03	1,5707E+00
	1297	1301	-9,2000E-04	-1,1000E-03	1,1957E+00
	1316	1314	-9,2000E-04	-8,8500E-04	9,6196E-01
Cross Girder # 6	1437	1435	-9,2000E-04	-1,2800E-03	1,3913E+00
	1443	1463	-9,2000E-04	-1,4500E-03	1,5761E+00
	1469	1474	-9,2000E-04	-1,3630E-03	1,4815E+00

Table 12 – Impact factor evaluation from the nodal vertical displacement difference between rails and T beams on right hand side of the track. Impact factors are also shown from the ratio between static and dynamic quantities.

Table 13 presents nodal vertical acceleration peaks of right and left rails and T beams.

	T beam Right	Vertical Acceleration Peak [m/s^2]	T beam Left Node #	Vertical Acceleration Peak [m/s^2]	Right Rail Node #	Vertical Acceleration Peak [m/s^2]	Left Rail Node #	Vertical Acceleration Peak [m/s^2]
Cross girder # 5	1113	1,185	1114	1,28	1115	21,116	1116	33,887
	1141	1,296	1142	1,442	1121	26,934	1122	32,086
	1152	1,326	1153	1,544	1147	28,149	1148	28,87
Diaphragms # 3 – 4	1273	1,578	1274	2,249	1275	30,45	1276	31,281
	1285	1,696	1286	2,178	1287	23,544	1288	31,624
	1301	1,574	1302	2,223	1297	41,633	1298	29,218
	1314	1,718	1315	2,332	1316	29,588	1317	52,239
Cross girder # 6	1435	1,126	1436	1,953	1438	37,953	1437	64,895
	1463	1,129	1464	1,603	1444	24,025	1443	37,603
	1474	1,196	1475	1,908	1470	28,172	1469	28,658

Table 13 - Nodal vertical acceleration peaks of right and left rails and T beams.

Table 14 presents nodal vertical acceleration peaks of the railway girder.

	Railway Girder Node #	Vertical Acceleration Peak [m/s^2]
Cross girder # 5	1110	1,107
	1130	1,174
	1149	1,223
Diaphragm # 3	1270	1,359
Diaphragm # 4	1311	1,562
Cross girder # 6	1432	1,086
	1452	1,038
	1471	1,024

Table 14 - Nodal vertical acceleration peaks of the railway girder.